Investigations Into the Development of New Methodologies for Organic Electrochemistry

Alex Christopher Seastram

This thesis is submitted for the degree of Doctor of Philosophy (PhD) at Cardiff University

July 2022

Summary

This thesis describes investigations into the development of new electrochemical methodologies applicable to organic synthesis.

Initial investigations were focused on the development of new strategies for the generation and utilisation of alkoxy radicals under electrochemical conditions. To this end, a new procedure for an electrochemical manganese-catalysed deconstructive chlorination of cycloalkanols was developed. In this study, tertiary cyclopropanols and cyclobutanols were conveniently converted into synthetically useful distally chlorinated ketones *via* alkoxy radical intermediates. This methodology utilises an inexpensive manganese (II) pre-catalyst to facilitate the synthesis of a diverse range of *β*- and *γ*-chloroketones (40 examples, 30-90% yield). Facile scale-up was also performed by employing a recirculating flow-electrochemistry system and mechanistic investigations, including the use of cyclic voltammetry, allowed the proposal of alkoxy radical intermediates.

Further work on the electrochemical generation of alkoxy radicals was then performed to overcome the limitations associated with the manganese-catalysed method. This work centred around the use of cerium (III) or (IV) salts to generate alkoxy radicals under electrochemical conditions. Following these unsuccessful investigations, the development of a photoelectrochemical system for the cerium-mediated generation of alkoxy radicals was subsequently explored.

Chapter 4 of this thesis then describes investigations into an electrochemical alkene hetero-difunctionalisation procedure that proceeds *via* a 1,4-nitrile migration. In this study, cyanohydrin substrates bearing a distal alkene were converted into synthetically useful 1,2-azidonitriles using a manganese (II) salt as an azide transfer reagent (28 examples, 27-75% yield). This methodology was then extended to perform electrochemical alkene sulfonylcyanation and trifluoromethylcyanation, as well as to access a trifunctionalised hexanenitrile from a functionalised malononitrile starting material. The utility of the products formed was demonstrated through orthogonal derivatisation, and mechanistic investigations, including cyclic voltammetry studies and a radical clock experiment, allowed the proposal of radical intermediates within the reaction mechanism.

List of Publications

1. B. D. W. Allen, M. D. Hareram, A. C. Seastram, T. McBride, T. Wirth, D. L. Browne and L. C. Morrill, *Org*. *Lett*., 2019, **21**, 9241–9246.
2. W. I. Nicholson, A. C. Seastram, S. A. Iqbal, B. G. Reed-Berendt, L. C. Morrill and D. L. Browne, *ChemSusChem*, 2020, **13**, 131–135.
3. W. I. Nicholson, J. L. Howard, G. Magri, A. C. Seastram, A. Khan, R. R. A. Bolt, L. C. Morrill, E. Richards and D. L. Browne, *Angew*. *Chem*., *Int*. *Ed*., 2021, **60**, 23128–23133.
4. M. D. Hareram, A. A. M. A. El Gehani, J. Harnedy, A. C. Seastram, A. C. Jones, M. Burns, T. Wirth, D. L. Browne and L. C. Morrill, *Org*. *Lett*., 2022, **24**, 3890–3895.
5. A. C. Seastram, M. D. Hareram, T. M. B. Knight and L. C. Morrill, *Chem*. *Commun*., 2022, **58**, 8658–8661.

Acknowledgements

It would be no exaggeration to say that if not for the support of countless people, this journey would not have been possible.

My first thanks go to my supervisor, Louis Morrill. Louie, thank you for your supervision and guidance throughout the last 5 years. I have learned and grown a great deal as a chemist and person over this time, and for your influence I am very grateful. I'd also like to thank Duncan Browne for his support during my first steps into an academic research lab. I would also like to extend my thanks to Rob Jenkins, James Griffiths, and Jamie Cross for their dedication to making the department run smoothly.

Throughout my time in the Morrill group, I've had the absolute privilege of sharing the lab and office with many wonderful people, from both the Morrill and Browne groups. I'd like to thank Kurt, Dan, Shyam, and Mubarak for all the fun times and laughter, and I wish every member I'm leaving behind all the best. I would also like to thank Mark Shuttleworth and Tom Knight, MChem students I supervised, for all their efforts during their projects.

There are some who deserve a special mention. Firstly, some of the guys who I had the pleasure of sharing the lab with during my earlier years: Ben Allen, thank you for showing me the ropes of electrochemistry and being a great source of knowledge during my first year. Ben R-B, I will always be grateful for your supervision during my MChem project and for all the shreds to the first draft of any presentation, my MChem thesis, and even one of the chapters to this thesis! I look forward to being lab mates with you once again! Deepak, we started our PhDs in electrochemistry together and shared much of the journey – I may be slightly envious that you got out a bit earlier but I'm here now! Thank you for being a great sounding board and for making the best curries I've ever had! Will, your strong-willed attitude made sharing a lab with you eventful to say the least, but I wouldn't have had it any other way, especially for the year we spent sharing a lab on shifts after the first lockdown of 2020! Roddy, I've missed your quick wit from the moment you left the lab, as well as your willingness to always help others when they're stuck with any sort of problem. I'm excited to share a lab with you again soon!

There are also some who deserve mention for making the latter stages of my PhD enjoyable and memorable: Albara, thanks for all the laughs and don't lose your creativity – all great things start with a crazy idea, and you're full of them! Matt, everyone should aspire to have your work ethic, keep smelling those chemicals! James, you're needy, cynical, and neurotic, but I wouldn't want you any other way. Thanks for all the tea, the laughs, and the friendship!

Special thanks must go to two guys in particular: Tom, your friendship has been a constant source of joy throughout this journey, it was an absolute pleasure to share a house with you, and there's no one I'd rather have taught me to ski, I'm looking forward to more laughs in the future! Andy, we started this journey together long before the PhD even began, not only in the lab but also as flat/housemates. Thanks for pushing me to always improve my chemistry knowledge, and the great times both in and out of the lab. I hope there are many more in the future!

There are also those outside of uni who deserve my gratitude for aiding me throughout this journey, maybe without realising it so much. Becky, John, Bain, Hannah, and Marcus, I couldn't ask for better friends. Our weekend getaways have been some of the absolute highlights of my last four years. You all never failed at taking my mind off things when they have been at their toughest, which I will always be grateful for. I can't wait for all our future trips.

Last but by no means least I have to thank my family for their unconditional support, even if none of you really know what I've been up to over the last 4 years!! Dan, Tash, Ozzy, Brody, David, Carly, John, Grandma, Grandpa, Dad, and of course my wonderful twinny, Rach! Thank you all for your unwavering support, not only during this PhD but also during the 22 years prior to it.

Finally, the most special mention is for you, Mum. You have been and are undoubtedly my number 1 supporter, without your support and encouragement throughout my whole life, this would not have been possible. Thank you for everything you've done for me, and for all that you will inevitably do for me in the future.

Abbreviations

1,10-phen	1,10-Phenanthroline
Ac	Acetyl
app	Apparent
aq.	Aqueous
BDD	Boron-doped diamond
BDE	Bond dissociation energy
bipy	Bipyridine
Bn	Benzyl
Boc	*tert*-Butyloxycarbonyl
br	Broad
CAN	Ceric ammonium nitrate
cat.	Catalytic
c-Bu	Cyclobutyl
CBz	Carboxybenzyl
conc.	Concentrated
c-Pen	Cyclopentyl
CV	Cyclic voltammetry
Cy	Cyclohexyl
d	Doublet
d.r.	Diastereomeric ratio
DBAD	Di-*tert*-butyl azodicarboxylate
DBU	1,8-Diazabicyclo[5.4.0]undec-7-ene
DCA	9,10-Dicyanoanthracene
DCE	1,2-Dichloroethane
DIAD	Di-*iso*-propyl azodicarboxylate
DMA	Dimethylacetamide
DMF	Dimethylformamide
DMPO	5,5-Dimethyl-1-pyrroline *N*-oxide
DMSO	Dimethyl sulfoxide
DMU	1,3-Dimethylurea

DPA	9,10-Diphenylanthracene
Equiv.	Equivalents
ESR	Electron spin resonance
Et	Ethyl
EWG	Electron-withdrawing group
Fc	Ferrocene
FTIR	Fourier-transform infrared
glyme	Dimethoxyethane
GSW	Galvanised steel wire
h	Hours
HAT	Hydrogen atom transfer
HFIP	1,1,1,3,3,3-Hexafluoropropan-2-ol
HRMS	High resolution mass spectrometry
IBX	2-Iodoxybenzoic acid
i-Pr	*iso*-Propyl
LED	Light-emitting diode
LMCT	Ligand to metal charge transfer
LRMS	Low resolution mass spectrometry
m	Multiplet
m	meta
M.p.	Melting Point
Me	Methyl
min	Minutes
NBS	*N*-Bromosuccinimide
n-Bu	Normal butyl
NCS	*N*-Chlorosuccinimide
n-Hex	Normal hexyl
NIS	*N*-Iodosuccinimide
NMR	Nuclear magnetic resonance
NSAID	Non-steroidal anti-inflammatory drug
o	ortho

p	para
PCET	Proton-coupled electron transfer
Petrol	Petroleum ether
Ph	Phenyl
Pin	Pinacolato
ppm	Part(s) per million
Py	Pyridine
q	Quartet
RBF	Round-bottom flask
rt	Room temperature
RVC	Reticulated vitreous carbon
s	Singlet
SOMO	Singly occupied molecular orbital
t	Triplet
TBA	Tetra-*n*-butylammonium
TBS	*tert*-Butyldimethylsilyl
t-Bu	*tert*-Butyl
TEA	Tetraethylammonium
TEMPO	2,2,6,6-Tetramethylpiperidine 1-oxyl
Tf	Trifluoromethane sulfonyl
TFA	Trifluoroacetic acid
TFE	2,2,2-Trifluoroethanol
THF	Tetrahydrofuran
TMS	Trimethylsilyl
TPPA	Tri(pyrrolidin-1-yl)phosphine oxide
Ts	Toluene sulfonyl
UV	Ultraviolet

Table of Contents

Chapter 1: Introduction

Chapter 2: Manganese-Catalysed Electrochemical Deconstructive Chlorination of Cycloalkanols *via* Alkoxy Radicals

Chapter 3: Investigations Into the (Photo)Electrochemical Generation of Alkoxy Radicals Using Cerium (III) and (IV) Salts

Chapter 4: Electrochemical Alkene Azidocyanation *via* 1,4-Nitrile Migration

Chapter 5: Experimental

Chapter 1: Introduction

Table of Contents

1.1 Synthetic Organic Electrochemistry

The origins of using electrochemistry – a branch of chemistry that focuses on the interconversion of electrical and chemical energy[1] – to enable organic transformations can be traced back to the invention of the first electric battery, or so called “Volta pile”, in 1800.[2] The subsequent application of this technology to the electrolysis of acetic acid, generating ethane gas, in the 1830s by Faraday first demonstrated the power of electrochemistry in driving non-spontaneous organic reactions.[3,4] This pioneering work served not only to establish many of the foundations, principles, and lexicon of electrochemistry (e.g., introduction of the terms *anode*, *cathode*, and *electrolysis*),[5] but also as the inspiration for the development of Kolbe electrolysis in 1847,[6] an important reaction that enables facile alkyl radical generation from widely available carboxylic acids.

The invention of the potentiostat by Hickling in 1942,[7] as well as the development of voltammetry techniques (polarography in 1922 and subsequently cyclic voltammetry (CV) in 1948),[8–10] enabled organic chemists to perform reactions at specific constant potentials. As opposed to the methodologies developed in the field in the 1800s that exclusively relied on *galvanostatic* conditions, where a constant current is applied, these reactions performed under *potentiostatic* conditions could be tuned to target the oxidation or reduction of specific functional groups.

The latter half of the 20th century saw further establishment of electrochemistry as a useful technology to aid organic synthesis, including the development of the Monsanto adiponitrile process, through which over 300000 tonnes of this key intermediate towards Nylon 66 is produced annually from acrylonitrile.[11–13] In 1975 the Shono oxidation was developed to allow for *α*-functionalisation of amides and carbamates,[14,15] and the scope of nucleophiles tolerated was expanded through the development of the “cation pool” concept by Yoshida in 1999.[16,17]

Synthetic organic electrochemistry should be attractive to organic chemists, offering a “greener”, alternative approach to organic synthesis by replacing stoichiometric quantities of chemical redox reagents with an electrical current.[18] The technique generally operates under mild conditions to deliver highly chemoselective transformations, and often can be scaled up with ease.[19] Despite the key advances highlighted above and the advantages that the technique can offer, the uptake of electrochemistry in the organic synthesis community has not been broad.

This is in part due to the lack of standardised equipment, with “home built” setups being favoured, which can lead to irreproducibility between laboratories as a result of the

sensitivity of electrolysis parameters.[20] Within the last decade commercially available setups have been developed to facilitate greater uptake within the community,[21,22] such as IKA's ElectraSyn and Screening System.[23,24] Another reason for this lack of uptake may be the perceived complexity of designing organic electrochemical reactions, with there being many aspects to consider that are unfamiliar to the traditional organic chemist.[19]

1.1.1 Considerations for Reaction Design

There are more aspects to consider when designing an electrochemical reaction for an organic transformation compared to a traditionally performed reaction. In an electrochemical setup a power source – in the form of a battery, potentiostat, or galvanostat – connected to two or three electrodes is required to provide electrical energy to the reaction. This contrasts with a traditional reaction where an input of thermal energy is often applied to drive reactions to the desired products. The bulk reaction media plays a vital role in the conductivity of the system, and the choice of solvent(s) and supporting electrolyte can have a drastic effect on the outcome of reactions. In some cases, the separation of the anode and cathode in different chambers may be necessary, and so a divided cell setup would be required as opposed to the more commonly used undivided cell. With the reaction setup considered, the chemist then must decide between performing the reaction under an applied constant current or a constant potential, with there being advantages and disadvantages to each choice. Finally, reactions can be performed with direct electrolysis of the substrates/reagents at the working electrode or mediated electrolysis can be performed.[25]

The key considerations for each constituent will now be discussed briefly.

1.1.1.1 Power Source

The power source is used to create a local oxidative environment at the anode and a local reductive environment at the cathode by pushing electrons from the anode to the cathode. Historically, the power sources used for electrochemical reactions have been either a galvanostat or a potentiostat. A galvanostat allows reactions to be performed under galvanostatic conditions, where a constant current is applied to the system. When using a potentiostat, the potential at the working electrode can be controlled. Modern electrochemical devices, colloquially referred to as potentiostats, can now operate as both types of power source.

Currently, electrochemical reactions for organic synthesis have almost exclusively been performed using direct current (DC), resulting in a unidirectional flow of electrons with

unchanging electrode polarity.[26] Much less investigated is the use of alternating current (AC) electrolysis despite the benefits that could be obtained.[27] The potential advantages to using AC include the minimisation of over oxidation/reduction products,[28,29] promoting reactions in the diffusion layer of electrochemically generated intermediates,[30,31] and potentially controlling the reactive species formed on the electrode surfaces.[32]

1.1.1.2 Electrode Material

Electrochemical systems comprise of at least two, and sometimes three, electrodes. Of the two electrodes always present, one is denoted as the "working" electrode – where the synthetically useful reaction occurs – and the other the "counter" electrode. The third electrode that can be employed is a "reference" electrode.[33] When a reference electrode is employed, the potentiostat controls the potential between the working and reference electrodes which is particularly useful when performing electrolysis under potentiostatic conditions – allowing specific electron transfer processes to be targeted. In the absence of a reference electrode, the potentiostat will instead control the potential difference between the working and counter electrodes. The anode and cathode can both be denoted as either the working or counter electrode depending on whether an anodic or cathodic process is being studied. Whilst a two electrode system is more frequently employed when performing synthetic reactions,[33] a reference electrode is always required when specific and accurate potentials are required, as is necessary when performing CV experiments (*vide infra*).[25]

When oxidation is desired anode materials that are carbon-based, such as graphite, reticulated-vitreous carbon (RVC), glassy carbon, and boron-doped diamond (BDD), as well as platinum are generally utilised. As anodic chemistry is frequently coupled with proton reduction at the cathode, electrodes with a low overpotential for proton reduction such as platinum or nickel are employed.[34,35] These electrodes with a low overpotential for proton reduction require less energy to facilitate the process than electrodes with a high overpotential, which is beneficial for the desired transformation. When reduction is desired, a wide array of cathode materials can be chosen, such as magnesium, aluminium, iron, or carbon-based electrodes which are all able to reduce organic compounds. Sacrificial anodes, which dissolve upon use, such as magnesium, iron, nickel, lead, or copper are often used in these reactions.[36]

As the electron transfer processes that occur on the electrode surfaces are heterogeneous in nature, the success and/or selectivity of an organic reaction under electrochemical conditions can be heavily dependent on the electrode material chosen.[37]

For example, in Xu and co-workers' 2017 report disclosing an electrochemical aromatic C-H amidination protocol, the authors observed vastly different yields of their cyclised products when the anode material was varied (Scheme 1.1).[38]

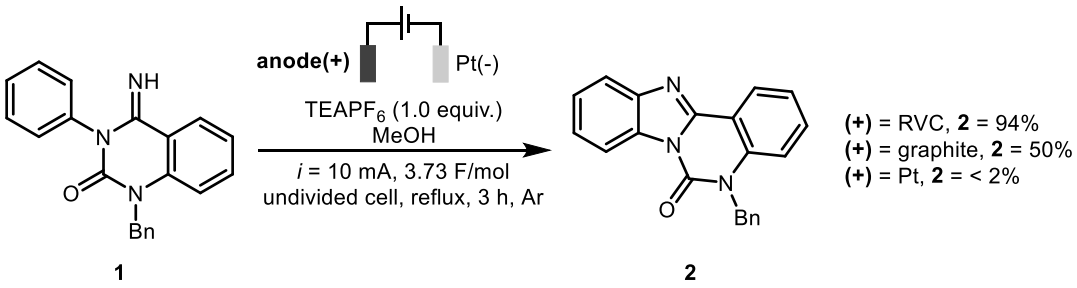

Scheme 1.1: Effect of anode material on Xu's electrochemical aromatic C-H amidination

When using RVC, a highly porous carbon-based electrode with a high surface area, a 94% yield of cyclised product **2** was obtained from amidine **1**. Upon substitution of the RVC anode for graphite, again a carbon-based electrode but with a smaller surface area, the yield of **2** almost halved to 50%. Complete inhibition of the reaction was observed when a platinum anode was employed.

The results obtained by Xu and co-workers is just one example that highlights how important the choice of electrode material can be for a successful reaction. Despite this importance, it can be difficult to predict which electrode material may be optimum for a specific process, with it often necessary to employ an empirical approach.[39]

When performing electrochemical reactions in organic media, which are less conductive than aqueous systems, electrodes with large surface areas such as RVC and carbon felt can be advantageous as they allow the application of higher currents with less of an increase in the overall cell potential compared to electrodes with smaller surface areas.[37,40,41]

1.1.1.3 Solvents and Supporting Electrolyte

Solvents and supporting electrolytes are intrinsically linked within the design of an electrochemical reaction, ensuring sufficient electric conductivity to allow electrolysis to occur at the electrode surface.[42] When designing an organic electrochemical reaction, there are a range of critical factors that must be considered which a traditional organic chemist may be unfamiliar with, including the operating potential range of the solvent. If the substrate of interest's (and/or any intermediates') oxidation or reduction potential lies outside the operating potential range of the solvent, the solvent will be preferentially

oxidised or reduced. Therefore, solvents with large operating potential ranges are preferred. The solvent must also solubilise all substrates/reagents, as well as the supporting electrolyte, and as a result polar solvents with high dielectric constants are frequently chosen.

Polar aprotic solvents such as MeCN, DMF, DMA, and DMSO are among the most commonly used in organic electrochemistry. These are often paired with a polar protic solvent such as AcOH, TFA, MeOH, and HFIP when studying oxidation processes, as they act as sacrificial substrates for proton reduction at the cathode.[25]

As organic solvents are generally non-conductive, supporting electrolytes are required to ensure the resistance of the system is not too high for the desired electrolysis to occur.[42,43] Supporting electrolytes provide positive and negative ions that carry charge through the system, reducing the resistance. Generally supporting electrolytes that are inert are desired, and of course they must be soluble in the solvents chosen. Interaction between the supporting electrolyte and the electrode surface forms a “double layer” that influences the diffusion of the substrate and/or intermediates to and from the electrode, thus differences in the electrolyte composition can impact the outcome of a reaction. commonly used electrolytes include salts with lithium or tetra-*n*-butylammonium (TBA) cations along with anions such as perchlorate, hexafluorophosphate, tetrafluoroborate, or halides.[44]

1.1.1.4 Divided vs. Undivided Cell

When looking to perform an organic reaction under electrochemical conditions, there are two common types of electrolytic cell to choose from, an undivided cell or a divided cell (Figure 1.1).[25,43]

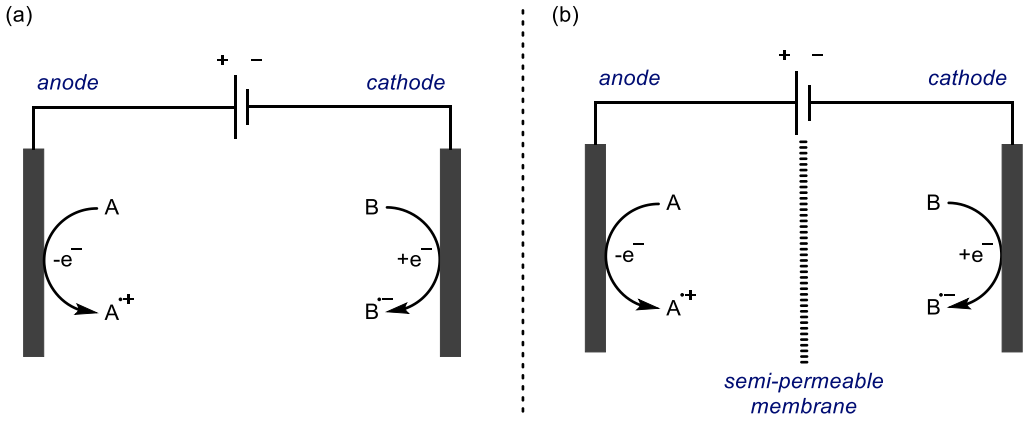

Figure 1.1: Diagram representing (a) an undivided cell; (b) a divided cell

An undivided cell is the most frequently used electrolytic cell in organic synthesis due to its greater simplicity compared to a divided cell. In an undivided cell (Figure 1.1a), both the desired electrochemical transformation at the working electrode and the counter reaction at the counter electrode occur within the same cell. In cases where an anodic oxidation reaction is being studied, should the substrates, reagents, intermediates, and/or products be sensitive to reduction at the cathode, it may be necessary to employ a divided cell.

In a divided cell (Figure 1.1b), the anode and cathode are situated in different chambers, separated by a semi-permeable membrane that allows charged species to migrate between the chambers. This ensures conductivity is maintained but without allowing mixing of the anolyte and catholyte.[43]

1.1.1.5 Constant Current vs. Constant Potential Electrolysis

As discussed above, there are two main types of electrolysis used to perform organic transformations, galvanostatic (constant current) and potentiostatic (constant potential) electrolysis.

Under galvanostatic conditions the current is controlled and maintained throughout the reaction, with no control over the observed potential. In these reactions, the initial potential that is observed is the oxidation/reduction potential of the most easily oxidised/reduced species, and the potential will remain constant until that species is consumed. At that point, the potential will increase rapidly until the oxidation/reduction potential of the next most easily oxidised/reduced species is reached. Should the next most easily oxidised/reduced species be the product, this will lead to the formation of side products. If the product's redox potential lies outside the operating potential range of the solvent and/or other additives, then these side reactions can be avoided.[43]

Constant current electrolysis allows for the utilisation of a simpler reaction setup than constant potential electrolysis, with there being no requirement for the employment of a reference electrode. Therefore, it is considered more convenient to work with and thus is the most common form of electrolysis employed for organic synthesis. Additionally, higher conversion of the substrate is also observed when a constant current is applied, as the potential will hold at the species' oxidation/reduction potential until full consumption is achieved. A disadvantage to constant current electrolysis is the possible lack of selectivity for the desired product that can result from over-oxidation or over-reduction of the product should its oxidation/reduction potential be reached during the reaction.

Under potentiostatic conditions the potential is controlled throughout the reaction with the observed current changing over time. In these reactions, the applied potential is chosen to selectively oxidise/reduce the compound of interest, and typically the current will start at a maximum due to the resistance of the system being at its lowest. As the substrate is consumed, the resistance of the system increases and as a result the current observed begins to decrease over time. To successfully perform potentiostatic reactions, the compound of interest's oxidation/reduction potential should first be determined through CV analysis (*vide infra*).[43]

Constant potential electrolysis can lead to a higher product selectivity being achieved as specific oxidation/reduction potentials of the substrate can be targeted. However, as the current decreases with time during a constant potential experiment, full conversion of the substrate is often not achieved in these reactions. Constant potential experiments may also require a reference electrode, making the setup more complicated than a constant current experiment.[25,45]

1.1.1.6 Direct vs. Mediated Electrolysis

Direct electrolysis, where the compound of interest is oxidised/reduced directly at the anode/cathode, involves a heterogeneous electron transfer process (Figure 1.2a). This process can at times be inefficient and can lead to the grafting of organic species to the working electrode, negatively impacting the reaction outcome/selectivity.[37,43,46] In these cases, one strategy that can be employed to overcome the inefficiency is through the use of a redox mediator to perform mediated electrolysis (Figure 1.2b).[37,43,46]

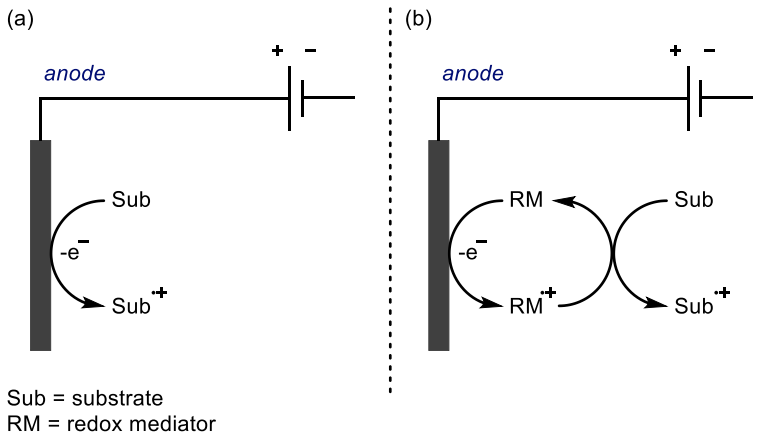

Figure 1.2: Schematics of (a) direct electrolysis; (b) mediated electrolysis

Mediated electrolysis is a hybrid between direct electrochemical electron transfers and homogeneous chemical redox reactions. A redox mediator, which can be employed in

catalytic quantities, can be oxidised directly at the anode and then the oxidised species can oxidise the substrate through a homogeneous electron transfer process (note: anodic oxidation is depicted in Figure 1.2, but redox mediators can also be used in cathodic reduction processes). An appropriate redox mediator must be sufficiently stable in both the oxidation states accessed to allow for electron transfer processes between the activated mediator and the substrate.

There are two distinct mechanism types for the homogeneous electron transfer between the activated redox mediator and the substrate depending on how the two interact with one another (Figure 1.3).

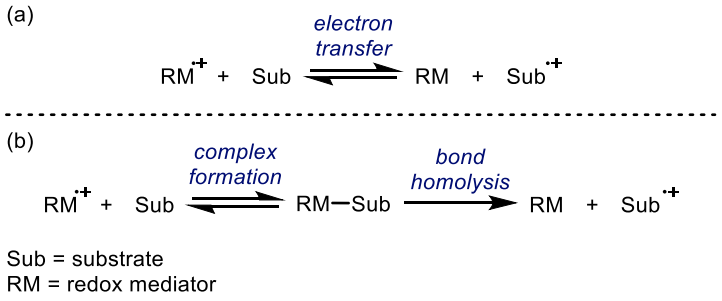

Figure 1.3: Mechanisms of electron transfer. (a) outer-sphere; (b) inner-sphere

In an outer-sphere mechanism, no bond is formed between the activated mediator and substrate and the electron transfer occurs through space. In an inner-sphere electron transfer, a homogeneous reaction occurs between the activated mediator and substrate or to form a new chemical bond, which can then homolyse to regenerate the mediator along with the newly oxidised substrate.[46]

Commonly employed redox mediators in organic electrochemistry include triarylamines,[47–59] triarylimidazoles,[60–64] and salts/complexes of metals such as manganese,[65–75] and nickel,[76–88] though this list is far from exhaustive.[5,46,89,90]

1.1.2 Cyclic Voltammetry

Cyclic voltammetry (CV) is an incredibly powerful analytical technique that can be employed to study the redox processes of organic compounds. It can also be used to gain mechanistic insight into electron transfer processes that may occur within organic reaction mechanisms.[91,92]

A typical CV setup is composed of a working electrode, a counter electrode, and a reference electrode, which have the same functions as described in section 1.1.1.2. The working electrode frequently employed is a glassy carbon disk, with a platinum wire

counter electrode. When the CV analysis is performed in organic media, a $Ag/AgNO_3$ reference electrode system is commonly used as it has a stable and well-defined equilibrium potential, and thus it is used a reference point for all measurements taken. The potential of Ag/Ag^+ reference electrodes can vary with parameters such as the solvent and electrolyte used. Therefore, an internal reference compound with a known oxidation/reduction potential is often added to ensure consistency between measurements, not only within the same laboratory but also in the wider community. Ferrocene (Fc) is a commonly used internal reference and all the oxidation potentials reported in this thesis are referenced to Fc/Fc^+.[93,94]

To visualise the process performed when running a CV, the applied potential can be plotted vs. time (Figure 1.4).

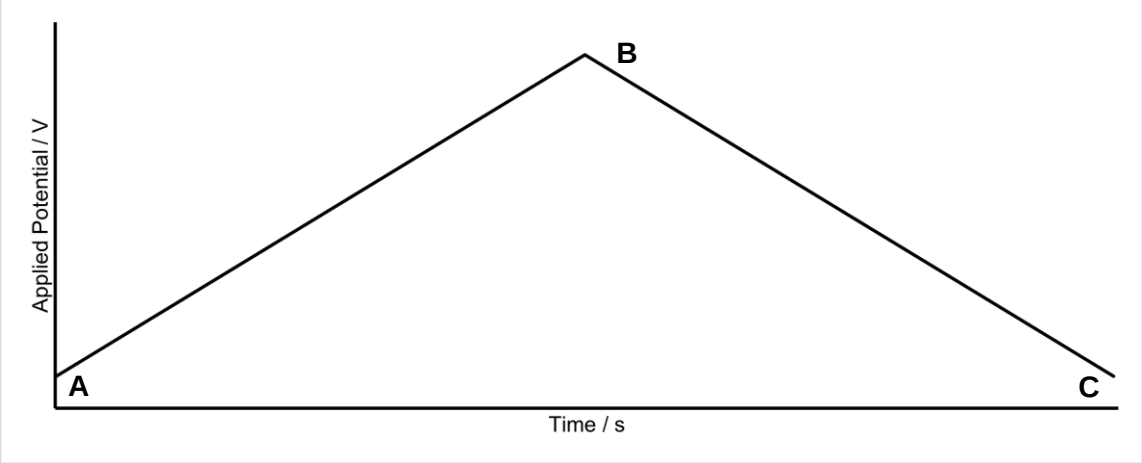

Figure 1.4: Applied potential vs time for a generic CV experiment

When performing a CV, the applied potential is changed with time from the start potential (**A**) to the switching potential (**B**). In the case of this CV, the starting potential is lower than the switching potential and therefore the sweep from **A** to **B** can be described as an oxidative sweep. Once the switching potential is reached, the reductive sweep then begins until the stop potential (**C**) is reached, at which point the experiment is complete.

During a CV, the current is measured as a function of the applied potential, where changes in current indicate the oxidation or reduction of a compound at the working electrode (Figure 1.5).

When a solution of Fc in MeCN is scanned to the switching potential (i.e., **A** to **B**), Fc is oxidised locally at the working electrode to Fc^+, resulting in an increase in the current measured until point **D**. This point coincides with decreasing concentration of Fc within

the diffusion layer that surrounds the working electrode. At point **D**, where the anodic current is reached at the oxidation potential (E_{ox}), the current observed is now dictated by the delivery of additional Fc *via* diffusion into the diffusion layer. Due to the now increased concentration of Fc^+ in the diffusion layer, the rate diffusion of Fc from the bulk solution slows, resulting in a decrease in the current observed from **D** to **B**. At the switching potential **B**, the scan direction is reversed until the stop potential **C** is reached. During this reverse sweep, the inverse process occurs where Fc^+ is reduced to Fc, and the same concentration effects are observed. At point **E** the cathodic current is reached at the reduction potential (E_{red}).

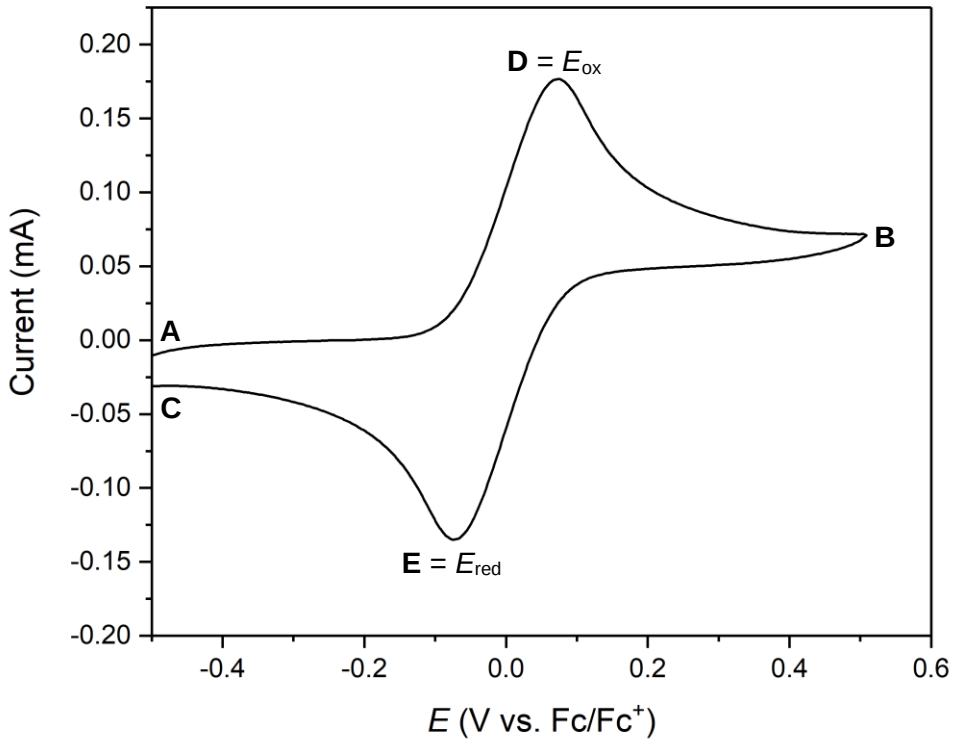

Figure 1.5: CV of Fc (6.0 mM) in MeCN (6 mL) with $LiClO_4$ (0.1 M). ***Scan rate: 100 mV/s***

For an electrochemically reversible process, one would expect that E_{ox} and E_{red} should be equal in value; however, as CV measurements are dependent on the diffusion of species from the bulk solution to the diffusion layer, separation of the two values is observed to give the characteristic “duck”-shaped voltammograms. The closer in values the two peaks are, the more reversible the electron transfer process is.

1.2 Recent Applications

In the last decade, there has been a resurgence in the use of electrochemistry within the synthetic organic chemistry community,[18] partly due to the development of standardised electrochemical reactors for processes in batch and flow.[21–24]

Electrochemical processes for organic synthesis can be organised into three main sections by reaction type: anodic oxidation, cathodic reduction, and paired electrolysis. In this section state-of-the-art developments in the field of organic electrochemistry that highlight the benefits that this technique can offer the synthesis community will be discussed.

1.2.1 Anodic Oxidation

In 2019, Xu and co-workers developed an electrochemical methodology for regio- and diastereoselective alkene vicinal diamination (Scheme 1.2).[49]

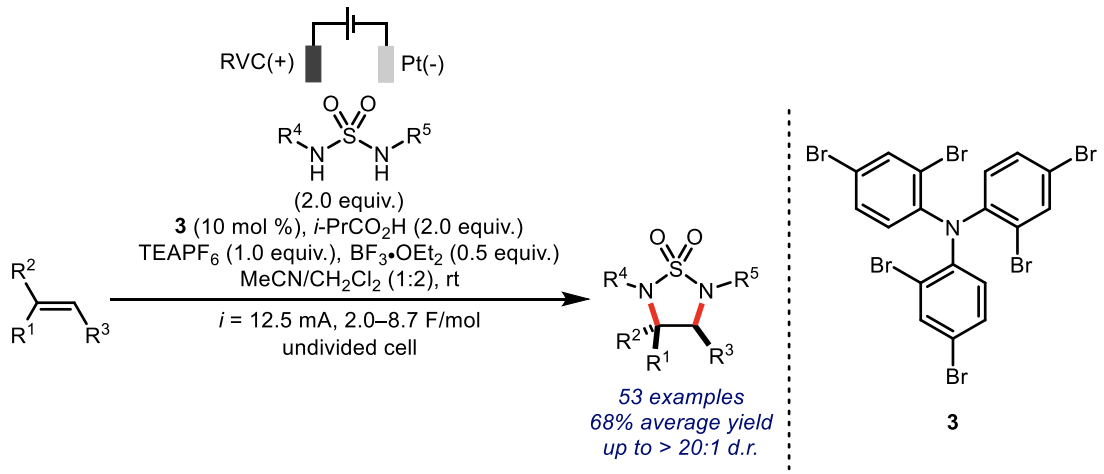

Scheme 1.2: Electrochemical alkene vicinal diamination

In this reaction, di- or trisubstituted alkenes are reacted with a sulfamide (2.0 equiv.) in the presence of triarylamine **3** (10 mol %) that acts as a redox mediator, *iso*-butyric acid (2.0 equiv.), $TEAPF_6$ (1.0 equiv.) and BF_3•OEt_2 (0.5 equiv.) in 1:2 $MeCN/CH_2Cl_2$. Reactions are performed under galvanostatic conditions (i = 12.5 mA) with an RVC anode and a platinum cathode, where 53 diaminated products were formed in a 68% average yield, with most examples formed in diastereomeric ratios of up to > 20:1 and excellent regioselectivities were observed for appropriate substrates. The method exhibits an exceptionally broad substrate scope, with a range of 1,1-di-, 1,2-di-, and trisubstituted alkenes bearing electron-rich and electron-poor aryl, heteroaryl, or alkyl substituents successfully converted to the desired products. A wide range of sulfamides were also

tolerated, and when unsymmetrical sulfamides were employed the products were formed regioselectively. Substrates bearing more than one alkene were also tolerated, with only the most electron-rich alkene reacting, highlighting the chemoselectivity of the transformation. Of particular interest is the success of the reaction when natural products such as estrone and quinine were employed as substrates, showing the potential applicability of this reaction to the late-stage functionalisation of pharmaceutically relevant compounds. The free vicinal diamines were easily furnished through deprotection of the sulfamide using either HBr or hydrazine.

Mechanistically, the reaction initiates with oxidation of the redox mediator **3** at the anode to form the triarylamine radical cation, which in turn oxidises the alkene to its radical cation (Scheme 1.3).

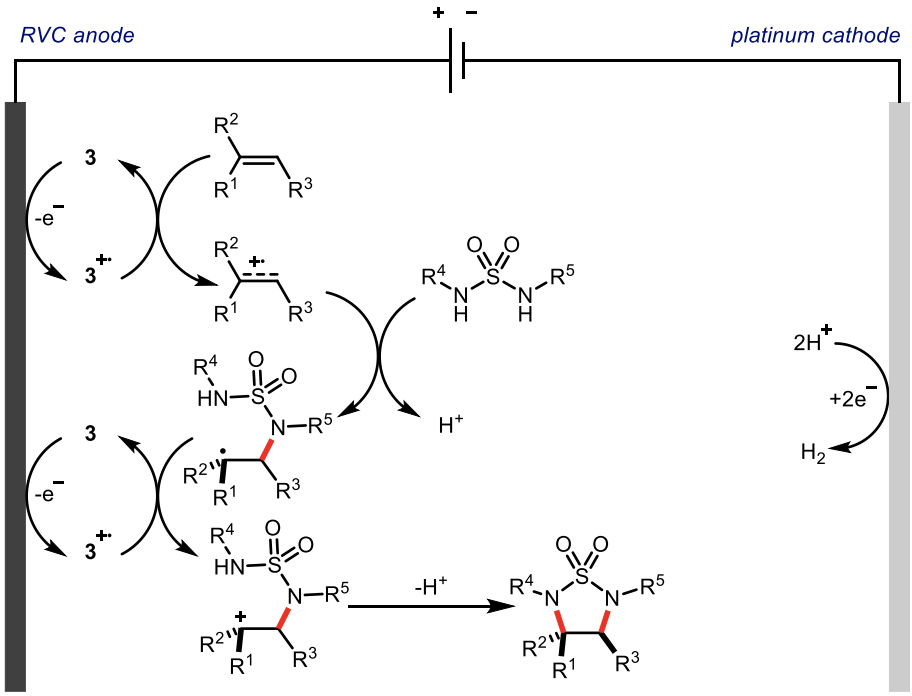

Scheme 1.3: Proposed mechanism for the electrochemical alkene vicinal diamination

Triarylamine **3** was found to be crucial to the outcome of the reaction, with the yield of the desired product decreasing significantly under direct electrolysis. This is proposed to be as a result of the propensity of alkene radical cations to undergo dimerisation at the anode surface.[95–97] The alkene radical cation, formed *via* electron transfer with the radical cation of **3**, then reacts with the sulfamide substrate to give an alkyl radical. It is in this step that the regioselectivity the authors observed is determined, with the less substituted nitrogen attacking the least hindered carbon of the radical cation, resulting in the most stable alkyl

radical intermediate. This alkyl radical then undergoes a single electron oxidation, either through another mediated process or directly at the anode to give a carbocation. Subsequent cyclisation then affords the sulfamide products.

This methodology offers an alternative strategy to well established methods for alkene vicinal diamination such as through using stoichiometric osmium (VIII) or hypervalent iodine organic oxidants. These strategies have obvious drawbacks such as environmental and safety issues through the generation of stoichiometric quantities of toxic waste, as well as cost, and often a compromise on functional group compatibility and diastereoselectivity is observed. This electrochemical method serves to overcome these limitations.

1.2.2 Cathodic Reduction

In the area of cathodic reduction processes, Baran and co-workers have developed an electrochemical alternative to the Birch reduction that facilitates the reduction of aromatic rings, as well as enabling other reductive transformations such as McMurry couplings and reductive cyclisations (Scheme 1.4).[98]

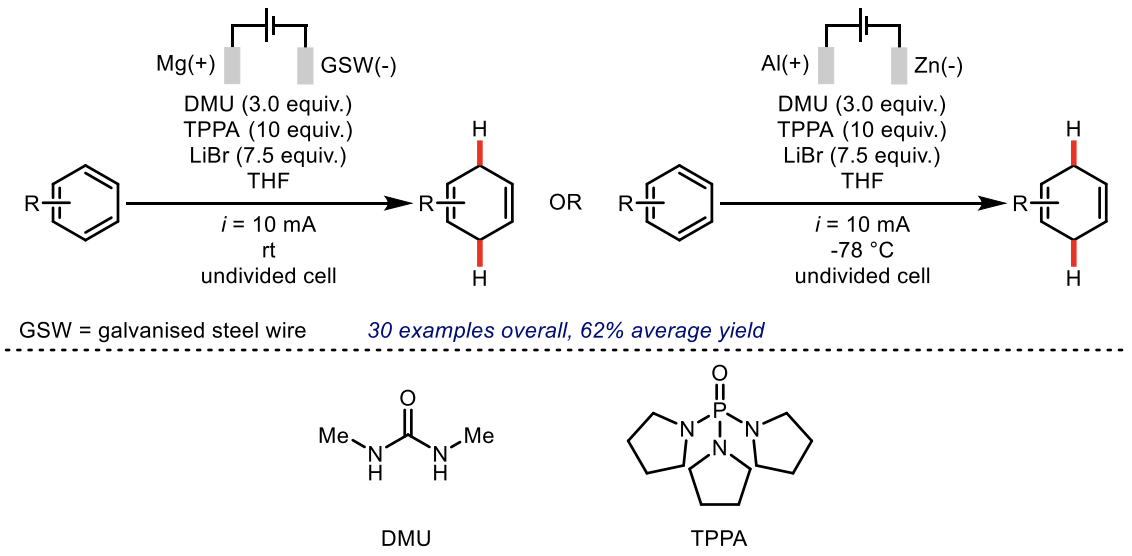

Scheme 1.4: Electrochemical "Birch" reduction

In this work an electrochemical system comprising of an aromatic compound, DMU (3.0 equiv.) as a proton source, TPPA (10 equiv.) as an additive, and LiBr (7.5 equiv.) as the supporting electrolyte in THF was electrolysed under a constant current of 10 mA to afford the cyclohexadiene species. Two sets of conditions were developed: in the first set of conditions a magnesium sacrificial anode and a galvanised steel wire (GSW) cathode

were employed at rt, and in the second set an aluminium sacrificial anode and a zinc cathode were used at -78 °C. Alternative proton sources to DMU reduced the selectivity for the desired product, likely due to an increase in competing proton reduction at the cathode. In the absence of TPPA a metallic substance presumed to be lithium metal, due to its violent reactivity with MeOH and water upon cleaning, accumulated on the cathode. TPPA has been employed to combat this phenomenon in lithium-ion batteries, and its activity translated well to this system. An extensive substrate scope was reported, including the reduction of both electron-poor and electron-rich aromatic rings, with the expected regioselectivity observed in those cases. Functional groups sensitive to reductions including carboxylic acids, carbamates, and silanes were tolerated well, but when compounds with ketones were subjected to the reaction, reduction to the alcohol was observed alongside reduction of the aromatic ring. A range of heterocycles, which are less frequently tolerated under traditional Birch reduction conditions, were successfully reduced under these electrochemical conditions. Bicyclic and tricyclic heterocycles generally saw reduction of the carbocyclic ring favoured over the heterocyclic portion. Natural product derivatives such as dextromethorphan and estrone were also successfully employed, and the utilisation of flow electrochemistry allowed the reaction to be performed on a 100 g scale with no decrease in the yields observed.

Extensive mechanistic studies, including the use of electroanalytical techniques (e.g., CV) and computational studies allowed the authors to propose the following reaction mechanism for this electrochemical alternative to the Birch reduction (Scheme 1.5).

The proposed reaction mechanism proceeds in a similar manner to the classical Birch reduction, with the representative reduction of naphthalene **4** shown. The process initiates with single electron reduction of **4** at the cathode to form radical anion **5** which is then protonated with DMU. The resulting radical **6** then undergoes another single electron reduction at the cathode to anion **7**, followed by protonation to deliver the desired reduced product **8**. Oxidation of the sacrificial anode material releases metal cations into the solution.

This methodology offers a vast improvement in terms of safety, functional group compatibility, and scalability when compared to the classic Birch reduction as well as to previously developed electrochemical analogues.[98–103] The previous electrochemical alternatives to the Birch reduction have suffered from poor selectivity with a range of unwanted by-products formed and side reactions occurring, including competing proton

reduction at the cathode and electrode passivation; all of which are overcome through this work.

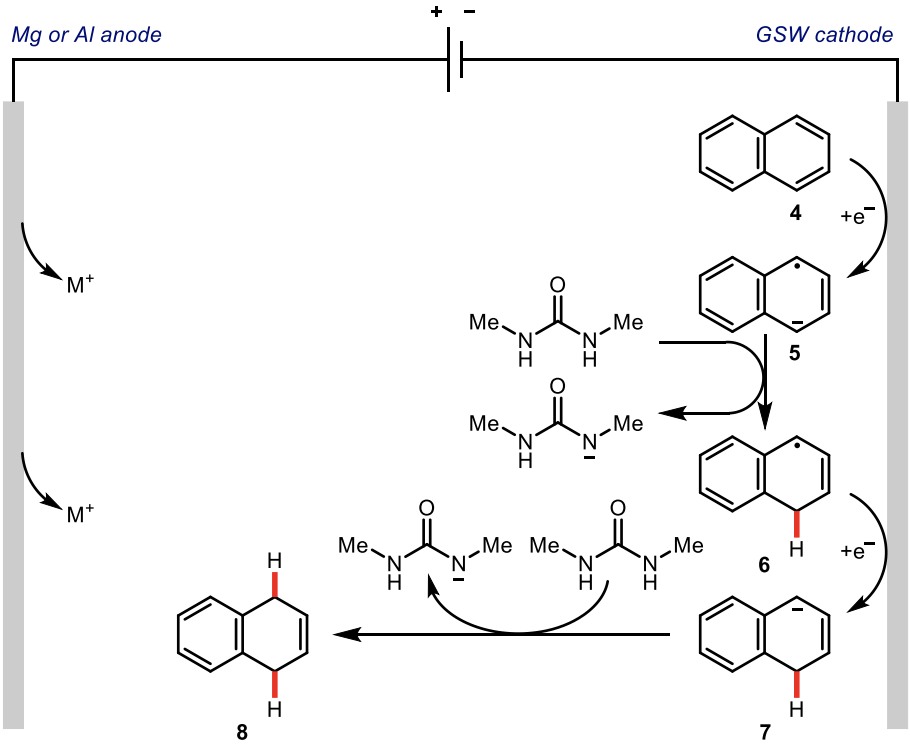

Scheme 1.5: Proposed mechanism for the electrochemical "Birch" reduction

1.2.3 Paired Electrolysis

Paired electrolysis, where synthetically useful redox processes occur at both electrodes in the same vessel are highly desirable in order to maximise the atom economy of a system, with no sacrificial reagents required.[5,104] In one such process, Mei and co-workers reported an electrochemical nickel-catalysed *C*(sp^3)-*C*(sp^2) cross-coupling utilising paired electrolysis (Scheme 1.6).[80]

Using this methodology, the authors were able to take indole-3-acetic acids and couple them with a range of aryl bromides under this electrochemical system. By employing a platinum anode and nickel foam cathode, $NiBr_2$•glyme complex (10 mol %) as catalyst, bipyridine ligand **9** (20 mol %), DBU (1.0 equiv.) as a base, and lutidinium perchlorate **10** (1.0 equiv.) as the supporting electrolyte in DMF and applying a constant current of 4 mA for 8 h, 46 examples of the desired cross-coupled products were obtained in a 62% average yield. An extensive substrate scope was demonstrated, with a plethora of aryl bromides employed successfully including the presence electron-withdrawing groups (e.g., CF_3), electron-donating groups (e.g., OMe), bi- and tricyclic rings, and hetero-

aromatics. Substrates with substitution at the 2-, 4-, and 5-positions of the indole were demonstrated, as well as various *N*-substituents. The method was also applied to the derivatisation of indomethacin, a NSAID used as to treat pain and fever.

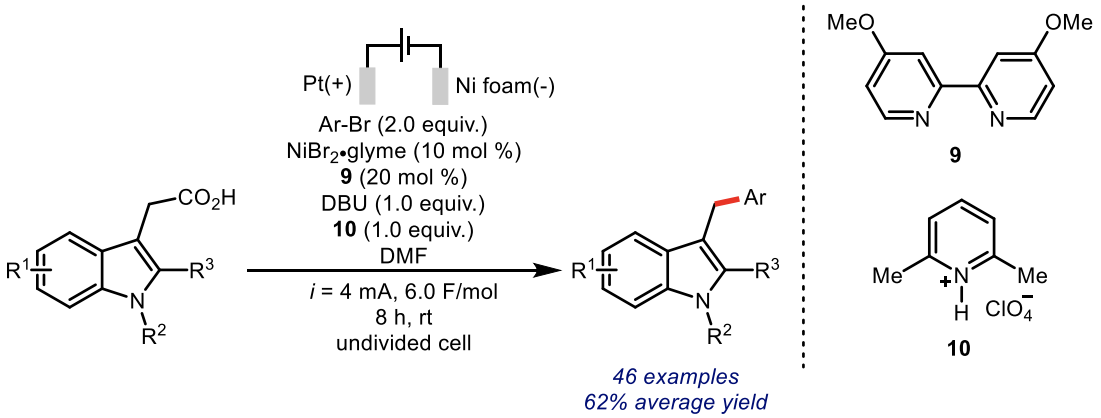

Scheme 1.6: Electrochemical nickel-catalysed decarboxylative C(sp³)-C(sp²) cross-coupling

The authors proposed the following reaction mechanism (Scheme 1.7).

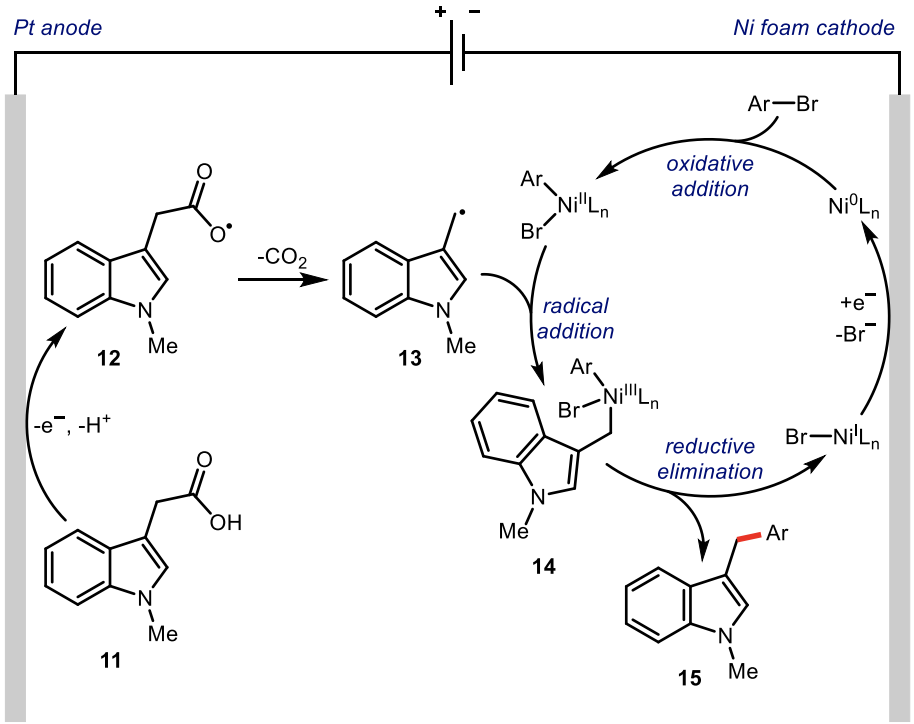

Scheme 1.7: Proposed mechanism for the electrochemical nickel-catalysed decarboxylative C(sp³)-C(sp²) cross-coupling

The proposed mechanism, with the representative cross-coupling of *N*-methylindole derivative **11** shown, initiates with formation of carboxyl radical **12** upon deprotonation of the carboxylic acid and single electron oxidation of the resulting carboxylate anion at the anode. Radical decarboxylation then affords alkyl radical **13**. Concurrently, a nickel (0) complex can be formed from the nickel (II) precursor through double reduction at the cathode. Following oxidative addition into the aryl-bromide bond a new nickel (II) species is then formed. Radical addition of **13** to this nickel (II) complex affords the nickel (III) species **14**, that can then undergo reductive elimination to afford the desired product **15** and a nickel (I) bromide. Loss of the bromide anion and single electron reduction of the nickel at the cathode regenerates the necessary nickel (0) complex.

There are previous reports of nickel-catalysed decarboxylative cross-couplings being performed under electrochemical conditions;[105,106] however, these reports require the use of redox active esters as pre-functionalised carboxylic acids as well as either a divided cell with a sacrificial reductant, or a sacrificial anode in an undivided cell. The methodology developed by Mei and co-workers is an advance on these previous works, allowing the use of the simpler undivided cell setup without needing a sacrificial anode, and the ability to directly use carboxylic acid substrates.

1.2.4 In Tandem with Other Enabling Technologies

As interest in synthetic organic electrochemistry has risen, so has the interest in the development of methodologies that utilise electrochemistry in tandem with complementary enabling technologies.

1.2.4.1 Photoelectrochemistry

Photoelectrochemistry can be employed to access organic transformations that are not possible under photochemical nor electrochemical conditions individually, or to improve reactions that require forcing conditions to proceed.[107]

In an example where their combination was utilised to excellent effect, the research groups of Lin and Lambert collaborated to report a photoelectrochemical procedure to access extremely strong reductants that enable the formation of aryl radicals from aryl chlorides and aryl bromides (Scheme 1.8).[108]

In this work, aryl chlorides or aryl bromides were reacted under photoelectrochemical conditions using DCA (5 mol %) as the redox mediator and photoredox catalyst, pyridine (20 mol %) as an additive, B_2Pin_2 (2.0 equiv.) as the SOMOphile, and $TBAPF_6$ (1.5 equiv.) as the supporting electrolyte in MeCN. A constant potential of 3.2 V was applied using a

zinc sacrificial anode and a graphite cathode in a divided cell and the solution was irradiated using blue LEDs until full consumption of the starting material.

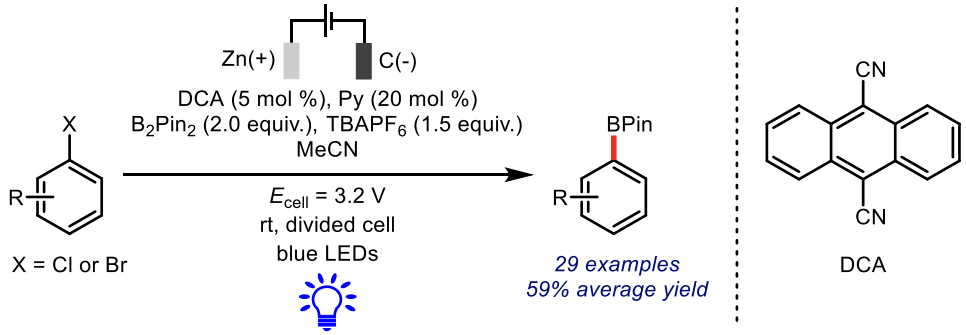

Scheme 1.8: Photoelectrochemical generation of highly reducing species

A broad tolerance of substituents on the aromatic ring were demonstrated by the authors, although electron-poor substrates gave higher yields than electron-rich substrates, as would be expected for reduction processes, and heteroaromatics also worked well. Generally, aryl bromides performed better than aryl chlorides, which the authors propose is because the reverse electron transfer process (the aryl radical anion reducing DCA), is more able to outcompete loss of chloride from the aryl radical anion compared to the loss of bromide when aryl bromides are employed. Functional groups that are sensitive to reducing conditions including esters, ketones, and carbamates remained intact, highlighting the chemoselectivity of the process. Amino acid derivatives were also successfully employed, including a derivative of L-leucine where no epimerisation of the stereogenic centre was observed.

Following mechanistic investigations involving the use of UV-vis spectroscopy and CV studies, the authors proposed the following mechanism (Scheme 1.9).

In the cathodic chamber the reaction initiates with single electron reduction of DCA at the graphite cathode to give a radical anion. Upon irradiation with blue LEDs, the excited state of the radical anion, which is a strong reductant with a reduction potential of -3.2 V vs. SCE, which can reduce the aryl halide (E_{red} ~ 1.9 to 2.9 V vs. SCE) to its corresponding aryl radical anion and regenerate DCA. Heterolysis of the C-X bond furnishes an aryl radical that then adds into the SOMOphile to form the desired borylated product. Oxidation of the zinc anode material releases zinc cations into the solution in the anodic chamber.

Through this work, the authors have developed a photoelectrochemical methodology that allows access to a highly reducing species which chemoselectively activates substrates

which are challenging to activate under solely photochemical conditions. This work is a conceptual advance that will allow the activation of other substrates that require large reduction potentials to be activated.

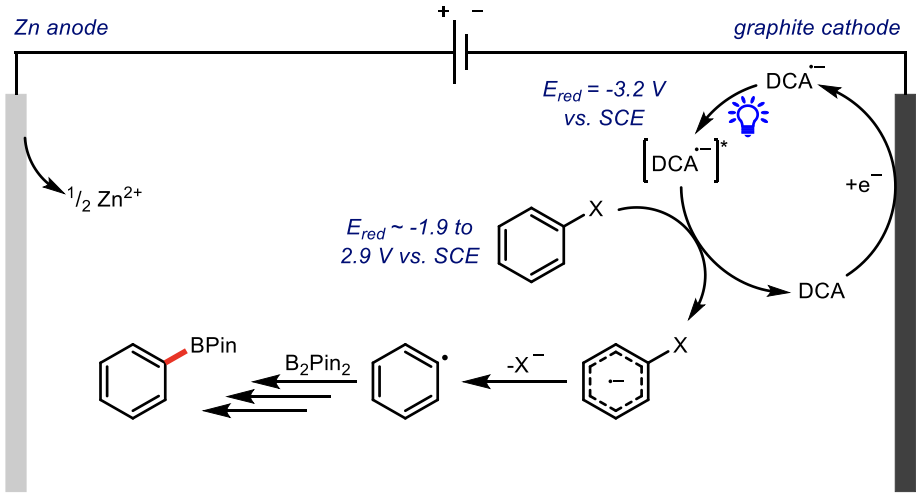

Scheme 1.9: Proposed mechanism for the photoelectrochemical generation of highly reducing species

1.2.4.2 Flow Electrochemistry

Flow chemistry offers many advantages to synthetic organic chemists for a multitude of reasons, one of which being the ease of scale-up that can be achieved.[109] As interest in utilising electrochemistry for organic synthesis has grown over the last decade, one avenue of research has been directed towards the development of flow electrochemistry systems.[110–112]

One recent example of a flow electrochemistry system comes from Noël and co-workers in 2021, where they reported an electrochemical aziridination of internal alkenes in a flow setup (Scheme 1.10).[113]

In this flow electrochemical system, a solution of the appropriate alkene and primary amine (5.0 equiv.), along with HFIP (5.0 equiv.) as a proton source, and cyclohexadiene **16** (0.5 equiv.) as an additive in MeCN is pumped through a microflow electrocell comprising of a graphite anode and a steel cathode. A flow rate of 0.15 mL/min is used and the reaction is performed under galvanostatic conditions to furnish the desired aziridine products. As a selection of the aziridines were unstable upon isolation, the crude aziridines were reacted with thiophenol **17** (1.2 equiv.) in the presence of BF_3•OEt_2 (10 mol %) in MeCN to give 1,2-aminosulfide products. Cyclohexadiene additive **16** was shown to prevent over-oxidation of the alkene at the anode. Due to the decreased

interelectrode distance compared to batch electrochemical setups, no supporting electrolyte is required for this process, as is frequently the case in flow electrochemical reactions.

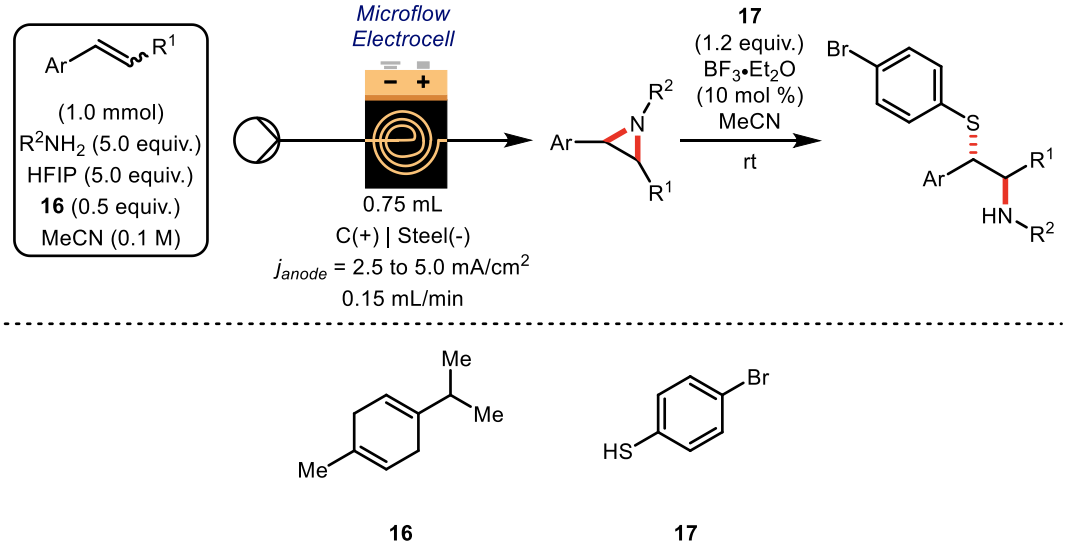

Scheme 1.10: Flow electrochemical alkene aziridination and subsequent derivatisation

The authors reported an extensive substrate scope, with 28 examples demonstrated. A wide selection of primary alkyl amines was tolerated, including the ethyl ester of glycine and the methyl ester of L-phenylalanine. Only alkenes with electron-neutral or electron-rich substituents were tolerated, with electron-poor alkenes likely having too high an oxidation potential to make the initial oxidation favourable. The process was also scaled up 10-fold with no difference in the yield of product obtained and the only change required being the increase in overall reaction time as more solution was passed through the microflow electrocell.

After mechanistic studies that included the use of CV, computational studies, and mechanistic experiments, the following mechanism was proposed for the transformation (Scheme 1.11).

The reaction begins with single electron oxidation of the alkene at the anode to form a radical cation. Reaction with the primary amine quenches the cation to give an alkyl radical intermediate. A second single electron oxidation at the anode and cyclisation furnishes the desired aziridine product. The counter reaction at the cathode is proton reduction to release hydrogen gas.

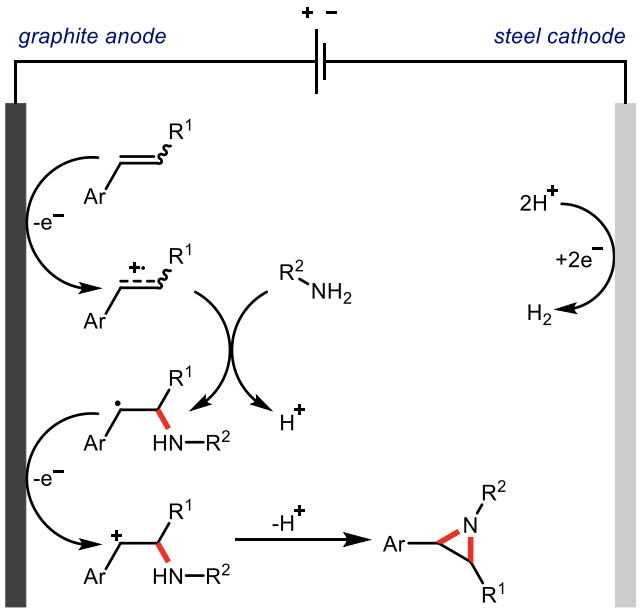

Scheme 1.11: Proposed mechanism for the electrochemical alkene aziridination in flow

Previous methods for synthesising aziridines electrochemically have required the use of pre-functionalised amines such as amino-phthalimides or sulfamates,[114–116] so being able to utilise primary alkyl amines, that need no deprotection and can still be further functionalised, is a vast improvement on those methods.

1.3 Summary and Outlook

To summarise, in recent years electrochemistry has re-emerged as a powerful technique to facilitate organic transformations, whilst offering advantages compared to traditional methods. An inherently green technology, electrochemistry allows the direct use of electricity to oxidise or reduce organic compounds without the requirement for chemical oxidants or reductants that may be of high molecular weight and/or have a high toxicity. As the applied potential can be tuned by the user, specific single electron processes can be targeted, leading to highly chemoselective transformations which in some cases offer higher functional group tolerance compared to processes that require chemical oxidants.

Further exploration into the combination of electrochemistry with other enabling technologies will further the interest in the field, with photoelectrochemistry allowing access to highly oxidising or highly reducing species and flow electrochemistry allowing the facile scale-up of electrochemical reactions.

One reason for the increased interest in electrochemical methodologies for organic synthesis has been the development of commercially available reactors, lowering the barrier for entry into the field for the traditional synthetic chemist. For instance, all the

batch electrochemical reactions disclosed in this thesis have been performed on one of these reactors, the ElectraSyn 2.0.

1.4 Aims and Objectives

The aims of this PhD were to investigate and develop new electrochemical methodologies in organic synthesis, with the objectives of developing sustainable and selective methodologies for performing important organic transformations. This was initially to be achieved by investigating the electrochemical generation and utilisation of alkoxy radicals, privileged motifs that allow access to a range of products through *β*-scission, hydrogen atom transfer (HAT) chemistry, or addition to *π*-systems (Chapters 2 and 3). Following the conclusion of these investigations, attention was then turned to the development of electrochemical alkene difunctionalisations (Chapter 4).

1.5 References

1 C. O. Oriakhi, in *Chemistry in Quantitative Language*, Oxford University Press, 2009.

2 A. G. A. Volta, *J. Nat. Philos. Chem. Arts*, 1800, **4**, 179–187.

3 M. Faraday, *Ann. Phys. Leipzeg*, 1834, **47**, 438.

4 H. Lund, *J. Electrochem. Soc.*, 2002, **149**, S21–S33.

5 M. Yan, Y. Kawamata and P. S. Baran, *Chem. Rev.*, 2017, **117**, 13230–13319.

6 H. Kolbe, *J. Prakt. Chem.*, 1847, **41**, 138.

7 A. Hickling, *Trans. Faraday Soc.*, 1942, **38**, 27–33.

8 J. Heyrevský, *Chem. List.*, 1922, **16**, 256–264.

9 J. Heyrovský, *Philos. Mag.*, 1923, **45**, 303–315.

10 J. E. B. Randles, *Trans. Faraday Soc.*, 1948, **44**, 327–338.

11 M. M. Baizer, *CHEMTECH*, 1980, **10**, 161.

12 T. Fuchigami, S. Inagi and M. Atobe, *Fundamentals and applications of organic electrochemistry: Synthesis, materials, devices*, 2014.

13 D. S. P. Cardoso, B. Šljukić, D. M. F. Santos and C. A. C. Sequeira, *Org. Process Res. Dev.*, 2017, **21**, 1213–1226.

14 T. Shono, H. Hamaguchi and Y. Matsumura, *J. Am. Chem. Soc.*, 1975, **97**, 4264–4268.

15 T. Shono, *Tetrahedron*, 1984, **40**, 811–850.

16 J. I. Yoshida, S. Suga, S. Suzuki, N. Kinomura, A. Yamamoto and K. Fujiwara, *J. Am. Chem. Soc.*, 1999, **121**, 9546–9549.

17 J. I. Yoshida and S. Suga, *Chem. - Eur. J.*, 2002, **8**, 2650–2658.

18 A. Wiebe, T. Gieshoff, S. Möhle, E. Rodrigo, M. Zirbes and S. R. Waldvogel, *Angew. Chem., Int. Ed.*, 2018, **57**, 5594–5619.

19 E. J. Horn, B. R. Rosen and P. S. Baran, *ACS Cent. Sci.*, 2016, **2**, 302–308.

20 S. B. Beil, D. Pollok and S. R. Waldvogel, *Angew. Chem., Int. Ed.*, 2021, 60, 14750–14759.

21 M. Yan, Y. Kawamata and P. S. Baran, *Angew. Chem., Int. Ed.*, 2018, **57**, 4149–4155.

22 C. Gütz, B. Klöckner and S. R. Waldvogel, *Org. Process Res. Dev.*, 2016, **20**, 26–32.

23 ElectraSyn 2.0 Package, https://www.ika.com/en/Products-Lab-Eq/Electrochemistry-Kit-csp-516/ElectraSyn-20-Package-cpdt-20008980/, (accessed 3 July 2022).

24 IKA Screening System Electrochemistry, https://www.ika.com/en/Products-Lab-Eq/Screening-System-csp-913/, (accessed 3 July 2022).

25 C. Kingston, M. D. Palkowitz, Y. Takahira, J. C. Vantourout, B. K. Peters, Y. Kawamata and P. S. Baran, *Acc. Chem. Res.*, 2020, **53**, 72–83.

26 Y. Kawamata, K. Hayashi, E. Carlson, S. Shaji, D. Waldmann, B. J. Simmons, J. T. Edwards, C. W. Zapf, M. Saito and P. S. Baran, *J. Am. Chem. Soc.*, 2021, **143**,

16580–16588.

27 S. Rodrigo, D. Gunasekera, J. P. Mahajan and L. Luo, *Curr. Opin. Electrochem.*, 2021, **28**, 100712.

28 L. E. Sattler, C. J. Otten and G. Hilt, *Chem. - Eur. J.*, 2020, **26**, 3129–3136.

29 E. O. Bortnikov and S. N. Semenov, *J. Org. Chem.*, 2021, **86**, 782–793.

30 S. Rodrigo, C. Um, J. C. Mixdorf, D. Gunasekera, H. M. Nguyen and L. Luo, *Org. Lett.*, 2020, **22**, 6719–6723.

31 C. Schotten, C. J. Taylor, R. A. Bourne, T. W. Chamberlain, B. N. Nguyen, N. Kapur and C. E. Willans, *React. Chem. Eng.*, 2021, **6**, 147–151.

32 B. Lee, H. Naito, M. Nagao and T. Hibino, *Angew. Chem., Int. Ed.*, 2012, **51**, 6961–6965.

33 M. Klein and S. R. Waldvogel, *Angew. Chem., Int. Ed.*, 2022, DOI: 10.1002/anie.202204140.

34 Y. A. Lyon, A. A. Roberts and D. R. McMillin, *J. Chem. Educ.*, 2015, **92**, 2130–2133.

35 J. E. Nutting, J. B. Gerken, A. G. Stamoulis, D. L. Bruns and S. S. Stahl, *J. Org. Chem.*, 2021, **86**, 15875–15885.

36 J. Chaussard, J. C. Folest, J. Y. Nedelec, J. Perichon, S. Sibille and M. Treupel, *Synthesis*, 1990, **5**, 369–381.

37 D. M. Heard and A. J. J. Lennox, *Angew. Chem., Int. Ed.*, 2020, **59**, 18866–18884.

38 H. B. Zhao, Z. W. Hou, Z. J. Liu, Z. F. Zhou, J. Song and H. C. Xu, *Angew. Chem., Int. Ed.*, 2017, **56**, 587–590.

39 A. M. Couper, D. Pletcher and F. C. Walsh, *Chem. Rev.*, 1990, **90**, 837–865.

40 J. M. Friedrich, C. Ponce-de-León, G. W. Reade and F. C. Walsh, *J. Electroanal. Chem.*, 2004, **561**, 203–217.

41 T. X. Huong Le, M. Bechelany and M. Cretin, *Carbon N. Y.*, 2017, **122**, 564–591.

42 L. Schulz and S. R. Waldvogel, *Synlett*, 2019, **30**, 275–285.

43 G. Hilt, *ChemElectroChem*, 2020, **7**, 395–405.

44 T. Shono, in *Comprehensive Organic Synthesis*, Elsevier, 1991, pp. 789–813.

45 M. Rafiee, M. N. Mayer, B. T. Punchihewa and M. R. Mumau, *J. Org. Chem.*, 2021, **86**, 15866–15874.

46 R. Francke and R. D. Little, *Chem. Soc. Rev.*, 2014, **43**, 2492–2521.

47 E. Steckhan, *Angew. Chem., Int. Ed.*, 1986, **25**, 683–701.

48 T. Fuchigami, M. Tetsu, T. Tajima and H. Ishii, *Synlett*, 2001, 1269–1271.

49 C. Y. Cai, X. M. Shu and H. C. Xu, *Nat. Commun.*, 2019, **10**, 4953.

50 S. Liu and M. Klussmann, *Org. Chem. Front.*, 2021, **8**, 2932–2938.

51 M. D. Hareram, A. A. M. A. El Gehani, J. Harnedy, A. C. Seastram, A. C. Jones, M. Burns, T. Wirth, D. L. Browne and L. C. Morrill, *Org. Lett.*, 2022, **24**, 3890–3895.

52 Y. Shen, K. Suzuki, M. Atobe and T. Fuchigami, *J. Electroanal. Chem.*, 2003, **540**, 189–194.

53 S. P. Young, S. C. Wang, D. J. Tantillo and R. D. Little, *J. Org. Chem.*, 2007, **72**,

4351–4357.

54 X. Wu, A. P. Davis and A. J. Fry, *Org. Lett.*, 2007, **9**, 5632–5636.

55 S. P. Young and R. D. Little, *J. Org. Chem.*, 2008, **73**, 6807–6815.

56 Y. S. Park and R. D. Little, *Electrochim. Acta*, 2009, **54**, 5077–5082.

57 X. Wu, A. P. Davis, P. C. Lambert, L. Kraig Steffen, O. Toy and A. J. Fry, *Tetrahedron*, 2009, **65**, 2408–2414.

58 L. J. Li, Y. Y. Jiang, C. M. Lam, C. C. Zeng, L. M. Hu and R. D. Little, *J. Org. Chem.*, 2015, **80**, 11021–11030.

59 C. Y. Cai and H. C. Xu, *Nat. Commun.*, 2018, **9**, 3551.

60 C. C. Zeng, N. T. Zhang, C. M. Lam and R. D. Little, *Org. Lett.*, 2012, **14**, 1314–1317.

61 N. T. Zhang, C. C. Zeng, C. M. Lam, R. K. Gbur and R. D. Little, *J. Org. Chem.*, 2013, **78**, 2104–2110.

62 N. N. Lu, S. J. Yoo, L. J. Li, C. C. Zeng and R. D. Little, *Electrochim. Acta*, 2014, **142**, 254–260.

63 N. N. Lu, N. T. Zhang, C. C. Zeng, L. M. Hu, S. J. Yoo and R. D. Little, *J. Org. Chem.*, 2015, **80**, 781–789.

64 K. Y. Zhang, N. N. Lu, S. J. Yoo, L. M. Hu, R. D. Little and C. C. Zeng, *Electrochim. Acta*, 2016, **199**, 357–365.

65 N. Fu, G. S. Sauer, A. Saha, A. Loo and S. Lin, *Science*, 2017, **357**, 575–579.

66 N. Fu, G. S. Sauer and S. Lin, *J. Am. Chem. Soc.*, 2017, **139**, 15548–15553.

67 L. Niu, C. Jiang, Y. Liang, D. Liu, F. Bu, R. Shi, H. Chen, A. D. Chowdhury and A. Lei, *J. Am. Chem. Soc.*, 2020, **142**, 17693–17702.

68 K. Y. Ye, G. Pombar, N. Fu, G. S. Sauer, I. Keresztes and S. Lin, *J. Am. Chem. Soc.*, 2018, **140**, 2438–2441.

69 K. Y. Ye, Z. Song, G. S. Sauer, J. H. Harenberg, N. Fu and S. Lin, *Chem. - Eur. J.*, 2018, **24**, 12274–12279.

70 N. Fu, Y. Shen, A. R. Allen, L. Song, A. Ozaki and S. Lin, *ACS Catal.*, 2019, **9**, 746–754.

71 L. Lu, N. Fu and S. Lin, *Synlett*, 2019, **30**, 1199–1203.

72 Z. Zhang, L. Zhang, Y. Cao, F. Li, G. Bai, G. Liu, Y. Yang and F. Mo, *Org. Lett.*, 2019, **21**, 762–766.

73 S. Tian, X. Jia, L. Wang, B. Li, S. Liu, L. Ma, W. Gao, Y. Wei and J. Chen, *Chem. Commun.*, 2019, **55**, 12104–12107.

74 J. Lai and M. A. Pericàs, *Org. Lett.*, 2020, **22**, 7338–7342.

75 T. H. Meyer, R. C. Samanta, A. Del Vecchio and L. Ackermann, *Chem. Sci.*, 2021, **12**, 2890–2897.

76 M. Durandetti, J. Y. Nédélec and J. Périchon, *J. Org. Chem.*, 1996, **61**, 1748–1755.

77 S. Condon, D. Dupré, G. Falgayrac and J. Y. Nédélec, *Eur. J. Org. Chem.*, 2002, 105–111.

78 B. L. Truesdell, T. B. Hamby and C. S. Sevov, *J. Am. Chem. Soc.*, 2020, **142**, 5884–5893.

79 H. J. Zhang, L. Chen, M. S. Oderinde, J. T. Edwards, Y. Kawamata and P. S. Baran, *Angew. Chem., Int. Ed.*, 2021, **60**, 20700–20705.

80 Z.-H. Wang, L. Wei, K.-J. Jiao, C. Ma and T.-S. Mei, *Chem. Commun.*, 2022, DOI: 10.1039/D2CC02641D.

81 J. A. Miranda, C. J. Wade and R. D. Little, *J. Org. Chem.*, 2005, **70**, 8017–8026.

82 D. Mikhaylov, T. Gryaznova, Y. Dudkina, M. Khrizanphorov, S. Latypov, O. Kataeva, D. A. Vicic, O. G. Sinyashin and Y. Budnikova, *Dalt. Trans.*, 2012, **41**, 165–172.

83 C. Li, Y. Kawamata, H. Nakamura, J. C. Vantourout, Z. Liu, Q. Hou, D. Bao, J. T. Starr, J. Chen, M. Yan and P. S. Baran, *Angew. Chem., Int. Ed.*, 2017, **56**, 13088–13093.

84 S. Sengmany, A. Ollivier, E. Le Gall and E. Léonel, *Org. Biomol. Chem.*, 2018, **16**, 4495–4500.

85 Y. Kawamata, J. C. Vantourout, D. P. Hickey, P. Bai, L. Chen, Q. Hou, W. Qiao, K. Barman, M. A. Edwards, A. F. Garrido-Castro, J. N. Degruyter, H. Nakamura, K. Knouse, C. Qin, K. J. Clay, D. Bao, C. Li, J. T. Starr, C. Garcia-Irizarry, N. Sach, H. S. White, M. Neurock, S. D. Minteer and P. S. Baran, *J. Am. Chem. Soc.*, 2019, **141**, 6392–6402.

86 R. J. Perkins, A. J. Hughes, D. J. Weix and E. C. Hansen, *Org. Process Res. Dev.*, 2019, **23**, 1746–1751.

87 D. Liu, H. X. Ma, P. Fang and T. S. Mei, *Angew. Chem., Int. Ed.*, 2019, **58**, 5033–5037.

88 Y. Mo, Z. Lu, G. Rughoobur, P. Patil, N. Gershenfeld, A. I. Akinwande, S. L. Buchwald and K. F. Jensen, *Science*, 2020, **368**, 1352–1357.

89 N. Chen and H. C. Xu, *Chem. Rec.*, 2021, **21**, 2306–2319.

90 C. A. Malapit, M. B. Prater, J. R. Cabrera-Pardo, M. Li, T. D. Pham, T. P. McFadden, S. Blank and S. D. Minteer, *Chem. Rev.*, 2022, **122**, 3180–3218.

91 N. Elgrishi, K. J. Rountree, B. D. McCarthy, E. S. Rountree, T. T. Eisenhart and J. L. Dempsey, *J. Chem. Educ.*, 2018, **95**, 197–206.

92 C. Sandford, M. A. Edwards, K. J. Klunder, D. P. Hickey, M. Li, K. Barman, M. S. Sigman, H. S. White and S. D. Minteer, *Chem. Sci.*, 2019, **10**, 6404–6422.

93 R. R. Gagne, C. A. Koval and G. C. Lisensky, *Inorg. Chem.*, 1980, **19**, 2854–2855.

94 S. Trasa'tti, *Pure Appl. Chem.*, 1986, **58**, 955–966.

95 G. Burgbacher and H. J. Schäfer, *J. Am. Chem. Soc.*, 1979, **101**, 7590–7593.

96 L. J. Johnston and N. P. Schepp, *J. Am. Chem. Soc.*, 1993, **115**, 6564–6571.

97 Y. Imada, Y. Okada, K. Noguchi and K. Chiba, *Angew. Chem., Int. Ed.*, 2019, **58**, 125–129.

98 B. K. Peters, K. X. Rodriguez, S. H. Reisberg, S. B. Beil, D. P. Hickey, Y. Kawamata, M. Collins, J. Starr, L. Chen, S. Udyavara, K. Klunder, T. J. Gorey, S. L. Anderson, M. Neurock, S. D. Minteer and P. S. Baran, *Science*, 2019, **363**, 838–845.

99 A. J. Birch, *Nature*, 1946, **158**, 60.

100 R. A. Benkeser and E. M. Kaiser, *J. Am. Chem. Soc.*, 1963, **85**, 2858–2859.

101 K. E. Swenson, D. Zemach, C. Nanjundiah and E. Kariv-Miller, *J. Org. Chem.*, 1983, **48**, 1777–1779.

102 E. Kariv-Miller, K. E. Swenson and D. Zemach, *J. Org. Chem.*, 1983, **48**, 4210–4214.

103 M. Ishifune, H. Yamashita, Y. Kera, N. Yamashita, K. Hirata, H. Murase and S. Kashimura, *Electrochim. Acta*, 2003, **48**, 2405–2409.

104 T. Wu and K. D. Moeller, *Angew. Chem., Int. Ed.*, 2021, **60**, 12883–12890.

105 H. Li, C. P. Breen, H. Seo, T. F. Jamison, Y. Q. Fang and M. M. Bio, *Org. Lett.*, 2018, **20**, 1338–1341.

106 T. Koyanagi, A. Herath, A. Chong, M. Ratnikov, A. Valiere, J. Chang, V. Molteni and J. Loren, *Org. Lett.*, 2019, **21**, 816–820.

107 J. P. Barham and B. König, *Angew. Chem., Int. Ed.*, 2020, **59**, 11732–11747.

108 H. Kim, H. Kim, T. H. Lambert and S. Lin, *J. Am. Chem. Soc.*, 2020, **142**, 2087–2092.

109 M. B. Plutschack, B. Pieber, K. Gilmore and P. H. Seeberger, *Chem. Rev.*, 2017, **117**, 11796–11893.

110 R. A. Green, R. C. D. Brown, D. Pletcher and B. Harji, *Org. Process Res. Dev.*, 2015, **19**, 1424–1427.

111 D. Pletcher, R. A. Green and R. C. D. Brown, *Chem. Rev.*, 2018, **118**, 4573–4591.

112 G. Laudadio, W. de Smet, L. Struik, Y. Cao and T. Noël, *J. Flow Chem.*, 2018, **8**, 157–165.

113 M. Ošeka, G. Laudadio, N. P. van Leest, M. Dyga, A. de A. Bartolomeu, L. J. Gooßen, B. de Bruin, K. T. de Oliveira and T. Noël, *Chem*, 2021, **7**, 255–266.

114 T. Siu and A. K. Yudin, *J. Am. Chem. Soc.*, 2002, **124**, 530–531.

115 J. Chen, W. Q. Yan, C. M. Lam, C. C. Zeng, L. M. Hu and R. D. Little, *Org. Lett.*, 2015, **17**, 986–989.

116 J. Li, W. Huang, J. Chen, L. He, X. Cheng and G. Li, *Angew. Chem., Int. Ed.*, 2018, **57**, 5695–5698.

Chapter 2: Manganese-Catalysed Electrochemical Deconstructive Chlorination of Cycloalkanols *via* Alkoxy Radicals

Table of Contents

2 Preface

This chapter discusses the development of a manganese-catalysed electrochemical deconstructive chlorination of cycloalkanols to furnish synthetically useful distally chlorinated ketones *via* alkoxy radicals. This methodology utilises an inexpensive manganese (II) pre-catalyst to synthesise a diverse range of *β*- and *γ*-chloroketones from cyclobutanols and cyclopropanols respectively in good yields (40 examples, 30-90% yield). A recirculating flow-electrochemistry system was employed to allow access to 1.20 g of product without a need for further purification. Mechanistic investigations were performed, including the use of cyclic voltammetry to propose the formation of an alkoxy radical intermediate.

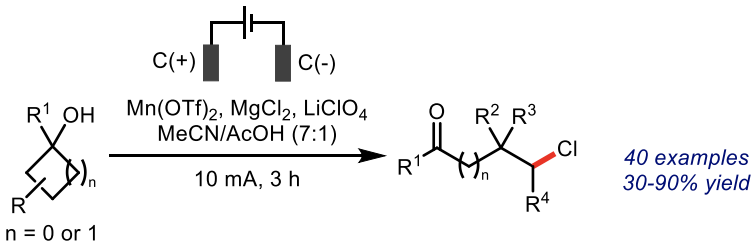

Publication: B. D. W. Allen, M. D. Hareram, A. C. Seastram, T. McBride, T. Wirth, D. L. Browne and L. C. Morrill, *Org. Lett.*, 2019, **21**, 9241–9246.

Acknowledgements

Benjamin D. W. Allen – PDRA responsible for reaction discovery, optimisation, and part of the substrate synthesis and substrate scope.

Mishra Deepak Hareram – PhD student responsible for part of the substrate synthesis and substrate scope.

Alex C. Seastram – Responsible for part of the substrate synthesis and part of the substrate scope. Responsible for the mechanistic studies.

Tom McBride – PhD student responsible for the flow electrochemistry.

Thomas Wirth – Co-supervisor of B. D. W. Allen, Cardiff University.

Duncan L. Browne – Supervisor of T. McBride and co-supervisor of B. D. W. Allen, UCL.

Louis C. Morrill – Supervisor, Cardiff University.

2.1 Introduction

2.1.1 Alkoxy Radicals

2.1.1.1 Reactivity Modes

Alkoxy radicals are highly transient, oxygen-centred radicals that exhibit a rich and diverse reactivity.[1,2] Reactivity modes that can be accessed by alkoxy radicals include hydrogen atom transfers (HAT),[3,4] addition to *π*-systems,[5,6] and *β*-scission processes (Figure 2.1).[7–9]

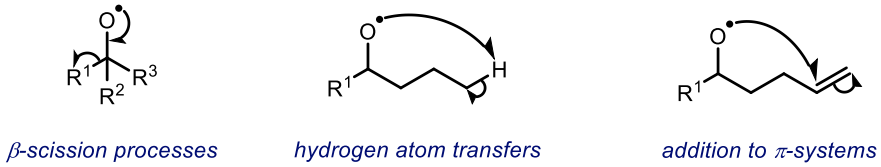

Figure 2.1: Reactivity modes of alkoxy radicals

HAT processes can allow for the formation of alkyl radicals from alkoxy radicals through both intra- and intermolecular processes. HATs of this type are favourable due to the difference in bond dissociation energy (BDE) between an RO-H bond vs. a C(sp^3)-H bond (~105 kcal/mol vs. ~98 kcal/mol).[10] This favourability allows for the selective activation of previously unreactive C-H bonds. The resulting alkyl radical can then be functionalised either from the radical directly,[11–16] or through an EC (electrochemical-chemical) type mechanism;[17] whereby the radical is oxidised/reduced, and the resulting ion is quenched in a polar fashion. The addition of alkoxy radicals to *π*-systems can lead to the formation of tetrahydrofurans or other *O*-heterocycles through intramolecular processes,[17–20] or the formation of ethers *via* intermolecular additions.[21–23] *β*-Scission processes of acyclic alcohols allow for the formation of new carbonyls along with new radical intermediates;[24,25] however, when cyclic alcohols are employed the carbonyl formed can be distally functionalised through a deconstructive functionalisation strategy.[9,26–31]

These privileged intermediates have been successfully employed in a range of transformations such as C-H functionalisation, C-C bond activation, and in the synthesis of heterocycles to access a wide range of products over the last 60 years, and have even been employed for the synthesis of biologically active compounds.[32–35]

2.1.1.2 Generation Methods

The generation of alkoxy radicals directly from aliphatic alcohols is challenging, and this is partly due to the high BDE of RO-H bonds (~105 kcal/mol).[10] As a result, traditional

methods of alkoxy radical generation involve the pre-functionalisation of alcohols followed by the homolysis of weak RO-X bonds, using radical initiators and/or thermal or UV photochemical activation (Scheme 2.1, top left),[18,36,37] the requirement of which can limit functional group tolerance.

More recently, methodologies have been developed to generate alkoxy radicals using transition metals in combination with stoichiometric oxidants (Scheme 2.1, top right).[38,39] These methods typically require the *in situ* formation of a metal-alkoxide complex followed by homolysis of the M-OR bond. The requirement for a stoichiometric quantity of chemical oxidant also reduces the functional group compatibility of this methodology, as with traditional approaches, and leads to the formation of stoichiometric waste that must be separated from the desired product.

Photocatalysis has been employed as a milder method for generating alkoxy radicals from a variety of radical precursors (Scheme 2.1, bottom left).[2,40,41] The ability to use visible light irradiation in place of UV irradiation or stoichiometric oxidants improves the utility of these methodologies, with improved functional group tolerances. Radical precursors such as peroxides,[42] and *N*-alkoxyphthalimides have been employed,[11,12] and more recently photochemical methods have been developed to allow access to alkoxy radicals directly from aliphatic alcohols.[30,31,43,44]

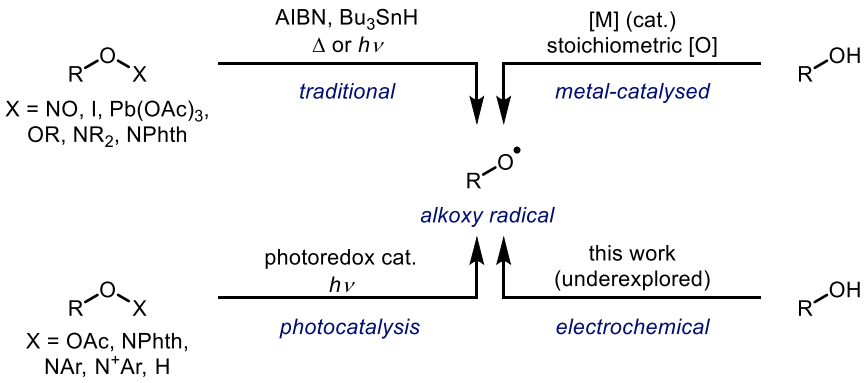

Scheme 2.1: Alkoxy radical generation methods

Organic electrochemistry offers an alternative but attractive approach to the generation of alkoxy radicals, due to its inherent ability to oxidise compounds without the requirement for often high molecular weight chemical oxidants, improving the atom economy and potentially the functional group compatibility of alkoxy radical generating methodologies. Despite these and other previously discussed benefits (see chapter 1), the development

of alkoxy radical generation methodologies under electrochemical conditions has thus far received little attention (Scheme 2.1, bottom right).[45–50]

2.1.1.3 Electrochemical Generation

In 1981, Swenton and co-workers reported an anodic dearomative dimethoxylation of methoxylated naphthalenes (Scheme 2.2a).[45]

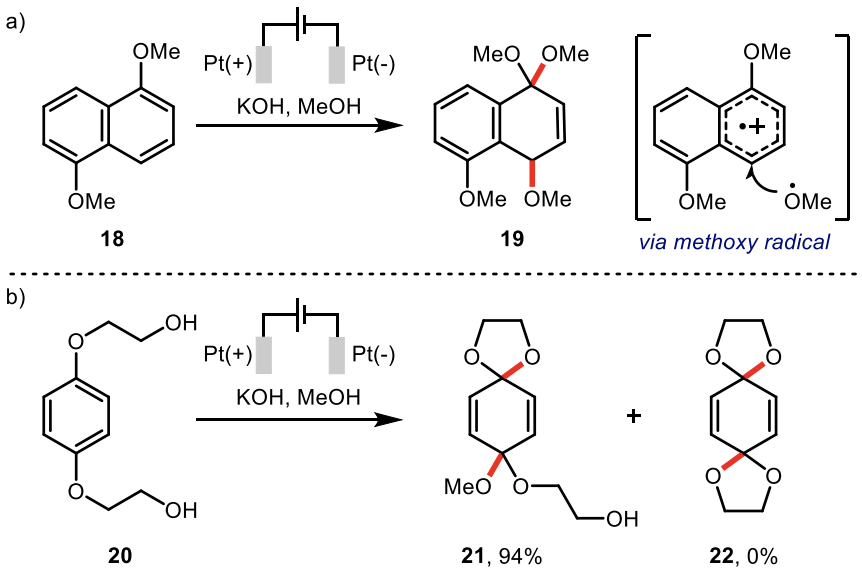

Scheme 2.2: a) Electrochemical dearomative dimethoxylation of methoxylated naphthalenes; b) Experimental evidence supporting methoxy radical formation

In this work, electron-rich aromatic systems such as dimethoxynaphthalene **18** are dearomatised with concurrent dimethoxylation to form products such as **19**, using a 1% methanolic solution of KOH under anodic conditions using platinum electrodes (Scheme 2.2a). The authors proposed two plausible mechanisms, firstly an ECEC type mechanism, whereby the aromatic system is oxidised to form a radical cation. This radical cation then reacts with a methoxide anion, before undergoing another oxidation to an aryl cation that is quenched with another equivalent of methoxide. The alternative proposal is an EEC_rC_p type mechanism, where methoxide is oxidised at the anode to form a methoxy radical which then reacts with the electrochemically generated aryl radical cation. This forms an aryl cation that is subsequently quenched by a methoxide anion.

In an attempt to distinguish between the two mechanisms, hydroquinone derived **20** was subjected to the reaction conditions (Scheme 2.2b). In the case of an ECEC type mechanism, diketal **22** was expected to be the observed product, due to the preference of the aryl radical cation to react intramolecularly with the tethered alcohol over an

intermolecular reaction with the methanol solvent. As diketal **21** was formed as the sole product, the authors concluded that this process goes through an EEC_rC_p mechanism. Despite these conclusions, the proposed EEC_rC_p mechanism can be disputed. Firstly, diketal **21** could still be the major product formed if an ECEC type mechanism is occurring, as the presence of methanol in solvent quantities decreases the favourability of intramolecular quenching of the aryl cation formed in the first step compared to quenching with the bulk solvent. Secondly, as no CV studies were performed, the proposal of concurrent oxidation of the electron-rich aromatic system and methoxide, as is required for a EEC_rC_p type mechanism, has no supporting evidence.

Following this, in 2012 Nishiyama and co-workers reported a similar dearomative dimethoxylation of electron-rich aromatic systems, this time using boron-doped diamond (BDD) as the anode material.[48] In this work, the authors provided more evidence for the formation of methoxy radicals *via* electron spin resonance (ESR) spectroscopy (Scheme 2.3).

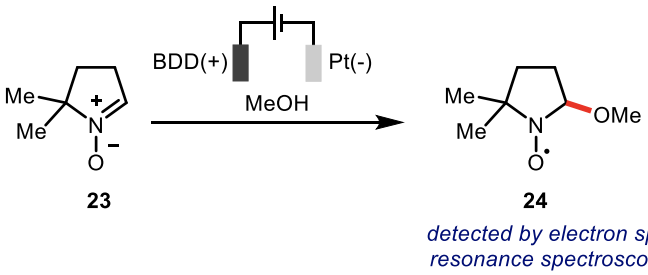

Scheme 2.3: Evidence for methoxy radical formation using ESR spectroscopy

When DMPO **23** was subjected to the reaction conditions as a radical trap, methoxy adduct **24** was detected by ESR spectroscopy,[51] supporting the generation of methoxy radicals under their conditions. Their studies by ESR also highlighted the requirement for expensive anode materials such as BDD or platinum, as due to the high oxidation potential of methoxide anions, their broad potential windows were essential for the generation of a sufficient concentration of methoxy radicals. This requirement inherently limits the wider application of this methodology to synthesis.

2.1.2 Deconstructive Functionalisation of Cycloalkanols

The *β*-scission of cyclic alkoxy radicals allows the furnishing of distally functionalised carbonyls *via* a transient alkyl radical intermediate and subsequent trapping of this radical with a SOMOphilic species. This process can be described as the deconstructive functionalisation of cycloalkanols (Scheme 2.4).[9]

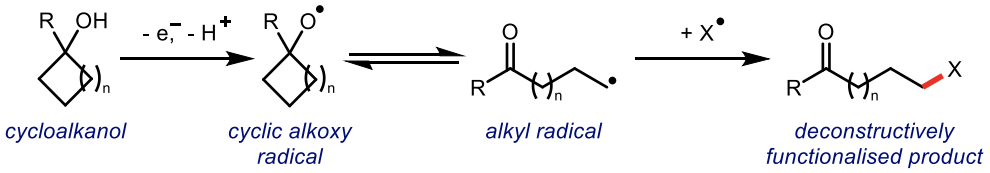

Scheme 2.4: Deconstructive functionalisation of cycloalkanols via β-scission of alkoxy radicals

In recent years, there have been many examples of such reactivity to form a range of distally functionalised ketones. Often, these processes require the use of a stoichiometric oxidant, either to mediate the process itself or to turn over the catalyst.

In 2015, Zhu and co-workers reported a manganese-catalysed deconstructive azidation of cyclobutanol (Scheme 2.5).[27]

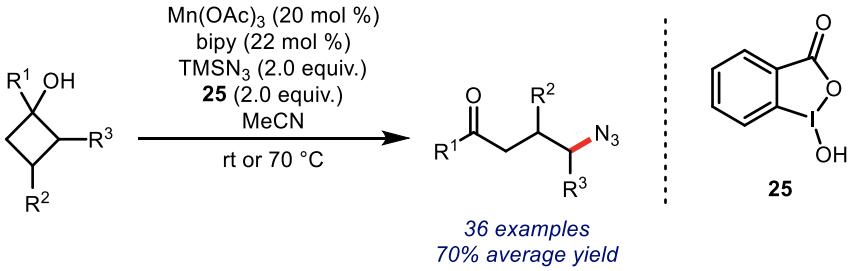

Scheme 2.5: Manganese-catalysed deconstructive azidation of cyclobutanols

This methodology utilises a manganese (III) catalyst in combination with $TMSN_3$ and hypervalent iodine reagent **25** to facilitate the formation of *γ*-azidoketones from cyclobutanols. This procedure exhibits a broad substrate scope, with 36 examples reported in an average isolated yield of 70%. Electron-rich and electron-poor (hetero)aromatic rings are tolerated in the 1-position, and additional substitution in the 2- and 3-positions of the cyclobutanol is also tolerated. However, this work does lack the demonstration of substrates containing functional groups sensitive to oxidations, such as such as primary or secondary alcohols, and only cyclobutanols were successfully ring opened. Within this manifold, **25** is required in a super-stoichiometric quantity to generate the manganese (V) species as per their proposed catalytic cycle.

In 2016, the Zhu group further expanded this reaction methodology to allow for the formation of new C-C bonds through the deconstructive cyanation and deconstructive alkynylation of cyclobutanols under their manganese catalysis manifold (Scheme 2.6).[52]

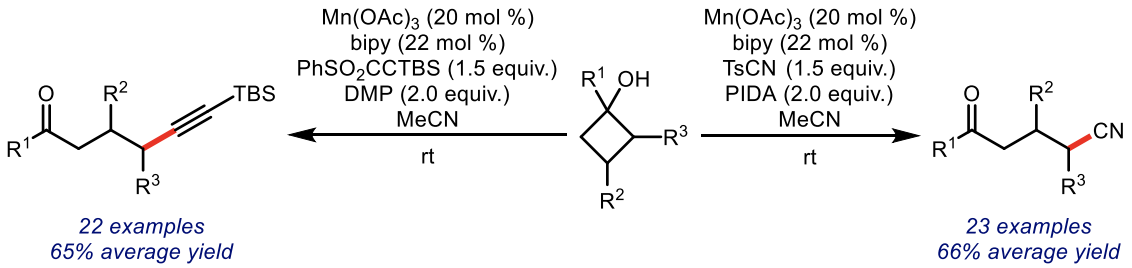

Scheme 2.6: Manganese-catalysed deconstructive cyanation and alkynylation of cyclobutanols

In this expansion of their previous methodology,[27] a range of cyclobutanols were successfully converted to *γ*-alkynyl and *γ*-cyanoketones. As in the previous work, a manganese (III) catalyst is utilised, in combination with either tosyl cyanide or TBS-protected phenylsulfonyl ethyne allowed conversion to the desired deconstructive functionalised products. The cyanation procedure included 23 examples with an average isolated yield of 66%, and the alkynylation procedure included 22 examples with an average isolated yield of 65%. Both procedures exhibit vast substrate scopes including substrates with electron-rich aryl, electron-poor aryl, heteroaryl, or alkyl substituents in the 1-position, and further substitution in the 2- and 3-positions of the cyclobutanol was also tolerated. As with the previous work, there is an absence of redox sensitive functional groups such as aldehydes or benzyl alcohols, and again only cyclobutanols could be ring opened.

Copper can also be used to initiate deconstructive functionalisations of cycloalkanols, as highlighted by Lopp and co-workers' report in 2015 of a copper-catalysed deconstructive trifluoromethylation of cyclopropanols (Scheme 2.7).[53]

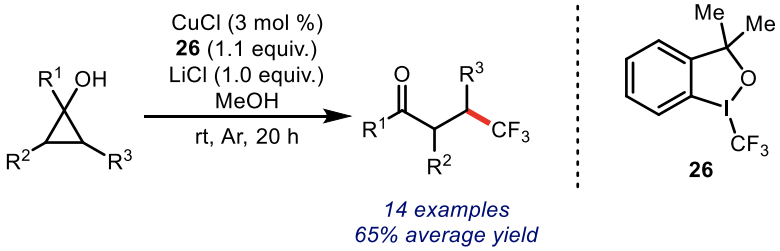

Scheme 2.7: Copper-catalysed deconstructive trifluoromethylation of cyclopropanols

This procedure utilises a copper (I) catalyst, in combination with LiCl and one of Togni's hypervalent iodine reagents,[54] **26**, to mediate the transformation and furnish *β*-trifluoromethylketones, with 14 examples reported in an average isolated yield of 65%. Hypervalent iodine reagent **26** serves a dual-purpose in the mechanism, acting both as the source of the trifluoromethyl group and as the oxidant required to access the active

copper (III) species. This methodology exhibits a moderately broad substrate scope, including substrates with alkyl, alkenyl, and aryl substituents in the 1-position, as well as further substitution in the 2- and 3-positions of the cyclopropanol. There is an absence of functional groups sensitive to oxidations, such as primary or secondary alcohols; however protected versions (e.g., silyl- and benzyl-protected alcohols) work under these conditions in good yields. This work is also limited to cyclopropanols, with no larger cycloalkanols reported within the scope. Also in 2015, the Xu group and Dai group reported similar procedures for copper-catalysed deconstructive trifluoromethylation of cyclopropanols.[55,56]

Deconstructive functionalisation processes have also been developed utilising photoredox catalysis. Pioneering work from Knowles and co-workers focused on the generation of alkoxy radicals using an iridium (III) photocatalyst under blue LED irradiation.[30] In the reaction, an intramolecular proton coupled electron transfer (PCET) process, occurs to access deconstructive hydrogenations of cycloalkanols (Scheme 2.8).

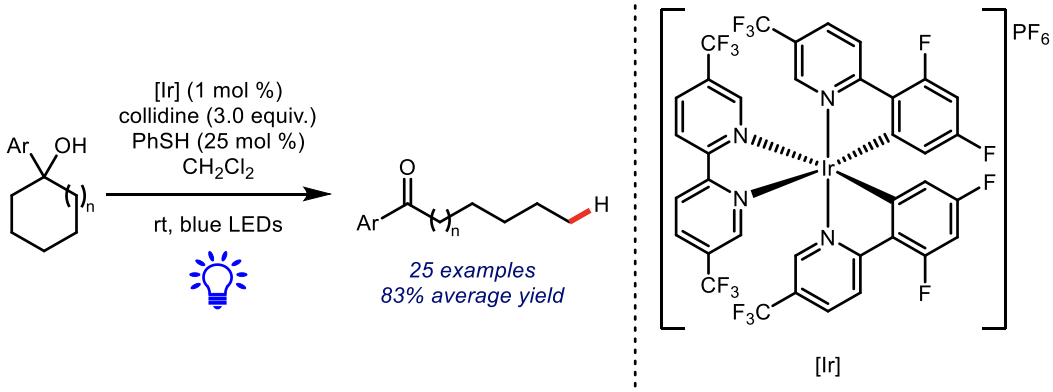

Scheme 2.8: Iridium photo-catalysed deconstructive hydrogenation of cycloalkanols

In this work, a range of electron-rich aromatic rings are oxidised to the corresponding aryl cations by the excited state of the iridium photocatalyst (Scheme 2.9).

Deprotonation of the alcohol by the collidine Brønsted base occurs with concomitant single electron reduction of the aryl cation to provide the alkoxy radical. Subsequent *β*-scission and intermolecular HAT then provides the deconstructive hydrogenated product.

This work has subsequently been expanded upon by Knowles and co-workers to perform ring expansion chemistry using a similar catalytic manifold,[57] and in 2020 Rueping and co-workers used an organic photocatalyst in tandem with nickel catalysis to access deconstructed arylation products *via* a PCET type mechanism.[31]

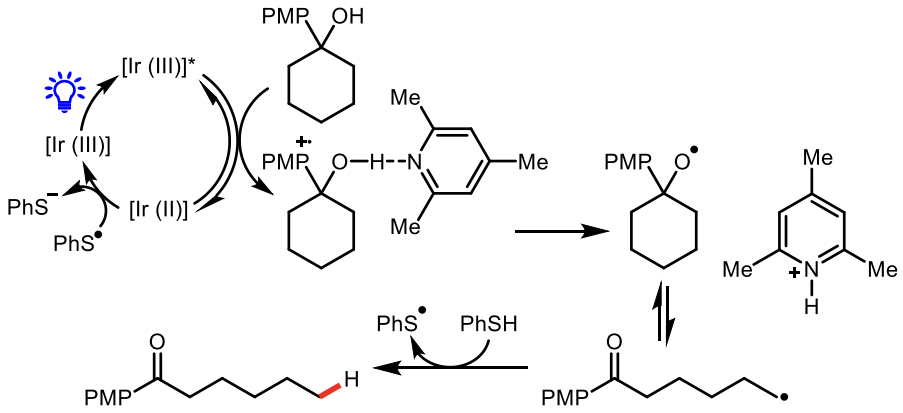

Scheme 2.9: Iridium photo-catalysed deconstructive hydrogenation of cycloalkanols mechanism

2.1.3 Deconstructive Chlorination of Cycloalkanols

Whilst there have been many reports of deconstructive functionalisation of cycloalkanols, there are few reports of deconstructive chlorination, giving access to synthetically useful distally chlorinated ketones.

In 2016, Zhu and co-workers reported a silver-catalysed deconstructive chlorination of cycloalkanols (Scheme 2.10).[58]

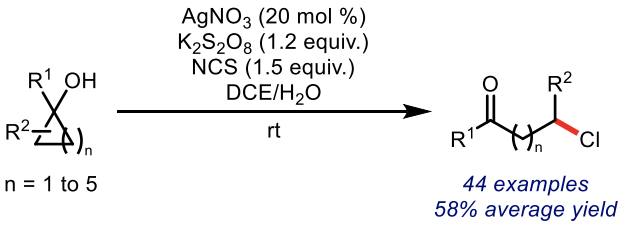

Scheme 2.10: Silver-catalysed deconstructive chlorination of cycloalkanols (Zhu)

In this procedure, cycloalkanols of various sizes (cyclopropanols to cycloheptanols) were successfully converted into the corresponding chloroketones using a silver (I) catalyst in combination with NCS as the chlorine source, and a stoichiometric quantity of potassium persulfate as the oxidant. Comprehensive substrate scopes are reported for the deconstructive chlorination of cyclopropanols and cyclobutanols into the corresponding *β*- and *γ*-chlorinated ketones, including the tolerance of electron-rich and electron-poor aryl substituents, as well as heteroaryl, alkyl, and alkenyl substituents in the 1-position. The substrate scopes reported for cyclopentanols, cyclohexanols, and cycloheptanols are more limited, with only halogens demonstrated to be tolerated on the aryl substituent in the 1-position. Overall, 44 examples are reported with an average isolated yield of 58%. This methodology was later expanded to the deconstructive bromination of cyclobutanols

using NBS in place of NCS, reporting 5 examples in 63% average isolated yield. This work shows no limitation in the ring size of the cycloalkanol being ring opened (in contrast to Zhu's previous work discussed in section 2.1.2),[27,52] as well as exhibiting a much broader substrate scope. However, drawbacks include the use of a stoichiometric quantity of potassium persulfate as the oxidant required for the process, as well as a lack of redox-active substituents demonstrated, including aldehydes and benzyl alcohols.

Concurrent with the above studies, Zhang and co-workers developed an alternative procedure for the silver-catalysed deconstructive chlorination of cycloalkanols (Scheme 2.11).[29]

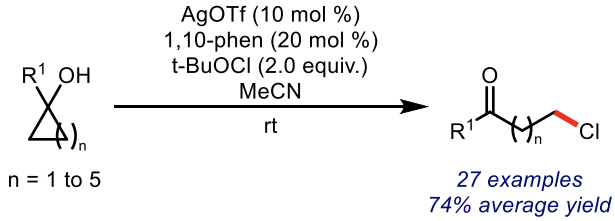

Scheme 2.11: Silver-catalysed deconstructive chlorination of cycloalkanols (Zhang)

As with the work of Zhu and co-workers, this methodology utilises a silver (I) catalyst to convert cycloalkanols, ranging from cyclopropanols to cycloheptanols, into the corresponding chloro-substituted ketones. In this work, silver triflate was used as the catalyst, along with 1,10-phenanthroline as a ligand, and a super-stoichiometric quantity of *tert*-butyl hypochlorite as both the oxidant and chlorine source. Overall, 27 examples are reported with an average isolated yield of 74%, primarily from the ring opening of cyclobutanols. In the 1-position, electron-poor aryl substituents, extended π-systems, and halo-substituted aryl substituents are all tolerated well; however, there are no examples where electron-rich aromatics or redox sensitive functional groups are present.

Later in the same year, Zhu and co-workers further developed their previously reported manganese-catalysed deconstructive functionalisation of cyclobutanols methodology to allow for deconstructive chlorination (Scheme 2.12).[59]

In this work, a manganese (II) catalyst was used in combination with TMS chloride as the chlorine source and hypervalent iodine reagent IBX as the super-stoichiometric oxidant to allow access to *γ*-chloroketones from cyclobutanols. This work exhibits a broad substrate scope, with 32 examples reported in a 76% average isolated yield. The scope shows tolerance of both electron-rich and electron-poor aryl substituents, including heteroaryl substituents in the 1-position. Further substitution in the 2- and 3-positions of

the cyclobutanol are also tolerated, and this reaction can be used to access ring expanded products. As with the previous work, there is also an absence of redox-sensitive functional groups being tolerated under these conditions. Although this work expands on the previous reports by the author so that deconstructive chlorination is now tolerated, this work reports no examples using larger rings, as was possible when a silver (I) salt was used.[58]

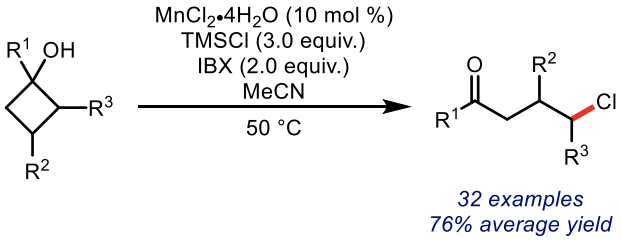

Scheme 2.12: Manganese-catalysed deconstructive chlorination of cyclobutanols

2.1.4 Electrochemical Manganese Catalysis

There is a growing focus on the use of metal catalysts as redox mediators for electrochemically mediated organic transformations,[60] and one metal that has received considerable interest is manganese.

In 2017, Lin and co-workers reported an electrochemical manganese-catalysed dichlorination of alkenes (Scheme 2.13).[61]

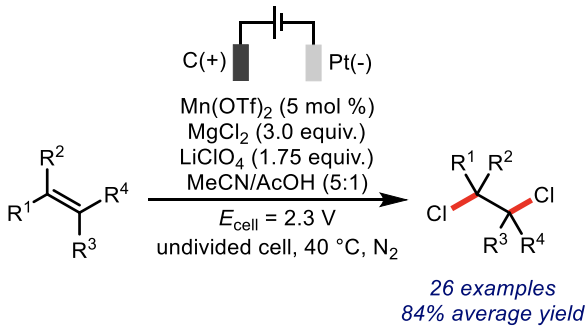

Scheme 2.13: Electrochemical manganese-catalysed alkene dichlorination

This methodology utilises a manganese (II) catalyst in combination with magnesium chloride to afford 1,2-dichloroalkanes from alkenes through potentiostatic electrolysis with a graphite anode and platinum cathode. This reaction exhibits an expansive substrate scope, with 26 reported examples in an average isolated yield of 84%. The scope includes reactions on monosubstituted acyclic alkenes, for example styrene and its

derivatives, with electron-donating and electron-withdrawing substituents on the phenyl ring both tolerated. Alkenes with 1,1-, 1,2-, and tri-substitution were successfully converted to the 1,2-dichloroalkanes also. Redox sensitive functional groups were tolerated within substrates, including alcohols, aldehydes, carboxylic acids, amines, sulfides, and aromatic *N*-heterocycles, highlighting the chemoselectivity that can be obtained under electrochemical conditions.

Following mechanistic investigations, including CV studies, the authors proposed the following reaction mechanism (Scheme 2.14).

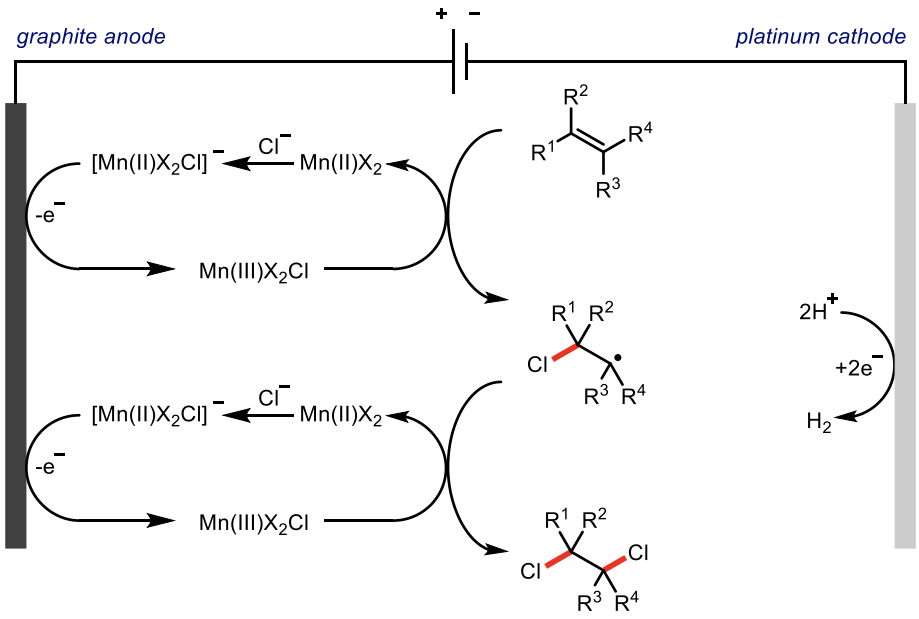

Scheme 2.14: Proposed mechanism of the electrochemical manganese-catalysed alkene dichlorination

The reaction initiates with the formation of an anionic manganese (II) chloride species that is first oxidised at the anode to the corresponding manganese (III) chloride, removing the requirement for a super-stoichiometric quantity of a chemical oxidant in this reaction manifold. This manganese (III) complex acts as a chlorine transfer reagent to deliver a chlorine atom to the alkene, resulting in the formation of a new alkyl radical. This alkyl radical then reacts with another equivalent of the anodically generated manganese (III) chloride to furnish the desired 1,2-dichloroalkane.

This system was developed from a related electrochemical alkene diazidation procedure developed by Lin and co-workers,[62] and this system was then applied to other electrochemical manganese-catalysed methodologies for alkene chlorotrifluoro-methylation,[63] and chloroalkylation.[64]

In a related study in 2019, Mo and co-workers reported an electrochemical procedure for the manganese-catalysed trifluoromethylation of electron-deficient alkenes followed by a subsequent radical cascade sequence to synthesise different azaheterocycles (Scheme 2.15).[65]

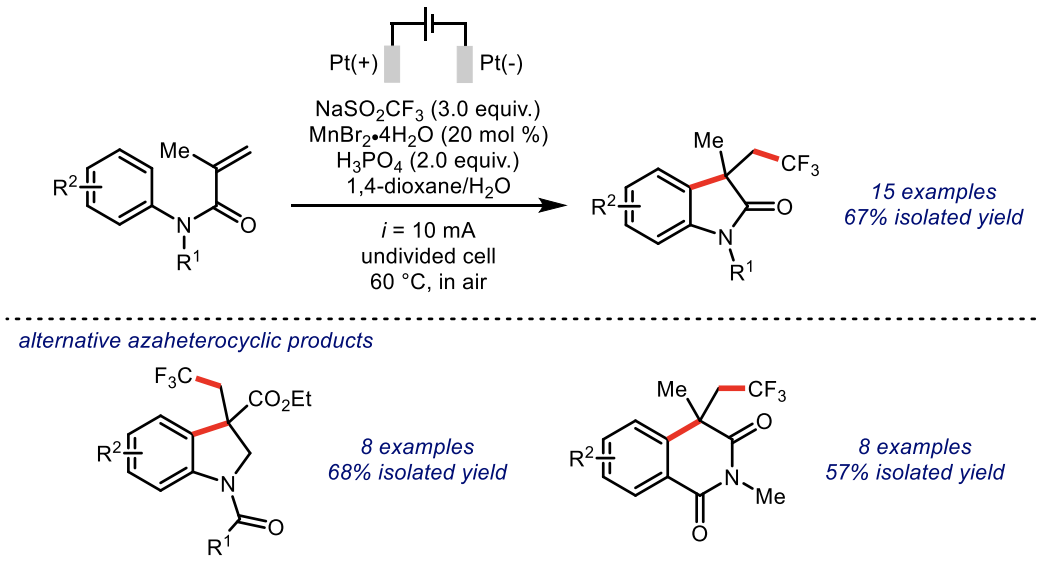

Scheme 2.15: Electrochemical manganese-catalysed alkene trifluoromethylation radical cascade

In this work, the authors reported conditions that enable electrochemical manganese-catalysed formations of oxindoles, indolines, and hydroisoquinoline-1,3-diones. In these reactions, a manganese (II) catalyst was used in combination with sodium trifluoromethanesulfinate and phosphoric acid to initiate radical cascade processes that afford these aza-heterocycle. Within the substrate scope, they reported 15 examples of oxindoles, 8 indolines, and 8 hydroisoquinoline-1,3-diones in an overall average isolated yield of 65%. Halogens, alkyl groups, and electron-withdrawing groups are tolerated well on the aromatic ring, with electron-donating groups giving lower yields. In contrast to the work of Lin and co-workers, there is a lack of redox-active functionalities such as aldehydes demonstrated, suggesting that the chemoselectivity obtained under electrochemical conditions is somewhat dependent on the reaction of interest.

2.1.5 Aims and Objectives

As described above, investigations into the generation and utilisation of alkoxy radicals electrochemically has been limited to the generation of methoxy radicals from methoxide, using expensive boron-doped diamond or platinum anodes. This has thus far hindered the development of applicable synthetic methodologies.

Taking inspiration from the works of Zhu,[27,52,59] and Lin,[61,62] we envisaged that an electrochemical system composed of a manganese (II) salt in combination with a chloride salt would facilitate the deconstructive chlorination of tertiary cycloalkanols under electrochemical conditions to furnish distally functionalised ketones. The use of a manganese (II) salt would allow us to circumvent the high oxidation potential required for the generation of alkoxy radicals directly at the anode. This in turn would allow us to develop a methodology that demonstrates a broad substrate scope, with traditionally redox sensitive functional groups being tolerated, and therefore making the method more applicable to the wider synthesis community.

2.2 Results and Discussion

2.2.1 Optimisation

Initial investigations, performed by Benjamin Allen (PDRA in the Morrill group), were focused on the use of manganese (II) salts to catalyse the deconstructive chlorination of 1-phenylcyclobutanol **27** to form *γ*-chlorinated ketone **28**. Optimisation studies then commenced and were performed by Benjamin Allen (Table 2.1). For a detailed optimisation, the data can be found in the supporting information for this published work.[66]

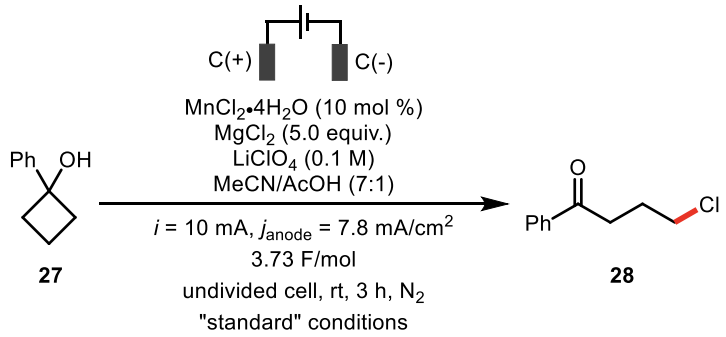

Entry[a]	Variation from "standard" conditions	Yield[b] (%)
1	None	82
2	No electricity	< 2
3	No $MnCl_2•4H_2O$	< 2
4	E_{cell} = 2.4 V	66
5	*i* = 12.5 mA	74
6	*i* = 7.5 mA	80
7	$TBAPF_6$ instead of $LiClO_4$	82
8	Pt foil cathode instead of graphite	82
9	Ni plate cathode instead of graphite	75
10	$Mn(OAc)_2•4H_2O$ instead of $MnCl_2•4H_2O$	82
11	**$Mn(OTf)_2$ instead of $MnCl_2•4H_2O$**	**97 (78)**
12[c]	LiCl instead of $MgCl_2$	64
13[c]	NaCl instead of $MgCl_2$	<2
14[c]	$MgCl_2$ (2.0 equiv.)	76
15[c]	$Mn(OTf)_2$ (5 mol %)	75
16[c,d]	Q = 2 F/mol	67

[a] Reactions performed using 0.3 mmol of **27** using the ElectraSyn 2.0 batch electrochemical reactor. [**27**] = 0.05 M. [b] Yield after 3 h as determined by ^{1}H NMR analysis of the crude reaction mixture with 1,3,5-trimethylbenzene as the internal standard. Isolated yield given in parentheses. [c] $Mn(OTf)_2$ as catalyst. [d] 96 min reaction time.

Table 2.1: Optimisation of the deconstructive chlorination of cycloalkanols

After an extensive optimisation, it was found that an electrochemical system utilising $MnCl_2•4H_2O$ (10 mol %) as catalyst, $MgCl_2$ (5.0 equiv.) as chloride source, and $LiClO_4$

(2.0 equiv.) as supporting electrolyte in MeCN/AcOH (7:1, [**27**] = 0.05 M), under galvanostatic conditions (i = 10 mA, j_{anode} = 7.8 mA/cm^2) with graphite electrodes at rt for 3 h (3.73 F/mol) under N_2, furnished **28** in an 82% yield by ^{1}H NMR (entry 1). This process was found to be reliant on both electricity and catalyst, with < 2% conversion to **28** obtained in the absence of either (entries 2 and 3). Variation of the electrolysis conditions by running the reaction at a constant cell potential (E_{cell} = 2.4 V) or altering the constant current applied (i = 12.5 mA or 7.5 mA) gave slightly decreased yields of **28** by ^{1}H NMR (66-80%, entries 4-6). Employing $TBAPF_6$ as supporting electrolyte, and a cathode of Pt foil or Ni plate also saw negligible changes to the yield of **28** obtained (entries 7-9). Upon evaluation of the manganese (II) salt, it was found that $Mn(OAc)_2$•$4H_2O$ also gave no change in the ^{1}H NMR yield obtained; however, using $Mn(OTf)_2$ improved the yield of **28** obtained to 97% by ^{1}H NMR, and the product could be isolated in a 78% yield (entries 10 and 11). Therefore for the rest of the optimisation studies, $Mn(OTf)_2$ was used as the catalyst.

Alteration of the chloride source from $MgCl_2$ to LiCl gave saw a drop in the yield obtained to 64% (entry 12), whereas using NaCl gave < 2% conversion to **28** (entry 13), presumably due to the poor solubility of NaCl in the MeCN/AcOH solvent system employed. It was also found that upon reduction of the amount of chloride source used and the catalyst loading synthetically useful yields of **28** could still be obtained (75-76%, entries 14 and 15). Finally, the reaction was run until only 2 F/mol of charge had passed, and a 67% yield of **28** was obtained. This indicated a Faradaic efficiency of 67% for this process (entry 16), suggesting that the majority of the electricity passed through the electrochemical cell is utilised productively. Therefore, the final optimised conditions for this process utilises $Mn(OTf)_2$ (10 mol %), $MgCl_2$ (5.0 equiv.), $LiClO_4$ (2.0 equiv.) in MeCN/AcOH (7:1, [**27**] = 0.05 M), under constant current conditions (i = 10 mA, j_{anode} = 7.8 mA/cm^2) with graphite electrodes at 25 °C for 3 h (3.73 F/mol) under N_2 (Scheme 2.16).

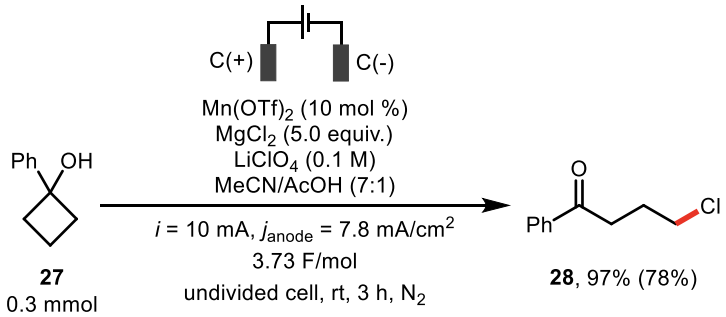

Scheme 2.16: Final optimised conditions

2.2.2 Substrate Scope

2.2.2.1 Substrate Synthesis

With optimised conditions in hand, attention was then turned to investigate the full scope of this reaction. Firstly, a range of 1-aryl-, alkyl-, alkenyl-, and alkynyl-cycloalkanols were synthesised to test under the parent reaction conditions, as well as a 3-aryl substituted oxetan-3-ol and azetidin-3-ol, using either a Grignard reagent or organolithium species (Scheme 2.17).

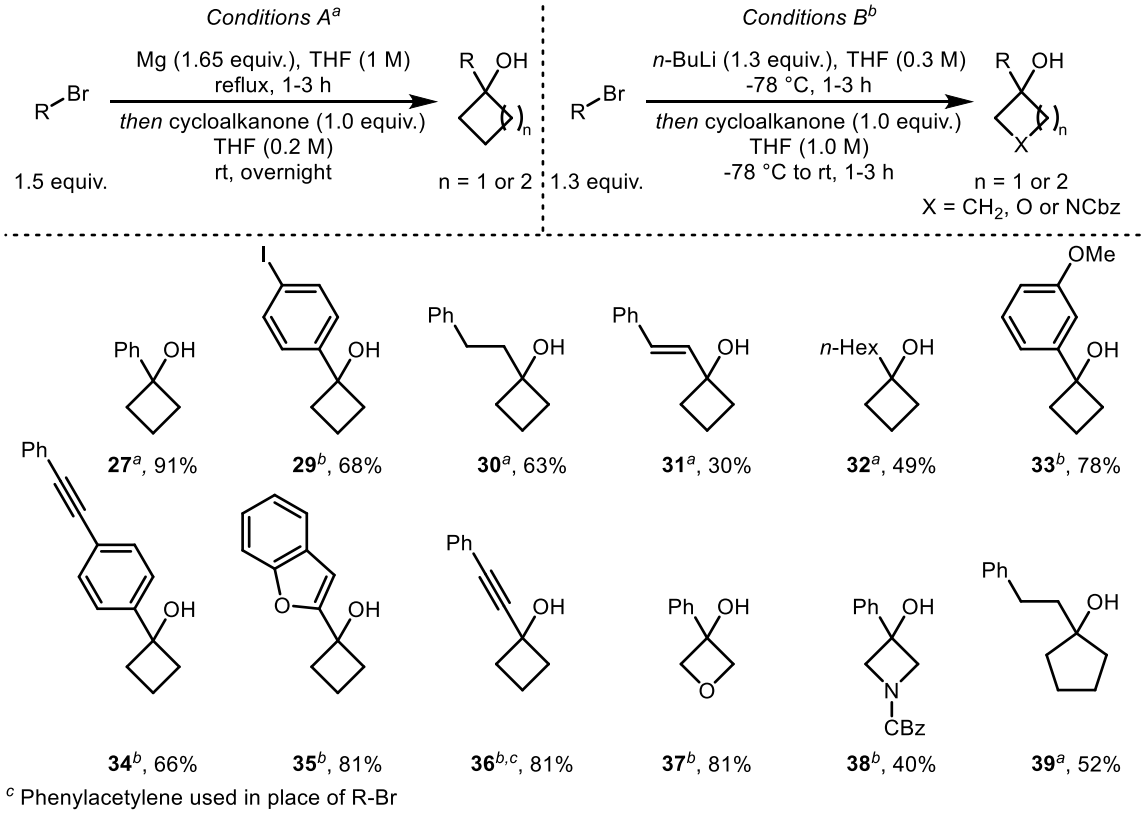

Scheme 2.17: Substrate synthesis of 1-substituted cycloalkanols

Under conditions A, the appropriate alkyl/alkenyl/aryl bromide (1.5 equiv.) was converted to the corresponding Grignard reagent by heating to reflux in THF with magnesium (1.65 equiv.) for 1-3 h. Upon formation of the Grignard, the solution was cooled and the appropriate cycloalkanone (1.0 equiv.) was added to afford the desired tertiary cycloalkanol. When using conditions B, the appropriate aryl halide (1.3 equiv.), or phenylacetylene (1.3 equiv.) was converted to the corresponding organolithium species using *n*-BuLi (1.3 equiv.) at -78 °C, before the appropriate electrophile (1.0 equiv.) was added to form the desired tertiary alcohol product. Through these two synthetic routes, a

range of 1-substituted cyclobutan-1-ols (**27**, **29-36**) were formed in good yields, as well as oxetan-3-ol **37**, azetidine-3-ol **38**, and cyclopentan-1-ol **39**.

A range of 1-alkylcycloalkan-1-ols were also synthesised utilising commercially available Grignard reagents (1.5 equiv.) and reacting them with the appropriate cycloalkanone (1.0 equiv.) (Scheme 2.18).

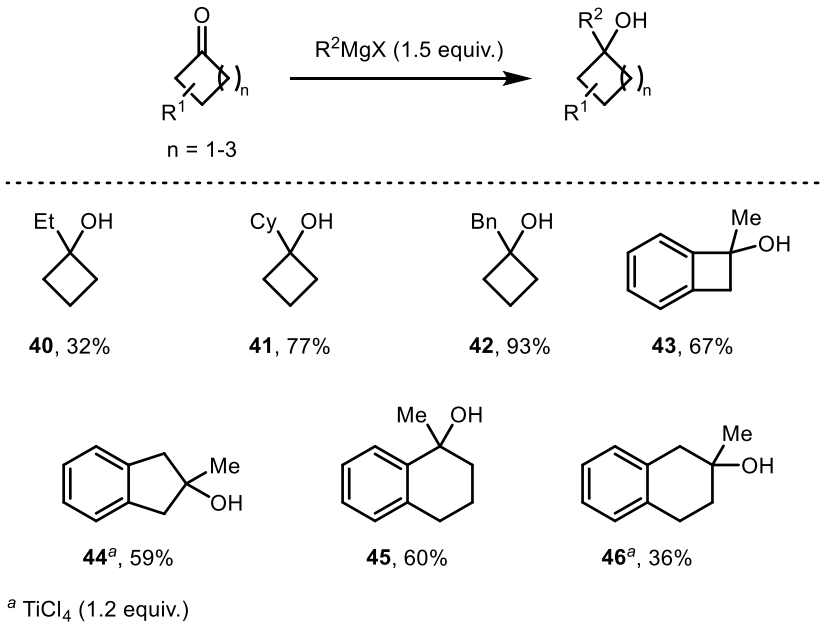

Scheme 2.18: Substrate synthesis of 1-alkyl cycloalkanols

Through this route, 1-ethyl, 1-cyclohexyl, and 1-benzyl cyclobutan-1-ols **40**-**42** were successfully synthesised. Fused cycloalkanols **43**-**46** were also formed in good yields. For the formation of **44** and **46**, $TiCl_4$ was used as a Lewis acid additive to allow for successful addition of the Grignard to the ketone.[67] When no Lewis acid was used a complex mixture of products were obtained, presumably due to the propensity of the Grignard reagent to act as a base and deprotonate the benzylic *α*-ketone hydrogens within the starting material.

For the synthesis of 1-alkylcyclopropan-1-ols the Kulinkovich reaction was utilised (Scheme 2.19).[68]

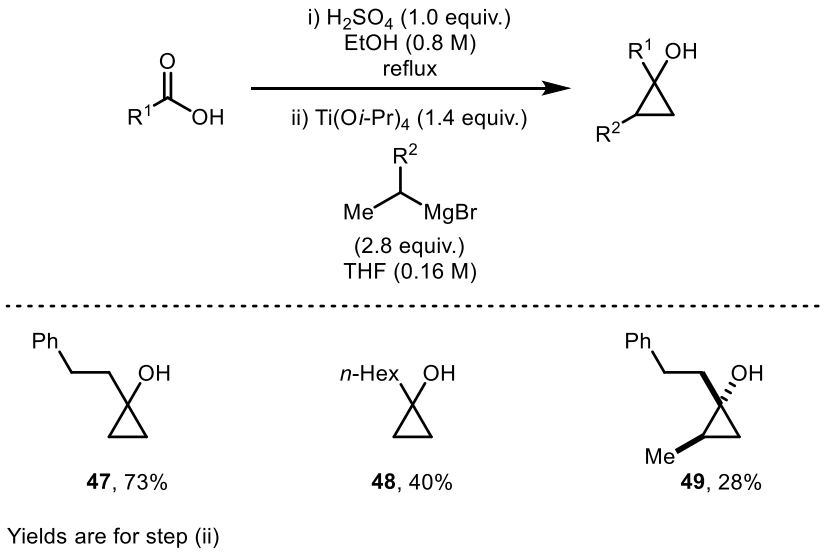

Scheme 2.19: Synthesis of 1-alkylcyclopropanols via Kulinkovich reaction

Firstly, the appropriate carboxylic acid (1.0 equiv.) was converted to the ethyl ester by heating to reflux in ethanol with sulfuric acid (1.0 equiv.). The ethyl esters obtained were then reacted with Ti(O*i*-Pr)$_4$ (1.4 equiv.) and the appropriate commercially available Grignard reagent (2.8 equiv.) in the Kulinkovich reaction to afford the desired 1-alkylcyclopropan-1-ol. Using this synthetic route, cyclopropan-1-ols **47**-**49** were successfully obtained in poor to good yields. In the case of **49**, the compound was obtained solely as the expected diastereoisomer.[69]

2.2.2.2 Substrate Scope

With synthesised substrates in hand, the full scope of this reaction was investigated.

Unfortunately, initial experiments immediately brought to light the sensitivity of the system towards electronic effects about the phenyl ring. It was observed that even weakly electron-donating groups on the phenyl ring in the *ortho*- or *para*-positions gave a significantly reduced yield (Scheme 2.20). Within this scheme, the reaction to form **50** was performed by me, and the reactions to form **51** to **54** were performed by either Benjamin Allen or Deepak Mishra.

Substrates with alkyl substituents in the *ortho*- or *para*-positions or containing an extended *π*-system showed either no appreciable formations of the desired products **50**-**53**, or a much-decreased yield, along with extensive decomposition of starting material. These observations are attributed to the more electron-rich aromatic ring, compared to the parent substrate **27**, increasing the favourability of C-O bond ionisation under the Brønsted and Lewis acidic reaction conditions through increased stabilisation

of the resulting carbocation. Gratifyingly, *meta*-substitution of mildly electron-donating groups were somewhat tolerated, with **54** isolated in a moderate 44% yield.

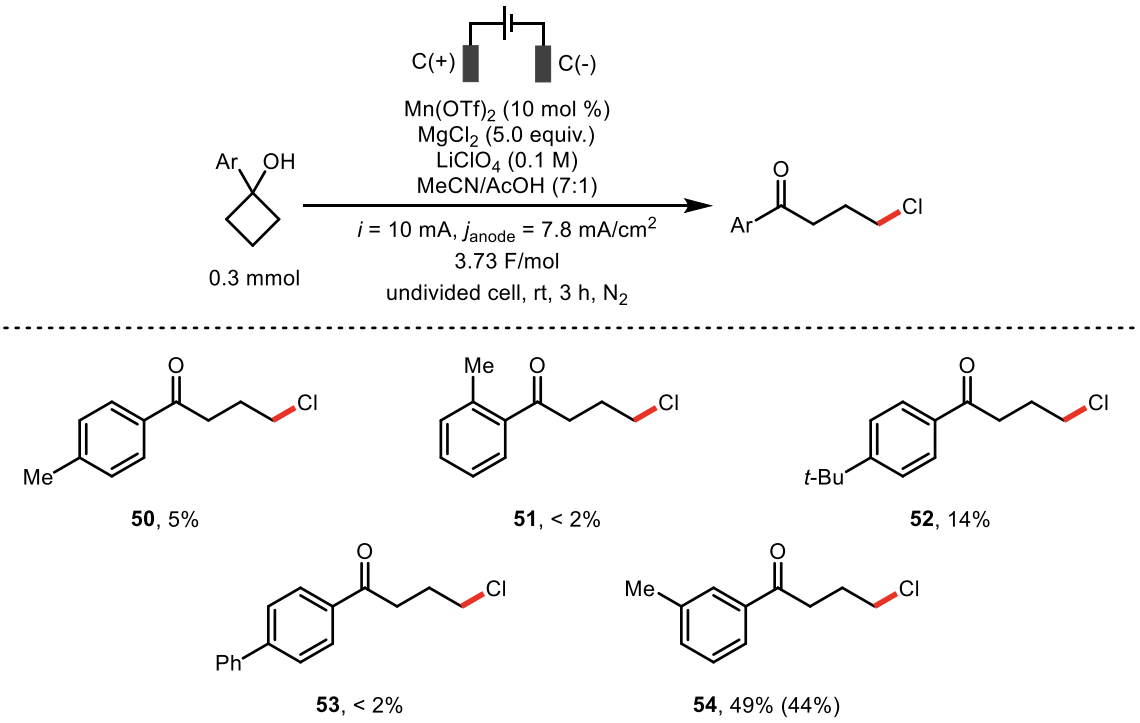

Yields as determined by ^{1}H NMR analysis of the crude reaction mixture using 1,3,5-trimethylbenzene as the internal standard quoted. Isolated yield given in parentheses.

Scheme 2.20: Initial substrate scope showing incompatibility of electron-rich substituents.

Attention was then turned to the re-optimisation of the system to better tolerate electron-donating substituents in the *ortho*- and *para*-positions. After another extensive optimisation using **55** as the optimisation substrate, performed by Benjamin Allen, it was found that by employing a slow addition of **55** over 2 h *via* a syringe pump and using TBAOAc as the supporting electrolyte in the place of $LiClO_4$, **52** could be obtained in a much improved 91% NMR yield and isolated in an 80% yield (Scheme 2.21).

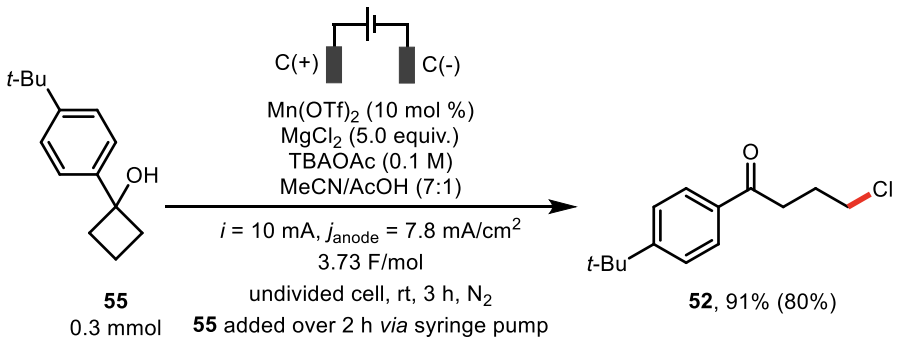

Yield as determined by ^{1}H NMR analysis of the crude reaction mixture using 1,3,5-trimethylbenzene as the internal standard quoted. Isolated yield given in parentheses.

Scheme 2.21: Re-optimised conditions for electron-rich substrates

With two applicable sets of conditions available for use depending on the electronic nature of the substrate, the full scope of the reaction was then evaluated. Firstly, substitution on the aromatic ring was evaluated (Scheme 2.22). In this section of the substrate scope, I was responsible for the formation and isolation of product **51**. Products **50**, **52**-**54** and **56**-**68** were formed and isolated by either Benjamin Allen or Deepak Mishra.

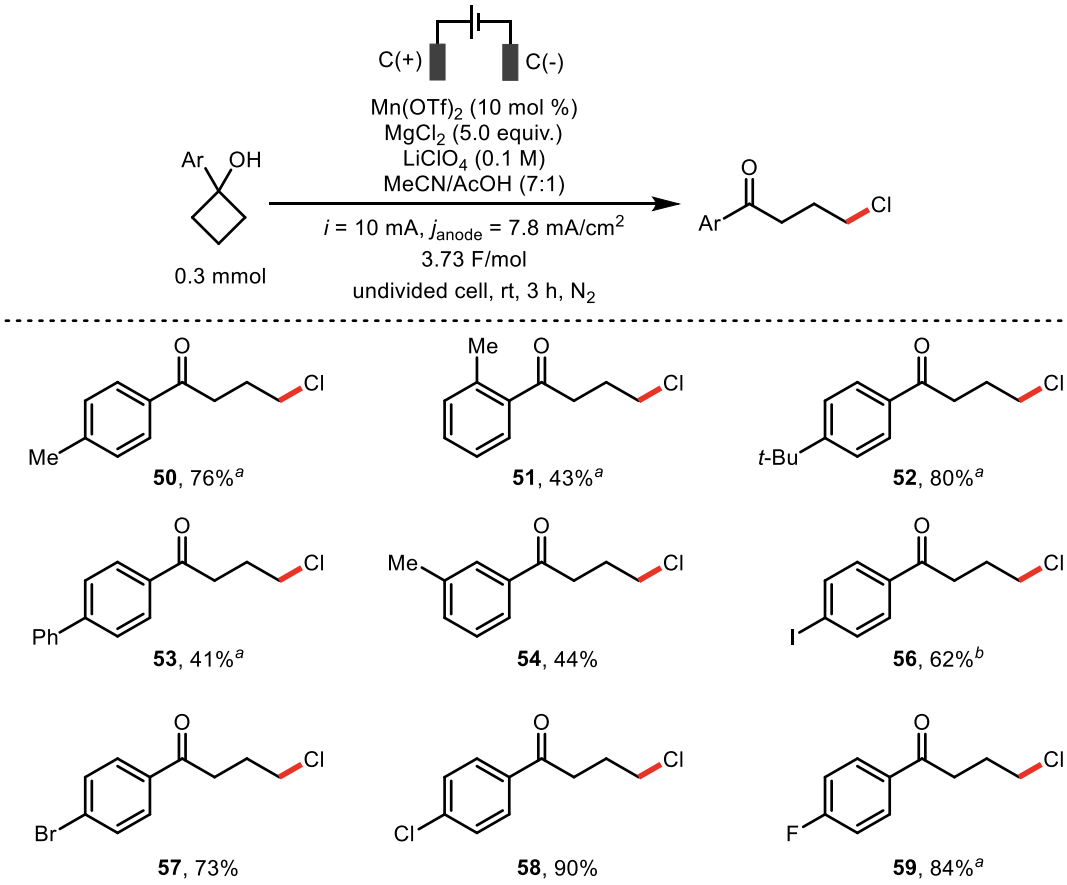

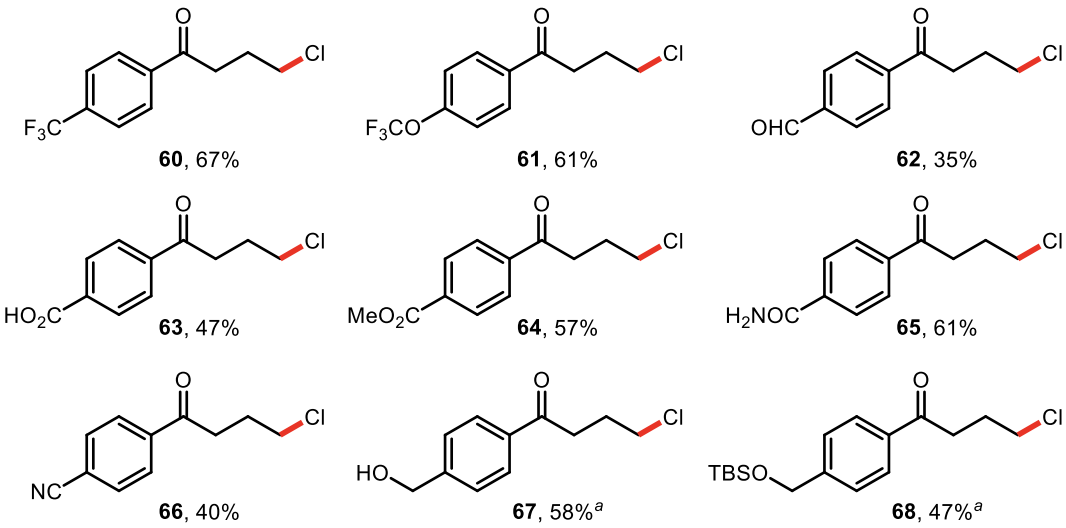

Isolated yields after chromatographic purification quoted. [a] Cycloalkanol added over 2 h *via* syringe pump, TBAOAc (0.1 M) as supporting electrolyte. [b] TBAOAc (0.1 M) as supporting electrolyte.

Scheme 2.22: Evaluation of substrates with aromatic ring substitution

By using one of the two aforementioned optimised conditions, a range of 1-arylcyclobutan-1-ols were converted to *γ*-chloroketones in good yields. Alkyl substitution is tolerated at any position within the aryl ring, and aryl substitution is tolerated in the *para*-position (**50**-**54**, 43-80%). Substrates with halogens in the *para*-position worked well, furnishing the desired products in excellent yields (**56**-**59**, 62-90%) and open the possibility for further derivatisation of the products. Electron-withdrawing groups (e.g., CF_3) are also compatible with the system (**60** and **61**, 67% and 61%). This electrochemical system exhibits excellent functional group tolerance, highlighted by the tolerance of redox active substituents such as an aldehyde, carboxylic acid, ester, amide, nitrile, benzylic primary alcohol, and a silyl ether (**62**-**68**, 35-61%). This tolerance is an improvement on the work of Zhu and co-workers,[59] where no substituents of this type were reported within their substrate scope.

Following the success of assessing substitution on the aromatic ring, we next sought to evaluate the compatibility of 1-alkylcyclobutanols in our system (Scheme 2.23). In this section of the substrate scope, I was responsible for the formation and isolation of products **69**, **71**, **73**, and **74**. Products **70** and **72** were formed and isolated by either Benjamin Allen of Deepak Mishra.

Within this part of the scope, all substrates were compatible with the original optimised conditions, with no requirement for a slow addition of the substrate to the reaction mixture. Good yields were obtained for all the isolable *γ*-chlorinated alkyl ketones (**70**-**74**). In the case of product **69**, the ^{1}H NMR yield is quoted to show that the reaction worked well;

however, the isolated yield was significantly reduced to 19% due to the volatility of the product.

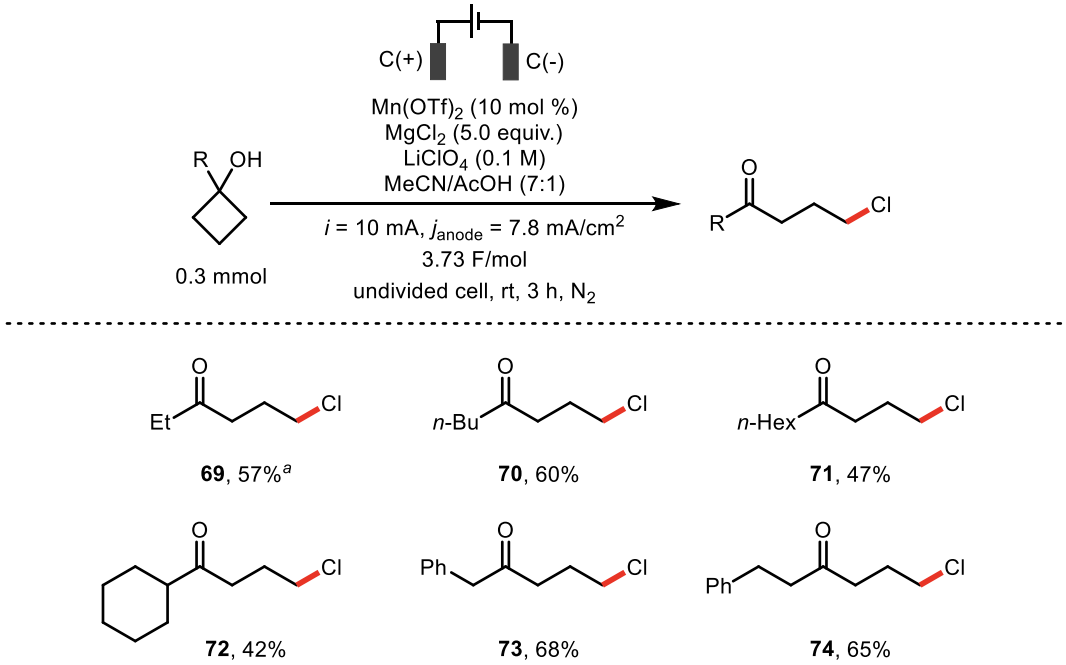

Isolated yields after chromatographic purification quoted. [a] Yield as determined by ^{1}H NMR analysis of the crude reaction mixture with 1,3,5-trimethylbenzene as the internal standard.

Scheme 2.23: Evaluation of substrates with alkyl substitution

Following this part of the scope, bicyclic systems as well as substrates with additional substitution in the 2- or 3-positions of the cyclobutanol ring were tested under the electrochemical conditions (Scheme 2.24). All the compounds **75**-**83** were synthesised and isolated by either Benjamin Allen or Deepak Mishra.

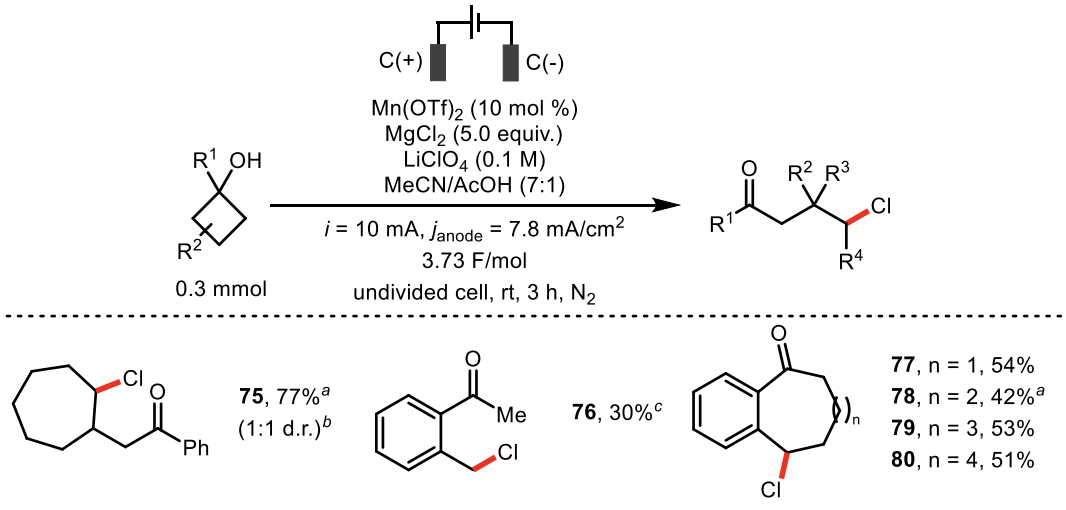

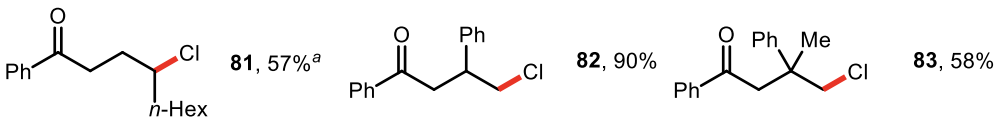

Isolated yields after chromatographic purification quoted. [a] Cycloalkanol added over 2 h *via* syringe pump, TBAOAc (0.1 M) as supporting electrolyte. [b] As determined by ^{1}H NMR analysis of the crude reaction mixture. [c] t = 6 h (7.46 F/mol).

Scheme 2.24: Bicyclic and poly-substituted cyclobutanol scope

The subjection of bicyclic systems to the reaction conditions enabled the formation of disubstituted cycloheptane **75** as well as the efficient synthesis of benzyl chlorides **76**-**80** in good yields (30-77%), including the formation of 7-, 8-, 9-, and 10-membered benzo-fused ring systems. Additional substitution around the cyclobutanol ring system allowed access to polysubstituted *γ*-chloroketones **81**-**83** in good to excellent yields (57-90%), with **81** obtained as the sole regioisomer.

Following this extensive scope of cyclobutanols, the deconstructive chlorination of 1-aryl and 1-alkylcyclopropan-1-ols was then explored (Scheme 2.25). Within this section of the substrate scope, I was responsible for the synthesis and isolation of compounds **86**-**88**, and compounds **84**, **85**, and **89** were made by either Benjamin Allen or Deepak Mishra.

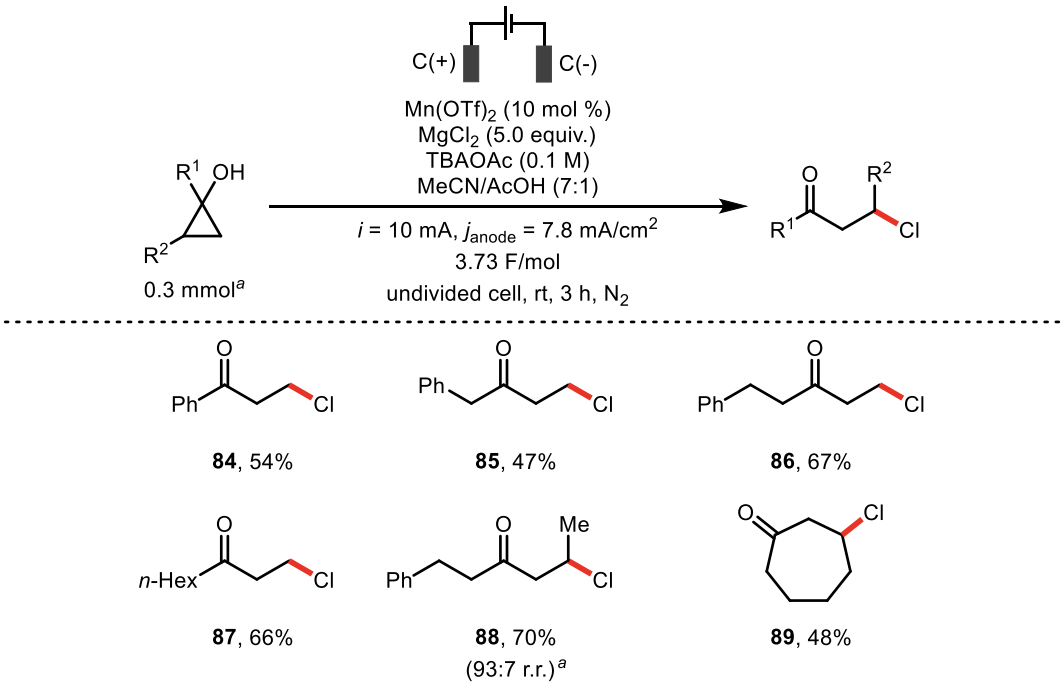

Isolated yields after chromatographic purification quoted. [a] Cyclopropanol added over 2 h *via* syringe pump. [b] As determined by ^{1}H NMR analysis of the crude reaction mixture.

Scheme 2.25: Cyclopropanol substrate scope

Several cyclopropan-1-ols can be efficiently converted into the corresponding *β*-chloroketones in good yields, including the formation of 1-phenylketone **84** and 1-alkylketones **85**-**88** (47-67% yields). Additional substitution in the 2-position of the cyclopropane ring is also tolerated, giving the secondary alkyl radical derived product **88** as the major regioisomer in good yield (70%). Bicyclic cyclopropanols are also tolerated, furnishing *β*-chlorinated cycloheptanone **89** in moderate yield (48%).

Despite the broad substrate scope demonstrated using this methodology, some limitations were discovered. A range of other cyclobutanol substrates proved unsuccessful in furnishing the desired *γ*-chloroketone under either set of optimised conditions (Figure 2.2).

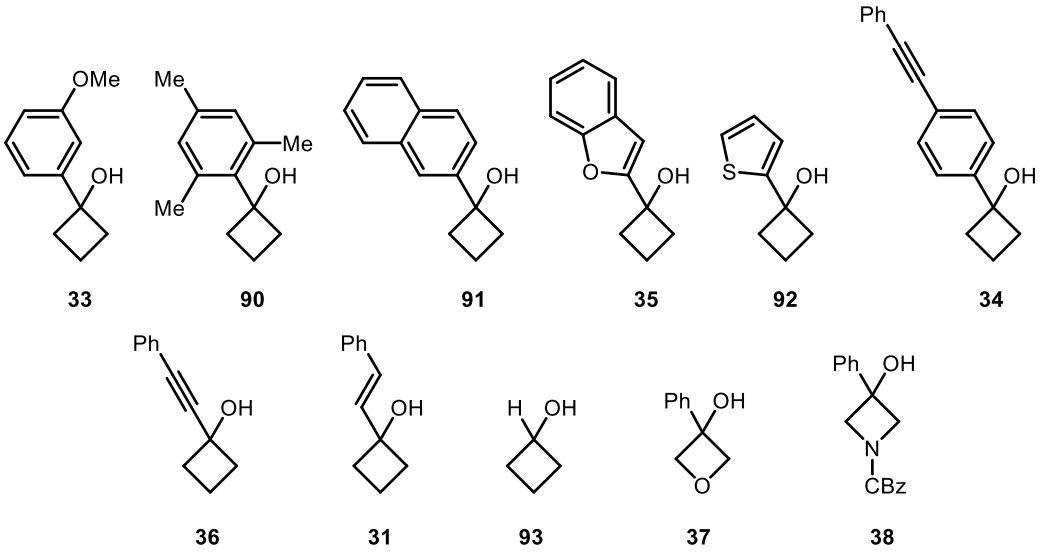

Figure 2.2: Unproductive cyclobutanol substrates

When 1-(*meta*-methoxyphenyl)cyclobutan-1-ol **33** was subjected to this electro-synthetic method, analysis of the crude reaction mixture by ^{1}H NMR indicated a 20% yield of the desired ring opened product, with no indication of recovered starting material. The poor yield may be due to the electron-rich nature of the aromatic ring allowing for undesired non-productive pathways to take place under the reaction conditions. When mesityl substrate **90** was tested, no desired product was observed by ^{1}H NMR analysis of the crude reaction mixture, nor was any recovered starting material detected. New signals in the region of 4.70 to 5.30 ppm were observed, indicating the potential formation of new alkenes that could occur *via* ionisation of the C-OH bond, which would be more favoured due to the electron-rich nature of the mesityl ring. Furthermore, the mesityl moiety may sterically shield the alcohol, inhibiting coordination to the manganese catalyst. This

hypothesis is supported by the lower yield obtained for the *ortho*-tolyl substrate **51** (43%) as compared to the *para*-tolyl substrate **50** (76%).

Naphthyl substituted cyclobutan-1-ol **91** formed the desired *γ*-chloroketone in a 10% NMR yield, and further attempts to improve this yield proved futile. Heteroaryl substituted cyclobutanols **35** and **92** gave a complex mixture of products, as did alkynyl and styryl substrates **31**, **34**, and **36**. What these substrates did in the reaction mixture is unclear; however, no desired products were observed in any case. Cyclobutanol **93** did give the desired *γ*-chloroaldehyde in a 36% yield by ^{1}H NMR; however, the product could not be isolated due to its volatility. Oxetan-3-ol **37** gave no product with only 50% remaining starting material, suggesting unwanted decomposition, and azetidinol **38** was unreactive, with 80% starting material returned by ^{1}H NMR.

Under these reaction conditions we were also limited to performing deconstructive chlorination on cyclopropanols and cyclobutanols. Cycloalkanols of higher order did not furnish the desired distally chlorinated ketones. A selection of the cyclopentanol and cyclohexanols tried under these reaction conditions are shown (Figure 2.3).

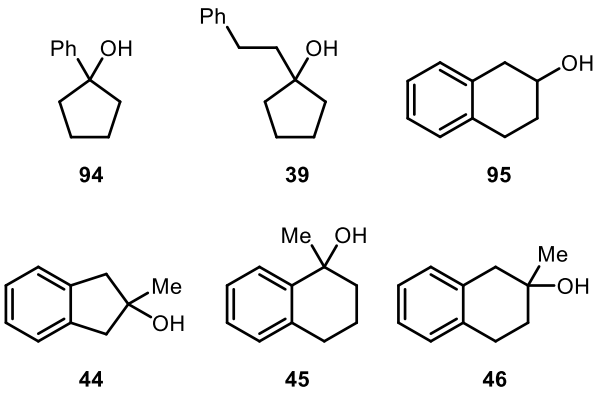

Figure 2.3: Unproductive cyclopentanol and cyclohexanol substrates

1-Phenylcyclopentanol **94** gave no desired *δ*-chlorinated ketone product and full decomposition of **94** was observed, which can be attributed to the increased propensity for C-OH bond ionisation and subsequent alkene formation compared to **27**. This in turn makes the ionisation faster than the desired *β*-scission process, which itself is slowed due to the significantly reduced ring strain of cyclopentanes compared to cyclobutanes.[70] Following this observation, it was hypothesised that by swapping the aryl group for a less electron-donating alkyl substituent, the rate of decomposition could be slowed. Therefore, substrate **39** was tested, resulting in the formation of no visible product with 70% recovery of **39**. This shows that despite inhibiting the suggested decomposition pathway, ring

opening of the cyclopentanol under these conditions is still unfavourable. Benzo-fused cyclohexanol **95** was also unreactive, giving 82% recovery of starting material with no formation of the desired product, whereas benzo-fused cycloalkanols **44**-**46** each gave no product with significant starting material decomposition.

2.2.3 Flow Electrochemistry Scale-up

Following completion of the substrate scope, the scalability of the electrochemical transformation was explored by translating the parent reaction to a flow electrochemical setup utilising the Ammonite8 flow cell reactor.[71] The work described in this section was performed by Tom McBride.

Initially, reaction parameters such as electrolyte loading, temperature, solvent ratio, applied current, residence time, and charge passed were evaluated under a single pass flow electrochemistry system (Scheme 2.26).

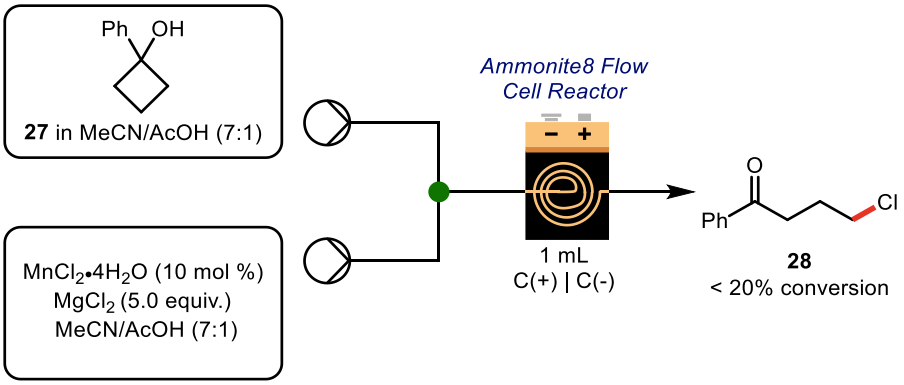

Scheme 2.26: Scale-up using single pass flow electrochemistry

Using a single pass flow electrochemistry setup, and through varying all the reaction parameters, the yield of **28** obtained could not be increased beyond 20% by ^{1}H NMR analysis of the crude reaction mixture, with significant quantities of **27** observed.

Therefore, the reaction was then transferred to a recirculating flow system (Scheme 2.27). Within this setup, a solution of **27**, $MnCl_2$•$4H_2O$, and $MgCl_2$ in MeCN/AcOH was recirculated (flow rate = 2.5 mL/min) through the Ammonite8 flow cell reactor, using a HPLC pump, with an applied current of 400 mA to obtain 1.20 g of **28** (78%) in just 5 h. Upon full consumption of **27** by TLC analysis of the reaction mixture, the solution was then passed through an inline purification system to yield **28** as a spectroscopically pure compound with no further purification necessary. Due to the decreased inter-electrode

distance within the Ammonite8 flow cell reactor, the requirement for supporting electrolyte was removed.

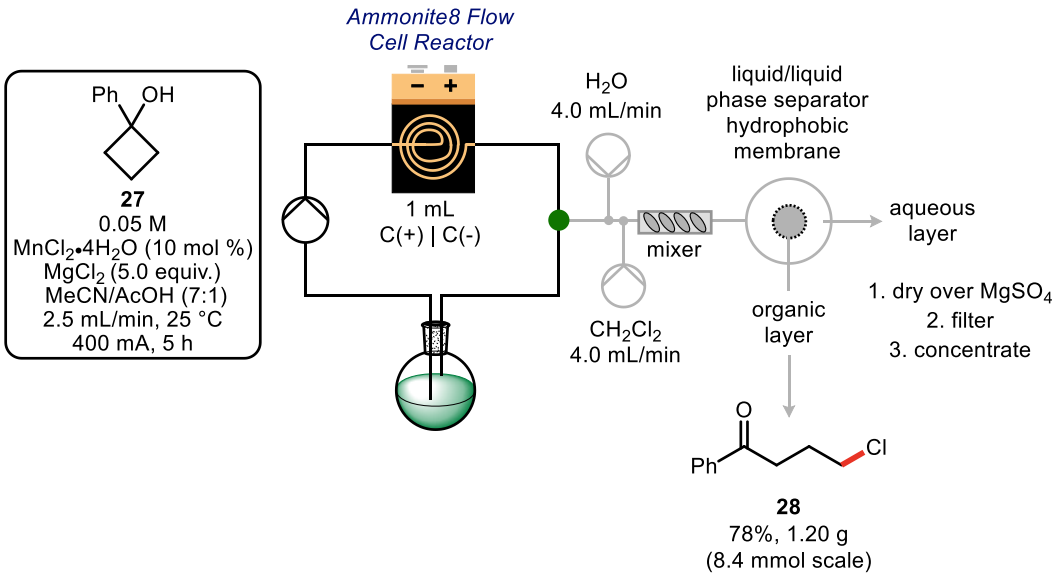

Scheme 2.27: Scale-up using recirculating flow electrochemistry

2.2.4 Mechanistic Studies

With the substrate scope completed, mechanistic studies were then performed to gain insight into how this reaction proceeds. This was achieved using both cyclic voltammetry (CV) as well as through experimental means.

2.2.4.1 Cyclic Voltammetry Studies

CV studies were employed to gain an insight into the mechanism of this electrochemical process.[72] Through this technique, single electron transfer events can be observed for each component of the reaction, as well as for their combinations, providing information on the relative oxidation potentials of each component of the reaction. Firstly, the $Mn(OTf)_2$ salt and $MgCl_2$ were studied using CV (Figure 2.4).

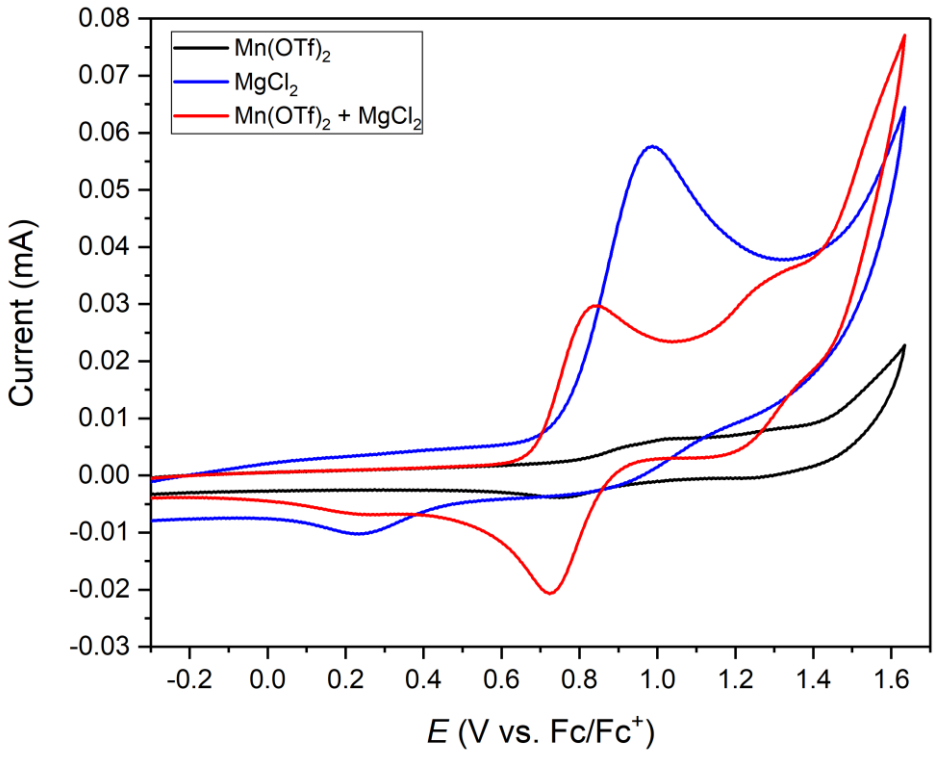

Figure 2.4: Cyclic voltammogram of $Mn(OTf)_2$, $MgCl_2$, and their mixture in MeCN with AcOH (60 mM) and $LiClO_4$ (0.1 M). ***a*** *(black line) – $Mn(OTf)_2$ (2.0 mM);* ***b*** *(blue line) – $MgCl_2$ (8.0 mM);* ***c*** *(red line) $Mn(OTf)_2$ (2.0 mM) and $MgCl_2$ (8.0 mM).* ***Scan rate: 100 mV/s***

It can be seen that $Mn(OTf)_2$ alone (black line) is redox inactive within the operating potential range of the solvent, whereas $MgCl_2$ (blue line) shows an irreversible oxidation event at ~1.0 V vs Fc/Fc^+ for the single electron oxidation of chloride anions to chlorine atoms. Upon the combination of $Mn(OTf)_2$ and $MgCl_2$ (red line), a new quasi-reversible oxidation event is observed at ~0.8 V vs Fc/Fc^+, providing evidence for the formation of a new compound that has a lower oxidation potential than $MgCl_2$. It is proposed that this species is an anionic $[Mn(II)X_2Cl]^-$ complex (X = OTf, OAc, or Cl) that is then able to be oxidised to $Mn(III)X_2Cl$ at the anode.[61]

Following these experiments, the effect of adding parent substrate **27** to the combination of $Mn(OTf)_2$ and $MgCl_2$ was then studied (Figure 2.5).

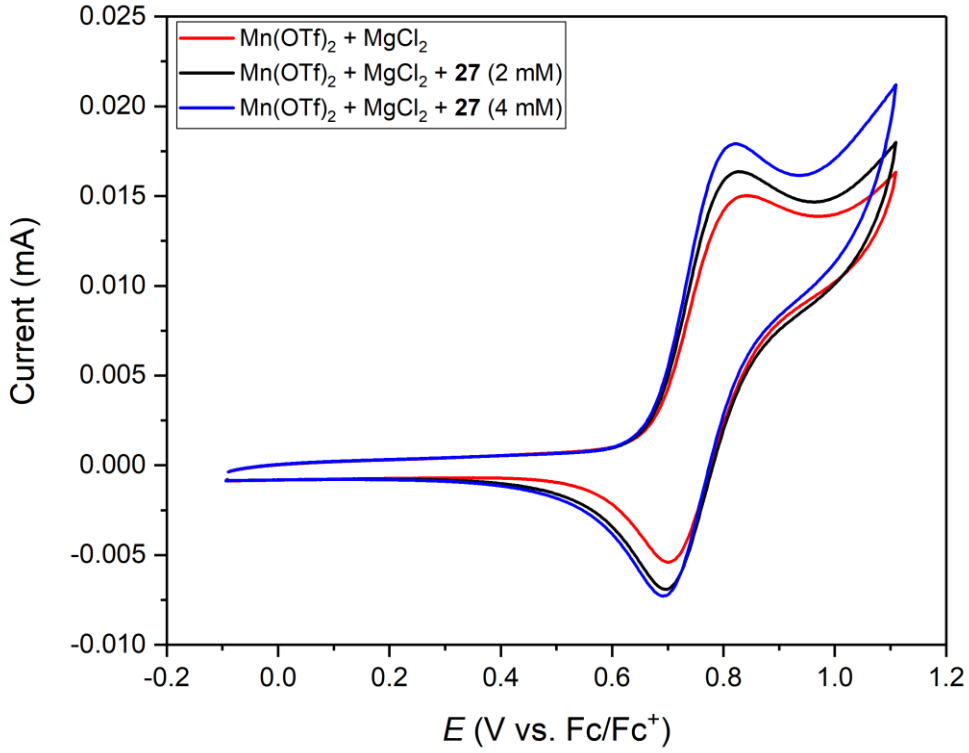

*Figure 2.5: Cyclic voltammogram of $Mn(OTf)_2$, $MgCl_2$, and **27** in MeCN with AcOH (60 mM) and $LiClO_4$ (0.1 M). **a** (red line) – $Mn(OTf)_2$ (2.0 mM) and $MgCl_2$ (8.0 mM); **b** (black line) – $Mn(OTf)_2$ (2.0 mM), $MgCl_2$ (8.0 mM), and **27** (2.0 mM); **c** (blue line) – $Mn(OTf)_2$ (2.0 mM), $MgCl_2$ (8.0 mM), and **27** (4.0 mM).* ***Scan rate: 20 mV/s***

In this voltammogram, it is evident that upon the addition of **27** to the mixture of $Mn(OTf)_2$ and $MgCl_2$ (black line) there is an increase in the current observed for the oxidation event when compared to the combination of $Mn(OTf)_2$ and $MgCl_2$ (red line). This increase in current is enhanced upon further addition of **27** (blue line). As the reduction event is still present, these observations perhaps suggest that the combination of **27** with the proposed $[Mn(II)X_2Cl]^-$ species forms a new complex, with the tertiary alcohol displacing either the chloride or one of the X ligands.

To ensure that both the $Mn(OTf)_2$ and $MgCl_2$ are necessary within the mechanistic framework of this transformation, combinations of each with **27**. Firstly $MgCl_2$, **27**, and their combination were studied (Figure 2.6).

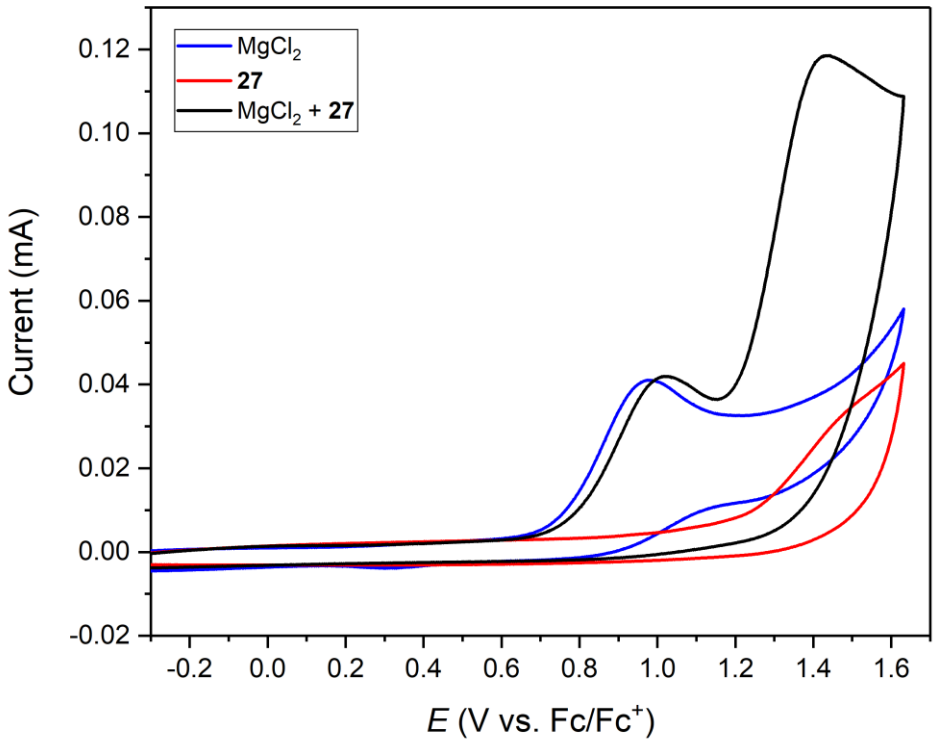

*Figure 2.6: Cyclic voltammogram of $MgCl_2$, **27**, and their mixture in MeCN with AcOH (60 mM) and $LiClO_4$ (0.1 M). **a** (blue line) – $MgCl_2$ (8.0 mM); **b** (red line) – **27** (4.0 mM); **c** (black line) – $MgCl_2$ (8.0 mM) and **27** (4.0 mM). **Scan rate: 50 mV/s***

The CV obtained of **27** (red line) shows that the substrate may start to oxidise at the anode as the potential pushes towards the operating potential window of the solvent. Upon the addition of $MgCl_2$ to **27** (black line), no new oxidation events with a lower oxidation potential than chloride is observed.

Next, $Mn(OTf)_2$, **27**, and their combination were then studied (Figure 2.7).

In this voltammogram, which was performed using a scan rate of 20 mV/s, the irreversible oxidation of the **27** (red line) can be observed at ~1.3 V vs. Fc/Fc^+. When the redox inactive $Mn(OTf)_2$ was added no new redox events were observed; however, a reduction in the current observed for the oxidation of **27** is observed. This perhaps is evidence for the formation of a Mn-alkoxide formation through displacement of a triflate ligand with the tertiary alcohol in **27**.

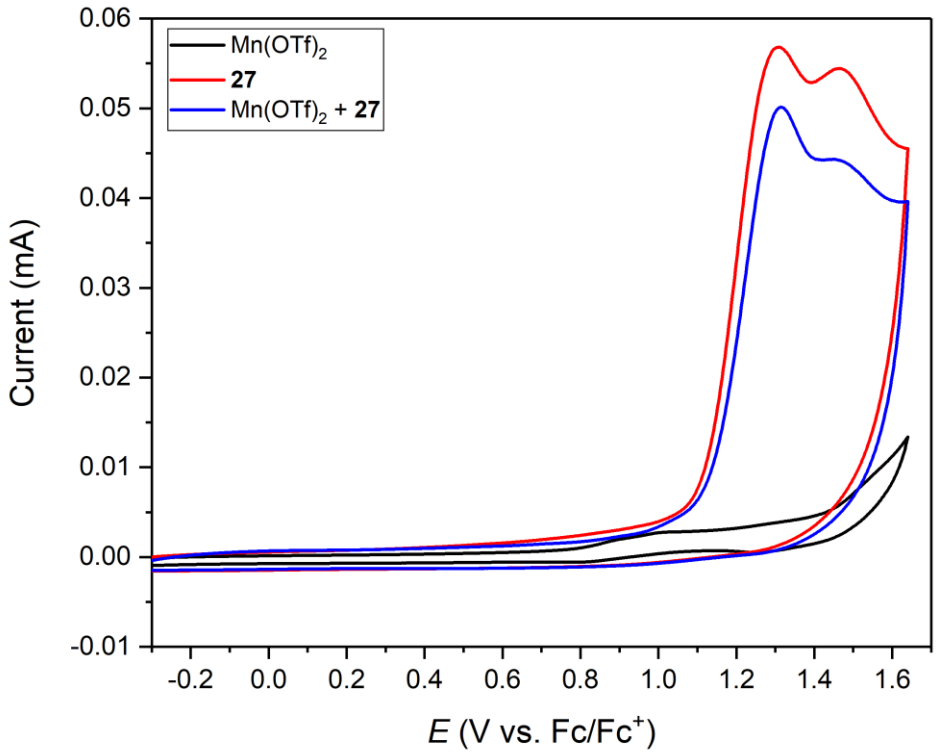

*Figure 2.7: Cyclic voltammogram of $Mn(OTf)_2$, **27**, and their mixture in MeCN with AcOH (60 mM) and $LiClO_4$ (0.1 M). **a** (black line) – $Mn(OTf)_2$ (2.0 mM); **b** (red line) – **27** (4.0 mM); **c** (blue line) – $Mn(OTf)_2$ (2.0 mM) and **27** (4.0 mM). **Scan rate: 20 mV/s***

2.2.4.2 Experimental Evidence

Following the CVs obtained in section 2.2.4.1, there are two plausible mechanistic pathways that the reaction could follow (Scheme 2.28).

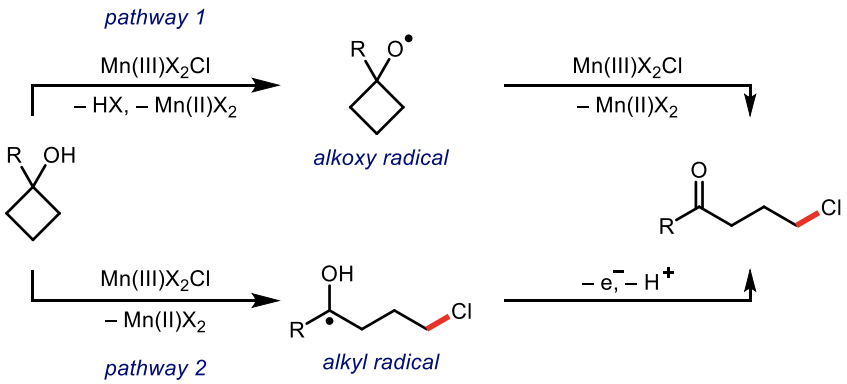

Scheme 2.28: Possible mechanistic pathways

The first pathway that could be followed would be initiated by interaction of the alcohol of with the anodically generated Mn(III) complex to furnish the alkoxy radical intermediate. This cyclic alkoxy radical can then undergo *β*-scission and reaction with another equivalent of the Mn(III)-chloride species to deliver the desired *γ*-chlorinated ketone. An alternative pathway would initiate with the Mn(III)-chloride complex acting as a chlorine transfer agent and delivering a chlorine atom to the 2-position of the cycloalkanol. This would result in the formation of an *α*-hydroxy alkyl radical, which after anodic oxidation and deprotonation would give the desired product also.

To distinguish between these two pathways, methyl ether **96** was synthesised from **27** *via* deprotonation of the alcohol with NaH (1.3 equiv.) and subsequent methylation of the resulting alkoxide with methyl iodide (5.0 equiv.) (Scheme 2.29).

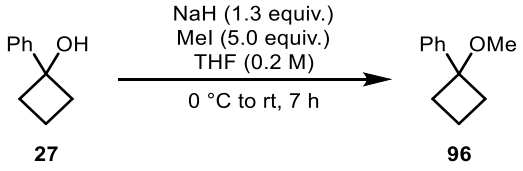

*Scheme 2.29: Formation of methyl ether **96***

It was thought that the absence of a hydroxyl functional group would prevent the formation of an alkoxy radical under the parent reaction conditions, meaning that if **28** was observed as the product, pathway 2 may be favoured. Therefore, methyl ether **96** was then subjected to the parent reaction conditions (Scheme 2.30).

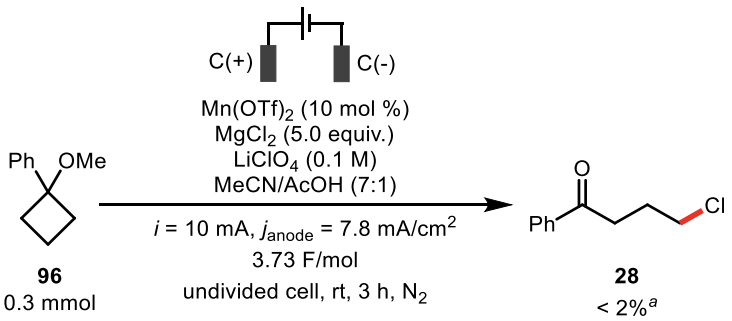

[a] As determined by ^{1}H NMR analysis of the crude reaction mixture using 1,3,5-trimethylbenzene as the internal standard.

*Scheme 2.30: Subjection of methyl ether **96** to the parent reaction conditions*

It was found that when **96** was subjected to the parent reaction conditions, **28** was not observed through ^{1}H NMR analysis of the crude reaction mixture, with an 82% recovery

of **96**. This observation suggests that the Mn(III)X_2Cl species does not promote ring opening in the absence of a hydroxyl functional group, therefore potentially indicating that pathway 1 may be favoured under these reaction conditions.

2.2.3.3 Proposed Mechanism

Following the mechanistic investigations discussed thus far in section 2.2.3, as well as literature precedent,[59,61] two reaction mechanisms can be proposed at this time (Scheme 2.31).

In the first possible mechanism (Scheme 2.31a), which goes *via* a free alkoxy intermediate, initiates through the formation of anionic Mn(II) alkoxide complex through coordination of the substrate to the Mn(II) species (X = anionic ligand, e.g., chloride, triflate, acetate). This anionic Mn(II) species is then oxidised to the corresponding Mn(III) alkoxide, which upon subsequent homolysis furnishes the alkoxy radical intermediate, as well as a regenerated Mn(II) species. This tertiary cyclic alkoxy radical can then undergo a reversible *β*-scission process to generate the transient primary alkyl radical, which is then trapped by an equivalent of anodically generated Mn(III)X_2Cl, furnishing a new C-Cl bond to deliver the desired distally chlorinated ketone. Hydrogen gas is evolved *via* proton reduction at the cathode.

In the second possible mechanism (Scheme 2.31b), the reaction also initiates with the formation of a Mn(III) alkoxide species through coordination of the cycloalkanol substrate to the Mn(II) species and subsequent oxidation at the anode. This Mn(III) species, with at least one chloride ligand, can then deliver a chlorine atom to the 2-position of the ring *via* a 5-membered transition state, with concurrent reduction of the Mn(III) centre to Mn(II). This results in a secondary alkyl radical in the *α*-position relative to the oxygen of the Mn(II) alkoxide. Oxidation of this radical at the anode forms an oxocarbenium species that is then quenched through ligand exchange with an anionic ligand (X = chloride, acetate, or triflate) to deliver the distally chlorinated ketone product. Again, hydrogen gas evolution occurs through proton reduction at the cathode.

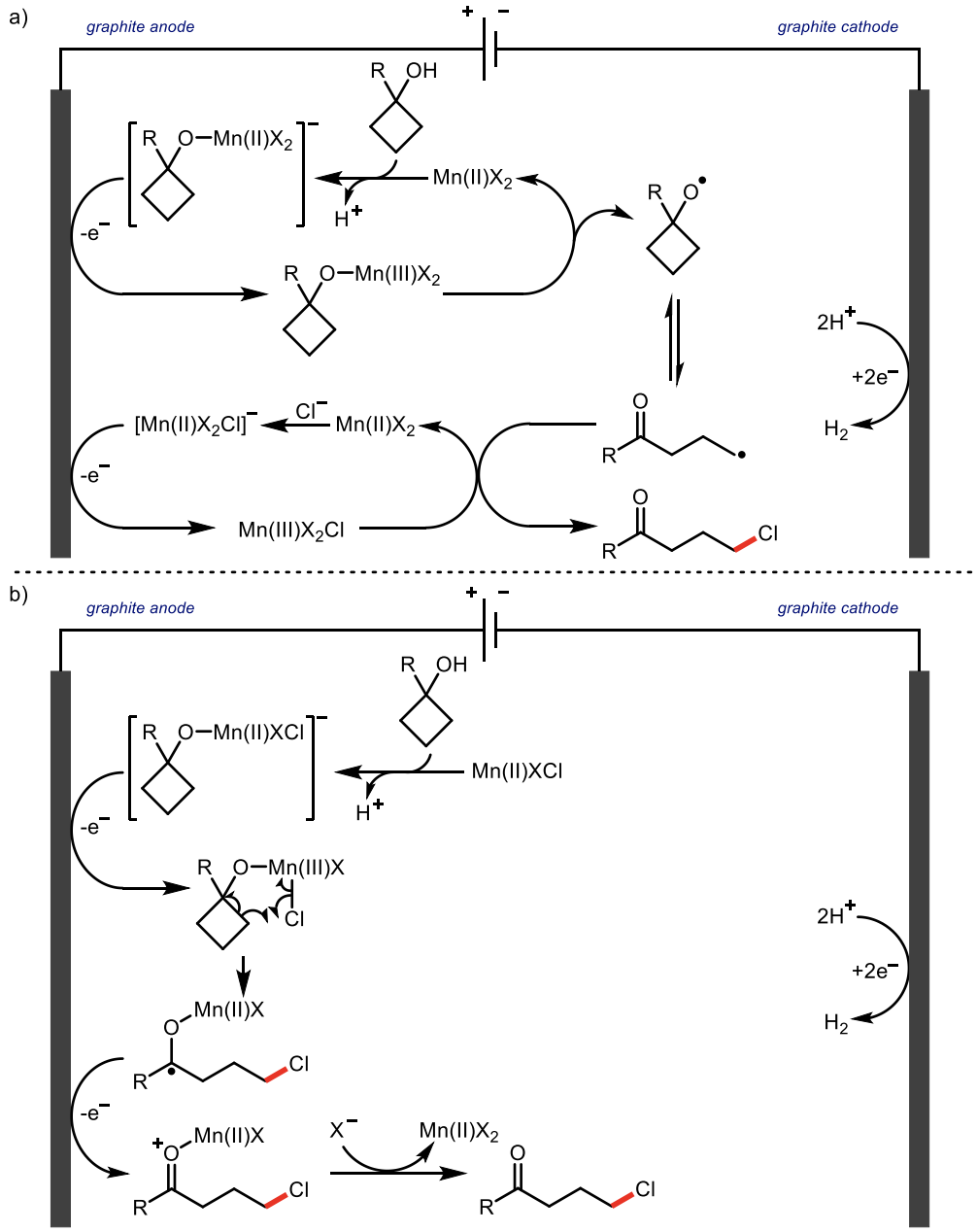

Scheme 2.31: Possible reaction mechanisms. (a) Mechanism through a free alkoxy radical intermediate; (b) Mechanism through which the ring opening is promoted by the manganese alkoxide species

2.3 Further Work

Further work in this area of research should focus on investigations into the development of a more general methodology for the electrochemical generation and utilisation of alkoxy radicals.

Currently, only deconstructive chlorination of cycloalkanols is possible using these reaction conditions. Further experiments to perform deconstructive bromination, iodination, trifluoromethylation, and azidation proved unsuccessful. Furthermore, this reaction is only applicable to the ring opening of cyclopropanols and cyclobutanols, with larger cycloalkanols failing under the reaction conditions.

Future work should focus on overcoming these limitations, as they significantly impact the applicability of this methodology to the wider synthetic chemistry community. For the development of alternative deconstructive functionalisations, it may be necessary to move away from manganese based systems to alternate metal salts (copper, silver, cerium) or away from metals completely by utilising other redox mediators such as triarylamines or triarylimidazoles.[73] When looking at developing methods for the ring opening of cyclopentanols and larger cycloalkanols, it may be necessary to move away from highly acidic proton sources to try and prevent decomposition pathways that can occur under acidic conditions.

It would also be prudent to develop a single pass, continuous flow electrochemical method to enable the facile scale-up of this method which would broaden the appeal of this process to the wider chemistry community, especially towards industrial applications.

Further studies should also be performed to give a clearer picture of how the reaction is proceeding mechanistically. Radical clock experiments could be performed by submitting substrates with a cyclopropyl ring at each of the carbons within the cyclobutanol ring to the reaction conditions. The observation of products where the cyclopropyl ring had opened would indicate the presence of radical intermediates.

Other mechanistic studies that could be performed include the use of EPR spectroscopy to observe the presence of alkoxy radials, potentially through the use of radical trapping agents such as DMPO.[48]

2.4 Conclusion

In conclusion, we have developed a new methodology for the generation and utilisation of alkoxy radicals through this electrochemical manganese-catalysed deconstructive chlorination of tertiary cycloalkanols. This methodology is applicable to the generation of

a broad range of synthetically useful *β*- and *γ*-chloroketones from the corresponding cyclopropanols and cyclobutanols. This procedure exhibits excellent functional group tolerance, with substrates containing a range of redox active functionalities, including aldehydes, benzylic alcohols, and nitriles tolerated to furnish the desired products. Mechanistic investigations, including the use of CV studies, provided a plausible mechanistic pathway *via* alkoxy radical intermediates.

2.5 References

1 P. Gray and A. Williams, *Chem. Rev.*, 1959, **59**, 239–328.

2 L. Chang, Q. An, L. Duan, K. Feng and Z. Zuo, *Chem. Rev.*, 2022, **122**, 2429–2486.

3 Ž. Čeković, *Tetrahedron*, 2003, **59**, 8073–8090.

4 M. Salamone and M. Bietti, *Acc. Chem. Res.*, 2015, **48**, 2895–2903.

5 J. Hartung, *Eur. J. Org. Chem.*, 2001, 619–632.

6 J. Hartung, T. Gottwald and K. Špehar, *Synthesis*, 2002, 1469–1498.

7 M. Murakami and N. Ishida, *Chem. Lett.*, 2017, **46**, 1692–1700.

8 X. Wu and C. Zhu, *Chin. J. Chem.*, 2019, **37**, 171–182.

9 S. P. Morcillo, *Angew. Chem., Int. Ed.*, 2019, **58**, 14044–14054.

10 S. J. Blanksby and G. B. Ellison, *Acc. Chem. Res.*, 2003, **36**, 255–263.

11 J. Zhang, Y. Li, F. Zhang, C. Hu and Y. Chen, *Angew. Chem., Int. Ed.*, 2016, **55**, 1872–1875.

12 C. Wang, K. Harms and E. Meggers, *Angew. Chem., Int. Ed.*, 2016, **55**, 13495–13498.

13 A. Hu, J. J. Guo, H. Pan, H. Tang, Z. Gao and Z. Zuo, *J. Am. Chem. Soc.*, 2018, **140**, 1612–1616.

14 X. Wu, M. Wang, L. Huan, D. Wang, J. Wang and C. Zhu, *Angew. Chem., Int. Ed.*, 2018, **57**, 1640–1644.

15 M. Wang, L. Huan and C. Zhu, *Org. Lett.*, 2019, **21**, 821–825.

16 Q. An, Z. Wang, Y. Chen, X. Wang, K. Zhang, H. Pan, W. Liu and Z. Zuo, *J. Am. Chem. Soc.*, 2020, **142**, 6216–6226.

17 A. R. Rivero, P. Fodran, A. Ondrejková and C. J. Wallentin, *Org. Lett.*, 2020, **22**, 8436–8440.

18 J. Hartung and F. Gallou, *J. Org. Chem.*, 1995, **60**, 6706–6716.

19 Y. Kim, K. Lee, G. R. Mathi, I. Kim and S. Hong, *Green Chem.*, 2019, **21**, 2082–2087.

20 E. Tsui, A. J. Metrano, Y. Tsuchiya and R. R. Knowles, *Angew. Chem., Int. Ed.*, 2020, **59**, 11845–11849.

21 A. L. Barthelemy, B. Tuccio, E. Magnier and G. Dagousset, *Angew. Chem., Int. Ed.*, 2018, **57**, 13790–13794.

22 W. Zheng, C. A. Morales-Rivera, J. W. Lee, P. Liu and M. Y. Ngai, *Angew. Chem., Int. Ed.*, 2018, **57**, 9645–9649.

23 B. J. Jelier, P. F. Tripet, E. Pietrasiak, I. Franzoni, G. Jeschke and A. Togni, *Angew. Chem., Int. Ed.*, 2018, **57**, 13784–13789.

24 K. Zhang, L. Chang, Q. An, X. Wang and Z. Zuo, *J. Am. Chem. Soc.*, 2019, **141**, 10556–10564.

25 Y. Chen, X. Wang, X. He, Q. An and Z. Zuo, *J. Am. Chem. Soc.*, 2021, **143**, 4896–4902.

26 J. Jingliang, L. X. Nguyen, D. R. Patterson and R. A. Flowers, *Org. Lett.*, 2007, **9**,

1323–1326.

27 R. Ren, H. Zhao, L. Huan and C. Zhu, *Angew. Chem., Int. Ed.*, 2015, **54**, 12692–12696.

28 J. J. Guo, A. Hu, Y. Chen, J. Sun, H. Tang and Z. Zuo, *Angew. Chem., Int. Ed.*, 2016, **55**, 15319–15322.

29 F. Q. Huang, J. Xie, J. G. Sun, Y. W. Wang, X. Dong, L. W. Qi and B. Zhang, *Org. Lett.*, 2016, **18**, 684–687.

30 H. G. Yayla, H. Wang, K. T. Tarantino, H. S. Orbe and R. R. Knowles, *J. Am. Chem. Soc.*, 2016, **138**, 10794–10797.

31 L. Huang, T. Ji and M. Rueping, *J. Am. Chem. Soc.*, 2020, **142**, 3532–3539.

32 D. R. Barton, J. M. Beaton, L. E. Geller and M. M. Pechet, *J. Am. Chem. Soc.*, 1961, **83**, 4076–4083.

33 P. de Armas, C. G. Francisco and E. Suárez, *J. Am. Chem. Soc.*, 1993, **115**, 8865–8866.

34 N. Hussain, D. O. Morgan, C. R. White and J. A. Murphy, *Tetrahedron Lett.*, 1994, **35**, 5069–5072.

35 S. Yamashita, A. Naruko, Y. Nakazawa, L. Zhao, Y. Hayashi and M. Hirama, *Angew. Chem., Int. Ed.*, 2015, **54**, 8538–8541.

36 G. Petrović and Ž. Čeković, *Tetrahedron Lett.*, 1997, **38**, 627–630.

37 S. Kim, T. A. Lee and Y. Song, *Synlett*, 1998, 471–472.

38 R. Ren and C. Zhu, *Synlett*, 2016, **27**, 1139–1144.

39 X. Wu and C. Zhu, *Chem. Rec.*, 2018, **18**, 587–598.

40 K. Jia and Y. Chen, *Chem. Commun.*, 2018, **54**, 6105–6112.

41 J. J. Guo, A. Hu and Z. Zuo, *Tetrahedron Lett.*, 2018, **59**, 2103–2111.

42 D. A. DiRocco, K. Dykstra, S. Krska, P. Vachal, D. V. Conway and M. Tudge, *Angew. Chem., Int. Ed.*, 2014, **53**, 4802–4806.

43 E. Tsui, H. Wang and R. R. Knowles, *Chem. Sci.*, 2020, **11**, 11124–11141.

44 A. Hu, J. J. Guo, H. Pan and Z. Zuo, *Science*, 2018, **361**, 668–672.

45 M. G. Dolson and J. S. Swenton, *J. Am. Chem. Soc.*, 1981, **103**, 2361–2371.

46 M. C. Carreño and M. Ribagorda, *J. Org. Chem.*, 2000, **65**, 1231–1234.

47 I. E. Markó, *Tetrahedron Lett.*, 2000, **41**, 4383–4387.

48 T. Sumi, T. Saitoh, K. Natsui, T. Yamamoto, M. Atobe, Y. Einaga and S. Nishiyama, *Angew. Chem., Int. Ed.*, 2012, **51**, 5443–5446.

49 S. Yajima, T. Saitoh, K. Kawa, K. Nakamura, H. Nagase, Y. Einaga and S. Nishiyama, *Tetrahedron*, 2016, **72**, 8428–8435.

50 M. A. Syroeshkin, I. B. Krylov, A. M. Hughes, I. V. Alabugin, D. V. Nasybullina, M. Y. Sharipov, V. P. Gultyai and A. O. Terent'ev, *J. Phys. Org. Chem.*, 2017, **30**, e3744.

51 E. G. Janzen and J. I. P. Liu, *J. Magn. Reson.*, 1973, **9**, 510–512.

52 R. Ren, Z. Wu, Y. Xu and C. Zhu, *Angew. Chem., Int. Ed.*, 2016, **55**, 2866–2869.

53 D. G. Kananovich, Y. A. Konik, D. M. Zubrytski, I. Järving and M. Lopp, *Chem.*

Commun., 2015, **51**, 8349–8352.

54 P. Eisenberger, S. Gischig and A. Togni, *Chem. - Eur. J.*, 2006, **12**, 2579–2586.

55 X. P. He, Y. J. Shu, J. J. Dai, W. M. Zhang, Y. S. Feng and H. J. Xu, *Org. Biomol. Chem.*, 2015, **13**, 7159–7163.

56 Y. Li, Z. Ye, T. M. Bellman, T. Chi and M. Dai, *Org. Lett.*, 2015, **17**, 2186–2189.

57 K. Zhao, K. Yamashita, J. E. Carpenter, T. C. Sherwood, W. R. Ewing, P. T. W. Cheng and R. R. Knowles, *J. Am. Chem. Soc.*, 2019, **141**, 8752–8757.

58 X. Fan, H. Zhao, J. Yu, X. Bao and C. Zhu, *Org. Chem. Front.*, 2016, **3**, 227–232.

59 L. Huan and C. Zhu, *Org. Chem. Front.*, 2016, **3**, 1467–1471.

60 A. Jutand, *Chem. Rev.*, 2008, **108**, 2300–2347.

61 N. Fu, G. S. Sauer and S. Lin, *J. Am. Chem. Soc.*, 2017, **139**, 15548–15553.

62 N. Fu, G. S. Sauer, A. Saha, A. Loo and S. Lin, *Science*, 2017, **357**, 575–579.

63 K. Y. Ye, G. Pombar, N. Fu, G. S. Sauer, I. Keresztes and S. Lin, *J. Am. Chem. Soc.*, 2018, **140**, 2438–2441.

64 N. Fu, Y. Shen, A. R. Allen, L. Song, A. Ozaki and S. Lin, *ACS Catal.*, 2019, **9**, 746–754.

65 Z. Zhang, L. Zhang, Y. Cao, F. Li, G. Bai, G. Liu, Y. Yang and F. Mo, *Org. Lett.*, 2019, **21**, 762–766.

66 B. D. W. Allen, M. D. Hareram, A. C. Seastram, T. McBride, T. Wirth, D. L. Browne and L. C. Morrill, *Org. Lett.*, 2019, **21**, 9241–9246.

67 M. T. Reetz, S. H. Kyung and M. Hüllmann, *Tetrahedron*, 1986, **42**, 2931–2935.

68 O. G. Kulinkovich, S. V. Sviridov and D. A. Vasilevski, *Synthesis*, 1991, **3**, 234.

69 C. P. Casey and N. A. Strotman, *J. Am. Chem. Soc.*, 2004, **126**, 1699–1704.

70 S. Wilsey, P. Dowd and K. N. Houk, *J. Org. Chem.*, 1999, **64**, 8801–8811.

71 R. A. Green, R. C. D. Brown, D. Pletcher and B. Harji, *Org. Process Res. Dev.*, 2015, **19**, 1424–1427.

72 C. Sandford, M. A. Edwards, K. J. Klunder, D. P. Hickey, M. Li, K. Barman, M. S. Sigman, H. S. White and S. D. Minteer, *Chem. Sci.*, 2019, **10**, 6404–6422.

73 R. Francke and R. D. Little, *Chem. Soc. Rev.*, 2014, **43**, 2492–2521.

Chapter 3: Investigations Into the (Photo)Electrochemical Generation of Alkoxy Radicals Using Cerium (III) and (IV) Salts

Table of Contents

3. Preface

This chapter discusses investigations towards the development of a new electrochemical methodology for the generation of alkoxy radicals using cerium (III/IV) salts to overcome the limitations discussed in chapter 2 (section 2.3). Attempts were made to develop a new electrochemical methodology that would allow for the ring opening of cyclopentanols and larger cycloalkanols, as well as to allow for alternative deconstructive functionalisation protocols to chlorination. Investigations were also made to utilise photochemistry in tandem with electrochemistry under this reaction system.

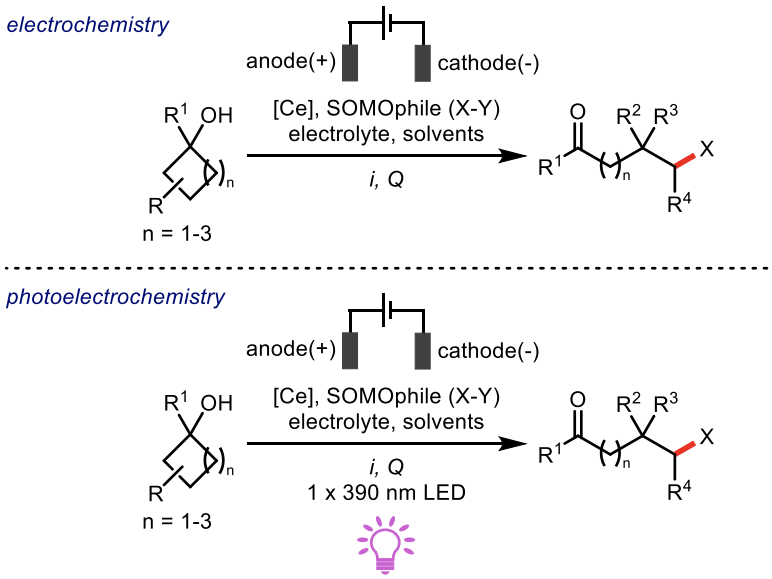

3.1 Introduction

As previously discussed in chapter 2, there have been four main strategies to generate alkoxy radicals for synthesis: traditional radical chemistry, transition metal catalysis (typically in tandem with stoichiometric chemical oxidants), photoredox catalysis, and to a lesser degree, electrochemistry (Scheme 3.1).[1,2]

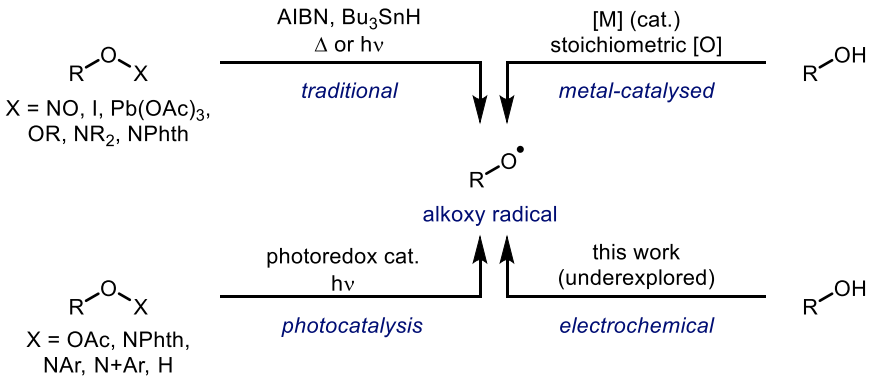

Scheme 3.1: Alkoxy radical generation methods

The use of cerium (IV) to generate alkoxy radicals has been extensively studied due to its ability to act as a single electron oxidant.[3,4] Alkoxy radicals have been generated using cerium under both traditional conditions and under photoredox catalysis.

3.1.1 Alkoxy Radical Generation using Cerium

The reactivity mode predominantly accessed by alkoxy radical generated using cerium (IV) has been *β*-scission, to perform deconstructive functionalisations of cycloalkanols *via* alkoxy radicals. Despite this, there are reports of cerium (IV) generated alkoxy radicals performing HATs, both intramolecularly and intermolecularly.

3.1.1.1 Deconstructive Functionalisation

Cerium (IV) sources were shown to allow the deconstructive functionalisation of cycloalkanols as early as 1972, when Meyer and Roček demonstrated the ability of ceric ammonium nitrate (CAN) to perform single electron oxidations of cyclobutanols, forming various ring opened products depending on the solvent composition.[5] This observation was refined to a more synthetically useful protocol in 2007, when Flowers and co-workers reported an approach to *β*-functionalised ketones *via* a cerium (IV) mediated deconstructive functionalisation of cyclopropanols (Scheme 3.2).[6]

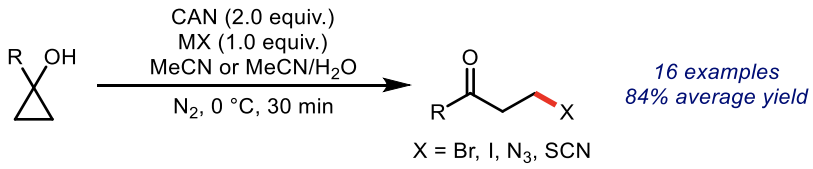

Scheme 3.2: Cerium (IV) mediated deconstructive functionalisation of cyclopropanols

This methodology utilises CAN as a stoichiometric oxidant for the formation of *β*-bromo-, iodo-, azido-, or thiocyanato-ketones from 1-substituted cyclopropanols and the appropriate salt, with 16 examples formed in an 84% average yield. This work allows facile access to synthetically useful products; however, the substrate scope is narrow and limited, with no examples demonstrating the tolerance of redox sensitive functional groups. The authors did later expand upon this work to include the ring opening of cyclobutanol substrates, although no examples using larger ring systems were subsequently reported.[7]

More recently, Gong and co-workers have reported similar ring openings of cyclobutanols using CAN to form homo-coupled products and to form tetralones (Scheme 3.3).[8,9]

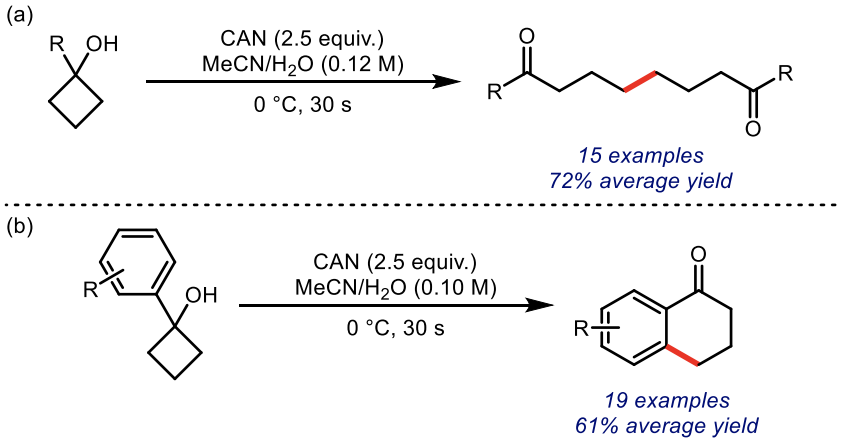

Scheme 3.3: Cerium (IV) mediated ring opening of cyclobutanols. (a) formation of homo-coupled products; (b) formation of tetralones

In these works, 1-substituted cyclobutanols were reacted with CAN (2.5 equiv.) in a 1:1 mixture of MeCN and water to give either the homo-coupled (15 examples, 72% average yield, Scheme 3.3a) or tetralone product (19 examples, 61% average yield, Scheme 3.3b). The reaction concentration seems to be crucial to the product selectivity, with a slightly higher concentration favouring the homo-coupled products, albeit electronic effects did favour the homo-coupled product in the tetralone formation substrate scope.

In the examples discussed thus far, a super-stoichiometric quantity of CAN has been utilised, with no attempts of a system where catalytic quantities could be utilised in combination with an oxidant demonstrated. This has been overcome using cerium (III) sources under photoredox catalysis, with Zuo and co-workers leading the way in developing this field.

In 2016, Zuo and co-workers reported a photocatalytic deconstructive amination of cycloalkanols *via* a cerium (III) chloride complex (Scheme 3.4).[10]

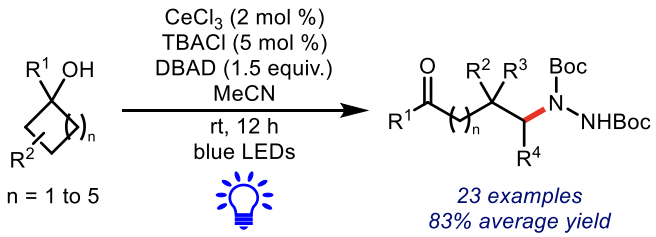

Scheme 3.4: Photocatalytic cerium-catalysed deconstructive amination of cycloalkanols

This methodology takes cycloalkanols (from cyclobutanols up to cyclooctanols) and conveniently transforms them into the corresponding distally aminated ketones using $CeCl_3$ (2 mol %) in combination with TBACl (5 mol %) as a chloride additive, and DBAD (1.5 equiv.) as the SOMOphile, with 23 examples reported in an 83% average yield. Generally, all substrates allowed the formation of the linear products shown, but when lower order secondary cyclobutanols and cyclopentanols were employed (R^1 = H), cyclic hemiaminal products were formed. Despite the broad substrate scope exhibited in terms of ring size, only substrates bearing relatively electron-neutral substituents were demonstrated, with no examples of strongly electron-donating or electron-withdrawing substituents. Only diazo compounds (DBAD or DIAD) were shown to act as the SOMOphile, due to the resulting electrophilic *N*-centred radical acting as the oxidant required to generate the active cerium (IV) species.

To overcome the limitation in the choice of SOMOphile for the transformation, a dual photocatalysis system was subsequently developed. By employing an anthracene based photoredox catalyst to act as an electron transfer mediator in tandem with the cerium (III/IV) system, privileged bridged lactones could be synthesised from simple cycloalkanols (Scheme 3.5).[11]

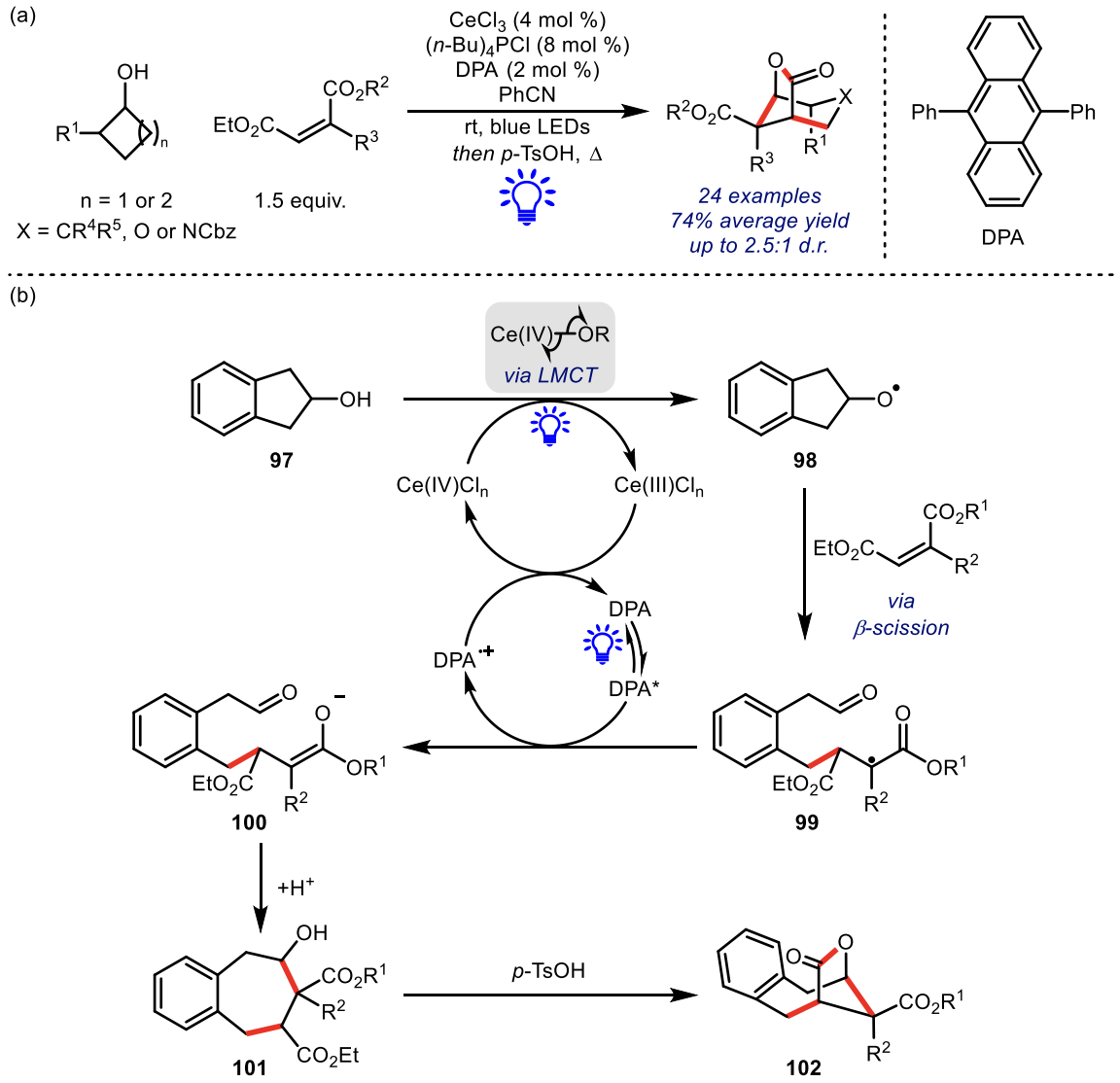

Scheme 3.5: Formation of bridged lactones via dual cerium and organic photocatalysis. (a) reaction scheme; (b) proposed mechanism

In this work, secondary cyclobutanols and cyclopentanols were rapidly converted into privileged bridged lactone motifs upon reaction with electron deficient alkenes *via* a cerium and organic photocatalyst dual manifold. These reactions only require 4 mol % of the cerium (III) salt and 2 mol % of 9,10-diphenylanthracene (DPA) as the organic photocatalyst, with 24 bridged lactones formed in an average yield of 74%, although the diastereoselectivity was generally poor with a maximum diastereomeric ratio of 2.5:1 observed (Scheme 3.5a).

Mechanistically, cycloalkanol **97** interacts with cerium (IV) to form a cerium (IV) alkoxide, which upon irradiation undergoes ligand to metal charge transfer (LMCT) to give alkoxy radical **98**, regenerating cerium (III) in the process (Scheme 3.5b). Ring opening of **98** *via* a *β*-scission process gives an alkyl radical that can add to the electron-deficient alkene,

giving a new alkyl radical intermediate **99**. Reduction by the excited state of DPA (DPA*) to enolate **100** and subsequent aldol reaction gives cycloheptanol **101**, which could also be isolated from the reaction. The addition of *p*-TsOH ensures complete lactonisation to **102**. This work highlights the ability of alkoxy radicals to allow the facile construction of complex and synthetically relevant compounds. The methodology for deconstructive functionalisation has been further developed to allow ketone (through *in situ* cyanohydrin formation) and lactol substrates to be used.[12,13]

Cerium (III/IV) photocatalysis has also been applied to acyclic alcohols. Firstly, König and co-workers reporting a cerium photocatalysed vicinal diol oxidative C-C bond cleavage in 2019 to give aldehydes.[14] Then, in a report with more application to synthesis, Zuo and co-workers reported a dehydroxymethylation of alcohols procedure that allowed the formation and reaction of alkyl radicals (Scheme 3.6).[15]

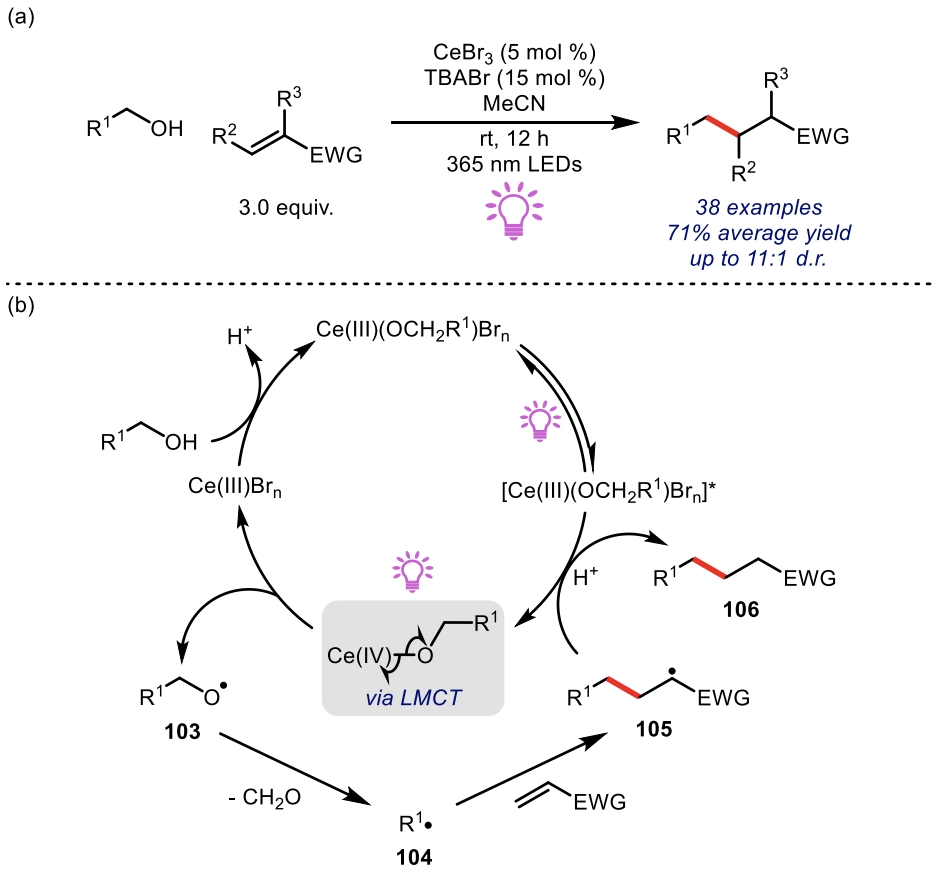

Scheme 3.6: Cerium photocatalysed alcohol dehydroxymethylation. (a) reaction scheme; (b) mechanistic proposal

In this work, simple alcohols are used to form alkyl radicals when irradiated with 365 nm LEDs in the presence of $CeBr_3$ (5 mol %) and TBABr (15 mol %). These alkyl radicals

then add to electron-deficient alkenes to form new alkane products, with 38 examples reported in a 71% average yield, and diastereomeric ratios of up to 11:1 were observed for appropriate examples (Scheme 3.6a). In this work more mechanistic studies were performed, including UV and Stern-Volmer quenching experiments, to allow the authors to propose a slightly different mechanism to that discussed in the previous example.

The authors propose a double-excitation mechanism, where the *in situ* formed cerium (IV) alkoxide is excited to the transient LMCT excited state and undergoes Ce-O bond homolysis to give alkoxy radical **103** and regenerates cerium (III) (Scheme 3.6b). Upon *β*-scission of **103**, alkyl radical **104** is formed with extrusion of formaldehyde. Addition of **104** to the electron-deficient alkene forms the new *α*-electron-withdrawing group alkyl radical **105**. This radical can be reduced by the excited state of the cerium (III) alkoxide complex (excited by 365 nm photons) and then protonated to give the desired product **106** whilst regenerating the cerium (IV) alkoxide complex ready for LMCT upon further irradiation. The alkyl radical formed upon *β*-scission, **104**, has since been used in a synergistic cerium and nickel catalysis protocol by the Zuo group to perform nickel cross-coupling reactions.[16]

3.1.1.2 Hydrogen Atom Transfers

This cerium photocatalysis approach to the generation of alkoxy radicals has also been applied to HAT chemistry, both intra- and intermolecularly. In 2018, Zuo and co-workers reported a selective *δ*-C-H functionalisation of alcohols using this methodology (Scheme 3.7).[17]

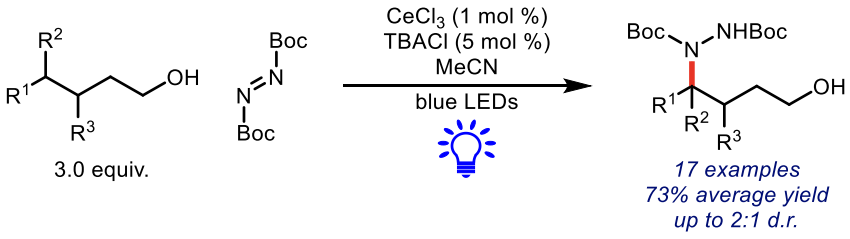

Scheme 3.7: Cerium photocatalysed δ-C-H functionalisation of alcohols

In this work, aliphatic alcohols can be selectively functionalised in the *δ*-position upon irradiation with blue LEDs when using $CeCl_3$ (1 mol %) and TBACl (5 mol %), to afford a range of *δ*-aminated alcohols. The authors reported 17 examples in an average yield of 73% with diastereomeric ratios of up to 2:1 for appropriate substrates. This work takes advantage of the higher BDE associated with O-H bonds vs. C-H bonds that make the HAT process thermodynamically favourable,[18] as well as the propensity of these systems

to proceed *via* a 6-membered cyclic transition state to selectively functionalise the *δ*-position.[2]

Subsequently, the Zuo group reported a related reaction that facilitates intermolecular HATs between alkoxy radicals and simple alkanes (Scheme 3.8).[19]

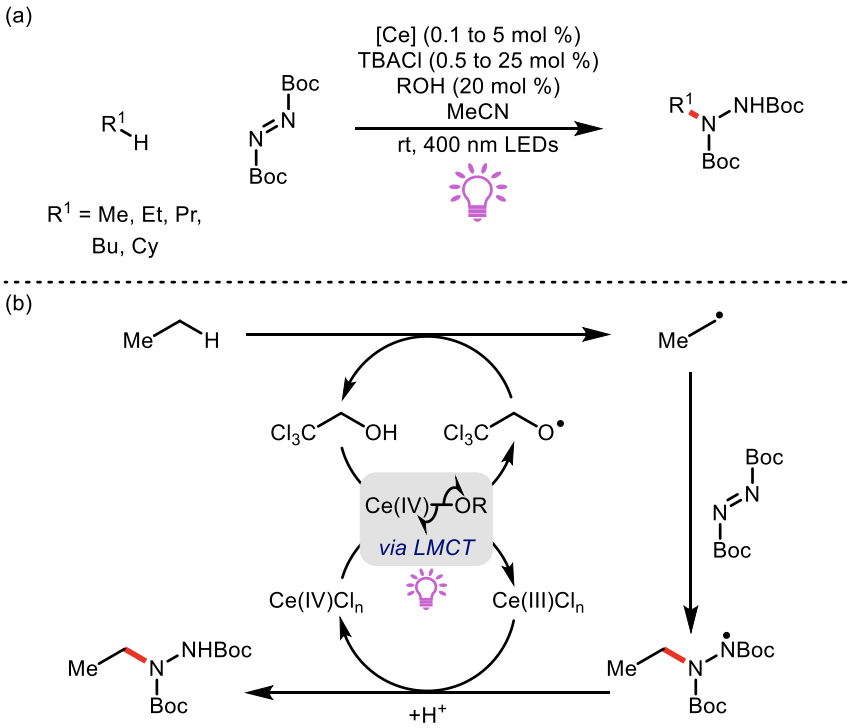

Scheme 3.8: Cerium photocatalysed alkane C-H functionalisation via alkoxy radials. (a) reaction scheme; (b) proposed mechanism

In this work, simple alkanes (methane, ethane, propane, butane, and cyclohexane) undergo C-H functionalisation in the presence of a simple alcohols (e.g., trichloroethanol) in catalytic quantities, a cerium (III) salt and TBACl under irradiation with 400 nm LEDs (Scheme 3.8a).

Mechanistically, an alkoxy radical is generated in a similar manner to as discussed previously (*via* photoinduced LMCT) which then abstracts a hydrogen from the simple alkane, again taking advantage of the higher BDE of O-H bonds vs. C-H bonds (Scheme 3.8b).[18] This process generates a new alkyl radical, as well as regenerates the alcohol catalyst, which then adds to the SOMOphile (DBAD) to give an *N*-centred radical. This *N*-centred radical acts as the terminal oxidant to regenerate the necessary cerium (IV) salt, and upon protonation the newly C-H aminated alkane product is furnished. Impressively, atmospheric pressures of propane and butane can be used to furnish the

aminated products. When using these gases, the products derived from the secondary alkyl radical are formed as the major products.

This work was later expanded in 2020 to allow for the generation of alkyl radicals on a vastly increased range of alkanes, as well as to expand the scope of the SOMOphiles that those alkyl radicals can be added to.[20]

3.1.2 Cerium Electrochemistry

There are few reports of cerium (III) being oxidised to cerium (IV) anodically for a synthetic transformation; however, in 2015 Moeller and co-workers reported an electrochemical oxidative condensation of syringaldehyde and 1,2-phenylenediamine to form benzimidazole using catalytic quantities of CAN (Scheme 3.9).[21]

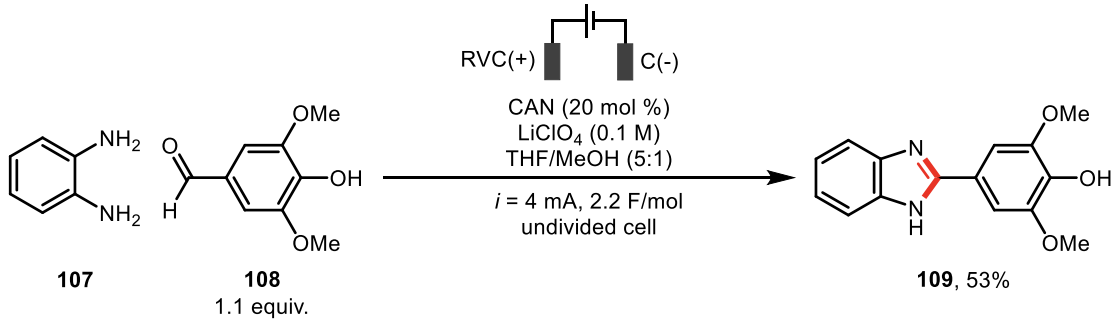

Scheme 3.9: Electrochemical cerium (IV)-catalysed oxidative condensation

In this reaction, 1,2-phenylenediamine **107** was electrolysed under galvanostatic conditions (*i* = 4 mA) along with syringaldehyde **108** (1.1 equiv.), CAN (20 mol %), and $LiClO_4$ (4.0 equiv.) in THF/MeOH (5:1). An RVC anode and a graphite cathode were employed, and the reaction was performed until 2.2 F/mol of charge had passed, furnishing the desired 2-arylbenzimidazole **109** in a 53% isolated yield. This reaction allowed the authors to synthesise one of the many electron-rich aromatic compounds they targeted in their work. Following this, in 2016 Moeller and co-workers then developed a paired electrolysis procedure in a divided cell. In the anodic chamber, they performed the same oxidative condensation reaction alongside a rhenium-catalysed CO_2 reduction to CO, in the cathodic chamber.[22]

3.1.3 Cerium Photoelectrochemistry

As discussed in chapter 1, photoelectrochemistry methodologies have received significant attention recently to allow access to transformations that are otherwise not possible using either photochemical or electrochemical approaches. In 2020, Xu and

co-workers applied a photoelectrochemical approach to a cerium-mediated decarboxylative C-H functionalisation of heteroarenes (Scheme 3.10).[23]

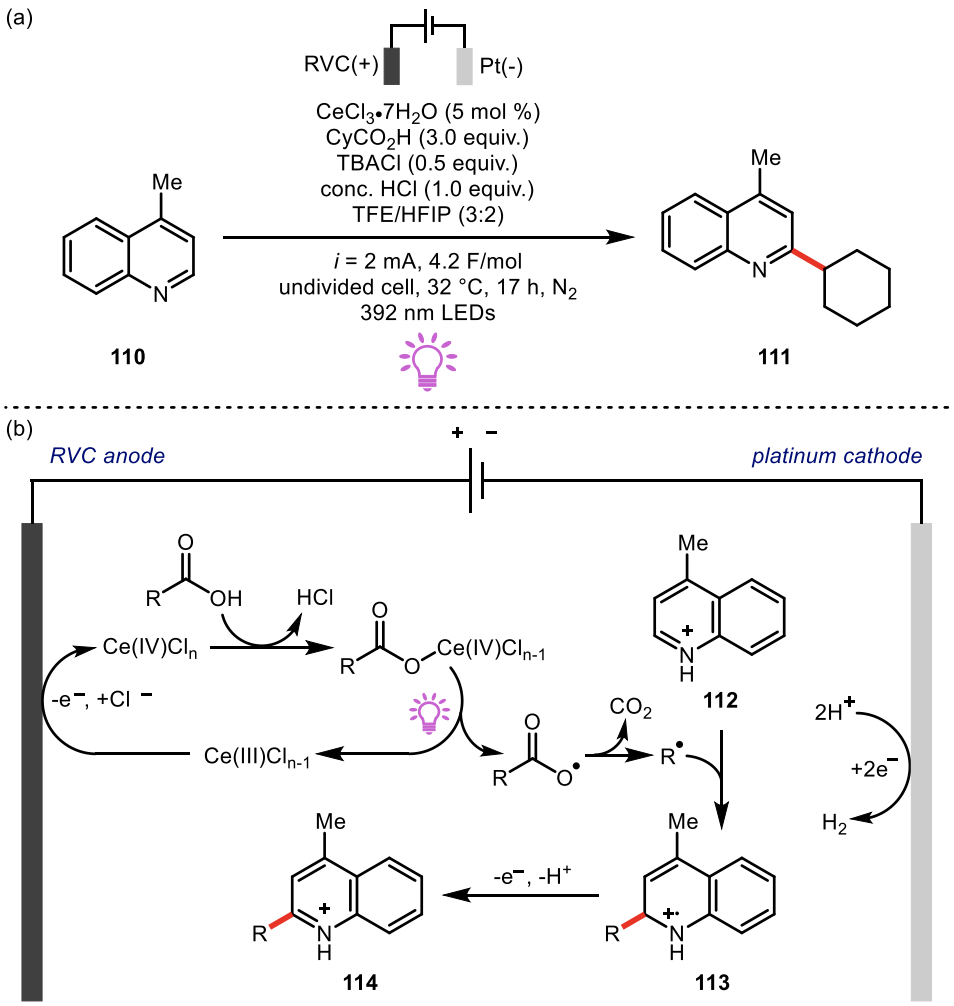

Scheme 3.10: Photoelectrochemical cerium-mediated decarboxylative C-H functionalisation of heteroarenes. (a) reaction scheme; (b) proposed mechanism

Using this procedure, heteroarenes such as lepidine **110** could be efficiently alkylated *via* a cerium-mediated radical decarboxylation under photoelectrochemical conditions to form cyclohexyl adduct **111** (Scheme 3.10a). The authors propose a photoelectrochemical cycle to generate a carboxyl radical, with the key Ce(IV)-O bond homolysis being initiated by irradiation with 392 nm LEDs (Scheme 3.10b). The resulting cerium (III) species is then oxidised back to cerium (IV) at the anode. The resulting carboxyl radical then undergoes radical decarboxylation to give an alkyl radical that can add to the protonated heteroarene SOMOphile **112** to give radical cation **113**. Subsequent single electron oxidation, either directly at the anode or by a cerium (IV) species, and re-aromatisation gives the protonated product **114** under the acidic

conditions. This photoelectrochemical approach, with cerium oxidation occurring at the anode, potentially allows for the use of a wide range of SOMOphiles. This is as the resulting radical species formed upon alkyl radical addition to the SOMOphile (e.g., **113**) is not required for re-oxidation of the cerium (III) species, as is the case with many of the previous examples discussed.

3.1.4 Aims and Objectives

The aim of the work disclosed in this chapter was to develop a new and alternate (photo)electrochemical system for the generation and reaction of alkoxy radicals. It was envisaged that this approach would allow us to overcome the limitations of the manganese-catalysed methodology developed in chapter 2, enabling ring opening of cycloalkanols of any size, and to enable deconstructive functionalisations other than chlorination.[24]

Taking inspiration from the seminal work of Zuo, as well as the work of Flowers, Moeller, and Xu, it was predicted that cerium (IV)-catalysed alkoxy radical generation and utilisation could be translated to an (photo)electrochemical system. It was hypothesised that the generation of cerium (IV) *via* anodic oxidation of cerium (III) would allow for compatibility of a wider range of SOMOphiles than disclosed in the works of Zuo. This in turn would enable the synthesis of a diverse selection of products, including the successful ring open cyclopentanols and larger cycloalkanols.

3.2 Results and Discussion

3.2.1 Substrate Synthesis

To commence our studies, the substrates that would be tested were first synthesised. Much like the work disclosed in chapter 2, a selection of tertiary cycloalkanols were synthesised from the corresponding cycloalkanones *via* addition of a Grignard reagent or an organolithium species (Scheme 3.11).

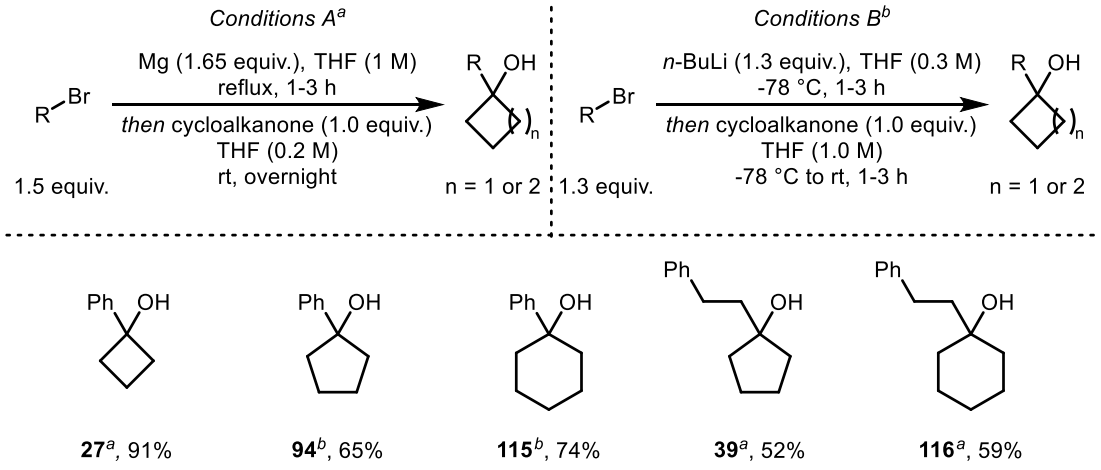

Scheme 3.11: Substrate synthesis

Using the Grignard procedure (conditions A), cyclobutanol **27**, cyclopentanol **39**, and cyclohexanol **116** were successfully synthesised using the previously generated phenylmagnesium bromide and phenethylmagnesium bromide respectively. 1-Phenyl substituted cyclopentanol **94** and cyclohexanol **115** were synthesised using the previously generated phenyl lithium species (conditions B). Good yields were obtained in the synthesis of all the substrates.

3.2.2 Preliminary Investigations

Initial investigations were focused on determining whether a stoichiometric quantity of cerium (IV) could facilitate the deconstructive functionalisation of cyclobutanol **27**, testing a small selection of SOMOphiles known to accept alkyl radicals; diphenyl disulfide **117**,[25–37] allyl sulfone **118**,[38–47] and benzothiazole **119** (Scheme 3.12).[48–56]

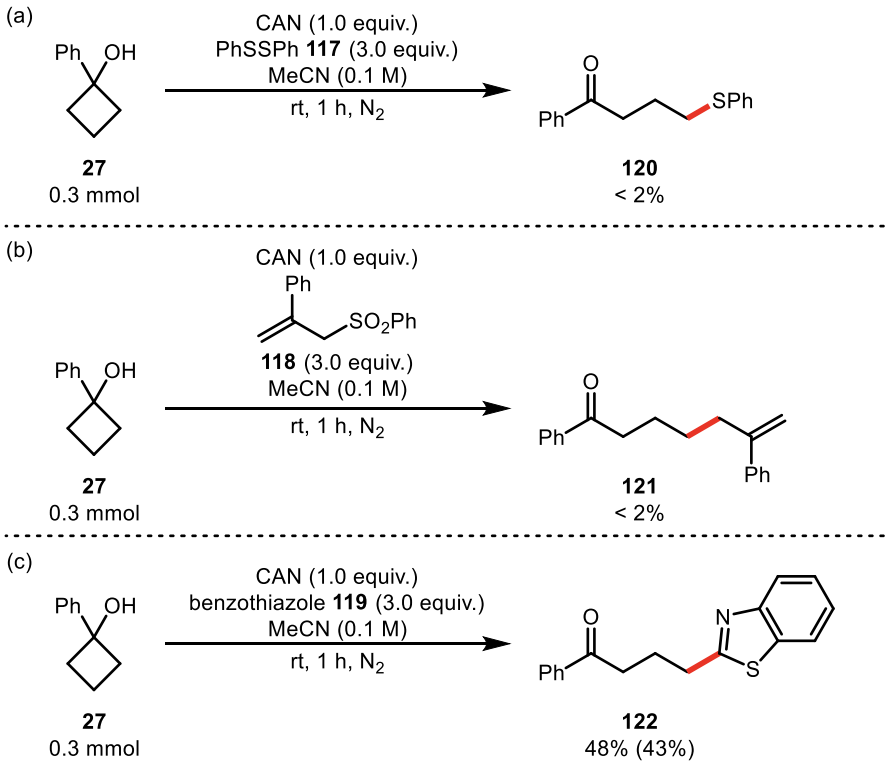

Yield as determined by ^{1}H NMR analysis of the crude reaction mixture with 1,3,5-trimethylbenzene as the internal standard. Isolated yield given in parentheses.

Scheme 3.12: Initial screening of SOMOphiles

In these preliminary investigations, **27** (0.3 mmol) was stirred in MeCN with CAN (1.0 equiv.) and the appropriate SOMOphile for 1 h to observe whether CAN could enable the deconstructive functionalisation of **27** using each SOMOphile. When diphenyl disulfide **117** (Scheme 3.12a) and allyl sulfone **118** (Scheme 3.12b) were tested, neither the desired sulfide **120**, nor the 1,1-disubstituted alkene **121** were observed upon ^{1}H NMR analysis of the crude reaction mixture. However, when benzothiazole was employed, *γ*-heteroaryl ketone **122** was successfully isolated in a 43% yield (Scheme 3.12c). This result highlights that CAN is able to facilitate the deconstructive heteroarylation of **27**.

With proof in hand that cerium (IV) can enable this transformation, attention then turned to translating this reaction to an electrochemical system that would allow the use of catalytic quantities of CAN, with the oxidation of cerium (III) to (IV) shown possible anodically (Table 3.1).[21–23]

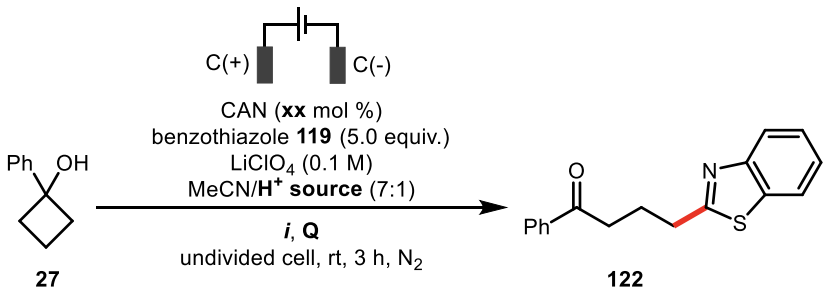

Entry[a]	xx (mol %)	H^+ source	*i* (mA)	Q (F/mol)	27[b] (%)	122[b] (%)
1	20	AcOH	5	1.87	40	44
2	20	MeOH	5	1.87	Observed	27
3	20	AcOH	-	-	93	6
4	0	AcOH	5	1.87	53	0

[a] Reactions performed using 0.3 mmol of cyclobutanol **27** using the ElectraSyn 2.0 batch electrochemical reactor. [**27**] = 0.05 M. [b] Yield as determined by ^{1}H NMR analysis of the crude reaction mixture with 1,3,5-trimethylbenzene as the internal standard.

Table 3.1: Initial electrochemical studies and test reactions

When **27** (0.3 mmol) was subjected to an electrochemical system composed of CAN (10 mol %), benzothiazole **119** (5.0 equiv.), and $LiClO_4$ (2.0 equiv.) in MeCN/AcOH (7:1) under a constant current of 5 mA for 3 h, **122** was obtained in a 44% yield by ^{1}H NMR analysis, with 40% recovery of **27** (entry 1). Changing the proton source from AcOH to MeOH afforded **122** in a 27% yield (entry 2). Control reactions were then performed, showing that both the applied current (entry 3) and CAN (entry 4) were necessary for successful conversion of **27** to **122**. The formation of some **122** in the absence of an applied current was expected as cerium (IV) is the oxidation state required for the transformation (see Scheme 3.12c). In the absence of CAN, only 53% of **27** was recovered, and this is presumably due to starting material decomposition under the electrolysis conditions when no productive pathway is possible.

From these results, we were satisfied that we had a working reaction that could be optimised; however, we first wanted to explore whether we would be able to apply the conditions to facilitate the ring opening of cyclopentanols and cyclohexanols, as well as explore using alternative SOMOphiles.

3.2.3 Screen of Cyclopentanols and Cyclohexanols

Initial attempts were focused on expanding the reaction so that cyclopentanols and cyclohexanols could be ring opened to form *δ*- and *ϵ*-substituted ketones respectively. The first substrates tried were the 1-phenyl substituted cyclopentanol **94** and cyclohexanol **115**, the direct analogues of cyclobutanol **27** (Table 3.2).

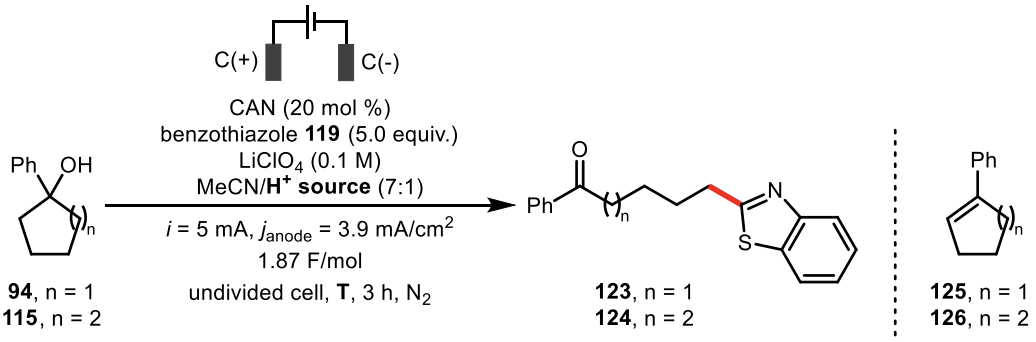

Entry[a]	n	H+ source	T (°C)	94/115[b] (%)	123/124[b] (%)	125/126[b] (%)
1	1	AcOH	rt	< 2	< 2	21
2	1	MeOH	rt	83	< 2	< 2
3	1	HFIP	rt	78	< 2	5
4	1	MeOH	50	78	< 2	4
5	1	HFIP	50	57	< 2	14
6	2	AcOH	rt	91	< 2	< 2
7	2	MeOH	rt	94	< 2	< 2
8	2	HFIP	rt	> 98	< 2	< 2
9	2	MeOH	50	> 98	< 2	< 2
10	2	HFIP	50	84	< 2	< 2

[a] Reactions performed using 0.3 mmol of cyclopentanol **94** or cyclohexanol **115** using the ElectraSyn 2.0 batch electrochemical reactor. [**94/115**] = 0.05 M. [b] Yield as determined by ^{1}H NMR analysis of the crude reaction mixture with 1,3,5-trimethylbenzene as the internal standard.

*Table 3.2: Testing of 1-phenylcyclopentan-1-ol **94** and 1-phenylcyclohexan-1-ol **115***

The reactions were performed using either **94** or **115** (0.3 mmol), CAN (20 mol %), **119** (5.0 equiv.), and $LiClO_4$ (2.0 equiv.) in a solvent system comprised of MeCN and a protic solvent that enables proton reduction at the cathode. A constant current of 5 mA was applied to the reaction, using graphite electrodes, for 3 h at the specified temperature. When using cyclopentanol **94** with AcOH at rt (entry 1), the observed product was alkene **125**.[57] There was no detection of the desired product **123** and full decomposition of **94** was observed. The formation of alkene **125** presumably proceeds *via* ionisation of the C-O bond upon protonation of the tertiary alcohol under the acidic conditions. Changing the proton source to the less acidic MeOH or HFIP suppressed the decomposition of **94** to **125** but did not enable the formation of **123** (entries 2 and 3). Increasing the reaction temperature to 50 °C only resulted in increased decomposition of **94** to **125**, with no **123** detected with either MeOH or HFIP as the proton source (entries 4 and 5).

Cyclohexanol **115** was also subjected to the same conditions as **94** (entries 6-10) and in these reactions a high recovery of **115** was observed in each reaction (> 80%), with no

detection of the desired heteroarylated product **124**. Interestingly, alkene **126** was not observed in any case.

Due to the observations that cyclobutanol **27** was ring opened to **122** more successfully with AcOH then MeOH as the proton source, and that cyclopentanol **94** decomposed when AcOH used, 1-phenethyl substituted cyclopentanol **39** and cyclohexanol **116** were then tested as model substrates. It was hypothesised that changing the substituent in the 1-position from a phenyl ring to a phenethyl chain would suppress the ionisation of the C-O bond in the presence of AcOH, which may lead to successful deconstructive heteroarylation to the corresponding products **127** and **128** (Table 3.3).

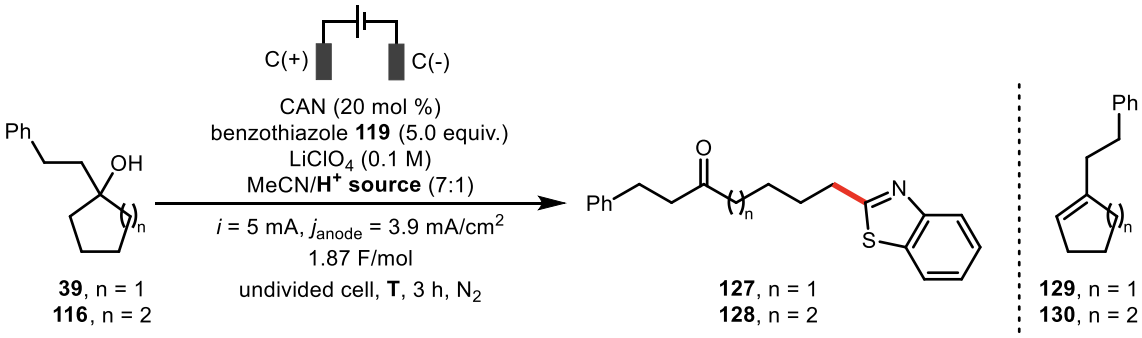

Entry[a]	n	H+ source	T (°C)	39/116[b] (%)	127/128[b] (%)	129/130[b] (%)
1	1	AcOH	rt	95	< 2	< 2
2	1	MeOH	rt	91	< 2	< 2
3	1	HFIP	rt	85	< 2	< 2
4	1	AcOH	50	70	< 2	< 2
5	1	MeOH	50	92	< 2	< 2
6	1	HFIP	50	79	< 2	< 2
7	2	AcOH	rt	88	< 2	< 2
8	2	MeOH	rt	90	< 2	< 2
9	2	HFIP	rt	80	< 2	< 2
10	2	AcOH	50	73	< 2	< 2
11	2	MeOH	50	79	< 2	< 2
12	2	HFIP	50	77	< 2	< 2

[a] Reactions performed using 0.3 mmol of cyclopentanol **39** or cyclohexanol **116** using the ElectraSyn 2.0 batch electrochemical reactor. [**39/116**] = 0.05 M. [b] Yield as determined by ^{1}H NMR analysis of the crude reaction mixture with 1,3,5-trimethylbenzene as the internal standard.

*Table 3.3: Testing of 1-phenethylcyclopentan-1-ol **39** and 1-phenethylcyclohexan-1-ol **116***

Cyclopentanol **39** and cyclohexanol **116** were each tested under the same reaction conditions, with reactions performed using AcOH, MeOH, or HFIP as the proton source at rt and at 50 °C. Although changing the substituent in the 1-position did prevent the

formation of the corresponding alkenes **129** and **130** as hoped, both **39** and **116** were remarkably unreactive under all conditions. The desired heteroarylated ketones **127** and **128** were not observed by ^{1}H NMR in any case, with large quantities (> 70%) of **39** and **116** recovered throughout.

The lack of reactivity observed with both cyclopentanols (**39** and **94**) and both cyclohexanols (**115** and **116**) aligns with the findings of Roček and co-workers, who found that cyclobutanol underwent significantly faster single electron oxidation with CAN than cyclopentanol ($k = 6.2\ M^{-1}s^{-1}$ vs. $2.2x10^{-5}\ M^{-1}s^{-1}$ in MeCN).[5] Due to the unreactive nature of these substrates, it seemed that attempts to solve the ring size limitation observed in the work disclosed in chapter 2 would not be overcome in this work. Therefore, attention then turned to exploring the compatibility of alternative SOMOphiles under this reaction system.

3.2.4 Screen of SOMOphiles

Firstly, a series of salts where subjected to the reaction condition to access one of two possible reactivity modes. In the first potential mode, anodically generated reactive radical species could be accessed from the anion, which could undergo radical-radical coupling with the alkyl radical intermediate formed after alkoxy radical *β*-scission. The second possibility was that a Ce(IV)-X species could be formed that could act as a transfer reagent for the anionic component, in a similar manner to the Mn(III)-Cl species observed in chapter 2 (Table 3.4).

The reactions were performed using cyclobutanol **27** (0.3 mmol), CAN (20 mol %), the appropriate salt (5.0 equiv.), and $LiClO_4$ (2.0 equiv.) in MeCN/AcOH (7:1) under a constant current of 5 mA for 3 h. Initially, the halide salts $MgCl_2$, KBr, and NaI were tested, along with NaN_3 and the trifluoromethyl radical source sodium trifluoromethanesulfinate. These were tested with the aim with the aim of forming the *γ*-halogenated ketones **28**, **131**, and **132**, *γ*-azido ketone **133**, and *γ*-trifluoromethyl ketone **134**; however, no product was observed by ^{1}H NMR in any case, with > 80% recovery of **27** (entries 1-5). During each of these experiments, the operating cell potential was lower than the potential observed when using **119** as the SOMOphile, possibly indicating that preferential oxidation of these anions was occurring at the anode over the oxidation of cerium (III) to (IV), leading to no reaction. NaCN was also tested and no *γ*-cyano ketone **125** was observed by ^{1}H NMR, with only 56% of **27** recovered, perhaps indicating that no productive electrochemical pathway leads to substrate decomposition.

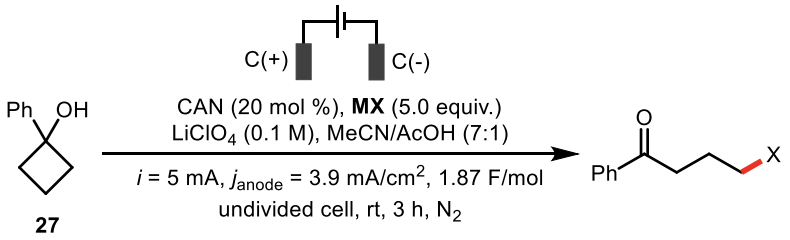

27

Entry[a]	MX	X	27[b] (%)	Product[b] (%)
1	$MgCl_2$	Cl (**28**)	81	< 2
2	KBr	Br (**131**)	97	< 2
3	NaI	I (**132**)	96	< 2
4	NaN_3	N_3 (**133**)	94	< 2
5	$NaSO_2CF_3$	CF_3 (**134**)	86	< 2
6	NaCN	CN (**135**)	56	< 2

[a] Reactions performed using 0.3 mmol of cyclobutanol **27** using the ElectraSyn 2.0 batch electrochemical reactor. [**27**] = 0.05 M. [b] Yield as determined by ^{1}H NMR analysis of the crude reaction mixture with 1,3,5-trimethylbenzene as the internal standard.

Table 3.4: Screen of salts

The results disclosed in table 3.4 seem to indicate that performing a radical-radical type coupling is not feasible under these reaction conditions, and that no Ce(IV)-X complex was being formed when using any of the salts tested. Therefore, to align more closely with the reaction using benzothiazole **119**, SOMOphiles that can act as radical traps were tested (Scheme 3.13).

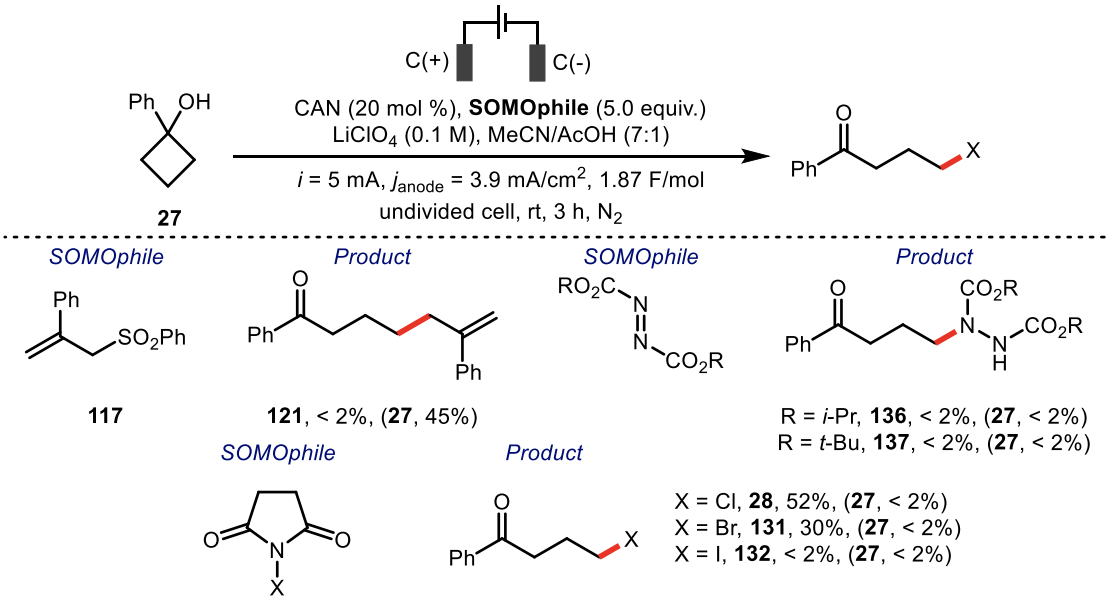

Yield as determined by ^{1}H NMR analysis of the crude reaction mixture with 1,3,5-trimethylbenzene as the internal standard. Recovery of **27** given in parentheses.

Scheme 3.13: Initial screen of SOMOphiles

The reactions were ran using the same conditions as when using the salts in Table 3.4, only with the appropriate SOMOphile (5.0 equiv.). When using allyl sulfone **117**, none of the desired alkene product **121** was observed by ^{1}H NMR, nor any alkene isomer products, and 45% of **27** was recovered. The azocarboxylates DIAD and DBAD were then tested, with neither of the corresponding hydrazines, **136** and **137**, being detected, and full decomposition of **27** was observed. *N*-Halosuccinimides were then tested, with NCS and NBS pleasingly giving the *γ*-chloro ketone **27** and *γ*-bromo ketone **131** in 52% and 30% yields by ^{1}H NMR respectively, although with no **27** remaining. On the other hand, NIS did not afford any of the *γ*-iodo analogue **132**, with the low operating potential observed indicating preferential oxidation of iodide to iodine over oxidation of cerium (III) to (IV).

Following the promising results observed when using NCS and NBS, control reactions were performed to ensure that both the CAN and the applied current were necessary for these transformations (Table 3.5).

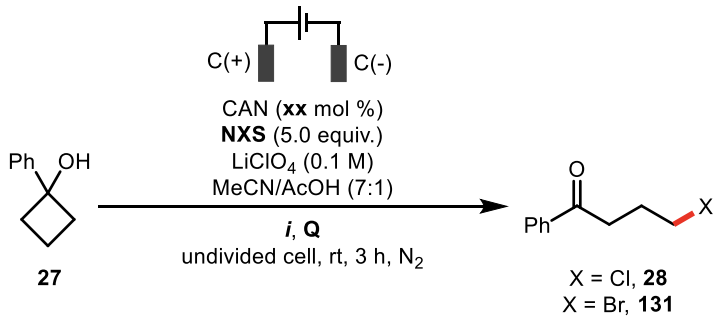

Entry[a]	X	xx (mol %)	*i* (mA)	Q (F/mol)	27[b] (%)	28/131[b] (%)
1	Cl	20	5	1.87	< 2	52
2	Cl	20	0	0	< 2	10
3	Cl	0	5	1.87	< 2	10
4	Br	20	5	1.87	< 2	30
5	Br	20	0	0	< 2	49
6	Br	0	5	1.87	< 2	9

[a] Reactions performed using 0.3 mmol of cyclobutanol **27** using the ElectraSyn 2.0 batch electrochemical reactor. [**27**] = 0.05 M. [b] Yield as determined by ^{1}H NMR analysis of the crude reaction mixture with 1,3,5-trimethylbenzene as the internal standard.

Table 3.5: Control reactions using NCS and NBS

When using NCS, 10% of **28** was detected by ^{1}H NMR both in the absence of CAN and without an applied current (entries 2 and 3). Interestingly, when using NBS the yield of **131** improved from 30% to 49% in the absence of an applied current, suggesting that cerium (III) can be re-oxidised to cerium (IV) under these reaction conditions (entry 5). In

the absence of CAN, the yield of **131** obtained was similar to using NCS (entry 6). The results suggest that the *N*-halosuccinimide, or intermediates originating from it, may be responsible for the regeneration of the active cerium (IV) species. A possible explanation may come from evaluation of the resulting succinimide radical upon halogen extraction and comparing it to the radical obtained when SOMOphile such as **119** is used (Scheme 3.14).

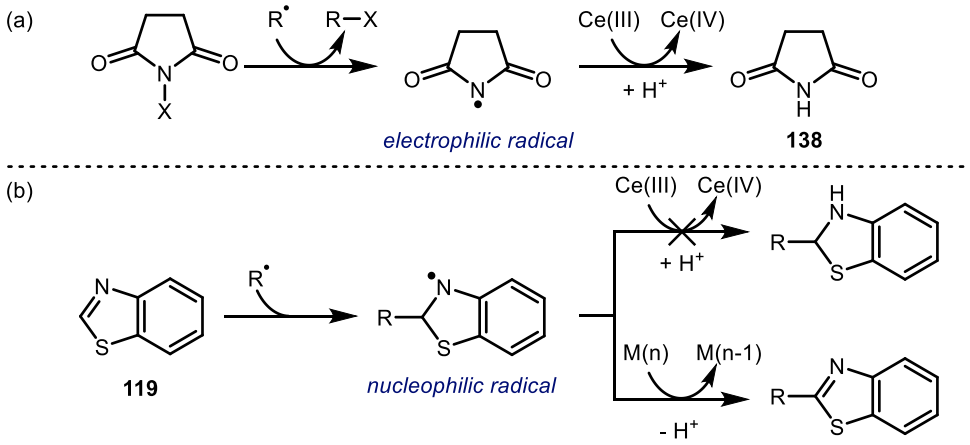

Scheme 3.14: Evaluation of radical intermediates when using different SOMOphiles

When using an *N*-halosuccinimide (Scheme 3.14a), an alkyl radical performs a halogen atom transfer to generate the succinimidyl radical. This radical can be characterised as being nucleophilic in nature as the corresponding anion is more stable than the corresponding cation. Therefore, this radical is susceptible to reduction and protonation to give succinimide **138**, which could be performed by cerium (III) to regenerate the necessary cerium (IV) species. As the N-Br bond in NBS is more susceptible to homolysis than the N-Cl bond in NCS, there may be a higher concentration of the succinimide radical available to oxidise cerium (III), perhaps explaining the increased yield obtained in the absence of an applied current when using NBS compared to using NCS.

When using benzothiazole **119** (Scheme 3.14b), addition of an alkyl radical forms a nitrogen centred radical which can be characterised as being nucleophilic in nature. Reduction and protonation, as in the case of the succinimidyl radical, is a reasonable pathway to follow; however, more favoured is oxidation and subsequent deprotonation which leads to rearomatisation of the benzothiazole moiety.

To prevent the auto-catalytic activity observed when using NBS, only SOMOphiles that would result in nucleophilic radicals upon interaction with the alkyl radical were subsequently tested (Scheme 3.15).

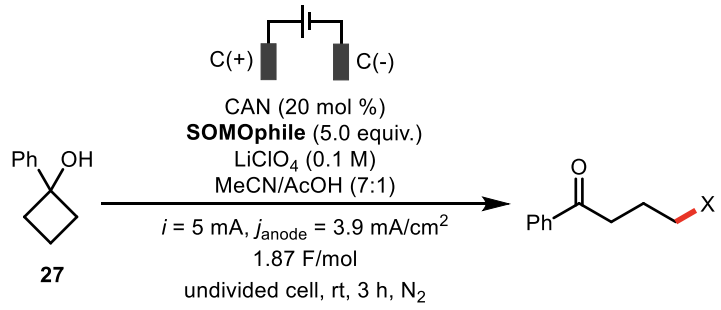

SOMOphile	*Product*	*SOMOphile*	*Product*
	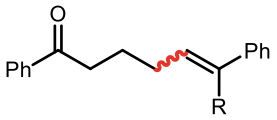	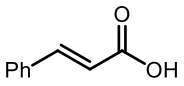	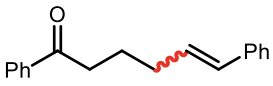
R = H, **139** R = Me, **140**	R = H, **141**, < 2%, (**27**, 41%) R = Me, **142**, < 2% (**27**, 53%)	**143**	**141**, < 2%, (**27**, 70%)
SOMOphile	*Product*	*SOMOphile*	*Product*
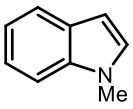	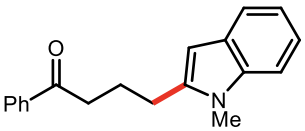	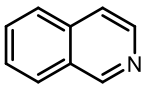	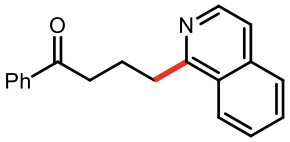
144	**145**, 31%, (**27**, 73%)	**146**	**147**, < 2%, (**27**, 88%)
SOMOphile	*Product*	*SOMOphile*	*Product*
	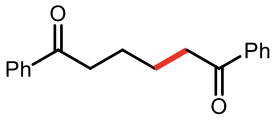	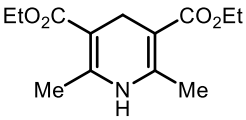	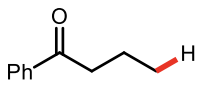
148	**149**, < 2%, (**27**, < 2%)	**150**	**151**, < 2%, (**27**, 89%)
SOMOphile	*Product*	*SOMOphile*	*Product*
	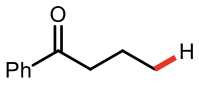	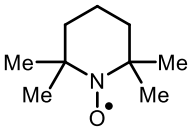	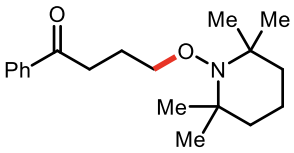
152	**151**, < 2%, (**27**, > 98%)	**153**	**154**, < 2%, (**27**, > 98%)

Yield as determined by ^{1}H NMR analysis of the crude reaction mixture with 1,3,5-trimethylbenzene as the internal standard. Recovery of **27** given in parentheses.

Scheme 3.15: Screen of SOMOphiles that result in nucleophilic radicals

Initial tests using styrene **139** and *α*-methylstyrene **140** only resulted in partial substrate decomposition (41% and 53% recovery of **27** respectively) and no detection of either isomer of the desired alkenes **141** and **142**. Utilisation of (*E*)-cinnamic acid **143**, which would also give the alkene product **141** upon radical addition followed by oxidative decarboxylation, was also not productive under the reaction conditions. *N*-Heterocycles

were also screened under the reaction conditions, with *N*-methyl indole **144** giving a 31% yield of **145** by ^{1}H NMR with full mass balance observed. Unfortunately, **145** could not be isolated from the reaction. Isoquinoline **146** was not successful as a SOMOphile, with **147** not observed and a high recovery of **27** obtained. When using **148**, the TBS-enol ether of acetophenone, the proton source was changed to MeOH; however, this did not prevent hydrolysis back to the ketone in the reaction, with a conversion back to acetophenone of > 90% observed. The desired dione **149** was not observed by ^{1}H NMR, and **27** had fully decomposed. Using a Hantzsch ester **150** and 1,4-cyclohexadiene **152** as hydrogen atom sources did not yield any of the desired butanone product **151**, again with high recoveries of **27** observed, likely due to preferential oxidation of the hydrogen atom sources to the corresponding pyridine derivative and benzene. Finally, TEMPO **153** was tested in the hope of forming hydroxylamine adduct **154** *via* a radical-radical coupling, but no product was observed by ^{1}H NMR.

After an extensive screen of various SOMOphiles, with most showing no signs of product formation, it was decided that focus should be brought back to optimising the reaction using benzothiazole as the SOMOphile. It was hoped that after optimal conditions were found that some of the SOMOphiles screened in this section may then be compatible under those new reaction conditions.

3.2.5 Optimisation of Benzothiazole System

With all attempts to ring open cyclopentanols and cyclohexanols (section 3.2.3) and attempts to utilise alternative SOMOphiles (section 3.2.4) proving unsuccessful, the original system utilising benzothiazole was revisited for optimisation. The first steps for this optimisation including the repetition of the initial hit obtained (Table 3.1, entry 1), which immediately brought to light irreproducibility problems with the electrochemical reaction system (Table 3.6).

All the reactions discussed in table 3.6 were performed by subjecting **27** (0.3 mmol), CAN (20 mol %), **119** (5.0 equiv.), and $LiClO_4$ (2.0 equiv.) in MeCN/AcOH (7:1) to a constant current of 5 mA for 3 h using graphite electrodes. Initial repeats of the original hit showed a remarkable variation in the yield of **122** obtained, ranging from 12% to 44% (entries 1-3). To attempt to identify a possible reason for the irreproducibility, each component of the reaction was changed methodically, with new graphite electrodes, and new batches of **27**, **119**, CAN, and $LiClO_4$ used (entries 4-8), with fresh solvents used in every case. Despite these changes, no trend was observed that could explain the irreproducibility of the reaction.

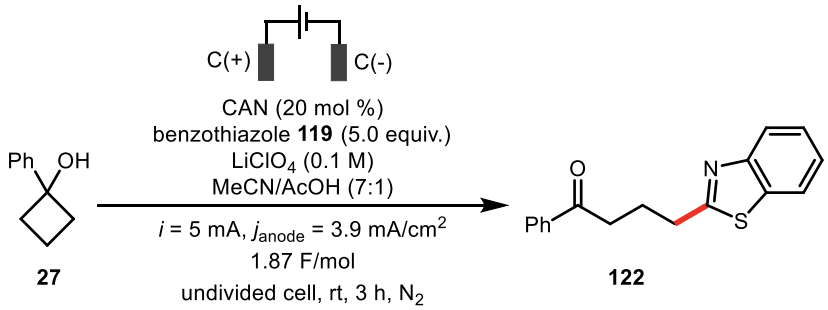

Entry[a]	27[b] (%)	122[b] (%)	Notes
1	40	44	N/A
2	40	32	N/A
3	60	12	N/A
4	55	11	New electrodes used
5	47	22	New batch of **27**
6	50	10	New bottle of **119**
7	56	8	New batch of CAN
8	51	33	New $LiClO_4$

[a] Reactions performed using 0.3 mmol of cyclobutanol **27** using the ElectraSyn 2.0 batch electrochemical reactor. [**27**] = 0.05 M. [b] Yield as determined by ^{1}H NMR analysis of the crude reaction mixture with 1,3,5-trimethylbenzene as the internal standard.

Table 3.6: Repetition of parent reaction using benzothiazole

It was thought that upon optimisation the reproducibility of the reaction could be improved. Due to the observation of significant amounts of **27** recovered when 1.87 F/mol of charge was passed, extending the amount of charge passed was first explored (Table 3.7).

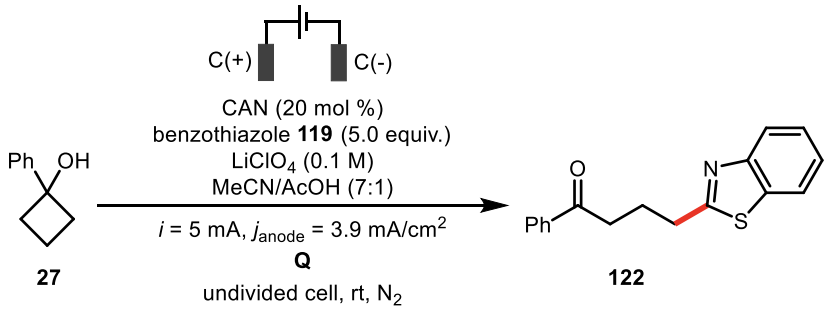

Entry[a]	Q (F/mol)	27[b] (%)	122[b] (%)
1	2.00	68	10
2	3.00	34	8
3	4.00	42	10

[a] Reactions performed using 0.3 mmol of cyclobutanol **27** using the ElectraSyn 2.0 batch electrochemical reactor. [**27**] = 0.05 M. [b] Yield as determined by ^{1}H NMR analysis of the crude reaction mixture with 1,3,5-trimethylbenzene as the internal standard.

Table 3.7: Screen of charge passed

The extension of the reaction time, to pass a higher charge, showed no improvement in the yield of **122** observed by ^{1}H NMR, with only decreases in the amount of **27** recovered. This suggested that there was no oxidation of cerium (III) to cerium (IV) occurring at the anode, leading to decomposition of **27** with no productive pathway to follow.

Attempts to improve the efficiency of electron transfer process between the anode and cerium (III) were made by altering the solvent system, the anode material, and the electrolyte (Table 3.8).

Initially, changes to the proton source were made, with MeOH, HFIP, and water tested, with decreases in the yield of **122** observed, significantly so when using HFIP and water, albeit with higher recoveries of **27** observed (entries 1-3). When using a THF/MeOH solvent system no **122** was detected either (entry 4). Utilisation of an RVC anode, in both MeCN/AcOH and THF/MeOH solvent systems showed low conversions of **27** to **122** (entries 5 and 6). Finally, the supporting electrolyte was changed from $LiClO_4$ to $TBAPF_6$, which also saw a decrease in the yield of **122** to 16% (entry 7).

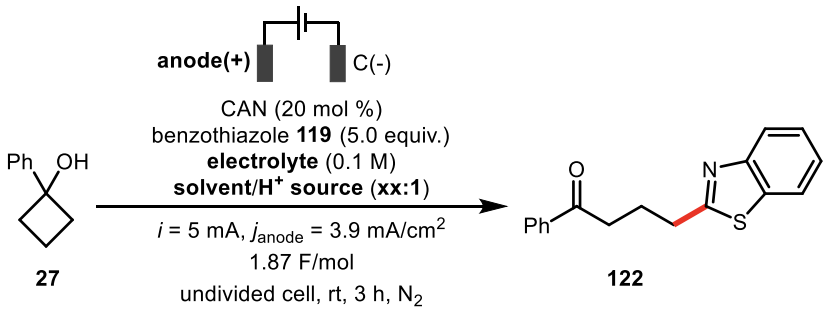

Entry[a]	Anode	Electrolyte	Solvent	H^+ source	27[b] (%)	122[b] (%)
1	graphite	$LiClO_4$	MeCN	MeOH	34	26
2	graphite	$LiClO_4$	MeCN	HFIP	71	14
3	graphite	$LiClO_4$	MeCN	H_2O	74	5
4	graphite	$LiClO_4$	THF	MeOH	66	< 2
5	RVC	$LiClO_4$	MeCN	AcOH	53	18
6	RVC	$LiClO_4$	THF	MeOH	74	4
7	graphite	$TBAPF_6$	MeCN	AcOH	40	16

[a] Reactions performed using 0.3 mmol of cyclobutanol **27** using the ElectraSyn 2.0 batch electrochemical reactor. [**27**] = 0.05 M. [b] Yield as determined by ^{1}H NMR analysis of the crude reaction mixture with 1,3,5-trimethylbenzene as the internal standard.

Table 3.8: Screen of solvent system, anode material, and electrolyte

With a range of conditions now screened with no success in improving the yield of **122** obtained, the effect of the reaction temperature was then explored (Table 3.9).

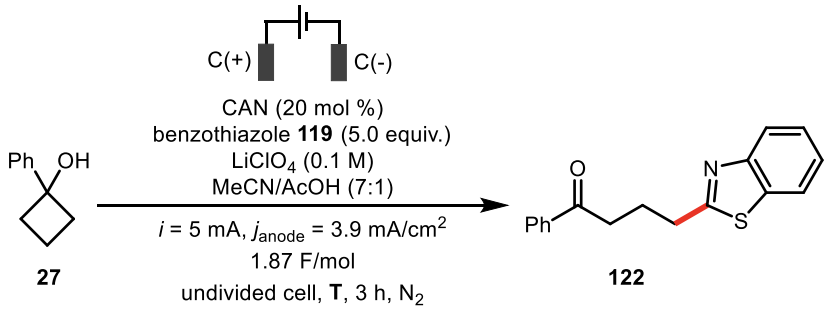

Entry[a]	T (°C)	27[b] (%)	122[b] (%)
1	0	49	14
2	25	28	10
3	40	30	10

[a] Reactions performed using 0.3 mmol of cyclobutanol **27** using the ElectraSyn 2.0 batch electrochemical reactor. [**27**] = 0.05 M. [b] Yield as determined by ^{1}H NMR analysis of the crude reaction mixture with 1,3,5-trimethylbenzene as the internal standard.

Table 3.9: Screen of temperature

Reactions were performed at 0 °C, 25 °C (in a temperature-controlled water bath, as opposed to all experiments performed at rt), and at 40 °C. It seems that temperature has little effect on the outcome of the reaction, with similar ^{1}H NMR yields of **27** obtained at all temperatures. The results do likely indicate that the source of the irreproducibility observed was not fluctuations in the ambient laboratory temperature day to day, with the reaction at 25 °C (entry 2) providing a much lower yield compared to the original hit.

At this point, the cerium source had remained consistent, with CAN used for all experiments. Therefore, $CeCl_3$ was tested in tandem with TBA salt additives, as in the work of Zuo discussed in section 1 (Table 3.10).[2,10,11,15,17,19,20]

In these reactions $CeCl_3$ was used as the cerium source (20 mol %), with TBABr or TBACl (40 mol %) and $LiClO_4$ (2.0 equiv.), or 2.0 equiv. of the TBA salt to act as the supporting electrolyte also. The change from CAN to $CeCl_3$ did not positively impact the yield, with no **122** observed by ^{1}H NMR in any of the reactions ran, perhaps suggesting that no cerium (IV) was anodically generated.

With no improvements observed in the yield of **122** obtained nor the reproducibility of the electrochemical process, attention was then turned to the development of a photoelectrochemical approach to perform the cerium-catalysed deconstructive heteroarylation.

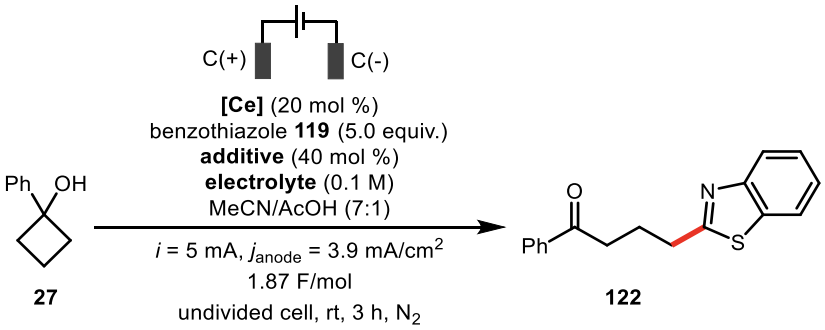

Entry[a]	[Ce]	Additive	Electrolyte	27[b] (%)	122[b] (%)
1	$CeCl_3$	TBABr	$LiClO_4$	96	< 2
2	$CeCl_3$	None	TBABr	> 98	< 2
3	$CeCl_3$	TBACl	$LiClO_4$	63	< 2
4	$CeCl_3$	None	TBACl	96	< 2

[a] Reactions performed using 0.3 mmol of cyclobutanol **27** using the ElectraSyn 2.0 batch electrochemical reactor. [**27**] = 0.05 M. [b] Yield as determined by ^{1}H NMR analysis of the crude reaction mixture with 1,3,5-trimethylbenzene as the internal standard.

Table 3.10: Screen of cerium source and additives

3.2.6 Photoelectrochemistry

Before commencing our studies on the photoelectrochemical generation of alkoxy radicals using cerium (III) sources, we first wanted to confirm that our photoelectrochemical system was set up correctly to ensure the validity of all results obtained in our studies. To do so, the photoelectrochemical decarboxylative C-H heteroarylation reported from Xu was performed in our system (Scheme 3.16).[23]

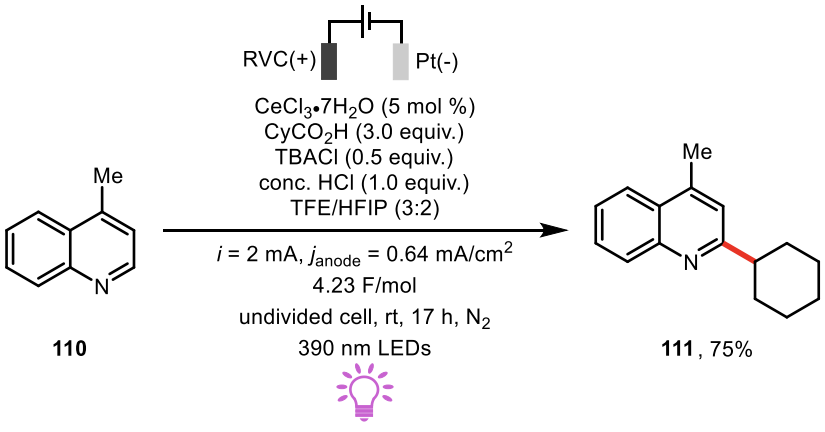

Yield as determined by ^{1}H NMR analysis of the crude reaction mixture with 1,3,5-trimethylbenzene as the internal standard.

Scheme 3.16: Repeat of Xu's photoelectrochemical decarboxylative C-H heteroarylation

Pleasingly, when Xu's reaction conditions were translated to an ElectraSyn vial and electrolysed under a constant current of 2 mA for 17 h under irradiation with 390 nm LEDs, the desired cyclohexyl substituted quinoline **111** was detected in a 75% yield by ^{1}H NMR. This result gave confidence that the photoelectrochemical system that had been set up was viable and that any subsequent results using the system could be trusted.

With the success of the control reaction, Xu's conditions were then translated to our desired reaction, the deconstructive heteroarylation of **27** under photoelectrochemical conditions (Table 3.11).

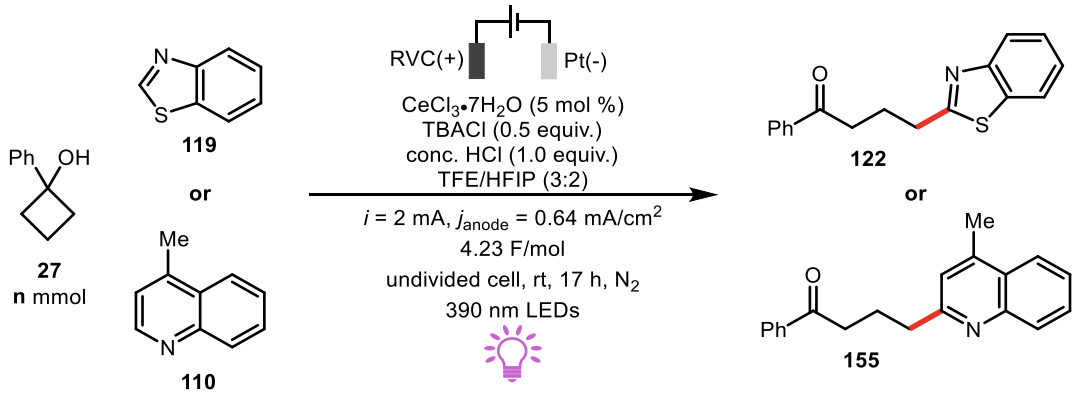

Entry[a]	n (mmol)	SOMOphile (equiv.)	27[b] (%)	122/155[b] (%)
1	0.3	**119** (3.0)	< 2	< 2
2	0.9	**119** (0.3)	< 2	< 2
3	0.3	**110** (3.0)	< 2	< 2
4	0.9	**110** (0.3)	< 2	< 2

[a] Reactions performed using 0.3 mmol of cyclobutanol **27** using the ElectraSyn 2.0 batch electrochemical reactor. [**27**] = 0.05 M. [b] Yield as determined by ^{1}H NMR analysis of the crude reaction mixture with 1,3,5-trimethylbenzene as the internal standard.

Table 3.11: Initial photoelectrochemical investigations

In these reactions, cyclobutanol **27** and either **119** or **110** were reacted with $CeCl_3$•$7H_2O$, TBACl, and conc. HCl in TFE/HFIP (3:2) under galvanostatic conditions (i = 2 mA) for 17 h with irradiation by 390 nm LEDs, to give either 2-substituted benzothiazole **122** or 2-substituted quinoline **155**. When using each SOMOphile, **27** was used both as the limiting reagent or in an excess (mimicking Xu's conditions); however, in no case was any product observed by ^{1}H NMR. There was also no detection of any **27** remaining at the end of any reaction, likely due to decomposition under the highly acidic conditions used.

To move away from the highly acidic conditions from using conc. HCl, a photoelectrochemical system with conditions more reminiscent of those utilised in section 3.2.5 were then employed, again using either benzothiazole **119** or lepidine **110** as

SOMOphiles to form the desired deconstructive heteroarylated products **122** or **155** (Table 3.12).

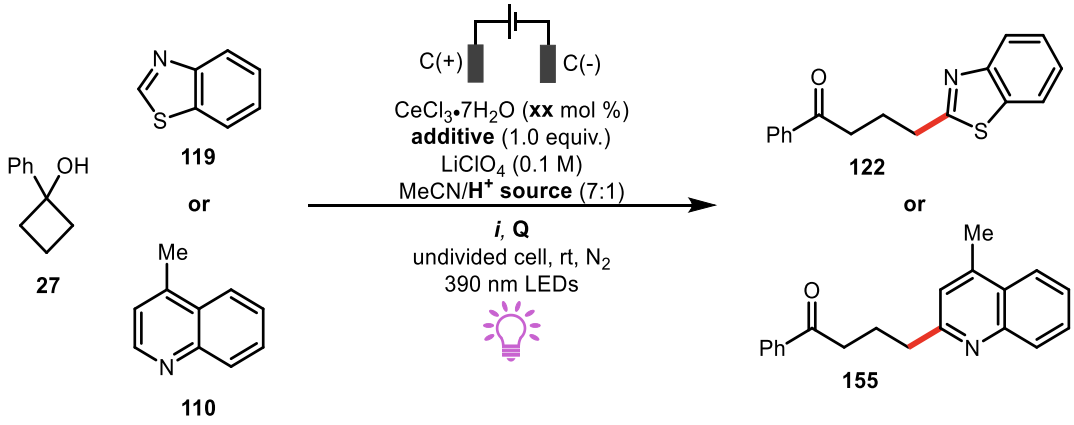

Entry[a]	xx (mol %)	SOMOphile (equiv.)	Additive	H^+ source	*i* (mA)	Q (F/mol)	27[b] (%)	122/155[b] (%)
1	5	**119** (1.5)	None	AcOH	2	4.2	< 2	< 2
2	5	**119** (1.5)	None	AcOH	2	2.0	20	< 2
3	5	**119** (1.5)	None	AcOH	5	2.0	51	< 2
4	10	**119** (1.5)	$MgCl_2$	AcOH	10	2.0	70	< 2
5	10	**119** (1.5)	TBACl	AcOH	10	2.0	73	< 2
6	10	**110** (1.5)	$MgCl_2$	AcOH	10	2.0	89	< 2
7	10	**110** (1.5)	TBACl	AcOH	10	2.0	> 98	< 2

[a] Reactions performed using 0.3 mmol of cyclobutanol **27** using the ElectraSyn 2.0 batch electrochemical reactor. [**27**] = 0.05 M. [b] Yield as determined by ^{1}H NMR analysis of the crude reaction mixture with 1,3,5-trimethylbenzene as the internal standard.

Table 3.12: Further photoelectrochemical investigations

In these reactions, **27** (0.3 mmol) was electrolysed under a constant current with $CeCl_3$•$7H_2O$ and $LiClO_4$ in the appropriate solvent system, along with the appropriate SOMOphile (1.5 equiv.) and additive (1.0 equiv.), whilst also being irradiated by 390 nm LEDs. Initially **119** was used as the SOMOphile (entries 1-7), and when a catalyst loading of 5 mol % was employed at a constant current of 2 mA until a charge of 4.2 F/mol (t = 17 h) had passed, no amount of **122** was detected by ^{1}H NMR with full decomposition of **27** (entry 1). When only 2.0 F/mol of charge was passed (t = 8 h), no **122** was observed again but 20% of **27** was recovered (entry 2). This suggests that **27** was decomposing during longer reactions. Therefore, the applied current was then increased to 5 mA, reducing the reaction time to 3 h 12 min. This again saw no detection of **122**, and another increase in the amount of **27** recovered to 51% by ^{1}H NMR (entry 3). The current was then increased again to 10 mA, along with the addition of a chloride salt additive that

seemed to be crucial to the reactivity observed by both Zuo[2,10,11,15,17,19,20] and Xu.[23] Using $MgCl_2$ or TBACl had no effect on the outcome of the reaction, with no **122** detected in either case along with high recovery of **27** (entries 4 and 5). The conditions of entries 4 and 5 were then repeated using lepidine **110**, with no **155** observed by ^{1}H NMR in either case.

With no products observed when utilising a photoelectrochemical set up and the irreproducibility of the system under standard electrochemical conditions, at this point investigations into this project were halted, in favour of pursuing more productive projects.

3.3 Conclusion

In conclusion, an electrochemical procedure for the cerium-catalysed deconstructive heteroarylation of cyclobutanols was discovered, meeting the objective of developing an alternative deconstructive functionalisation to chlorination. Attempts to perform deconstructive functionalisations on a selection of cyclopentanols and cyclohexanols were unsuccessful.

Unfortunately, this process was discovered to be extremely unpredictable and irreproducible, with vastly different results obtained when the reaction was repeated. Further studies to improve the process in terms of efficiency and reliability yielded no positive results. Taking inspiration from Xu and co-workers,[23] a photoelectrochemical system was then designed to overcome these problems encountered in the electrochemical system; however, no promising results were observed during this part of the investigation.

After the culmination of this project, the Zeng group has since reported two examples of photoelectrochemical generation of methoxy radicals using anodically generated cerium (IV) and catalytic quantities of methanol.[58,59] In these reports, photoinduced LMCT initiated homolysis of the Ce(IV)-O bond gives a methoxy radical that performs intermolecular HAT, furnishing silyl radicals or alkyl radicals and regenerating the methanol. Then in mid-2022, Lei and co-workers reported an adaptation of the Zeng work towards the deconstructive functionalisation of cycloalkanols, in essence achieving the aims and objectives we had set out to during this work.[60] In the methodology they report, the presence of 4-*tert*-butylpyridine was crucial to the success of the reaction, as in its absence no product is observed.

3.4 References

1 P. Gray and A. Williams, *Chem. Rev.*, 1959, **59**, 239–328.

2 L. Chang, Q. An, L. Duan, K. Feng and Z. Zuo, *Chem. Rev.*, 2022, **122**, 2429–2486.

3 T. L. Ho, *Synthesis*, 1973, **1973**, 347–354.

4 V. Sridharan and J. C. Menéndez, *Chem. Rev.*, 2010, **110**, 3805–3849.

5 K. Meyer and J. Rocek, *J. Am. Chem. Soc.*, 1972, **94**, 1209–1214.

6 J. Jingliang, L. X. Nguyen, D. R. Patterson and R. A. Flowers, *Org. Lett.*, 2007, **9**, 1323–1326.

7 B. M. Casey, C. A. Eakin and R. A. Flowers, *Tetrahedron Lett.*, 2009, **50**, 1264–1266.

8 H. Zeng, P. Pan, J. Chen, H. Gong and C. J. Li, *Eur. J. Org. Chem.*, 2017, 1070–1073.

9 J. Fang, L. Li, C. Yang, J. Chen, G. J. Deng and H. Gong, *Org. Lett.*, 2018, **20**, 7308–7311.

10 J. J. Guo, A. Hu, Y. Chen, J. Sun, H. Tang and Z. Zuo, *Angew. Chem., Int. Ed.*, 2016, **55**, 15319–15322.

11 A. Hu, Y. Chen, J. J. Guo, N. Yu, Q. An and Z. Zuo, *J. Am. Chem. Soc.*, 2018, **140**, 13580–13585.

12 Y. Chen, J. Du and Z. Zuo, *Chem*, 2020, **6**, 266–279.

13 J. Du, X. Yang, X. Wang, Q. An, X. He, H. Pan and Z. Zuo, *Angew. Chem., Int. Ed.*, 2021, **60**, 5370–5376.

14 J. Schwarz and B. König, *Chem. Commun.*, 2019, **55**, 486–488.

15 K. Zhang, L. Chang, Q. An, X. Wang and Z. Zuo, *J. Am. Chem. Soc.*, 2019, **141**, 10556–10564.

16 Y. Chen, X. Wang, X. He, Q. An and Z. Zuo, *J. Am. Chem. Soc.*, 2021, **143**, 4896–4902.

17 A. Hu, J. J. Guo, H. Pan, H. Tang, Z. Gao and Z. Zuo, *J. Am. Chem. Soc.*, 2018, **140**, 1612–1616.

18 S. J. Blanksby and G. B. Ellison, *Acc. Chem. Res.*, 2003, **36**, 255–263.

19 A. Hu, J. J. Guo, H. Pan and Z. Zuo, *Science*, 2018, **361**, 668–672.

20 Q. An, Z. Wang, Y. Chen, X. Wang, K. Zhang, H. Pan, W. Liu and Z. Zuo, *J. Am. Chem. Soc.*, 2020, **142**, 6216–6226.

21 B. H. Nguyen, R. J. Perkins, J. A. Smith and K. D. Moeller, *J. Org. Chem.*, 2015, **80**, 11953–11962.

22 M. J. Llorente, B. H. Nguyen, C. P. Kubiak and K. D. Moeller, *J. Am. Chem. Soc.*, 2016, **138**, 15110–15113.

23 X. L. Lai, X. M. Shu, J. Song and H. C. Xu, *Angew. Chem., Int. Ed.*, 2020, **59**, 10626–10632.

24 B. D. W. Allen, M. D. Hareram, A. C. Seastram, T. McBride, T. Wirth, D. L. Browne and L. C. Morrill, *Org. Lett.*, 2019, **21**, 9241–9246.

25 F. Dénès, C. H. Schiesser and P. Renaud, *Chem. Soc. Rev.*, 2013, **42**, 7900–7942.

26 F. Dénès, M. Pichowicz, G. Povie and P. Renaud, *Chem. Rev.*, 2014, **114**, 2587–2693.

27 B. Du, B. Jin and P. Sun, *Org. Lett.*, 2014, **16**, 3032–3035.

28 P. F. Wang, X. Q. Wang, J. J. Dai, Y. S. Feng and H. J. Xu, *Org. Lett.*, 2014, **16**, 4586–4589.

29 X. Wu and Y. Wang, *Tetrahedron Lett.*, 2018, **59**, 1240–1243.

30 M. M. Midland and H. C. Brown, *J. Am. Chem. Soc.*, 1971, **93**, 3291–3293.

31 G. A. Russell and H. Tashtoush, *J. Am. Chem. Soc.*, 1983, **105**, 1398–1399.

32 D. H. R. Barton, D. Bridon and S. Z. Zard, *Tetrahedron Lett.*, 1984, **25**, 5777–5780.

33 J. P. Light, M. Ridenour, L. Beard and J. W. Hershberger, *J. Organomet. Chem.*, 1987, **326**, 17–24.

34 G. A. Russell, P. Ngoviwatchai, H. Tashtoush and J. Hershberger, *Organometallics*, 1987, **6**, 1414–1419.

35 G. A. Russell, P. Ngoviwatchai, H. I. Tashtoush, A. Pla-Dalmau and R. K. Khanna, *J. Am. Chem. Soc.*, 1988, **110**, 3530–3538.

36 R. Y. Tang, P. Zhong and Q. L. Lin, *Synthesis*, 2007, 85–91.

37 J. Zhao, H. Fang, J. Han, Y. Pan and G. Li, *Adv. Synth. Catal.*, 2014, **356**, 2719–2724.

38 S. Donck, A. Baroudi, L. Fensterbank, J. P. Goddard and C. Ollivier, *Adv. Synth. Catal.*, 2013, **355**, 1477–1482.

39 A. Baralle, L. Fensterbank, J. P. Goddard and C. Ollivier, *Chem. - Eur. J.*, 2013, **19**, 10809–10813.

40 V. Corcé, L. M. Chamoreau, E. Derat, J. P. Goddard, C. Ollivier and L. Fensterbank, *Angew. Chem., Int. Ed.*, 2015, **54**, 11414–11418.

41 A. Dossena, S. Sampaolesi, A. Palmieri, S. Protti and M. Fagnoni, *J. Org. Chem.*, 2017, **82**, 10687–10692.

42 J. F. Zhao, P. Gao, X. H. Duan and L. N. Guo, *Adv. Synth. Catal.*, 2018, **360**, 1775–1779.

43 S. Sumino, M. Uno, H. J. Huang, Y. K. Wu and I. Ryu, *Org. Lett.*, 2018, **20**, 1078–1081.

44 J. Bin Han, A. Guo and X. Y. Tang, *Chem. - Eur. J.*, 2019, **25**, 2989–2994.

45 X. Chen, X. Gong, Z. Li, G. Zhou, Z. Zhu, W. Zhang, S. Liu and X. Shen, *Nat. Commun.*, 2020, **11**, 2756.

46 M. M. Zhang, S. H. Li, J. L. Tu, Q. Q. Min and F. Liu, *Org. Chem. Front.*, 2020, **7**, 622–627.

47 P. Ranjan, S. Pillitteri, G. Coppola, M. Oliva, E. V. Van der Eycken and U. K. Sharma, *ACS Catal.*, 2021, **11**, 10862–10870.

48 W. M. Zhao, X. L. Chen, J. W. Yuan, L. B. Qu, L. K. Duan and Y. F. Zhao, *Chem. Commun.*, 2014, **50**, 2018–2020.

49 S. Paul and J. Guin, *Chem. - Eur. J.*, 2015, **21**, 17618–17622.

50 P. Liu, W. Liu and C. J. Li, *J. Am. Chem. Soc.*, 2017, **139**, 14315–14321.

51 S. C. Lu, H. S. Li, S. Xu and G. Y. Duan, *Org. Biomol. Chem.*, 2017, **15**, 324–327.

52 Q. Huang and S. Z. Zard, *Org. Lett.*, 2018, **20**, 1413–1416.

53 J. Genovino, Y. Lian, Y. Zhang, T. O. Hope, A. Juneau, Y. Gagné, G. Ingle and M. Frenette, *Org. Lett.*, 2018, **20**, 3229–3232.

54 Z. Li, X. Wang, S. Xia and J. Jin, *Org. Lett.*, 2019, **21**, 4259–4265.

55 S. Samanta and A. Hajra, *J. Org. Chem.*, 2019, **84**, 4363–4371.

56 D. S. Li, T. Liu, Y. Hong, C. L. Cao, J. Wu and H. P. Deng, *ACS Catal.*, 2022, **12**, 4473–4480.

57 K. M. Boy, J. M. Guernon, D. S. Zuev, L. Xu, Y. Zhang, J. Shi, L. R. Marcin, M. A. Higgins, Y. J. Wu, S. Krishnananthan, J. Li, A. Trehan, D. Smith, J. H. Toyn, J. E. Meredith, C. R. Burton, S. R. Kimura, T. Zvyaga, X. Zhuo, K. A. Lentz, J. E. Grace, R. Denton, J. S. Morrison, A. Mathur, C. F. Albright, M. K. Ahlijanian, R. E. Olson, L. A. Thompson and J. E. Macor, *ACS Med. Chem. Lett.*, 2019, **10**, 312–317.

58 Y. Jiang, K. Xu and C. Zeng, *CCS Chem.*, 2022, **4**, 1796–1805.

59 Z. Tan, X. He, K. Xu and C. Zeng, *ChemSusChem*, 2022, **15**, e202102360.

60 Z. Yang, D. Yang, J. Zhang, C. Tan, J. Li, S. Wang, H. Zhang, Z. Huang and A. Lei, *J. Am. Chem. Soc.*, 2022, DOI: 10.1021/JACS.2C05520.

Chapter 4: Electrochemical Alkene Azidocyanation *via* 1,4-Nitrile Migration

Table of Contents

4. Preface

This chapter discusses the development of a new electrochemical methodology for the azidocyanation of alkenes *via* 1,4-nitrile migration to furnish synthetically useful 1,2-azidonitrile products from cyanohydrin substrates. Utilising an inexpensive manganese (II) salt as an azide transfer reagent, a diverse range of 1,2-azidonitriles could be synthesised in good yields (28 examples, 27-75% yield). This methodology was also extended to electrochemical alkene sulfonylcyanation and trifluoromethyl-cyanation procedures, as well as to access a trifunctionalised hexanenitrile from a functionalised malononitrile starting material. Product utility was then demonstrated through the orthogonal derivatisation of the 1,2-azidonitrile product. Mechanistic investigations were performed, including the use of cyclic voltammetry and a radical clock experiment to propose the radical migration mechanism.

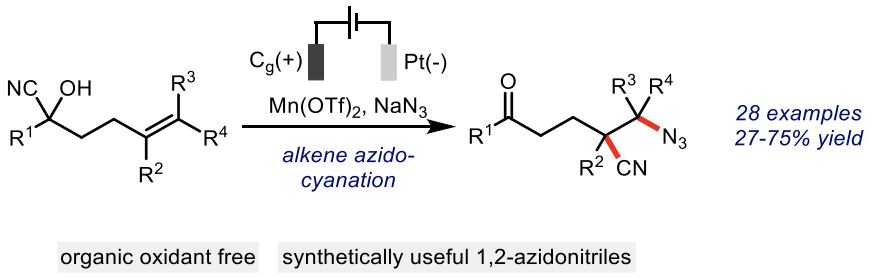

Publication: A. C. Seastram, M. D. Hareram, T. M. B. Knight and L. C. Morrill, *Chem. Commun.*, 2022, **58**, 8658–8661.

Acknowledgements

Alex C. Seastram – Responsible for reaction optimisation, design of the substrate scope, most of the substrate synthesis and scope, product derivatisation, and the mechanistic studies. Supervised the initial investigations and reaction discovery.

Mishra Deepak Hareram – PhD student responsible for part of the substrate synthesis and substrate scope.

Thomas M. B. Knight – MChem student responsible for the initial investigations and reaction discovery.

Louis C. Morrill – Supervisor, Cardiff University.

4.1 Introduction

Alkenes are an extremely versatile functional groups which exhibit a wide range of reactivity, allowing for facile construction of new C-C and C-heteroatom bonds through traditional methods such as hydroborations, epoxidations, Diels-Alder cycloadditions, and dihydroxylations.

Recently, there has been great interest in developing new methodologies for alkene difunctionalisation using electrochemistry.

4.1.1 Electrochemical alkene difunctionalisation

Electrochemistry has emerged as a powerful, efficient, and sustainable tool to perform intermolecular alkene difunctionalisation reactions.[1–3] Mechanistically, these new advances can be separated into three distinct categories (Scheme 4.1).[4]

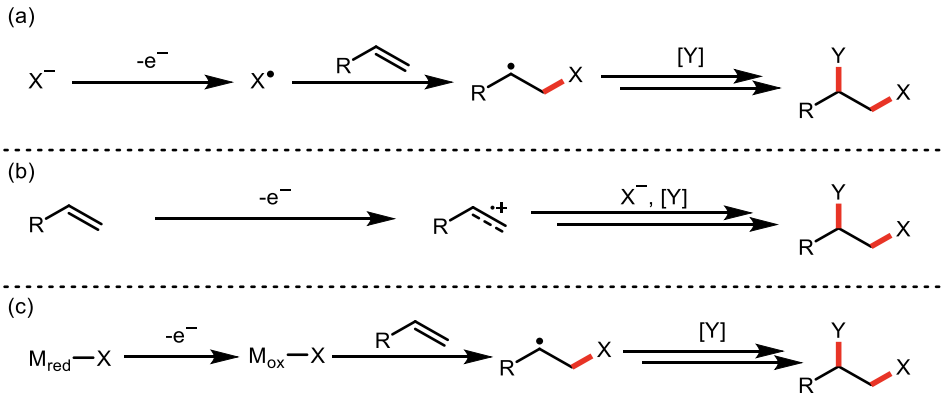

Scheme 4.1: Mechanisms for electrochemical alkene difunctionalisation; (a) Type 1; (b) Type 2; (c) Type 3

In type 1 (Scheme 4.Wa), direct oxidation of a nucleophilic species generates a radical intermediate which then initiates alkene addition.[5–14] This is in contrast to type 2 (Scheme 4.Wb), where the alkene is oxidised to the corresponding radical cation prior to difunctionalisation.[15–18] Finally in type 3 (Scheme 4.Wc), a pre-formed redox catalyst is oxidised, and controls the addition of radical intermediates across the alkene.[19–23]

Utilising the strategy outlined in category 3, Lin and co-workers developed an electrochemical manganese-catalysed diazidation of alkenes protocol in 2017 (Scheme 4.2).[19]

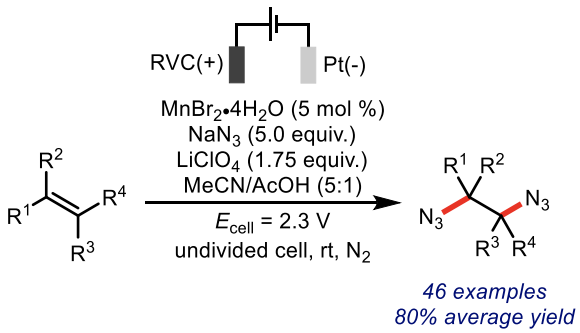

Scheme 4.2: Electrochemical manganese-catalysed alkene diazidation

Similarly to the electrochemical manganese-catalysed alkene dichlorination discussed in Chapter 2,[20] this methodology utilises a manganese (II) catalyst, in this case in combination with NaN_3, to afford 1,2-diazidoalkanes from alkenes through potentiostatic electrolysis with an RVC anode and platinum cathode. This reaction exhibits an expansive substrate scope, with 46 reported examples in an average isolated yield of 80%. The scope includes reactions on monosubstituted acyclic alkenes, for example styrene and its derivatives, including substrates with either electron-donating or electron-withdrawing substituents on the phenyl ring. Alkenes with any substitution are tolerated, with examples of 1,1-, 1,2-, tri-, and tetrasubstituted acyclic alkenes, as well as di-, tri-, and tetrasubstituted cyclic alkenes being successfully converted to the 1,2-diazidoalkanes. Electron-rich heterocycles such as benzoxazole and indole also afford the desired products, generally with good to high diastereoselectivity. Redox sensitive functional groups are also tolerated within substrates, including alcohols, aldehydes, amines, sulfides, and *N*-heterocycles, highlighting the selectivity that can be obtained under electrochemical conditions. Finally, substrates containing functional groups sensitive to nucleophiles were tested, with high yields of products containing halides, esters, or epoxides being obtained. The products were also smoothly converted into the corresponding vicinal diamines.

Following a type 3 mechanistic pathway, an anionic manganese (II) azide species is first oxidised at the anode to the corresponding manganese (III) azide (Scheme 4.3), removing the requirement for a super-stoichiometric quantity of a chemical oxidant in this reaction manifold. This manganese (III) complex acts as an azide transfer reagent to deliver an azide to the alkene, resulting in the formation of a new carbon centred radical. This alkyl radical then reacts with another equivalent of the anodically generated manganese (III) azide to furnish the desired 1,2-diazidoalkane.

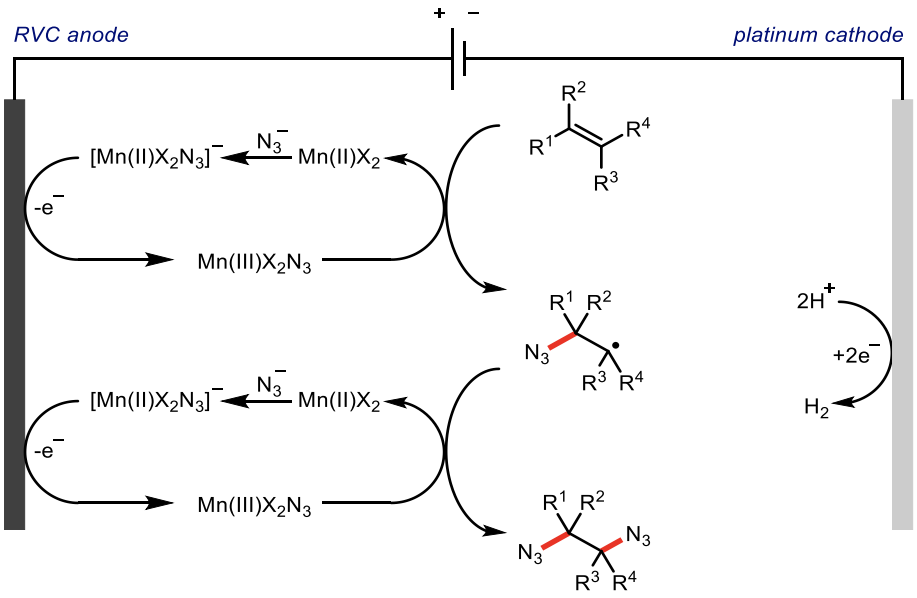

Scheme 4.3: Electrochemical manganese-catalysed alkene diazidation proposed mechanism

This procedure was also modified to allow for a manganese-catalysed alkene dichlorination,[20] and subsequently an organocatalysed variant of the diazidation protocol was developed utilising aminoxyl catalysts (TEMPO derivatives).[22]

4.1.2 Alkene Difunctionalisation *via* Functional Group Migration

In recent years, functional group migration has been developed into a useful strategy for the hetero-difunctionalisation of alkenes (Scheme 4.4).[24]

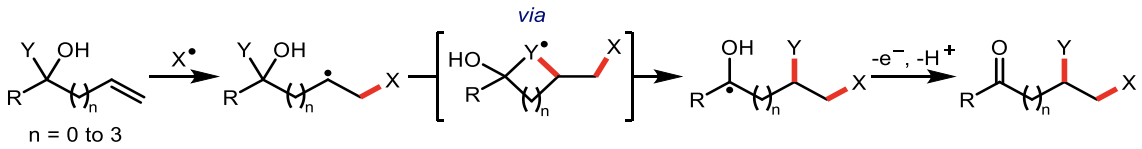

Scheme 4.4: Functional group migration strategy

Generally, tertiary alcohol substrates have been employed with the desired functional group installed at the *α*-position. Initially, the mechanism follows a similar pathway to either the type 1 or type 3 pathways discussed in section 4.1.1, where an *in situ* generated radical adds, or is delivered to, the alkene resulting in an internal alkyl radical. This radical then initiates migration of the pre-installed functional group *via* a cyclic intermediate. The newly generated *α*-hydroxy alkyl radical is oxidised to form the ketone after deprotonation.

This strategy has been well developed using traditional redox chemistry to facilitate intramolecular nitrile,[25–30] alkynyl,[31–33] heteroaryl,[28,29,33–38] carbonyl,[29,33,39] and oximinyl migration.[28,33,38]

Despite there being reports of 1,2- and 1,3-functional group migrations (n = 0 or 1, Scheme 4.4), the more common strategy is to employ 1,4- and 1,5-functional group migrations (n = 2 or 3, Scheme 4.4). This is because the 5- and 6-membered transition states accessed during the migration step are more favoured than the 3- or 4-membered transition states that are required for 1,2- or 1,3-migration.

4.1.2.1 Electrochemical Strategies

Electrochemistry has also been employed to perform alkene hetero-difunctionalisations *via* this functional migration strategy, allowing for facile generation of the radicals required to initiate the process through addition to the alkene, without the requirement for stoichiometric oxidants.[40–47]

Pan and co-workers have led the way in this field, with two reports, in 2018 and 2019, disclosing electrochemical alkene hetero-difunctionalisations through radical additions of sulfonyl and fluoroalkyl radicals to initiate 1,4-migration of alkynes, alkenes, and heteroaromatics (Scheme 4.5).[40,42]

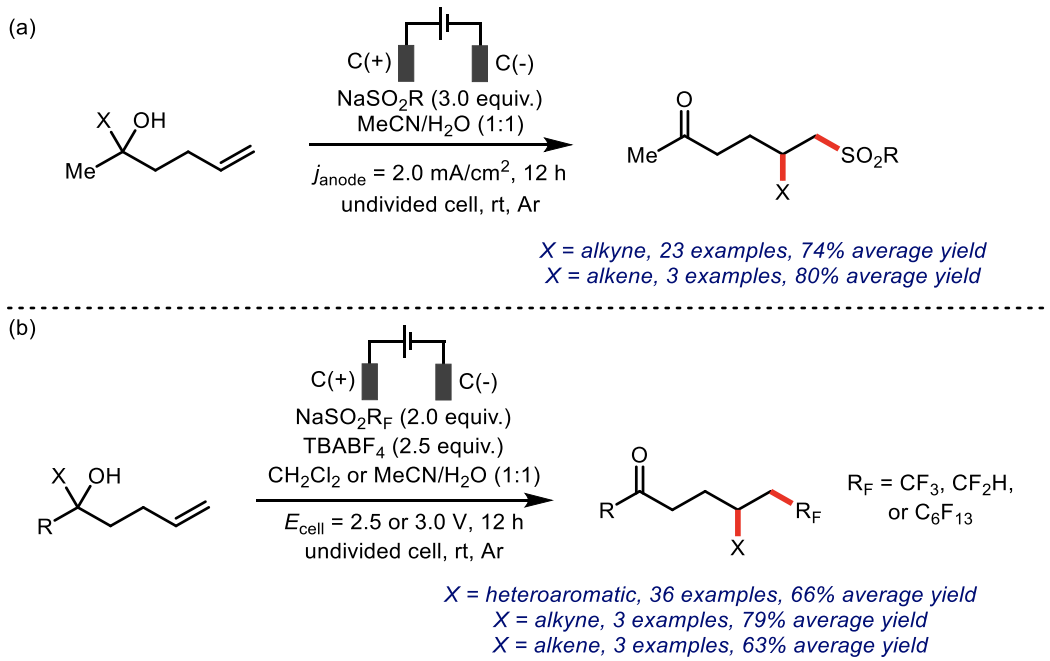

Scheme 4.5: Electrochemical alkene hetero-difunctionalisation via 1,4-migration through the addition of (a) sulfonyl radicals; (b) fluoroalkyl radicals

The first report, in 2018, disclosed the addition of anodically generated sulfonyl radicals to the alkene and subsequent migration of either alkynes (23 examples, 74% average yield) or alkenes (3 examples, 80% average yield) (Scheme 4.5a).[40] A range of phenylacetylene derived alkynes were successfully migrated, with mildly electron-donating (alkyl) and electron-withdrawing (CN, CF_3) groups on the aryl ring being tolerated well. A diverse selection of sodium sulfinates were also demonstrated, allowing the formation of both aryl and alkyl substituted sulfones.

Following this, the authors reported a similar methodology to migrate heteroaromatics (36 examples, 66% average yield), alkynes (3 examples, 79% average yield), and alkenes (3 examples, 63% average yield) upon addition of an anodically generated fluoroalkyl (CF_3, CF_2H, or C_6F_{13}) radicals to the alkene (Scheme 4.5b).[42] Using this methodology, an extensive substrate scope was demonstrated with variations of the R group, the migrating group, and the fluoroalkyl radical all working well.

In 2018, Guo and co-workers reported the electrochemical sulfonyl-heteroarylation of alkenes *via* 1,4- or 1,5-heteroaryl migration (Scheme 4.6).[41]

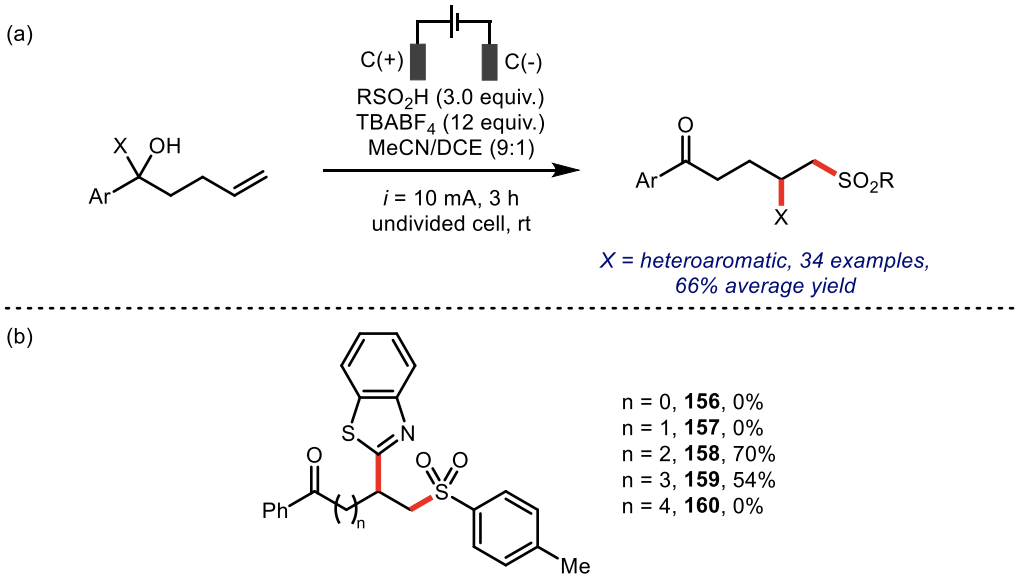

Scheme 4.6: (a) Electrochemical alkene sulfonyl-heteroarylation; (b) Effect of chain length

In a similar procedure to the one used by Pan and co-workers, the authors were able to generate sulfonyl radicals at the anode from the sulfinic acids, then add them to the alkene to initiate heteroaryl migration (Scheme 4.6a). A diverse substrate scope was demonstrated, with various aryl rings, sulfinic acids, and heteroaromatic groups utilised. A study probing the effect of chain length on the yield obtained was also reported

(Scheme 4.6b). It was observed that the reaction only took place when n = 2 or 3 (products **158** and **159**), with no observations of products **156**, **157**, or **160** with shorter or longer chains (n = 0, 1, 4). This is somewhat expected, due to the lower energy 5- and 6-membered transition states accessed during these 1,4- and 1,5-heteroaryl migrations.

4.1.3 Aims and Objectives

As described thus far in section 4.1, functional group migration is an extremely powerful tool to enable hetero-difunctionalisation of alkenes, with many examples that disclose the migration of various functional groups upon radical addition to the alkene. Organic electrochemistry has also emerged as an efficient and sustainable method for difunctionalisation of alkenes through this reaction manifold.

Taking inspiration from the works of Zhu[25] and Lin,[19] as well as Pan[40,42] and Guo,[41] we sought to develop an electrochemical system that would allow for the generation of radical intermediates that would add to an alkene and facilitate nitrile migration in order to access privileged products. Despite the extensive literature reporting nitrile migration within this reaction class using traditional chemistry (i.e., using stoichiometric oxidants), under electrochemical conditions this has not been reported. It was envisaged that the ability to remove the requirement for stoichiometric chemical oxidants would allow us to develop an electrochemical method that demonstrates a broad substrate scope, with redox sensitive functional groups tolerated.

4.2 Results and Discussion

4.2.1 Preliminary Investigations

To begin our investigations, cyanohydrin **163** was first synthesised as the parent substrate from benzoyl chloride (Scheme 4.7).

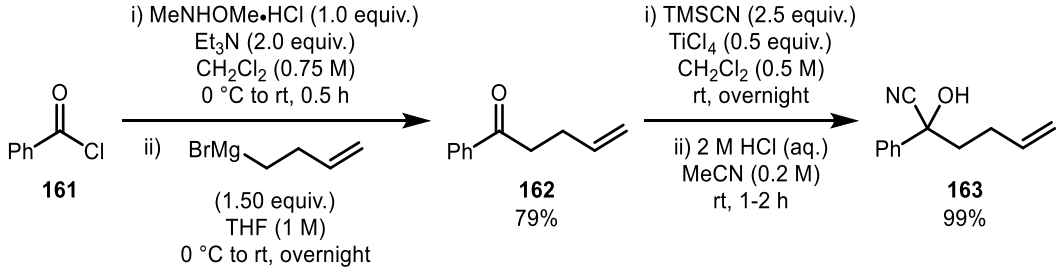

*Scheme 4.7: Synthesis of cyanohydrin **163***

In this two-step procedure, benzoyl chloride **161** was first converted to a Weinreb amide and reacted with the Grignard reagent of 4-bromobut-1-ene to afford ketone **162** in a 79% yield after column chromatography on a 50 mmol scale. Subsequent reaction of **162** with TMSCN in the presence of $TiCl_4$ afforded the corresponding TMS-protected cyanohydrin, which after deprotection with 2 M HCl (aq.) furnished **163** in a 99% yield without purification. Attempts to purify **163** by column chromatography on silica gel, basified silica gel (using triethylamine), basic alumina, or vacuum distillation all resulted in decomposition back to **162**. As a result, **163** and all other cyanohydrins discussed in this chapter were used without further purification.

With the parent substrate in hand, attention was then turned to subjecting **163** to electrochemical systems that would enable alkene trifluoromethylcyanation *via* 1,4-nitrile migration (Scheme 4.8). These reactions were performed by Thomas Knight under my supervision.

Firstly, cyanohydrin **163** was subjected to conditions similar to those utilised by Pan and co-workers to facilitate their electrochemical alkene sulfonylalkynylation (Scheme 4.8a).[40] Using **163** (0.3 mmol) in combination with sodium trifluoromethanesulfinate (3.0 equiv.) in a 1:1 mixture of MeCN and water under a constant current of 2.5 mA for 12 h saw < 2% of the desired product **164**, along with no recovery of **163**. Changing the conditions to those used in Pan's electrochemical alkene trifluoromethyl-heteroarylation, by adding $TBABF_4$ (2.5 equiv.) as supporting electrolyte and changing to a 10:1 mixture of CH_2Cl_2 and water solvent system saw the same result (Scheme 4.8b).[42]

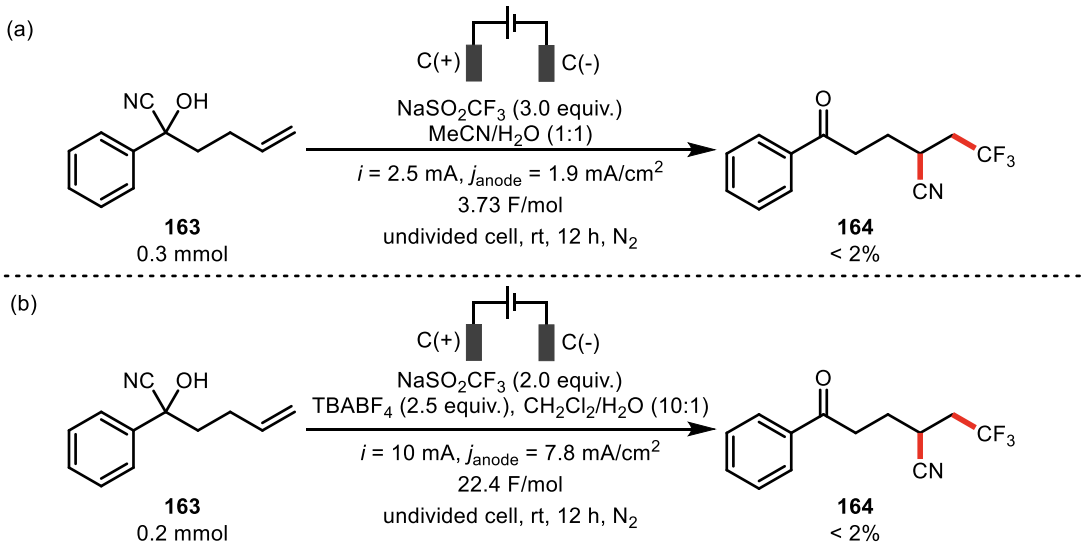

Yields as determined by ^{1}H NMR analysis of the crude reaction mixture using 1,3,5-trimethylbenzene as the internal standard.

Scheme 4.8: Initial studies for electrochemical alkene trifluoromethylcyanation

With the substrate seemingly unstable under the reaction conditions, some stability studies were performed to identify the cause of the instability (Table 4.1).

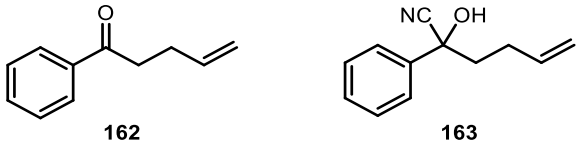

162 **163**

Entry[a]	Reagent	Electrolyte	Solvent	Time (h)	162[b] (%)	163[b] (%)
1	None	None	MeCN/H_2O (1:1)	1	< 2	73
2	$NaSO_2CF_3$ (3.0 equiv.)	None	MeCN/H_2O (1:1)	1	49	32
3	$NaSO_2CF_3$ (3.0 equiv.)	$TBABF_4$ (1.0 equiv.)	MeCN/H_2O (1:1)	1	49	35
4	None	None	MeCN/DCE (9:1)	24	< 2	82
5	$NaSO_2Tol$ (3.0 equiv.)	None	MeCN/DCE (9:1)	24	< 2	85
6	$NaSO_2Tol$ (3.0 equiv.)	$TBABF_4$ (1.0 equiv.)	MeCN/DCE (9:1)	24	< 2	83

[a] Studies performed using 0.3 mmol of cyanohydrin **163** in the conditions stated. [**163**] = 0.05 M.
[b] Yield as determined by ^{1}H NMR analysis of the crude reaction mixture with 1,3,5-trimethylbenzene as the internal standard.

*Table 4.1: Stability studies of **163***

When **163** was stirred in a 1:1 mixture of MeCN and water for 1 h, only 73% was observed by ^{1}H NMR, showing some decomposition was occurring just in the solvent system (entry 1). The addition of sodium trifluoromethanesulfinate (3.0 equiv.) aided significant decomposition of **163**, with ketone precursor **162** obtained as the main decomposition product (49%, entry 2), with similar results obtained when a supporting electrolyte was added (entry 3). Changing the solvent system to MeCN/DCE saw a much-improved stability of **163**, with > 80% observed after 24 h, even when sodium *p*-toluenesulfinate and a supporting electrolyte were added (entries 4-6). These results indicate that **163** is unstable under the aqueous conditions often required to solubilise the sodium trifluoromethanesulfinate but is much more stable when in organic media. Therefore, alternative alkene difunctionalisations were targeted.

An electrochemical alkene azidocyanation was then targeted. Inspiration was sought from conditions used in Lin and co-workers' electrochemical alkene difunctionalisation (Scheme 4.9).[48] This reaction was performed by Thomas Knight under my supervision.

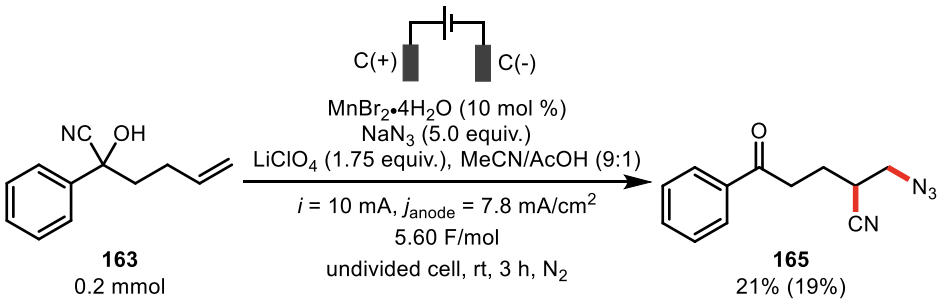

Yield as determined by ^{1}H NMR analysis of the crude reaction mixture using 1,3,5-trimethylbenzene as the internal standard. Isolated yield given in parentheses.

Scheme 4.9: Electrochemical alkene azidocyanation

When **163** was subjected to an electrochemical system composed of $MnBr_2$•$4H_2O$ (10 mol %) as an azide transfer reagent, NaN_3 (5.0 equiv.), and $LiClO_4$ (1.75 equiv.) as supporting electrolyte in MeCN/AcOH (9:1), with a constant current of 10 mA for 3 h, the desired product **165** was obtained in a 21% yield by ^{1}H NMR and was successfully isolated in a 19% yield. This represented an initial hit for the desired transformation; therefore, optimisation of the process was then targeted.

4.2.2 Optimisation

Following the successful formation of the desired 1,2-azidonitrile product (**165**), attention then turned to optimising this reaction.

Firstly, the electrode materials were screened under galvanostatic conditions with the reaction scale increased from 0.2 mmol to 0.3 mmol (Table 4.2).

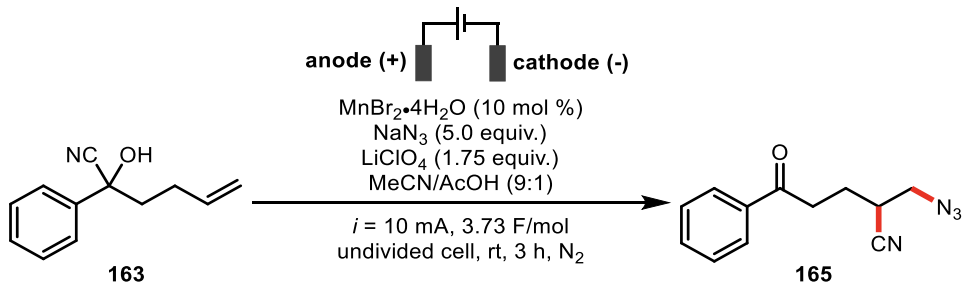

Entry[a]	Anode	Cathode	163[b] (%)	165[b] (%)
1	Graphite	Graphite	35	23
2	**Graphite**	**Pt foil**	**32**	**31**
3	RVC	Graphite	22	25
4	RVC	Pt foil	53	17

[a] Reactions performed using 0.3 mmol of cyanohydrin **163** using the ElectraSyn 2.0 batch electrochemical reactor. [**163**] = 0.05 M. [b] Yield after 3 h as determined by ^{1}H NMR analysis of the crude reaction mixture with 1,3,5-trimethylbenzene as the internal standard.

Table 4.2: Electrode material screen

Upon increasing the reaction scale from 0.2 mmol to 0.3 mmol, a similar yield of **165** was obtained by ^{1}H NMR (entry 1). By changing the cathode material from graphite to platinum foil, the ^{1}H NMR yield of **165** could be increased to 31%, with a similar recovery of **163** after 3 h (entry 2). This is presumably due to platinum's increased ability to facilitate proton reduction, making the electrochemical system more efficient. This contrasts with using an RVC anode and a graphite cathode (entry 3), where despite the slight increase in NMR yield of **165** compared to a graphite-graphite electrode system (entry 1), a significant decrease in the recovery of **163** was observed. Subsequently, a reaction with an RVC anode and platinum foil cathode saw a decrease in the NMR yield of **165**, albeit with an improved recovery of **163** (entry 4).

It was therefore decided that an electrode system composed of a graphite anode and platinum foil cathode would be used in all subsequent reactions. Next, a range of manganese (II) salts were employed as the azide transfer reagent (Table 4.3).

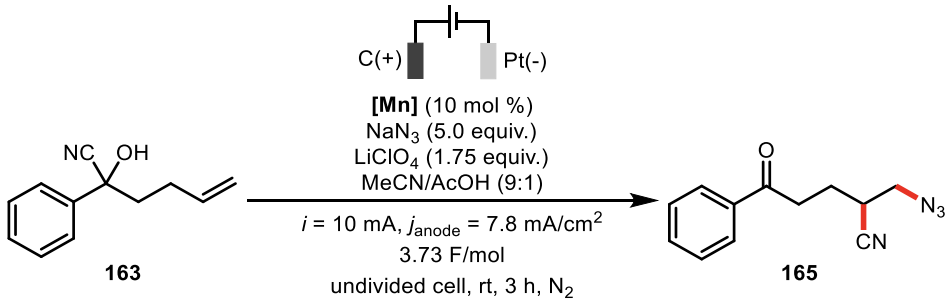

Entry[a]	[Mn]	163[b] (%)	165[b] (%)
1	$MnBr_2•4H_2O$	32	31
2	$Mn(acac)_2$	31	29
3	$MnCl_2•4H_2O$	21	31
4	$Mn(OAc)_2$	41	19
5	$Mn(OAc)_2•4H_2O$	37	33
6	**$Mn(OTf)_2$**	**37**	**31**

[a] Reactions performed using 0.3 mmol of cyanohydrin **163** using the ElectraSyn 2.0 batch electrochemical reactor. [**163**] = 0.05 M. [b] Yield after 3 h as determined by ^{1}H NMR analysis of the crude reaction mixture with 1,3,5-trimethylbenzene as the internal standard.

Table 4.3: Manganese (II) salt screen

Within this screen, it was found that the electrochemical alkene azidocyanation was agnostic with respect to the manganese (II) salts employed, with similar ^{1}H NMR yields of **165** delivered, with the exception of $Mn(OAc)_2$ where decomposition of **163** to ketone **162** was also observed (10%, entry 4). As $Mn(OAc)_2•4H_2O$ and $Mn(OTf)_2$ returned the greatest quantities of **163** out of the manganese (II) salts (entries 5 and 6), these were left as the best candidates moving forward. Due to the observation that ketone **162** (5%) was formed when using $Mn(OAc)_2•4H_2O$, $Mn(OTf)_2$ was chosen as the most efficient azide transfer reagent for the rest of the optimisation.

Subsequent studies then looked at how the identity of the proton source used in the reaction, and the ratio of MeCN to the proton source, would affect this transformation (Table 4.4).

Initially, it was found that moving from AcOH to fluorinated alcohols severely hindered the reaction (entries 2 and 3), with significant formation of **162** in both cases (39% and 24% respectively). This observation is attributed to the insolubility of sodium azide in these solvent systems, preventing formation of the desired Mn(III)-N_3 azide transfer reagent. Alternative organic acids were then tested, with a drop in yield from 31 to 20% by ^{1}H NMR seen when using formic acid (entry 4). When TFA was used as the proton source, an increase in the ^{1}H NMR yield of **165** was observed (48%, entry 5). Due to the increased acidity of TFA (pK_a = 12.65 in MeCN) compared to AcOH (pK_a = 23.51 in MeCN)[49], there

is a higher concentration of protons available for proton reduction at the cathode making the overall electrochemical system more efficient. Upon evaluation of the MeCN:TFA ratio (entries 6 and 7), it was found that a 9:1 ratio was the most desirable and was therefore carried forward.

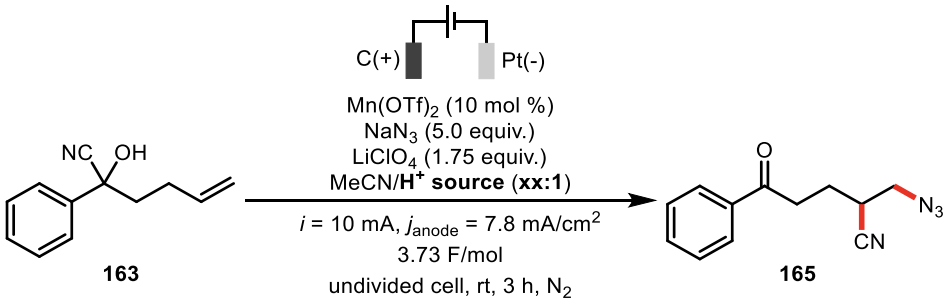

Entry[a]	H^+ source	Solvent Ratio	163[b] (%)	165[b] (%)
1	AcOH	9:1	37	31
2	HFIP	9:1	17	< 2
3	TFE	9:1	13	< 2
4	Formic Acid	9:1	40	20
5	**TFA**	**9:1**	**29**	**48**
6	TFA	4:1	31	27
7	TFA	19:1	17	51

[a] Reactions performed using 0.3 mmol of cyanohydrin **163** using the ElectraSyn 2.0 batch electrochemical reactor. [**163**] = 0.05 M. [b] Yield after 3 h as determined by ^{1}H NMR analysis of the crude reaction mixture with 1,3,5-trimethylbenzene as the internal standard.

Table 4.4: Proton source screen

The next stage of the optimisation investigated various supporting electrolytes, and how they affected the reaction efficiency (Table 4.5).

Initially a range of supporting electrolytes bearing a TBA or tetraethylammonium (TEA) cation were screened, with no improvement in the yield obtained when using $LiClO_4$, including $TBAN_3$ which could also act as an azide source (entries 1-7). Therefore, the loading of $LiClO_4$ as the supporting electrolyte was screened (entries 8-11), where it was found that the highest yield obtained was obtained with no supporting electrolyte used (52%, entry 11). This suggests that the sodium azide is also able to act as the supporting electrolyte within this reaction.

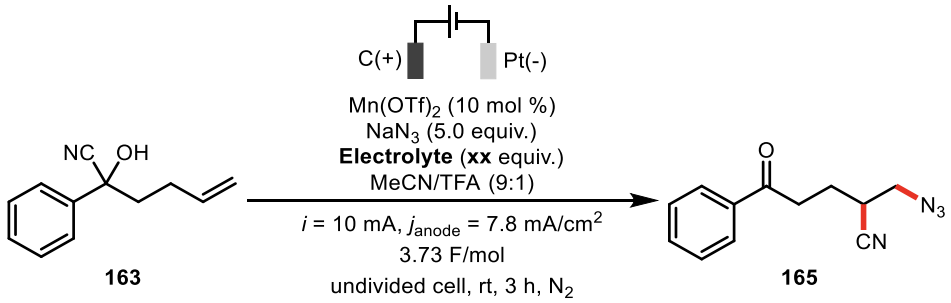

Entry[a]	Electrolyte	Loading (equiv.)	163[b] (%)	165[b] (%)
1	$LiClO_4$	1.75	29	48
2	$TBAPF_6$	1.75	34	34
3	$TBABF_4$	1.75	36	23
4	TBAOAc	1.75	7	16
5	$TBAClO_4$	1.75	23	47
6	$TEABF_4$	1.75	42	29
7	$TBAN_3$	1.75	7	26
8	$LiClO_4$	3.00	28	43
9	$LiClO_4$	2.00	29	36
10	$LiClO_4$	1.00	20	47
11	**None**	**0.00**	**21**	**52**

[a] Reactions performed using 0.3 mmol of cyanohydrin **163** using the ElectraSyn 2.0 batch electrochemical reactor. [**163**] = 0.05 M. [b] Yield after 3 h as determined by ^{1}H NMR analysis of the crude reaction mixture with 1,3,5-trimethylbenzene as the internal standard.

Table 4.5: Supporting electrolyte screen

Following the discovery that removing the supporting electrolyte increased the yield of **165** by ^{1}H NMR, the source and loading of azide anions were then studied (Table 4.6).

Swapping out NaN_3 for $TBAN_3$ saw a significant reduction in the yield of **165** observed by ^{1}H NMR from 52% to 14% (entry 2), along with diminished mass balance. Other azide sources such as $TMSN_3$ were not considered due to a lack of availability at the time of the study. As a result, the loading of NaN_3 was then explored, and it was found that decreasing the loading to 2.5 equiv. again had a significant, negative impact on the yield observed (5%, entry 3); however, increasing the loading beyond 5 equivalents to 7.5 and 10 equiv. had negligible impact on the ^{1}H NMR yield of **165** obtained (entries 4 and 5), with a detrimental effect on the mass balance when 10 equiv. was used. A loading of 5.0 equiv. was seen as optimal to develop a methodology with minimal waste and was therefore carried forward for the rest of the optimisation.

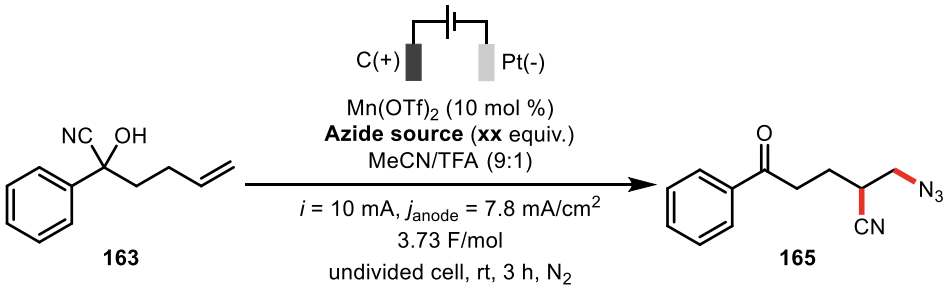

Entry[a]	Azide Source	Loading (equiv.)	163[b] (%)	165[b] (%)
1	**NaN_3**	**5.0**	**21**	**52**
2	$TBAN_3$	5.0	11	14
3	NaN_3	2.5	42	5
4	NaN_3	7.5	20	51
5	NaN_3	10	< 2	56

[a] Reactions performed using 0.3 mmol of cyanohydrin **163** using the ElectraSyn 2.0 batch electrochemical reactor. [**163**] = 0.05 M. [b] Yield after 3 h as determined by ^{1}H NMR analysis of the crude reaction mixture with 1,3,5-trimethylbenzene as the internal standard.

Table 4.6: Azide source screen

Next, the effect of the loading of $Mn(OTf)_2$ on the efficiency of azide transfer to **163** was investigated (Table 4.7).

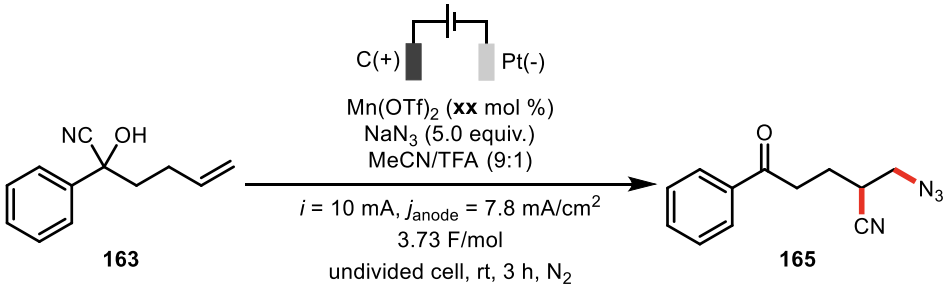

Entry[a]	Loading (mol %)	163[b] (%)	165[b] (%)
1	**10**	**21**	**52**
2	2.5	36	33
3	5.0	40	27
4	20	27	34

[a] Reactions performed using 0.3 mmol of cyanohydrin **163** using the ElectraSyn 2.0 batch electrochemical reactor. [**163**] = 0.05 M. [b] Yield after 3 h as determined by ^{1}H NMR analysis of the crude reaction mixture with 1,3,5-trimethylbenzene as the internal standard.

Table 4.7: $Mn(OTf)_2$ loading screen

It was observed that when the loading of $Mn(OTf)_2$ was reduced from 10 mol % to 2.5 and 5.0 mol % the ^{1}H NMR yield of **165** was reduced to 33% and 27% respectively (entries 2 and 3), and upon increasing to 20 mol % the conversion to **165** also reduced

to 34% (entry 4). A loading of 10 mol % therefore is optimal for efficient azide delivery to the substrate (entry 1).

With the reaction conditions screened, attention was then turned to optimisation of the electrochemical parameters, starting with the electrolysis conditions (Table 4.8).

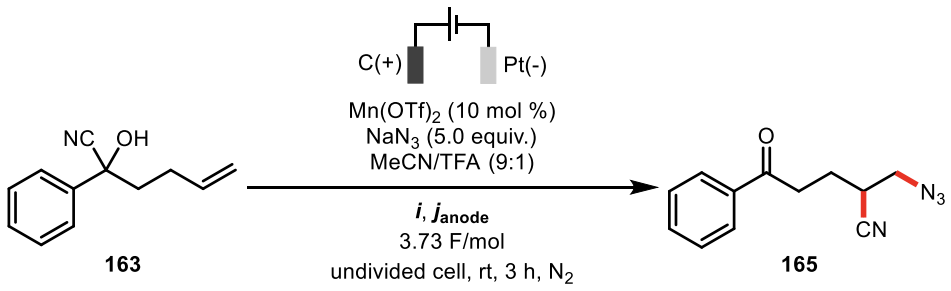

Entry[a]	Conditions	163[b] (%)	165[b] (%)
1[c]	***i* = 10 mA; j_{anode} = 7.8 mA/cm^2**	**21**	**52**
2[d]	*i* = 4 mA; j_{anode} = 3.1 mA/cm^2	< 2	23
3[e]	*i* = 8 mA; j_{anode} = 6.2 mA/cm^2	35	30
4[f]	*i* = 12 mA; j_{anode} = 9.4 mA/cm^2	36	32
5[g]	*i* = 20 mA; j_{anode} = 15.6 mA/cm^2	34	38
6	E_{cell} = 2 V	< 2	46

[a] Reactions performed using 0.3 mmol of cyanohydrin **163** using the ElectraSyn 2.0 batch electrochemical reactor. [**163**] = 0.05 M. [b] Yield as determined by ^{1}H NMR analysis of the crude reaction mixture with 1,3,5-trimethylbenzene as the internal standard. [c] 3 h reaction time. [d] 7 h 30 min reaction time. [e] 3 h 45 min reaction time. [f] 2 h 30 min reaction time. [g] 1 h 30 min reaction time.

Table 4.8: Electrolysis condition screen

Reduction of the current applied from 10 mA to 4 mA saw a significant decrease in the ^{1}H NMR yield of **165** from 52% to 23%, as well as in the overall mass balance (entry 2). This result suggests that at this current, the rate of electron transfer processes is not fast enough to facilitate formation of **165** in an appreciable amount before decomposition of **163** and/or reaction intermediates occurs. An applied current of 8 mA also saw a decrease in the quantity of **165** observed, albeit with no loss in the overall mass balance (entry 3). Increasing the current to from 10 mA to 12 and 20 mA saw reductions in the yield of **165** obtained by ^{1}H NMR (entries 4 and 5) but consistent presence of **163**. This perhaps highlights an inefficiency in the electrochemical system, where the charge passed is not utilised productively within these reduced reaction times. Running the reaction under potentiostatic conditions (entry 6) saw a decreased yield of **165** by ^{1}H, a reduced mass balance, and an increase in the reaction time (compared to entry 1).

Therefore, the original electrolysis conditions using an applied current of 10 mA was chosen as optimal.

Following screening of all the reaction parameters the reaction time was then studied (Table 4.9).

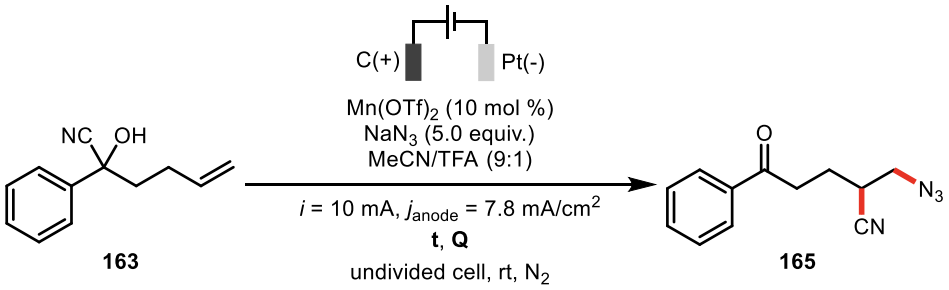

Entry[a]	Reaction Time	Q (F/mol)	163[b] (%)	165[b] (%)
1	3 h	3.73	21	52
2	1 h 36 min	2.00	46	29
3	**4 h**	**4.97**	**< 2**	**55 (51)**
4	5 h	6.22	< 2	42
5	6 h	7.46	< 2	41

[a] Reactions performed using 0.3 mmol of cyanohydrin **163** using the ElectraSyn 2.0 batch electrochemical reactor. [**163**] = 0.05 M. [b] Yield as determined by ^{1}H NMR analysis of the crude reaction mixture with 1,3,5-trimethylbenzene as the internal standard. Isolated yield given in parentheses.

Table 4.9: Reaction time screen

Initially, the reaction was run until 2.00 F/mol of charge had passed (t = 1 h 36 min, entry 2), yielding 29% of **165** by ^{1}H NMR. As this transformation is requires two single electron oxidations to proceed, this result indicates a charge efficiency of 29% for this electrochemical reaction, again highlighting that there is an inefficiency within the electrochemical system. It was then found that increasing the reaction time from 3 h to 4 h delivered a comparable amount of **165** (entry 3), but 5 and 6 h did not have the desired outcome of an improved yield of **165** (entries 4 and 5). These results highlight the instability of the **163** and/or reaction intermediates within the reaction for an extended period, as well as potentially **165** itself.

In an attempt to improve the yield further, the identity of the bulk solvent was then studied, to see if alternative solvents were able to stabilise **163**, **165**, and any reaction intermediates (Table 4.10).

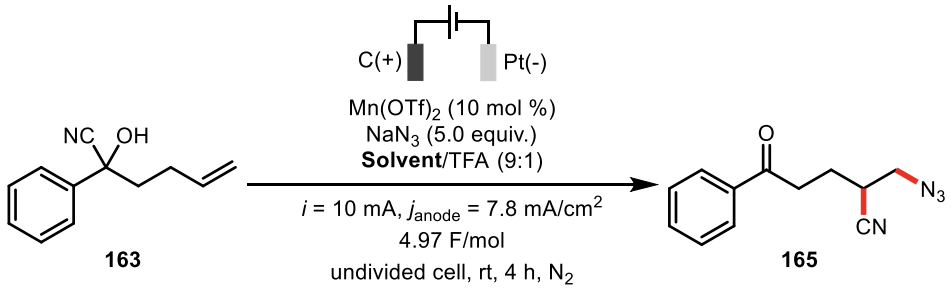

Entry[a]	Solvent	163[b] (%)	165[b] (%)
1	**MeCN**	**< 2**	**55 (51)**
2	THF	> 98	< 2
3	DMF	51	14
4	DMA	69	10
5	DMSO	12	32

[a] Reactions performed using 0.3 mmol of cyanohydrin **163** using the ElectraSyn 2.0 batch electrochemical reactor. [**163**] = 0.05 M. [b] Yield as determined by ^{1}H NMR analysis of the crude reaction mixture with 1,3,5-trimethylbenzene as the internal standard. Isolated yield given in parentheses.

Table 4.10: Solvent screen

All the solvents tested showed no improvement in the yield obtained, with a THF/TFA solvent system returning **163** quantitatively (entry 2). Alternative polar aprotic solvents DMF, DMA, and DMSO showed significantly reduced ^{1}H NMR yields of **165**, although with an increased mass balance when using DMF or DMA (entries 3-5).

With all avenues exhausted to improve the yield of **165**, the conditions of Table 4.10 entry 1 were found to be optimal for this electrochemical alkene azidocyanation process, and a variation from "standard" conditions table was then composed, presented below (Table 4.11).

After the extensive optimisation disclosed above, it was found that an electrochemical system utilising $Mn(OTf)_2$ (10 mol %) as an azide transfer reagent and NaN_3 (5.0 equiv.) as both azide source and supporting electrolyte in MeCN/TFA (9:1, [**163**] = 0.05 M), under galvanostatic conditions (i = 10 mA, j_{anode} = 7.8 mA/cm^2) with a graphite anode and platinum foil cathode at rt for 4 h (4.97 F/mol) under N_2, enabled the azidocyanation of **163** to furnish **165** in a 55% yield by ^{1}H NMR, with a 51% isolated yield obtained (entry 1). No conversion was observed in the absence of electricity (entry 2), and the yield of **165** was reduced in the absence of $Mn(OTf)_2$ (entry 3). In the absence of the azide transfer reagent, this process would presumably occur *via* a type 1 alkene difunctionalisation mechanism (Scheme 4.1) through the addition of free azidyl radicals, generated at the anode, to the alkene. Employing a constant cell potential (E_{cell} = 2.4 V) saw **165** obtained in a 55% yield by ^{1}H NMR, albeit in an increased reaction time (entry 4).

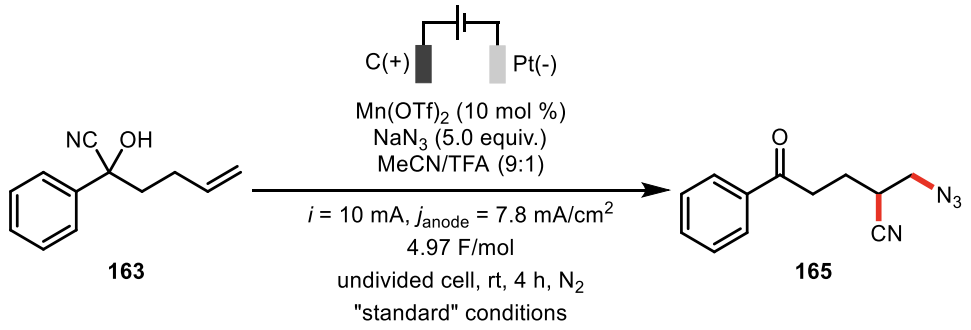

Entry[a]	Variation from "standard" conditions	163[b] (%)	165[b] (%)
1	**None**	**< 2**	**55 (51)**
2	No electricity	94	< 2
3	No $Mn(OTf)_2$	34	23
4	E_{cell} = 2.4 V	< 2	55
5[c]	i = 12.5 mA, j_{anode} = 9.8 mA/cm^2	4	32
6[d]	i = 7.5 mA, j_{anode} = 5.9 mA/cm^2	< 2	42
7	$LiClO_4$ (1.75 equiv.) as supporting electrolyte	20	38
8	Graphite cathode instead of Pt foil	6	23
9	Ni plate cathode instead of Pt foil	10	43
10	$MnBr_2.4H_2O$ instead of $Mn(OTf)_2$	< 2	34
11	$Mn(OAc)_2.4H_2O$ instead of $Mn(OTf)_2$	< 2	48
12	AcOH instead of TFA	20	30
13	NaN_3 (2.5 equiv.)	29	19
14	$Mn(OTf)_2$ (5 mol %)	8	50
15[e]	Q = 6.22 F/mol	< 2	42

[a] Reactions performed using 0.3 mmol of cyanohydrin **163** using the ElectraSyn 2.0 batch electrochemical reactor. [**163**] = 0.05 M. [b] Yield as determined by ^{1}H NMR analysis of the crude reaction mixture with 1,3,5-trimethylbenzene as the internal standard. Isolated yield given in parentheses. [c] 192 min reaction time. [d] 320 min reaction time. [e] 300 min reaction time.

Table 4.11: Deviation from "standard" conditions table

Galvanostatic conditions were preferred because of the consistent reaction times associated, and variation in the applied current had a detrimental effect on the yield of **165** (entries 5 and 6), as did the addition of $LiClO_4$ (1.75 equiv.) as supporting electrolyte (entry 7). Furthermore, substituting the platinum cathode for graphite or nickel plate (entries 8 and 9) did not aid in increasing the productivity of **165**. Employing alternative manganese (II) salts as azide transfer reagents also resulted in decreased yields of **165** by ^{1}H NMR (entries 10 and 11). Substituting TFA for AcOH as the proton source also resulted in a reduced conversion to **165** (entry 12), presumably due to the decreased solubility of NaN_3 observed in this solvent system. It was found that reducing the NaN_3 loading to 2.5 equiv. significantly lowered the ^{1}H NMR yield of **165** from 55 to 19% (entry 13), but a negligible impact on yield was observed upon reducing the $Mn(OTf)_2$ loading to 5 mol % (entry 14). Finally, increasing the reaction time further to 5 h saw a

decrease in the ^{1}H NMR yield of **165** to 42%, suggesting that the product may be somewhat unstable under the reaction conditions. Evidence supporting this was obtained when **165** was subjected to the "standard" reaction conditions for 4 h, and only 64% was returned by ^{1}H NMR analysis of the crude reaction mixture (Scheme 4.10).

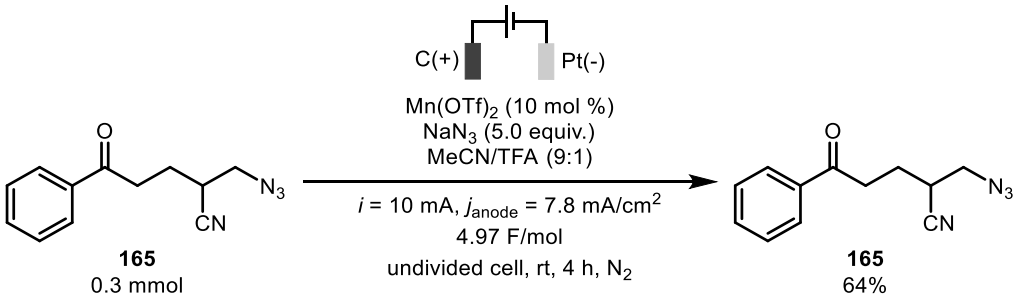

*Scheme 4.10: Re-subjection of **165** to the "standard" reaction conditions*

The final optimised conditions for this process therefore utilises $Mn(OTf)_2$ (10 mol %) and NaN_3 (5.0 equiv.) in MeCN/TFA (9:1, [**163**] = 0.05 M), under constant current electrolysis (i = 10 mA, j_{anode} = 7.8 mA/cm^2) with a graphite anode and platinum foil cathode at rt under N_2 for 4 h (4.97 F/mol) (Scheme 4.11).

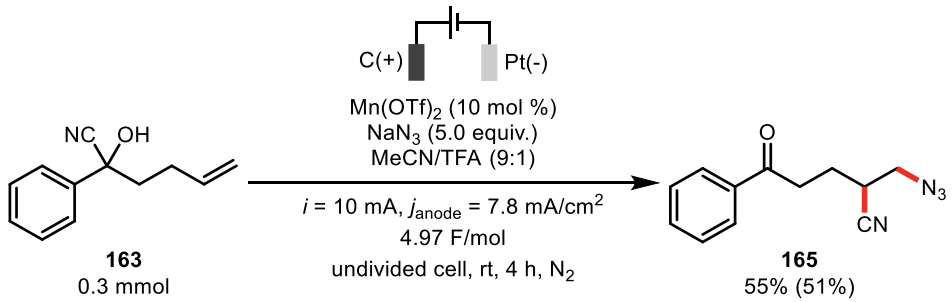

Scheme 4.11: Final optimised conditions for the electrochemical alkene azidocyanation

4.2.3 Substrate Scope

4.2.3.1 Substrate Synthesis

With optimised conditions in hand, attention was then turned to investigate the full scope of this reaction. In order to do so, a range of cyanohydrins were synthesised from the corresponding ketones to test under the parent reaction conditions (Scheme 4.12).

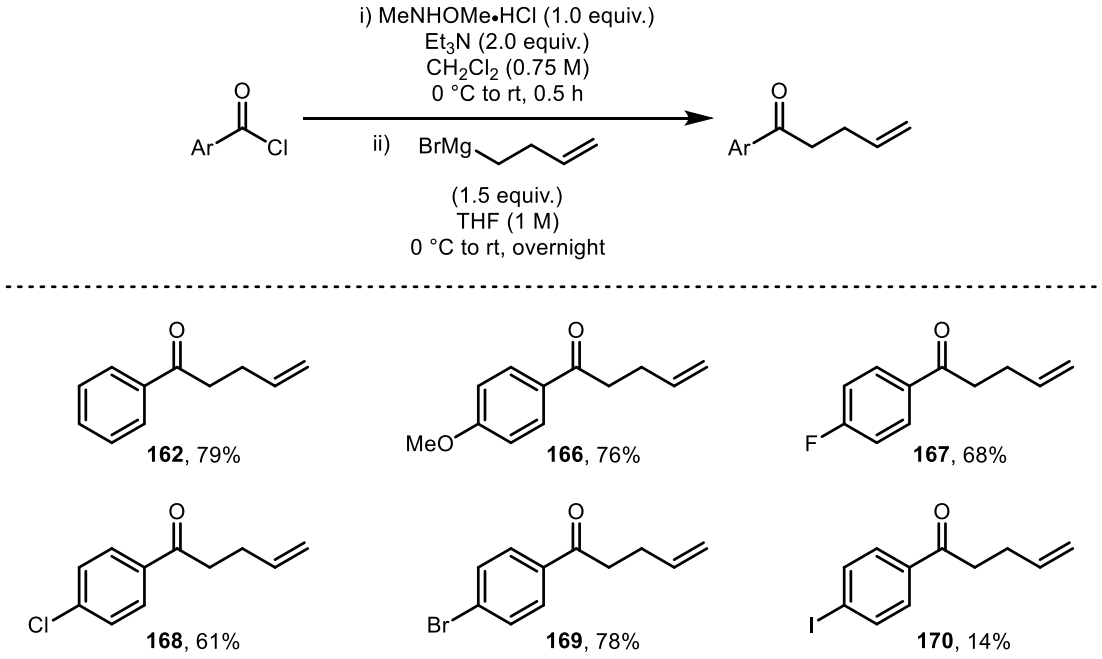

Scheme 4.12: Substrate synthesis of aromatic ketones from acid chlorides

Initially, a range of substituted aromatic acid chlorides were converted into the Weinreb amides using *N*,*O*-dimethylhydroxylamine hydrochloride (1.0 equiv.) and triethylamine (2.0 equiv.), and subsequently reacted with the Grignard reagent of 4-bromobut-1-ene (1.5 equiv.) to furnish the desired ketones. This synthetic route was chosen over alternative strategies as the use of Weinreb amides as the electrophile allows for selective mono-addition of the Grignard reagent to furnish the desired ketones. This is advantageous over alternative strategies such as Grignard addition to aldehydes followed by oxidation (multi-step), or slow addition of the Grignard directly to the acid chloride at low temperatures (side-reaction control). Using this route, aryl ketones substituted with a methoxy group and the halogens (**162**-**170**) in the *para* position were successfully synthesised, generally in good yields.

In the cases where the corresponding acid chlorides weren't readily available or accessible, the substituted aryl bromides could be used (Scheme 4.13).

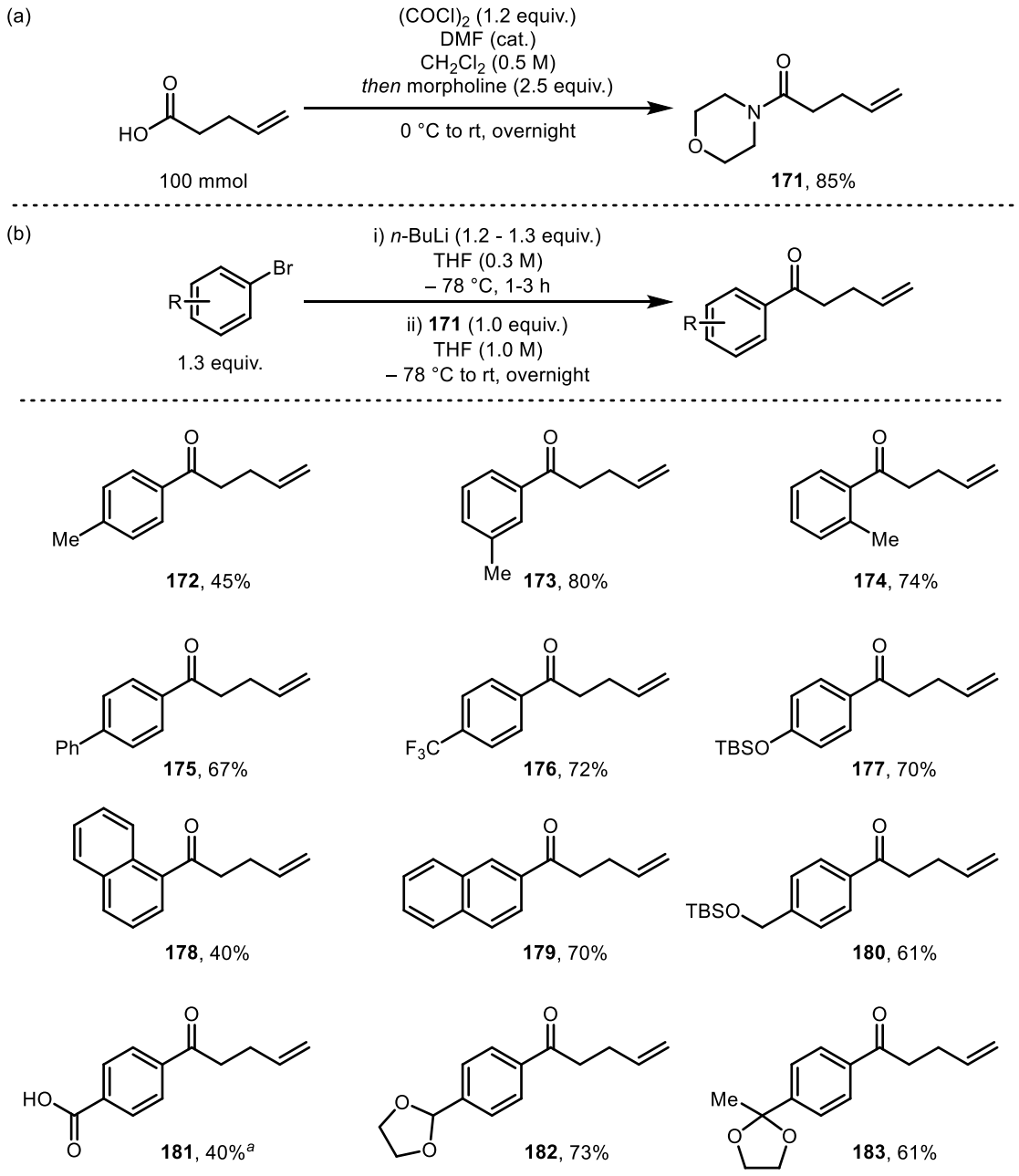

[a] *n*-BuLi (2.6 equiv.) used.

*Scheme 4.13: (a) Synthesis of morpholino amide **171**; (b) Substrate synthesis of aromatic ketones from aryl halides and **171***

Firstly, morpholino amide **171** was synthesised on a 100 mmol scale from 4-pentenoic acid *via in-situ* acid chloride formation using oxalyl chloride (1.2 equiv.) and catalytic DMF, followed by the addition of morpholine (2.5 equiv.) (Scheme 4.13a). The aryl bromide (1.3 equiv.) was treated with *n*-BuLi (1.3 equiv.) under lithium-halogen exchange conditions to form the corresponding aryl organolithium species which was in turn reacted with **171** (1.0 equiv.) to afford the desired ketones (Scheme 4.13b). Through this synthetic

route, a range of ketones (**172**-**183**) with various substitutions on the aromatic core were successfully synthesised in good yields, including keto-acid **181**, which required double the amount of *n*-BuLi to account for initial deprotonation of the carboxylic acid.

For the synthesis of alkyl ketones, an alternative synthetic route was utilised (Scheme 4.14). The ketones in this scheme were synthesised by Deepak Mishra.

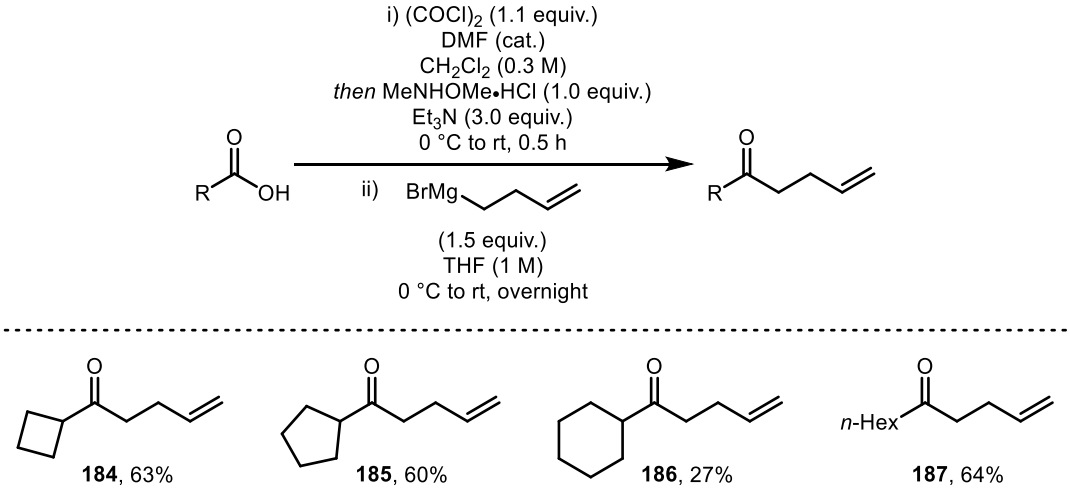

Scheme 4.14: Synthesis of alkyl ketones from carboxylic acids

Firstly, the appropriate carboxylic acid (1.0 equiv.) was transformed into the corresponding acid chloride using oxalyl chloride (1.1 equiv.) and catalytic DMF. Subsequent reaction with *N*,*O*-dimethylhydroxylamine hydrochloride (1.0 equiv.) and triethylamine (3.0 equiv.) afforded the Weinreb amide. Reaction of the Weinreb amide with the Grignard reagent of 4-bromobut-1-ene (1.5 equiv.) gave the desired alkyl ketones (**184**-**187**) in acceptable yields.

Ketones with various substitution patterns on the alkene, as well as substrates with substitution on the alkyl chain, and with an elongated alkyl chain were synthesised *via* enolate chemistry (Scheme 4.15).

Firstly, the appropriate *β*-ketoester was deprotonated using sodium hydride (1.0 equiv.) and the resulting enolate was then reacted with the necessary allylic bromide (1.1 equiv.), affording the desired *α*-alkylated *β*-ketoester. Heating the *β*-ketoester to reflux in methanolic NaOH (4.0 equiv.) initiated saponification and decarboxylation to give the desired ketone. Using this strategy, a range of ketones with various substitution patterns on the alkene (**188**-**192**) were synthesised in good yields, as well as tetralone **193** and a ketone with an extended alkyl chain (**194**).

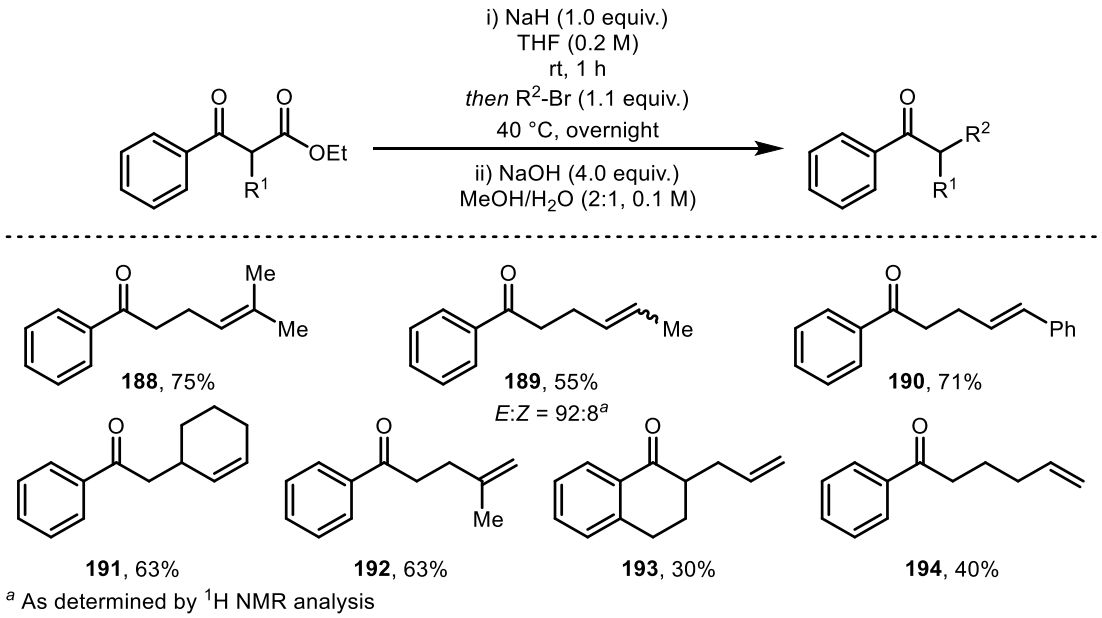

Scheme 4.15: Synthesis of substrates with alkenyl substitution

Some ketones required alternative methods to be synthesised, as summarised in Scheme 4.16.

Firstly, (4-Bromophenyl)ketone **169** could be derivatised to benzonitrile **195** in an 87% yield and boronic ester **196** in a 68% yield *via* a Rosenmund-von Braun reaction with CuCN and palladium-catalysed Miyaura borylation respectively (Scheme 4.16a).

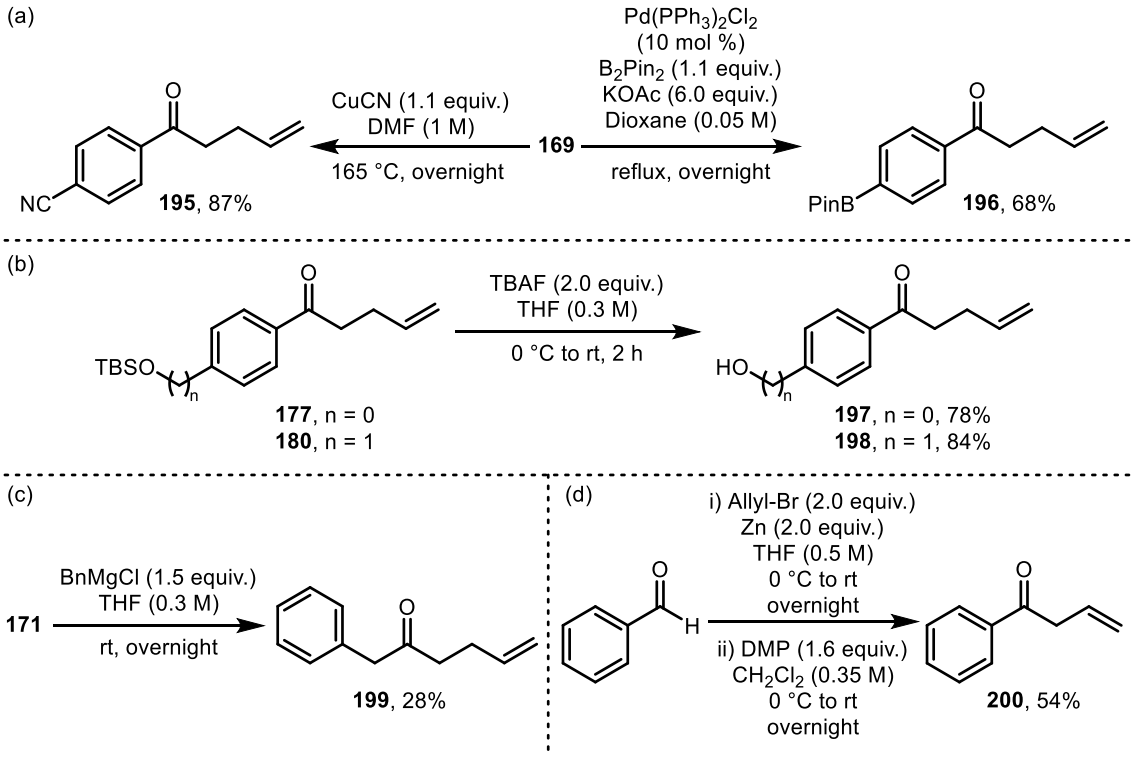

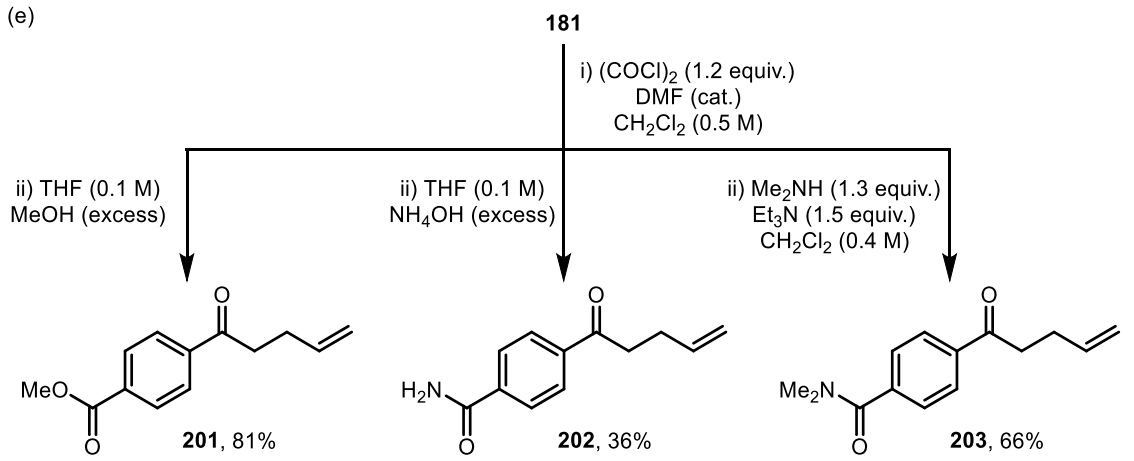

*Scheme 4.16: (a) Derivatisation of (4-bromophenyl)ketone **169**; (b) Deprotection of TBS-protected phenol **177** and benzyl alcohol **180**; (c) Synthesis of benzyl ketone **199**; (d) Synthesis of allyl ketone **200** via Barbier reaction and oxidation; (e) Formation of carboxylic acid derivatives **201**, **202**, and **203***

TBS-protected phenol **177** and TBS-protected benzyl alcohol **180** were smoothly converted to the free phenol **197** and alcohol **198** in 78% and 84% yields respectively upon reaction with TBAF (Scheme 16b). Benzyl ketone **199** was made through the addition of the commercially available BnMgCl to morpholino amide **171** (Scheme 16c). Allyl ketone **200** was made *via* a two-step procedure from benzaldehyde, firstly Barbier reaction with allyl bromide and zinc afforded the homoallyl alcohol which was oxidised to **200** by Dess-Martin oxidation (Scheme 16d). Finally, derivatisation of keto-acid **181** *via* the corresponding acid chloride allowed easy access to ester **201**, benzamide **202**, and dimethyl benzamide **203** (Scheme 16e).

Following the synthesis of the desired ketones, they were each converted into the corresponding cyanohydrins using TMSCN and titanium (IV) chloride, followed by an acidic work up with 2 M HCl (aq.) (Scheme 4.17).

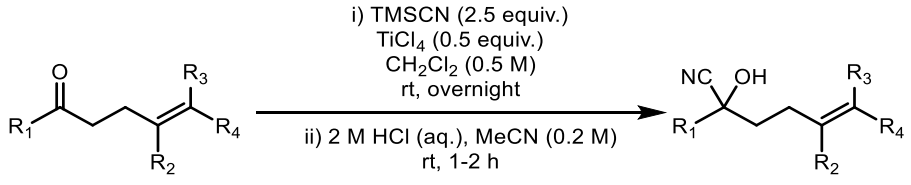

163, R = H, 99%
204, R = 4-Me, 86%
205, R = 3-Me, 94%
206, R = 2-Me, 96%
207, R = 4-Ph, 95%
208, R = 4-CF_3, 99%
209, R = 4-CN, 99%
210, R = 4-F, 95%
211, R = 4-Cl, 99%
212, R = 4-Br, 96%
213, R = 4-I, 96%
214, R = 4-OMe, 96%
215, R = 4-CH_2OH, 98%
216, R = 4-OH, 99%
217, R = 4-OTBS, 84%
218, R = 4-BPin, 98%
219, R = 4-CO_2H, 86%
220, R = 4-CO_2Me, 95%
221, R = 4-$CONH_2$, 77%
222, R = 4-$CONMe_2$, 89%

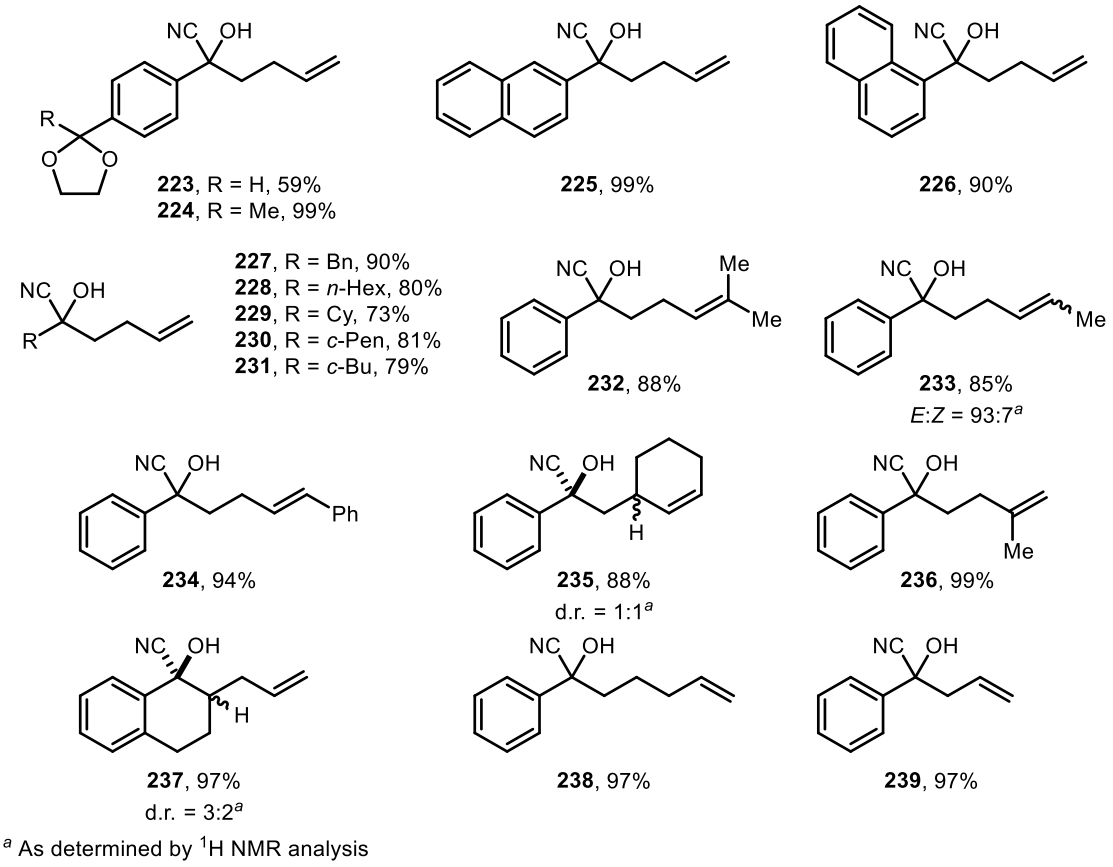

Scheme 4.17: Synthesis of cyanohydrins

As with parent cyanohydrin **163**, purification of these cyanohydrins was not possible, with decomposition back to the ketones observed during purification by chromatographic methods. Generally, the synthesis of these cyanohydrins (**163**, **204**-**239**) proceeded smoothly and to completion by ^{1}H NMR, with yields reported using crude masses. Unfortunately, attempts to deprotect acetal **223** and ketal **224** to the corresponding aldehyde and ketone containing cyanohydrins were unsuccessful, with concurrent decomposition of the cyanohydrin back to the ketone observed.

4.2.3.2 Substrate Scope

With synthesised substrates in hand, attention was then turned to investigate the full scope of this reaction, starting with aryl cyanohydrins with various substitution on the aromatic ring (Scheme 4.18).

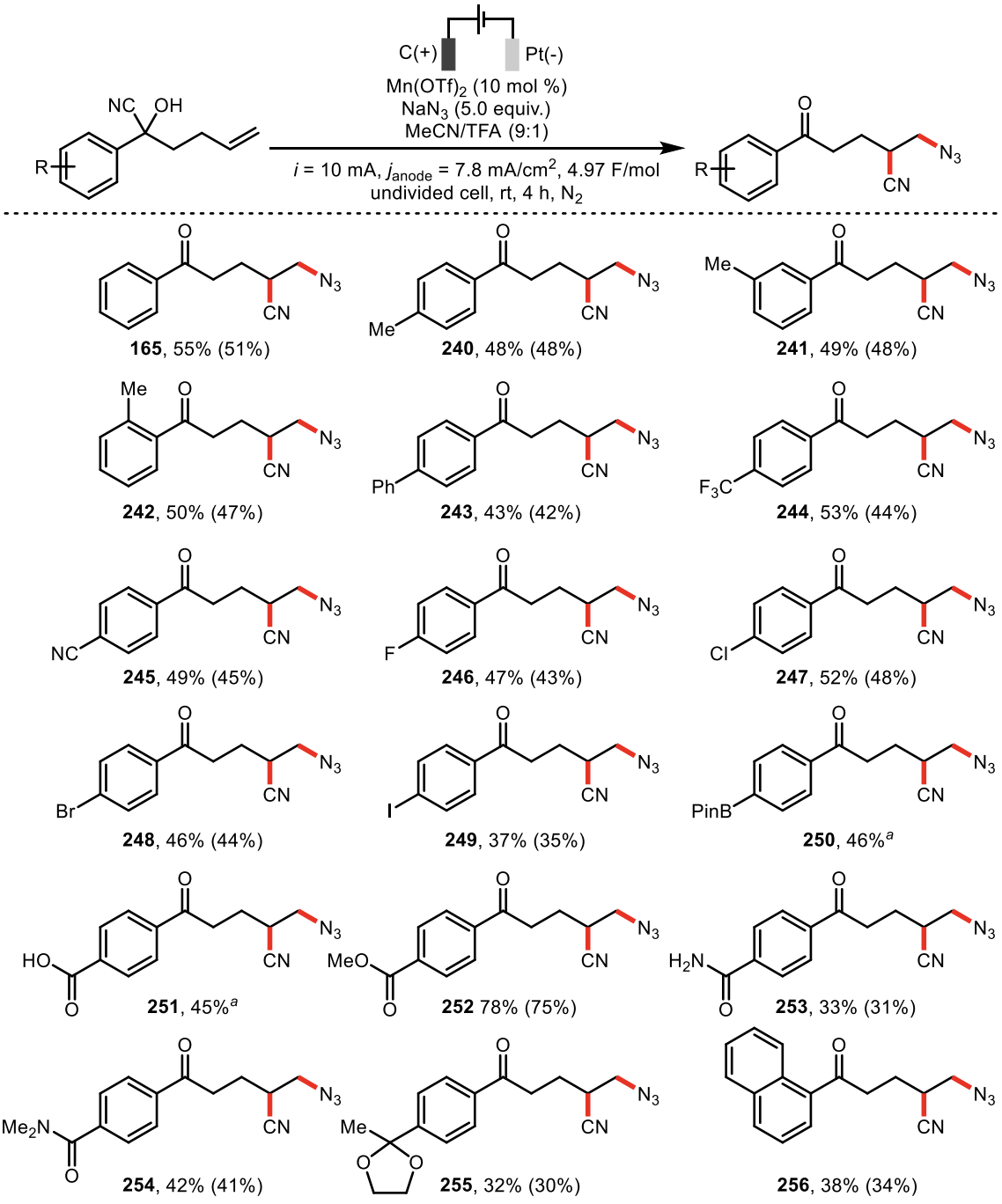

Yields as determined by ^{1}H NMR analysis of the crude reaction mixture using 1,3,5-trimethylbenzene as the internal standard quoted. Isolated yield given in parentheses. [a] 5 h (Q = 6.22 F/mol)

Scheme 4.18: Substrate scope – variation of aryl substitution

Generally, all successful cyanohydrin substrates performed similarly under this electrochemical reaction to the parent substrate **163**. It was found that steric hinderance around the aromatic ring did not appreciably impact the reaction, with 4-Me, 3-Me, and 2-Me substitution tolerated (**240**-**242**). Various substituents could also be incorporated well, with biphenyl **243**, and products containing electron-withdrawing groups (**244** and **245**) obtained in good yields. The halogens were also tolerated in the *para* position, as

was pinacol-borane (**246**-**250**), providing products that could potentially be further derivatised, in good yields. This electrochemical method exhibits good functional group tolerance, as demonstrated by the presence of a carboxylic acid, methyl ester, primary amide, tertiary amide, and ketal in the *para* position in moderate to excellent yields (**251**-**255**). Methyl ester **252** was pleasingly obtained in a 75% isolated yield, suggesting that this mesomerically withdrawing substituent may stabilise intermediates in the reaction, disfavouring any non-productive pathways that may hinder the reaction otherwise. The aromatic ring could also be extended, with 1-naphthyl product **256** obtained in a 34% isolated yield.

Following evaluation of aromatic substitution within the substrates, where good functional group tolerance was observed, a range of alkyl cyanohydrins were then tested within this electrochemical reaction (Scheme 4.19). Products **258**-**261** were synthesised and isolated by Deepak Mishra.

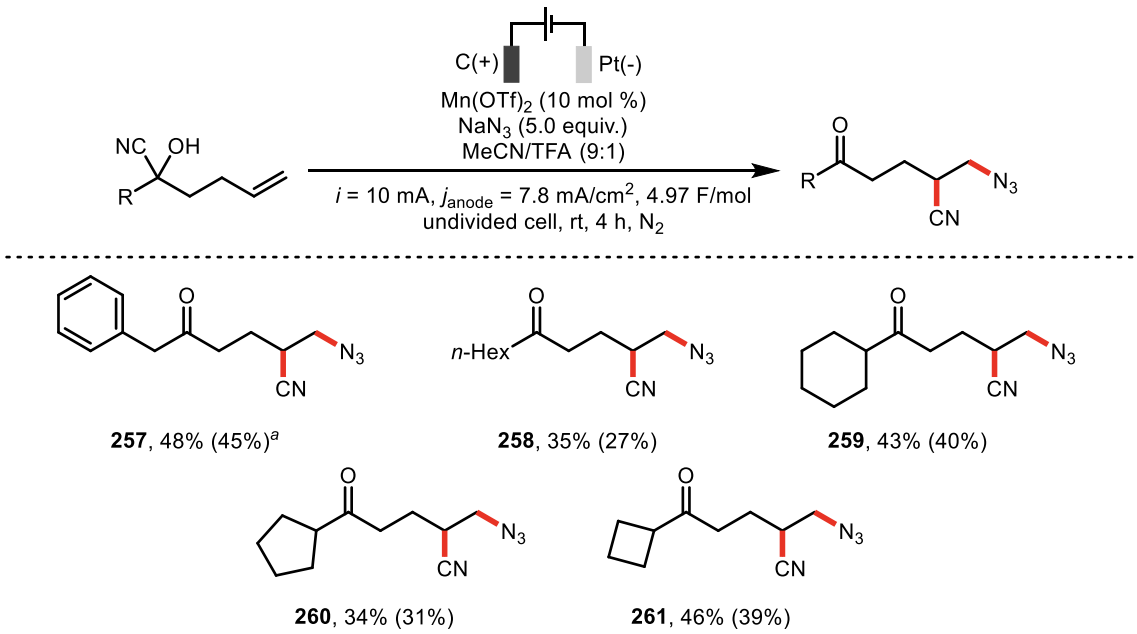

Yields as determined by ^{1}H NMR analysis of the crude reaction mixture using 1,3,5-trimethylbenzene as the internal standard quoted. Isolated yield given in parentheses. [a] 5 h (Q = 6.22 F/mol)

Scheme 4.19: Substrate scope – alkyl cyanohydrins

The alkyl cyanohydrins tested performed well under these reaction conditions, providing access to benzyl ketone **257** in a comparable yield to parent product **163**, albeit with a longer reaction time of 5 h required. The performance of other alkyl cyanohydrins varied, with cyclohexyl and cyclobutyl ketones **259** and **261** obtained in higher yields than *n*-hexyl and cyclopentyl ketones **258** and **260**.

Substrates with substitution on the alkene or alkyl chain were then tested under the reaction conditions (Scheme 4.20).

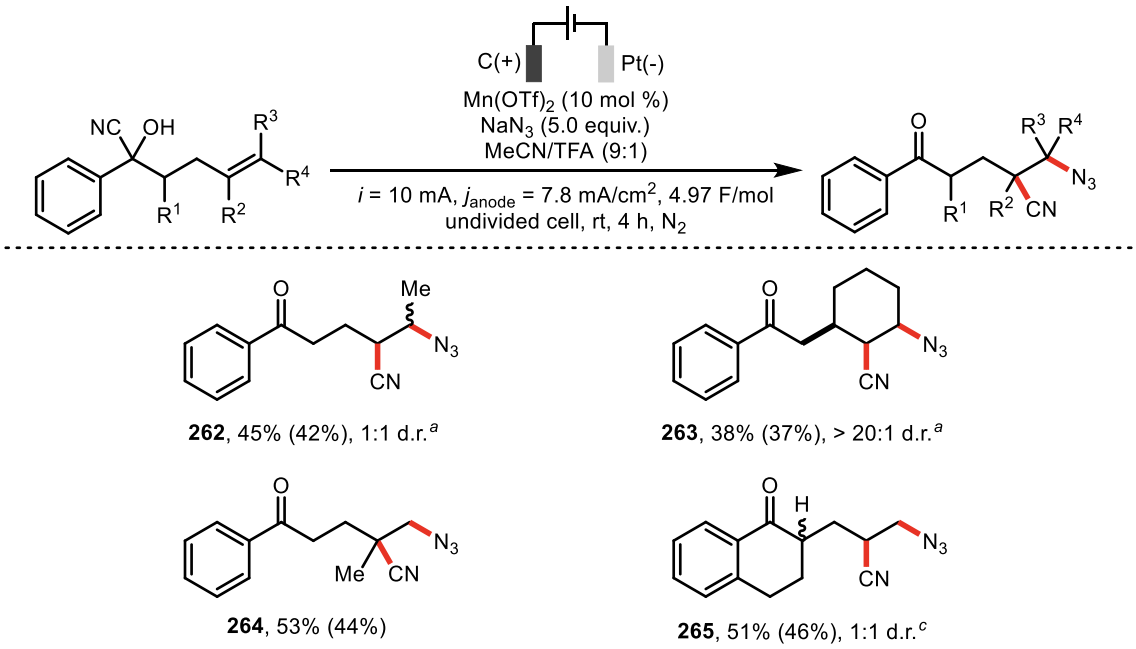

Yields as determined by ^{1}H NMR analysis of the crude reaction mixture using 1,3,5-trimethylbenzene as the internal standard quoted. Isolated yield given in parentheses. [a] As determined by ^{1}H NMR analysis of the crude reaction mixture.

Scheme 4.20: Substrate scope – alkyl chain and alkenyl substitution

Substitution on the alkene allowed for the formation of secondary alkyl azides **262** and **263** in good yields. **262** was formed as a 1:1 mixture of diastereoisomers, whereas **263** which was formed as a single diastereoisomer by ^{1}H NMR, presumably due to the conformational rigidity of the cyclohexane ring. Quaternary nitrile **264** was also formed in a 44% isolated yield, and subjection of 1-tetralol **237** led to the synthesis of 1-tetralone **265** as a 1:1 mixture of diastereoisomers.

Despite the broad substrate scope exhibited in this reaction, with a wide range of products formed and functional groups tolerated, there were limitations discovered. Cyanohydrin substrates that failed to furnish the desired 1,2-azidonitrile products under the electrochemical reaction conditions are shown in Figure 4.1.

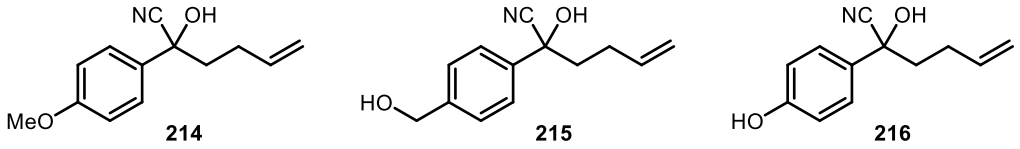

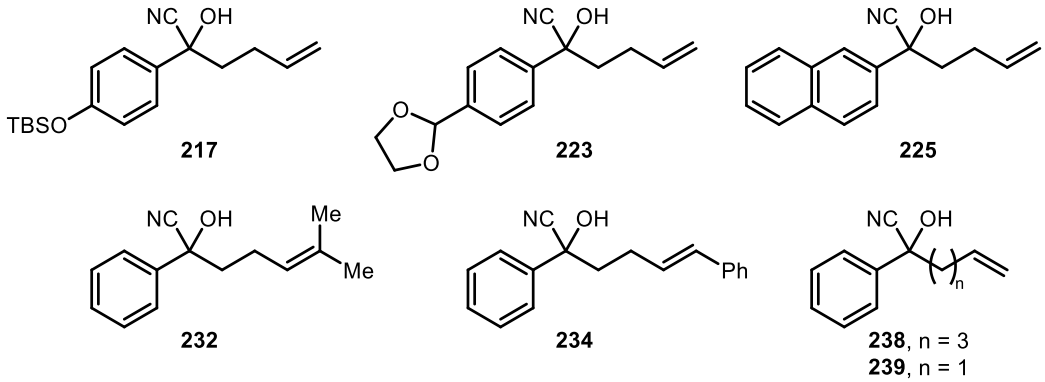

Figure 4.1: Incompatible substrates

When *para*-methoxyphenyl cyanohydrin **214** was subjected to this electrochemical reaction, analysis of the crude reaction mixture by ^{1}H NMR indicated just a 23% yield of the desired product, with only 7% of **214** recovered. This lower yield observed may be due to a decreased stability of **214** and/or intermediates within the reaction, favouring unproductive pathways. The identity of any side-products was not able to be confirmed, but perhaps they could be through the use of LCMS or other analytical techniques. Further optimisation towards this substrate may allow for improved performance.

When benzyl alcohol **215** was used, two 1,2-azidonitrile products were obtained in a 1:1 mixture and 34% combined yield by ^{1}H NMR. Of the two products obtained, one contained the benzyl alcohol functional group intact, and the other was identified as the benzaldehyde analogue, indicating that this process is not completely tolerant of redox sensitive functional groups. Attempts to prevent the oxidation of the benzyl alcohol to the benzaldehyde in the reaction using potentiostatic conditions (E_{cell} = 2.4 and 2.0 V) proved unsuccessful, with a 1:1 mixture of the two products formed on each attempt. Phenol **216** was showed only starting material decomposition, with no desired product observed by ^{1}H NMR and only 55% of **216** recovered. As with **214**, any side-products could not be identified. TBS-protected phenol **217** performed similarly to **216**, giving a 10% yield by ^{1}H NMR of the desired product, with 43% recovery of **217**. Further optimisation towards this substrate may also give an improvement in the yield obtained.

Acetal **223** gave a complex mixture of products which could not be identified, although there was possibly some substitution on the 1,3-dioxolane ring, perhaps through some Shono-type reactivity of the electron-rich ring. 2-Naphthyl cyanohydrin **225** was unreactive, with only a 15% yield observed by ^{1}H NMR, but this potentially could be improved through further substrate specific optimisation. Isoprenyl substrate **232** and styrenyl substrate **234** were completely unreactive and unstable to the reaction conditions, with no product and < 10% of the substrates observed by ^{1}H NMR in either

case. Attempts to shorten or elongate the alkyl chain also proved unsuccessful, with neither **238** nor **239** delivering the desired product, and whereas 37% of **239** was recovered, no **238** was observed by ^{1}H NMR analysis of the crude reaction mixture and a complex mixture of side-products observed.

4.2.3.3 Alternative Transformations

Following complete evaluation of the substrate scope for the electrochemical azidocyanation of alkenes, alternate transformations were then investigated under this electro-synthetic manifold (Scheme 4.21).

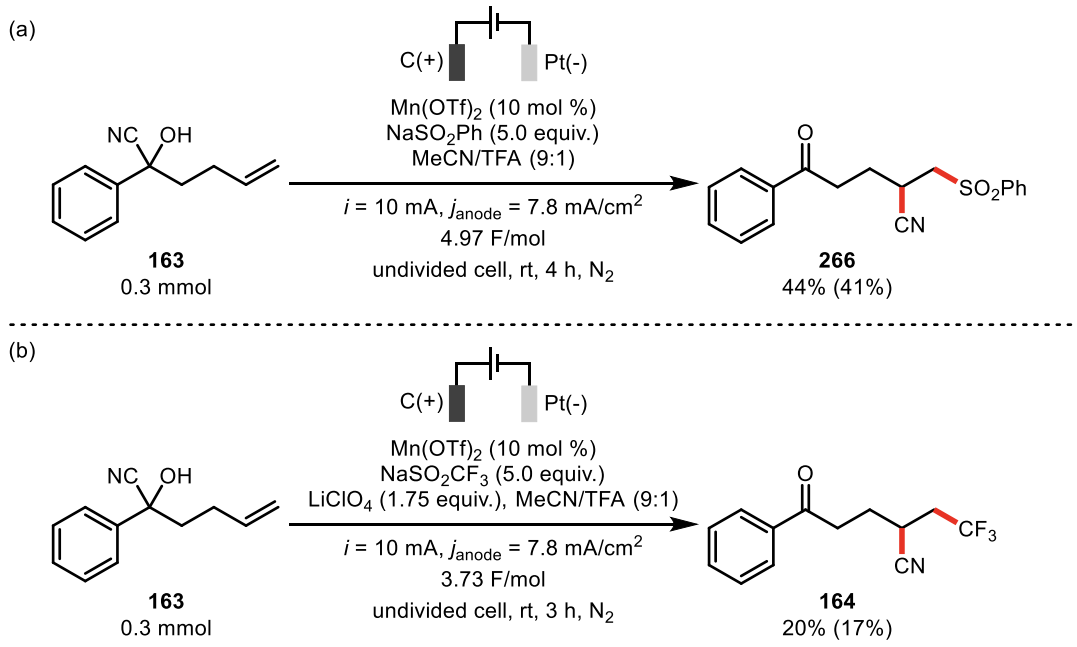

Yields as determined by ^{1}H NMR analysis of the crude reaction mixture using 1,3,5-trimethylbenzene as the internal standard quoted. Isolated yield given in parentheses.

Scheme 4.21: Addition of alternative radicals. (a) Electrochemical alkene sulfonylcyanation; (b) Electrochemical alkene trifluoromethylcyanation

Simply by substituting the sodium azide for sodium benzenesulfinate, sulfone **266** was obtained in a 44% yield by ^{1}H NMR and was isolated in a 41% yield (Scheme 4.21a). When sodium trifluoromethanesulfinate was used 1,2-trifluoromethylnitrile **164** was formed in a 20% ^{1}H NMR yield, and isolated in a 17% yield (Scheme 4.21b). In this example $LiClO_4$ was required as supporting electrolyte to decrease the resistance of the system, with high potentials observed in its absence. These reactions demonstrate the ability to initiate nitrile migration *via* the addition of sulfonyl or trifluoromethyl radicals to the alkene in this electrochemical system.

Subsequently, malononitrile **268** was synthesised and subjected to this electrochemical reaction to perform diazidation of the substrate as well as nitrile migration (Scheme 4.22).

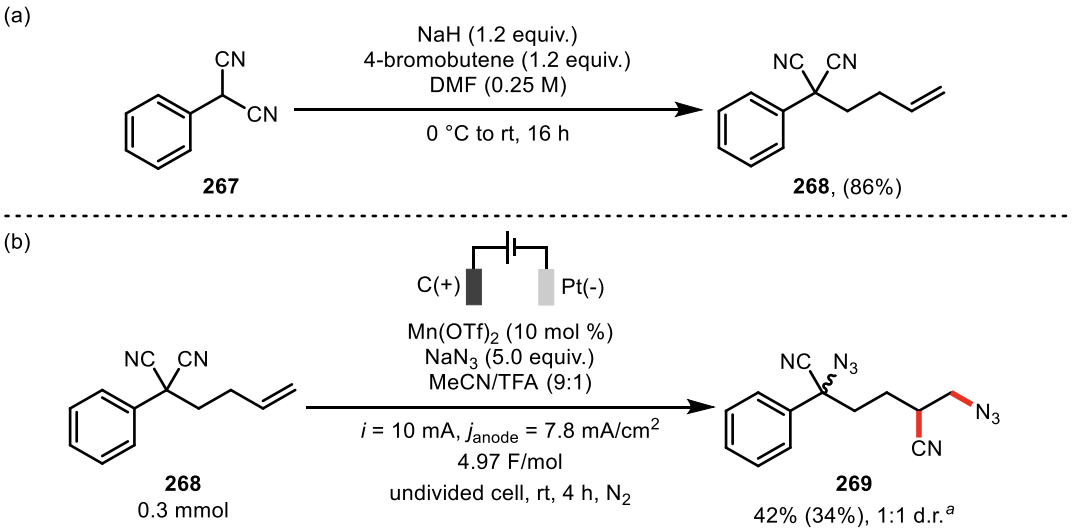

Yields as determined by ^{1}H NMR analysis of the crude reaction mixture using 1,3,5-trimethylbenzene as the internal standard quoted. Isolated yield given in parentheses.

*Scheme 4.22: (a) Synthesis of malononitrile substrate **4-DB**; (b) Subjection of **4-DB** to the parent reaction conditions*

Malononitrile **268** was synthesised from 2-phenylmalononitrile **267** through deprotonation with sodium hydride followed by alkylation with 4-bromobut-1-ene and was obtained in an 86% isolated yield (Scheme 4.22a). Subjection of **268** to the "standard" electrochemical system furnished trifunctionalised hexanenitrile **269** in a 42% yield by ^{1}H NMR in a 1:1 diastereomeric ratio (Scheme 4.22b).

4.2.3.4 Product Derivatisations

With the scope of this reaction fully investigated, focus was turned to demonstrating the utility product **165** through its orthogonal derivatisation (Scheme 4.23).

It was found that the azide substituent could be smoothly converted to 1,4-disubstituted-1,2,3-triazole **270** *via* a copper (I)-catalysed azide-alkyne cycloaddition (CuAAC) procedure (Scheme 4.23a).[50] Reacting **165** with phenyl acetylene in the presence of a catalytic quantity of $CuSO_4$ and sodium ascorbate as an organic reductant allowed for the formation of **270** regioselectively.[51] Furthermore, the ketone could be converted to hydrazone **271** *via* condensation with benzhydrazide in an 88% isolated yield (Scheme 4.23b).[52] Attempts to derivatise the nitrile through hydrolysing the nitrile to a carboxylic acid under basic conditions proved unsuccessful, resulting in the formation of side products, including the elimination of azide to form a terminal alkene.

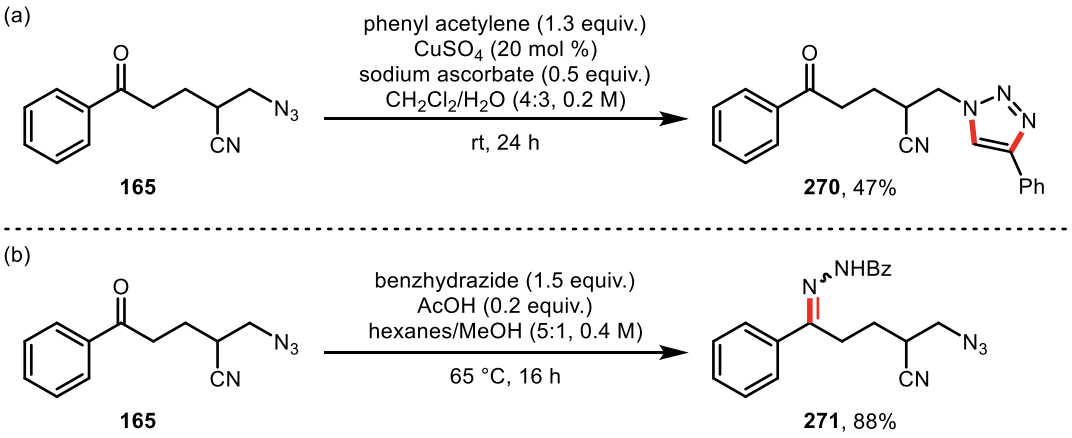

Scheme 4.23: Orthogonal product derivatisations. (a) CuAAC; (b) Hydrazone condensation

4.2.4 Reaction Scale-up

4.2.4.1 Flow electrochemistry

Upon complete evaluation of the substrate scope, as well as the orthogonal derivatisation of **165**, the scalability of the electrochemical transformation was then explored using flow electrochemistry. To do so, the parent reaction was translated to a flow electrochemistry set up using the Ammonite8 flow cell electrochemical reactor.[53]

Initially, a single pass flow electrochemical system was explored, with the current applied investigated (Table 4.12).

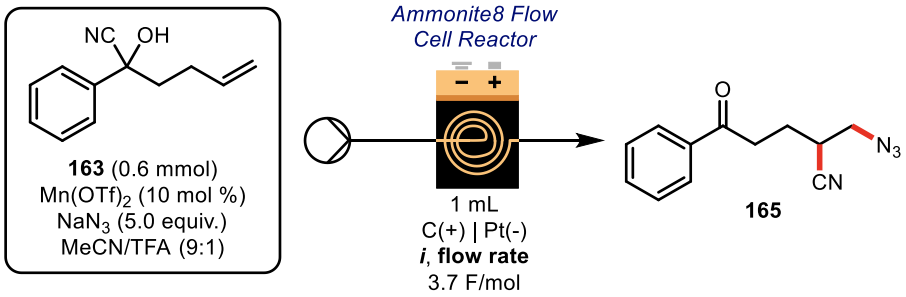

Entry[a]	Current (mA)	Flow rate (mL/min)	163[b] (%)	165[b] (%)
1	300	1.0	62	11
2	400	1.4	58	12
3	500	1.7	64	6
4	600	2.0	57	9

[a] Reactions performed using 0.6 mmol of cyanohydrin **163** in a flow electrochemical set up using the Ammonite8 flow cell electrochemical reactor. [**163**] = 0.05 M. [b] Yield after 3 h as determined by ^{1}H NMR analysis of the crude reaction mixture with 1,3,5-trimethylbenzene as the internal standard.

Table 4.12: Scale-up using single pass flow electrochemistry

In this system, **163** (0.6 mmol) was dissolved in a 9:1 mixture of MeCN and TFA (0.05 M) along with $Mn(OTf)_2$ (10 mol %) and sodium azide (5.0 equiv.). The solution was drawn up into a syringe and loaded onto a syringe pump set to the appropriate flow rate and passed through the Ammonite8 cell reactor with the appropriate current applied.

With changes in current being made, the flow rate also had to be changed to keep the amount of charge passed consistent between experiments. Initially, a current of 300 mA was applied, which resulted in only an 11% yield of **165** by ^{1}H NMR and 62% recovery of **163** (entry 1). Increasing the applied current from 300 mA up to 600 mA (with concurrent increases in the flow rate) showed similar results throughout (entries 2-4). These results highlight that a single pass through the Ammonite8 cell reactor is not sufficiently efficient to induce the electrochemical transformation or for long enough to see an appreciable formation of **165**. These observations are consistent with the previous investigations which revealed there is a lack of charge efficiency of the parent reaction.

To combat this, it was thought that employing a recirculating flow electrochemical system, which would access a prolonged residence time in the Ammonite8 cell reactor, hence potentially allowing access to a higher yield of **165** (Table 4.13).

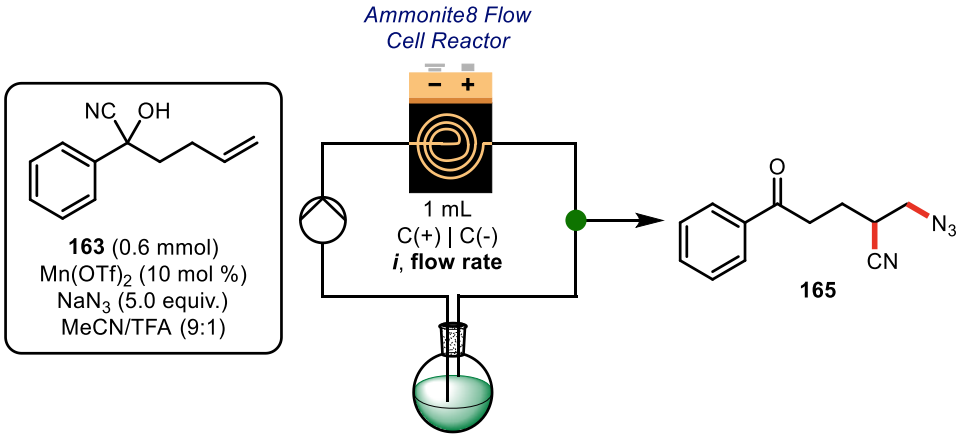

Entry[a]	Current (mA)	Flow rate (mL/min)	Time (min)	163[b] (%)	165[b] (%)
1	400	1.0	60	20	2
2	400	2.5	15	47	2
3	300	2.5	15	43	8

[a] Reactions performed using 0.6 mmol of cyanohydrin **163** in a flow electrochemical set up using the Ammonite8 flow cell electrochemical reactor. [**163**] = 0.05 M. [b] Yield after 3 h as determined by ^{1}H NMR analysis of the crude reaction mixture with 1,3,5-trimethylbenzene as the internal standard.

Table 4.13: Scale-up using recirculating flow electrochemistry

In this recirculating flow system, a solution of **163** (0.6 mmol), Mn(OTf) (10 mol %), and sodium azide (5.0 equiv.) in a 9:1 mixture of MeCN and TFA was pumped through the Ammonite8 cell reactor using a HPLC pump at the desired flow rate for the specified time with the appropriate current applied.

Initially, a current of 400 mA was applied and a flow rate of 1 mL/min selected, with the solution recirculated for 60 min, after which a 2% yield of **165** was obtained by ^{1}H NMR, with just 20% of **163** recovered (entry 1). To see whether the low yield obtained was due to the products instability within the electrochemical system, the reaction time was decreased to 15 min, with the flow rate increased to 2.5 mL/min where a similar yield of **165** was obtained, albeit with an increased recovery of **163** (entry 2). Reduction of the current to 300 mA resulted in a slightly improved yield of **165** (entry 3). These results seem to indicate that within the flow electrochemical system the rate of undesired side reactions/decomposition pathways is higher than that of the desired transformation. Throughout these experiments, the reaction mixture also seemed to facilitate blockages within the HPLC pumps used, potentially due to the corrosive nature of TFA. As a result, the attempts to scale-up the reaction using flow electrochemistry were ceased, and a scale-up within a batch electrochemical reactor was explored.

4.2.4.2 Batch Scale-up

The scale-up within a batch electrochemical system allowed for 1.0 mmol of **163** to be processed (Scheme 4.24).

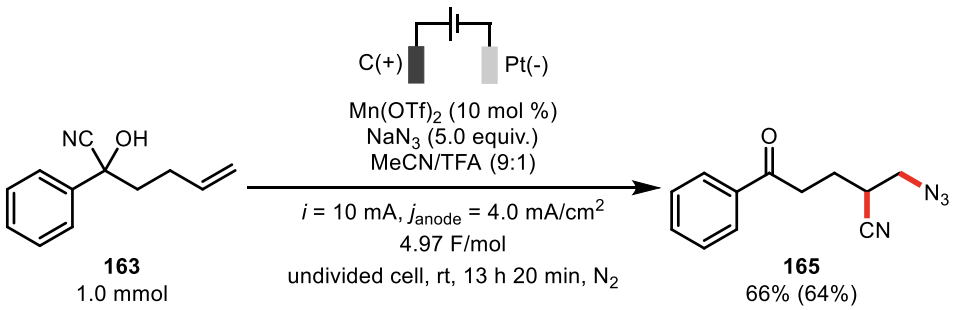

Yield as determined by ^{1}H NMR analysis of the crude reaction mixture using 1,3,5-trimethylbenzene as the internal standard quoted. Isolated yield given in parentheses.

Scheme 4.24 Scale-up in a batch electrochemical system

Upon scale-up from 0.3 to 1.0 mmol reaction, with the reaction time increased to 13 h 20 min (in order to pass the same amount of charge as on a 0.3 mmol scale), **165** could be obtained in a 66% yield by ^{1}H NMR, and isolated in a 64% yield. The reason for the improved yield compared to the reaction on a 0.3 mmol scale is unclear; however, it may

be that the increased volume of solvent used in the larger vial lowers the current density from 7.8 mA/cm^2 to 4.0 mA/cm^2, which may prevent decomposition of the starting material or reaction intermediates at the electrodes.

4.2.5 Mechanistic Studies

Mechanistic studies were then performed to gain insight into how this reaction proceeds. This was achieved using both cyclic voltammetry (CV) as well as through experimental means.

4.2.5.1 Cyclic Voltammetry Studies

Cyclic voltammetry (CV) was employed in order to gain an insight into the mechanism of this electrochemical process.[54] Through this technique, single electron transfer events can be observed for each component of the reaction, as well as for their combinations, providing information on the relative oxidation potentials of each component of the reaction. Firstly, the $Mn(OTf)_2$ salt and $TBAN_3$, used in place of sodium azide due to increased solubility in organic solvents, were studied using CV (Figure 4.2).

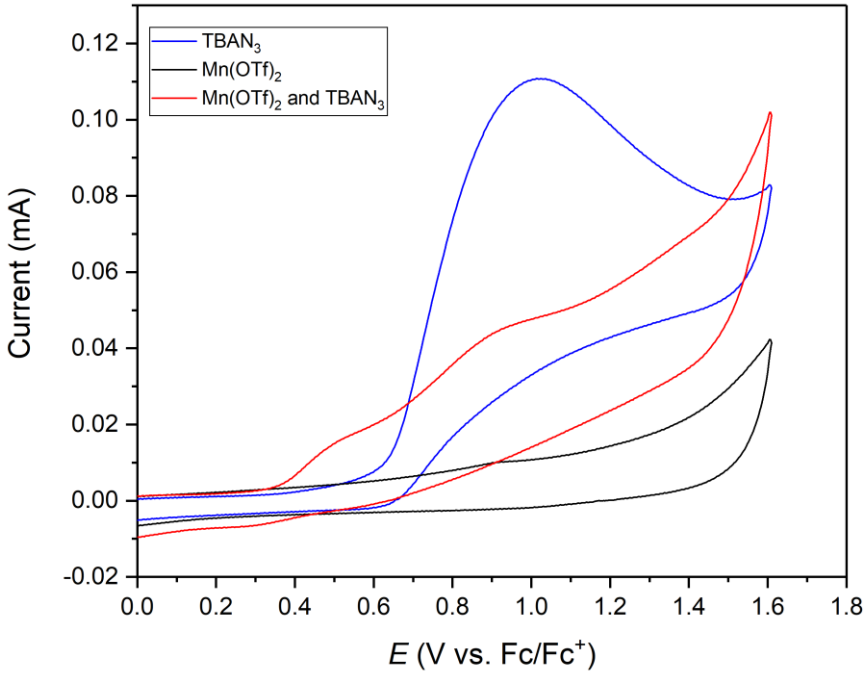

*Figure 4.2: Cyclic Voltammogram of $Mn(OTf)_2$, $TBAN_3$, and their mixture in MeCN (6 mL) with AcOH (240 µL) and $LiClO_4$ (0.1 M). **a** (black line) – $Mn(OTf)_2$ (2.0 mM); **b** (blue line) – $TBAN_3$ (10 mM); **c** (red line) – $Mn(OTf)_2$ (2.0 mM) and $TBAN_3$ (10 mM). **Scan rate: 100 mV/s***

From this voltammogram, it can be seen that $Mn(OTf)_2$ alone (black line) is redox inactive within the operating range of the solvent, whereas $TBAN_3$ (red line) shows an irreversible oxidation event at ~1.0 V vs Fc/Fc^+ for the single electron oxidation of azide anions to azidyl radicals. Upon the combination of $Mn(OTf)_2$ and NaN_3, a new series of irreversible redox events are observed, starting at ~0.5 V vs Fc/Fc^+, providing evidence for the formation of a new compound that has a lower oxidation potential than $TBAN_3$. It is proposed that this species is an anionic $[Mn(II)X_2N_3]^-$ complex (X = OTf, OAc, or N_3) that is then oxidised at the anode to $Mn(III)X_2N_3$.[48]

4.2.5.2 Experimental Evidence

To determine whether the reaction proceeds *via* a radical mechanism a radical clock experiment was designed. Cyclopropyl substituted cyanohydrin **274** was first synthesised from cyclopropanecarboxylic acid (Scheme 4.25). This substrate was synthesised by Deepak Mishra.

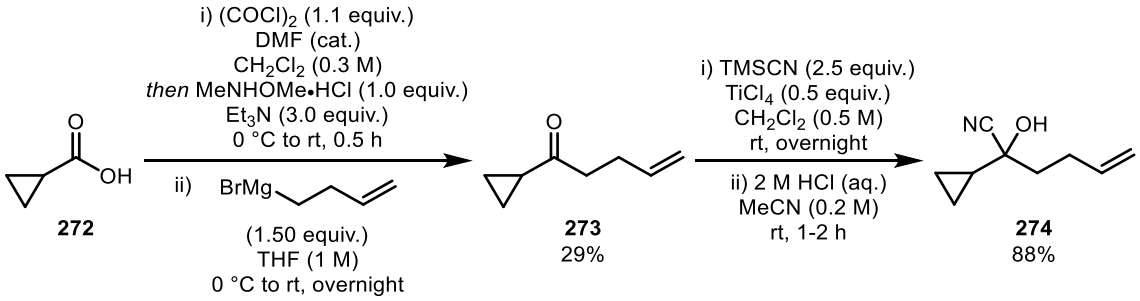

*Scheme 4.25: Synthesis of **274***

Cyclopropanecarboxylic acid **272** was first transformed into the corresponding Weinreb amide *via* the acid chloride, then the Grignard reagent of 4-bromobut-1-ene was added to furnish ketone **273** in a 29% yield. Upon reaction of **273** with TMSCN in the presence of $TiCl_4$, followed by acid mediated removal of the TMS group delivered cyanohydrin **274** in an 88% yield.

Once synthesised, **274** was then subjected to the parent reaction conditions as a radical clock experiment (Scheme 4.26). This reaction was performed by Deepak Mishra.

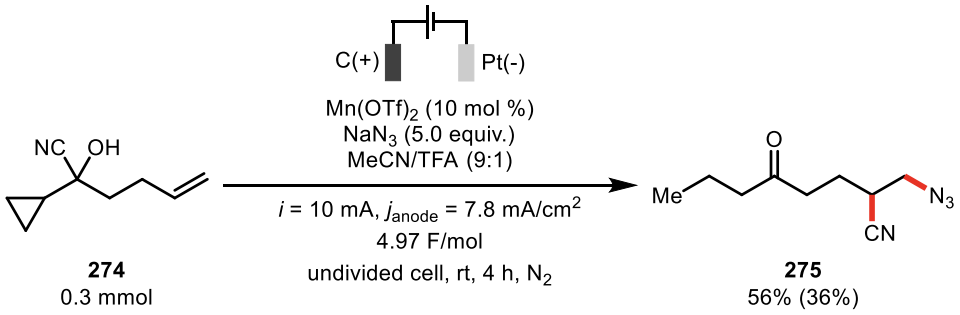

Yield as determined by ^{1}H NMR analysis of the crude reaction mixture using 1,3,5-trimethylbenzene as this internal standard quoted. Isolated yield given in parentheses.

Scheme 4.26: Radical clock experiment

Upon subjection of **274** to the electrochemical conditions, ring opened product **275** was obtained as the sole product of the reaction in a 56% yield by ^{1}H NMR (36% isolated). The delivery of **275** signifies the presence of radical intermediates within the operative reaction mechanism.

4.2.5.3 Proposed Mechanism

Following the mechanistic investigations disclosed thus far in section 4.2.5, as well as literature precedent,[25,48] the following plausible reaction mechanism is proposed (Scheme 4.28).

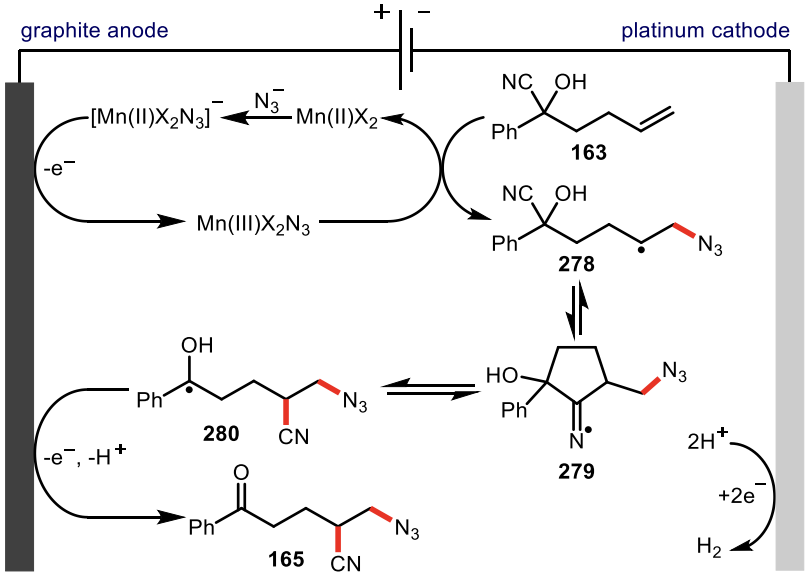

Scheme 4.28: Proposed reaction mechanism

Firstly, through the combination of Mn(II)X_2 and NaN_3, anionic species [Mn(II)X_2N_3]$^-$ is formed, which can then be oxidised at the anode to give Mn(III)X_2N_3. This intermediate

can act as an azide transfer reagent to deliver the azide to cyanohydrin **163**, furnishing secondary alkyl radical intermediate **278**. Intramolecular interception of this radical by the nitrile *via* a 5-exo-dig cyclisation affords iminyl radical **279**, which can subsequently undergo *β*-scission to give *α*-hydroxy alkyl radical **280**. A second oxidation at the anode, followed by proton loss affords 1,2-azidonitrile **165**. Hydrogen gas is evolved *via* proton reduction at the cathode.

4.3 Further Work

Further work in this area of research should focus on the development of alternative electrochemical alkene hetero-difunctionalisations *via* functional group migrations.

The work discussed in this chapter does have its limitations. Namely, only 1,4-nitrile migration can be performed under the developed conditions, with attempts to perform 1,3- and 1,5-nitrile migration through shortening or extending the alkyl chain between the cyanohydrin and alkene proving unsuccessful. A possible reason for this may be the instability of the cyanohydrin substrate and/or reaction intermediates under the current electrochemical conditions.

At this time, the electrochemical alkene sulfonylcyanation and trifluoromethylcyanation have been demonstrated, and further optimisation through screening of the various reaction conditions may allow for an improvement in the efficiency of these reactions. The use of the alternative reagents required for these transformations may allow for improved stability of the cyanohydrin starting materials under the reaction conditions.

There are also opportunities to develop electrochemical alkene hetero-difunctionalisation reactions using alternative substrates, with the nitrile swapped for other functional groups such as carbonyls and oximinyl groups. These substrates may be more stable than cyanohydrins under the reaction conditions, allowing for the development of a more general methodology than the one discussed in this chapter.

4.4 Conclusion

In conclusion, we have developed a new methodology for hetero-difunctionalisation of alkenes through this electrochemical alkene azidocyanation procedure.[55] This methodology is applicable across various alkene containing cyanohydrins, providing access to a broad range of synthetically useful 1,2-azidonitriles (28 examples). Tolerance of redox sensitive functional groups demonstrated, including nitriles, carboxylic esters, and benzamides. The utility of these products was demonstrated through orthogonal derivatisation using chemoselective transformations like the well understood CuAAC. The

method could also be extended to perform alkene sulfonylcyanation and trifluoromethylcyanation, simply by swapping sodium azide for the appropriate salt thus demonstrating the applicability of the developed methodology. By extension, a functionalised malononitrile starting material was also utilised to deliver a trifunctionalised hexanenitrile, which could be derivatised further. Mechanistic investigations, including the use of CV studies and a radical clock experiment, allowed the proposal of a plausible mechanistic pathway involving radical intermediates, in conjunction with known literature.

4.4 References

1 K. Y. Ye, G. Pombar, N. Fu, G. S. Sauer, I. Keresztes and S. Lin, *J. Am. Chem. Soc.*, 2018, **140**, 2438–2441.

2 G. M. Martins, B. Shirinfar, T. Hardwick and N. Ahmed, *ChemElectroChem*, 2019, **6**, 1300–1315.

3 J. C. Siu, N. Fu and S. Lin, *Acc. Chem. Res.*, 2020, **53**, 547–560.

4 W. Zhang and S. Lin, *J. Am. Chem. Soc.*, 2020, **142**, 20661–20670.

5 F. Xu, L. Zhu, S. Zhu, X. Yan and H. C. Xu, *Chem. - Eur. J.*, 2014, **20**, 12740–12744.

6 Y. Yuan, Y. Cao, Y. Lin, Y. Li, Z. Huang and A. Lei, *ACS Catal.*, 2018, **8**, 10871–10875.

7 Y. Yuan, Y. Chen, S. Tang, Z. Huang and A. Lei, *Sci. Adv.*, 2018, **4**, eaat5312.

8 Y. Wang, L. Deng, H. Mei, B. Du, J. Han and Y. Pan, *Green Chem.*, 2018, **20**, 3444–3449.

9 L. Sun, Y. Yuan, M. Yao, H. Wang, D. Wang, M. Gao, Y. H. Chen and A. Lei, *Org. Lett.*, 2019, **21**, 1297–1300.

10 S. Zhang, L. Li, J. Zhang, J. Zhang, M. Xue and K. Xu, *Chem. Sci.*, 2019, **10**, 3181–3185.

11 M. J. Luo, B. Liu, Y. Li, M. Hu and J. H. Li, *Adv. Synth. Catal.*, 2019, **361**, 1538–1542.

12 M. Xiong, X. Liang, X. Liang, Y. Pan and A. Lei, *ChemElectroChem*, 2019, **6**, 3383–3386.

13 X. Q. Mou, L. C. Ren, M. Zhang, M. Wang, Y. F. Jin, Q. X. Guan, A. Cai, S. M. Zhang, H. Ren, Y. Zhang and Y. Z. Chen, *Org. Lett.*, 2022, **24**, 1405–1411.

14 J. Yang, G. Li, K. Yu, B. Xu and Q. Chen, *J. Org. Chem.*, 2022, **87**, 1208–1217.

15 R. Feng, J. A. Smith and K. D. Moeller, *Acc. Chem. Res.*, 2017, **50**, 2346–2352.

16 C. Y. Cai and H. C. Xu, *Nat. Commun.*, 2018, **9**, 3551.

17 P. Xiong, H. Long and H. C. Xu, *Asian J. Org. Chem.*, 2019, **8**, 658–660.

18 Q. H. Teng, Y. Sun, Y. Yao, H. T. Tang, J. R. Li and Y. M. Pan, *ChemElectroChem*, 2019, **6**, 3120–3124.

19 N. Fu, G. S. Sauer, A. Saha, A. Loo and S. Lin, *Science*, 2017, **357**, 575–579.

20 N. Fu, G. S. Sauer and S. Lin, *J. Am. Chem. Soc.*, 2017, **139**, 15548–15553.

21 J. C. Siu, G. S. Sauer, A. Saha, R. L. MacEy, N. Fu, T. Chauviré, K. M. Lancaster and S. Lin, *J. Am. Chem. Soc.*, 2018, **140**, 12511–12520.

22 J. C. Siu, J. B. Parry and S. Lin, *J. Am. Chem. Soc.*, 2019, **141**, 2825–2831.

23 L. Lu, N. Fu and S. Lin, *Synlett*, 2019, **30**, 1199–1203.

24 X. Wu and C. Zhu, *Acc. Chem. Res.*, 2020, **53**, 1620–1636.

25 Z. Wu, R. Ren and C. Zhu, *Angew. Chem., Int. Ed.*, 2016, **55**, 10821–10824.

26 M. Ji, Z. Wu, J. Yu, X. Wan and C. Zhu, *Adv. Synth. Catal.*, 2017, **359**, 1959–1962.

27 R. Ren, Z. Wu, L. Huan and C. Zhu, *Adv. Synth. Catal.*, 2017, **359**, 3052–3056.

28 D. Chen, Z. Wu, Y. Yao and C. Zhu, *Org. Chem. Front.*, 2018, **5**, 2370–2374.

29 M. Ji, Z. Wu and C. Zhu, *Chem. Commun.*, 2019, **55**, 2368–2371.

30 C. Chang, H. Zhang, X. Wu and C. Zhu, *Chem. Commun.*, 2022, **58**, 1005–1008.

31 X. Tang and A. Studer, *Chem. Sci.*, 2017, **8**, 6888–6892.

32 Y. Xu, Z. Wu, J. Jiang, Z. Ke and C. Zhu, *Angew. Chem., Int. Ed.*, 2017, **56**, 4545–4548.

33 J. Yu, D. Wang, Y. Xu, Z. Wu and C. Zhu, *Adv. Synth. Catal.*, 2018, **360**, 744–750.

34 Z. Wu, D. Wang, Y. Liu, L. Huan and C. Zhu, *J. Am. Chem. Soc.*, 2017, **139**, 1388–1391.

35 M. Wang, Z. Wu, B. Zhang and C. Zhu, *Org. Chem. Front.*, 2018, **5**, 1896–1899.

36 X. J. Wei and T. Noël, *J. Org. Chem.*, 2018, **83**, 11377–11384.

37 H. Zhang, X. Wu, Q. Zhao and C. Zhu, *Chem. - An Asian J.*, 2018, **13**, 2453–2457.

38 N. Tang, S. Yang, X. Wu and C. Zhu, *Tetrahedron*, 2019, **75**, 1639–1646.

39 Z. L. Li, X. H. Li, N. Wang, N. Y. Yang and X. Y. Liu, *Angew. Chem., Int. Ed.*, 2016, **55**, 15100–15104.

40 Y. Gao, H. Mei, J. Han and Y. Pan, *Chem. - Eur. J.*, 2018, **24**, 17205–17209.

41 M. W. Zheng, X. Yuan, Y. S. Cui, J. K. Qiu, G. Li and K. Guo, *Org. Lett.*, 2018, **20**, 7784–7789.

42 Z. Zou, W. Zhang, Y. Wang, L. Kong, G. Karotsis, Y. Wang and Y. Pan, *Org. Lett.*, 2019, **21**, 1857–1862.

43 C. Chen, J. C. Kang, C. Mao, J. W. Dong, Y. Y. Xie, T. M. Ding, Y. Q. Tu, Z. M. Chen and S. Y. Zhang, *Green Chem.*, 2019, **21**, 4014–4019.

44 H. I. Jung, Y. Kim and D. Y. Kim, *Org. Biomol. Chem.*, 2019, **17**, 3319–3323.

45 Y. J. Kim and D. Y. Kim, *Org. Lett.*, 2019, **21**, 1021–1025.

46 J. C. Kang, Y. Q. Tu, J. W. Dong, C. Chen, J. Zhou, T. M. Ding, J. T. Zai, Z. M. Chen and S. Y. Zhang, *Org. Lett.*, 2019, **21**, 2536–2540.

47 Z. Guan, H. Wang, Y. Huang, Y. Wang, S. Wang and A. Lei, *Org. Lett.*, 2019, **21**, 4619–4622.

48 N. Fu, G. S. Sauer and S. Lin, *Nat. Protoc.*, 2018, **13**, 1725–1743.

49 F. Eckert, I. Leito, I. Kaljurand, A. Kütt, A. Klamt and M. Diedenhofen, *J. Comput. Chem.*, 2009, **30**, 799–810.

50 X. Creary, A. Anderson, C. Brophy, F. Crowell and Z. Funk, *J. Org. Chem.*, 2012, **77**, 8756–8761.

51 F. Himo, T. Lovell, R. Hilgraf, V. V Rostovtsev, L. Noodleman, K. B. Sharpless and V. V Fokin, *J. Am. Chem. Soc.*, 2005, **127**, 210–216.

52 X. L. Yang, X. X. Peng, F. Chen and B. Han, *Org. Lett.*, 2016, **18**, 2070–2073.

53 R. A. Green, R. C. D. Brown, D. Pletcher and B. Harji, *Org. Process Res. Dev.*, 2015, **19**, 1424–1427.

54 C. Sandford, M. A. Edwards, K. J. Klunder, D. P. Hickey, M. Li, K. Barman, M. S. Sigman, H. S. White and S. D. Minteer, *Chem. Sci.*, 2019, **10**, 6404–6422.

55 A. C. Seastram, M. D. Hareram, T. M. B. Knight and L. C. Morrill, *Chem. Commun.*, 2022, **58**, 8658–8661.

Chapter 5: Experimental

Table of Contents

5.1 General Information

Unless otherwise stated, all non-electrochemical reactions were conducted in flame-dried glassware under an atmosphere of dry nitrogen, sealed with septum seals and were stirred with Teflon-coated magnetic stirrer bars. Unless otherwise stated, all electrochemical reactions were performed using oven-dried ElectraSyn vials under an atmosphere of dry nitrogen, sealed with an ElectraSyn Teflon cap fitted with the appropriate electrodes and were stirred with Teflon-coated magnetic stirrer bars. Dry acetonitrile (MeCN), dichloromethane (CH_2Cl_2), diethyl ether (Et_2O) and tetrahydrofuran (THF) were obtained after passing these previously degassed solvents through activated alumina columns (Mbraun, SPS-800). Tetra-*n*-butylammonium hexafluorophosphate ($TBAPF_6$) and tetra-*n*-butylammonium tetrafluoroborate ($TBABF_4$) were recrystallised from ethanol or water, respectively, and dried in an oven before use. All other solvents and commercial reagents were used as supplied without further purification unless otherwise stated.

All electrochemical reactions were conducted using an ElectraSyn 2.0 apparatus, purchased from IKA. Graphite, reticulated vitreous carbon (RVC), and platinum foil electrodes were purchased from IKA and are of uniform dimensions. Graphite electrodes were also cut from a sheet of carbon foil (2 mm thickness) purchased from Goodfellow. The electrodes were cut to the dimension of 8 mm × 52 mm using a Startrite Bandsaw (model 18-T-5), with a Starrett Durate SFB High Carbon Steel Blade, 2870 mm × 10 mm × 0.65 mm, 3 mm pitch, regular tooth. Graphite electrodes could be used several times by renewing the top surface of the graphite, this was achieved by scraping away the top layer with a razor blade, sonicating in MeCN for 5 minutes, followed by oven-drying for at least 30 mins. Platinum electrodes were cut from a sheet of platinum foil (0.05 mm thickness) purchased from Goodfellow using scissors. Platinum electrodes were washed with water and acetone, then burned over a Bunsen burner before every reaction.

Cyclic voltammetry (CV) experiments were conducted using a Metrohm Autolab PGSTAT204, controlled using Nova 2.1 software. The working electrode was a glassy carbon disc (3 mm dia., BASi part number MF-2012), the counter electrode was a Pt-wire (BASi part number MW-4130) and a $Ag/AgNO_3$ reference electrode was used (BASi part number MF-2052).

Room temperature (rt) refers to 20–25 °C. Ice/water and CO_2(s)/acetone baths were used to obtain temperatures of 0 °C and -78 °C respectively. All reactions involving heating were conducted using DrySyn blocks and a contact thermometer.

Analytical thin layer chromatography was carried out using aluminium plates coated with silica (Kieselgel 60 F_{254} silica) and visualisation was achieved using ultraviolet light (254 nm), followed by staining with a 1% aqueous $KMnO_4$ solution. Flash column chromatography was performed using Kieselgel 60 silica in the solvent system stated.

Melting points were recorded on a Gallenkamp melting point apparatus and are reported corrected by linear calibration to benzophenone (47-49 °C) and benzoic acid (121-123 °C).

Infrared spectra were recorded on a Shimadzu IRAffinity-1 Fourier Transform ATR spectrometer as thin films using a Pike MIRacle ATR accessory. Characteristic peaks are quoted (v_{max} / cm^{-1}).

^{1}H, ^{13}C and ^{19}F NMR spectra were obtained on a Bruker Avance 300 (300 MHz ^{1}H, 75 MHz ^{13}C), Bruker Avance 400 (400 MHz ^{1}H, 101 MHz ^{13}C, 376 MHz ^{19}F) or a Bruker Avance 500 (500 MHz ^{1}H, 126 MHz ^{13}C) spectrometer at rt unless otherwise stated and in the solvent stated. Chemical shifts are reported in parts per million (ppm) relative to the residual solvent signal. All coupling constants, *J*, are quoted in Hz. Multiplicities are reported with the following symbols: br = broad, s = singlet, d = doublet, t = triplet, q = quartet, m = multiplet, app = apparent and combinations of these were used to denote higher order multiplicities.

High resolution mass spectrometry (HRMS, *m/z*) data was acquired at Cardiff University on a Micromass LCT Spectrometer.

“Petrol” refers to the fraction boiling in the range of 40-60 °C unless otherwise stated.

Current density values for the anode, j_{anode}, were calculated by dividing the current, *i*, passed during electrolysis by the exposed active surface area of the anode. The exposed active surface of the electrode was calculated to be the submerged surface of the electrode that was directly facing the other electrode, since electrons travel through the shortest available circuit (See Figure S1). See electrochemical General Procedures for specific current density values.

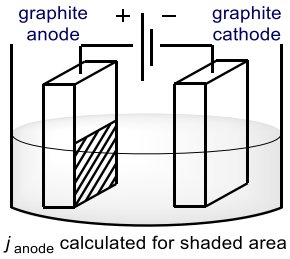

Figure 5.1: Current density calculation visual aid

5.2 Manganese-Catalysed Electrochemical Deconstructive Chlorination of Cycloalkanols *via* Alkoxy Radicals

5.2.1 Substrate Synthesis

General Procedure 1 – Generation and Addition of Grignard Reagents to Cycloalkanones

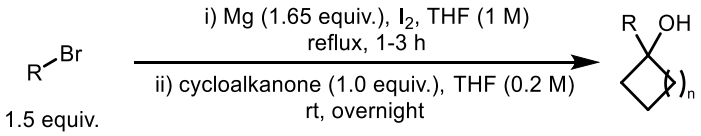

To a three-necked RBF fitted with a condenser, stopper, and septum seal was added magnesium (1.65 equiv.) and the system was flame-dried. After cooling, a crystal of iodine was added before the system was subjected to vacuum-nitrogen exchange cycles (× 3). Anhydrous THF (1 M with respect to the R-Br) was added, followed by dropwise addition of R-Br (1.50 equiv.). After complete addition, the mixture was stirred for 5 min at rt or until the exotherm had ceased, before being heated at reflux for 2-3 h. The reaction was allowed to cool to rt, then further cooled to 0 °C. A solution of the cycloalkanone (1.00 equiv.) in anhydrous THF (0.2 M) was added slowly and the reaction was stirred overnight at rt before being quenched with a saturated solution of NH_4Cl (aq.), and a few drops of 1 M HCl (aq.). EtOAc was added, the layers were separated, and the aqueous layer was further extracted with EtOAc (× 3). The combined organics were washed with brine, dried over $MgSO_4$, filtered, and concentrated under reduced pressure. The resultant crude material was purified by flash column chromatography to afford the desired compound.

General Procedure 2 – Addition of Commercially Available Grignard Reagents to Cycloalkanones

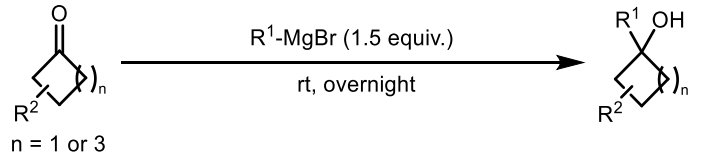

To a flame-dried RBF fitted with a septum seal was added a commercially available Grignard reagent (1.50 equiv.). After cooling to 0 °C, the cycloalkanone (1.00 equiv.) was added dropwise. After complete addition, the resulting mixture was stirred overnight at rt

before being quenched with a saturated solution of NH_4Cl (aq.), and a few drops of 1 M HCl (aq.). Et_2O was added, the layers were separated, and the aqueous layer was further extracted with Et_2O (× 3). The combined organics were washed with brine, dried over $MgSO_4$, filtered, and concentrated under reduced pressure. The resultant crude material was purified by flash column chromatography to afford the desired compound.

General Procedure 3 – Generation and Addition of Organolithium Reagents to Cycloalkanone

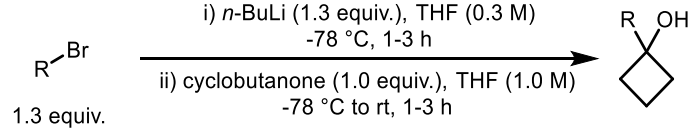

To a flame-dried RBF fitted with a septum seal was added a solution of R-Br (1.30 equiv.) in anhydrous THF (0.3 M). The mixture was cooled to -78 °C, and a solution of *n*-BuLi in hexanes (1.30 equiv.) was added dropwise. The reaction mixture was left to stir for 1-3 h before a solution of the cycloalkanone (1.00 equiv.) in anhydrous THF (1.0 M) was added dropwise. The solution was left to stir for 1-3 h whilst warming to rt. Water was added dropwise, followed by EtOAc, and the layers were separated. The aqueous layer was further extracted with EtOAc (× 3). The combined organics were washed with brine, dried over $MgSO_4$, filtered, and concentrated under reduced pressure. The resultant crude material was purified by flash column chromatography to afford the desired compound.

General Procedure 4 – Synthesis of Ethyl Esters

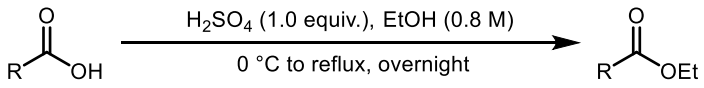

To a RBF charged with the appropriate carboxylic acid (1.00 equiv.) in EtOH (0.8 M) was added conc. H_2SO_4 (1.00 equiv.) dropwise at 0 °C. After complete addition, the mixture was heated at reflux overnight. The reaction was cooled to rt and concentrated under reduced pressure. The resulting residue was dissolved in CH_2Cl_2 and washed with 1 M NaOH (aq.) (× 3). The combined organics were dried over $MgSO_4$, filtered, and concentrated under reduced pressure to afford the ester that was used without further purification.

General Procedure 5 – Synthesis of Cyclopropanols *via* Kulinkovic Reactions

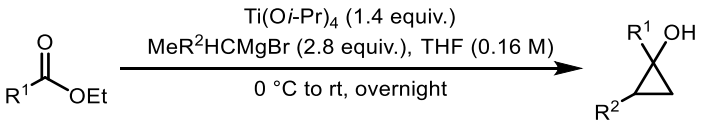

To a flame-dried RBF fitted with a septum seal was added the appropriate ester (1.00 equiv.) and Ti(O*i*-Pr)$_4$ (1.40 equiv.) in anhydrous THF (0.17 M). The mixture was cooled to 0 °C and a commercially available Grignard reagent (2.80 equiv.) was added dropwise. After complete addition the resulting mixture was stirred at rt overnight. Water was added, and the resulting precipitate was filtered through celite under vacuum and washed with EtOAc. The layers of the filtrate were separated, and the aqueous layer was further extracted with EtOAc (× 2). The combined organics were dried over $MgSO_4$, filtered, and concentrated under reduced pressure. The resultant crude material was purified by flash column chromatography to afford the desired compound.

5.2.2 Characterisation of Substrates

1-Phenylcyclobutan-1-ol (27)

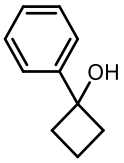

27

Prepared according to General Procedure 1 using magnesium turnings (2.01 g, 82.5 mmol), bromobenzene (7.90 mL, 75.0 mmol), and cyclobutanone (3.74 mL, 50.0 mmol). The resultant crude material was purified by flash column chromatography (10-20% EtOAc/petrol, silica gel) to afford **27** (6.78 g, 91%) as a white solid.

R_f = 0.13 (10% EtOAc/petrol); **M.p.:** 43-46 °C; **^{1}H NMR (500 MHz, DMSO-*d*$_6$)** δ_H = 1.57 – 1.69 (1H, m), 1.85 – 1.97 (1H, m), 2.21 – 2.31 (2H, m), 2.34 – 2.41 (2H, m), 5.44 (1H, s), 7.20 – 7.24 (1H, m), 7.29 – 7.36 (2H, m), 7.45 – 7.50 (2H, m); **^{13}C NMR (126 MHz, DMSO-*d*$_6$)** δ_C = 12.7, 37.2, 75.1, 124.8, 126.3, 127.9, 147.7.

These data are consistent with those previously reported in the literature.[1]

1-(4-Iodophenyl)cyclobutan-1-ol (29)

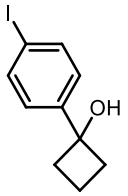

29

Prepared according to General Procedure 3 using 1,4-diiodobenzene (2.14 g, 6.50 mmol) in THF (22 mL, 0.3 M), *n*-BuLi (2.83 mL, 2.3 M in hexanes, 6.50 mmol), and cyclobutanone (374 µL, 5.00 mmol) in THF (5 mL, 1.0 M). The resultant crude material was purified by flash column chromatography (5% EtOAc/hexanes, silica gel) to afford **29** (929 mg, 68%) as an off-white solid.

R_f = 0.16 (10% EtOAc/hexanes); **M.p.:** 66-69 °C; **FTIR** (ν_{max} cm^{-1}, thin film) 3335 (br), 2980, 2940, 1489, 1389, 1223, 1128, 1103, 1078, 1005, 961, 839, 812, 642, 523; **^{1}H NMR (500 MHz, $CDCl_3$)** δ_H = 1.64 – 1.75 (1H, m), 1.95 – 2.08 (2H, m, O*H*), 2.31 – 2.40 (2H, m), 2.48 – 2.55 (2H, m), 7.23 – 7.27 (2H, m), 7.67 – 7.71 (2H, m); **^{13}C NMR (126 MHz, $CDCl_3$)** δ_C = 13.1, 37.1, 76.9, 92.9, 127.2, 137.6, 146.1; **HRMS** (EI+) $C_{10}H_{11}IO$ $[M-H_2O]^+$ requires 255.9749, found 255.9760 (+4.3 ppm).

1-Phenethylcyclobutan-1-ol (30)

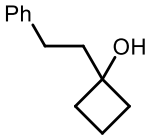

30

Prepared according to General Procedure 1 using magnesium turnings (201 mg, 8.25 mmol), (2-bromoethyl)benzene (1.02 mL, 7.50 mmol), and cyclobutanone (374 µL, 5.00 mmol). The resultant crude material was purified by flash column chromatography (10% EtOAc/hexanes, silica gel) to afford **30** (552 mg, 63%) as a colourless oil.

R_f = 0.15 (10% EtOAc/hexanes); **FTIR** (ν_{max} cm^{-1}, thin film) 3325 (br), 2932, 1605, 1497, 1459, 1250, 1158, 1103, 1057, 949, 748, 694; **^{1}H NMR (500 MHz, $CDCl_3$)** δ_H = 1.51 – 1.65 (2H, m), 1.75 – 1.83 (1H, m), 1.91 – 1.93 (2H, m), 1.99 – 2.09 (2H, m), 2.09 – 2.15 (2H, m), 2.70 – 2.74 (2H, m), 7.17 – 7.25 (3H, m), 7.27 – 7.32 (2H, m); **^{13}C NMR (126 MHz, $CDCl_3$)** δ_C = 12.3, 30.1, 36.2, 41.5, 75.5, 125.9, 128.5, 128.6, 142.7; **HRMS** (EI+) $C_{12}H_{16}O$ $[M]^+$ requires 176.1201, found 176.1199 (-1.1 ppm).

(*E*)-(2-Bromovinyl)benzene (281)

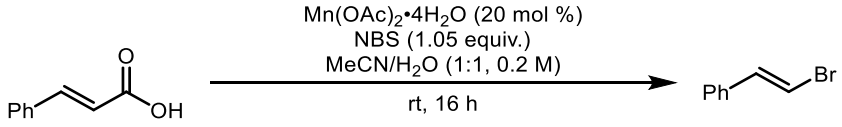

143 **281**

Following a modified literature procedure,[2] (*E*)-cinnamic acid **143** (1.48 g, 10.0 mmol), NBS (1.87 g, 10.5 mmol), and $Mn(OAc)_2•4H_2O$ (490 mg, 2.00 mmol) were dissolved in a 1:1 mixture of MeCN and water (50 mL, 0.2 M), and the mixture was stirred at rt for 16 h. The reaction mixture was then diluted with water (20 mL), and the aqueous layer was extracted with EtOAc (50 mL × 3). The combined organics were then dried over $MgSO_4$, filtered, and concentrated under reduced pressure. The resultant crude material was purified by flash column chromatography (1% EtOAc/petrol, silica gel) to afford **281** (609 mg, 33%) as a light-yellow oil.

R_f = 0.70 (1% EtOAc/petrol); **FTIR** (ν_{max} cm^{-1}, thin film) 3075, 3024, 2369, 1607, 1574, 1497, 1447, 1221, 1184, 1177, 1072, 937, 727, 689, 565, 492; **^{1}H NMR (500 MHz, $CDCl_3$)** δ_H = 6.77 (1H, d, *J* 14.0), 7.11 (1H, d, *J* 14.0), 7.27 – 7.35 (5H, m); **^{13}C NMR (126 MHz, $CDCl_3$)** δ_C = 106.7, 126.2, 128.4, 128.9, 136.1, 137.3; **HRMS** (EI+) C_8H_7Br $[M]^+$ requires 181.9731, found 181.9729 (-1.1 ppm).

(*E*)-1-Styrylcyclobutan-1-ol (31)

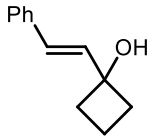

31

Prepared according to General Procedure 1 using magnesium turnings (175 mg, 7.20 mmol), **281** (879 mg, 4.80 mmol), and cyclobutanone (299 µL, 4.00 mmol). The resultant crude material was purified by flash column chromatography (5% EtOAc/petrol, silica gel) to afford **31** (207 mg, 30%) as a pale-yellow solid.

R_f = 0.14 (10% EtOAc/hexanes); **M.p.:** 41-44 °C; **^{1}H NMR (500 MHz, $CDCl_3$)** δ_H = 1.63 – 1.73 (1H, m), 1.82 – 1.92 (2H, m), 2.20 – 2.28 (2H, m), 2.29 – 2.36 (2H, m), 6.52 (1H, d, *J* 16.0), 6.67 (1H, d, *J* 16.0), 7.22 – 7.27 (1H, m), 7.30 – 7.35 (2H, m), 7.40 – 7.43 (2H, m); **^{13}C NMR (126 MHz, $CDCl_3$)** δ_C = 12.4, 36.6, 75.4, 126.6, 127.0, 127.7, 128.7, 134.1, 137.0.

These data are consistent with those previously reported in the literature.[3]

1-Hexylcyclobutan-1-ol (32)

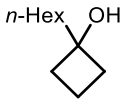

32

Prepared according to General Procedure 1 using magnesium turnings (201 mg, 8.25 mmol), 1-bromohexane (1.05 mL, 7.50 mmol), and cyclobutanone (374 µL, 5.00 mmol). The resultant crude material was purified by flash column chromatography (5% EtOAc/hexanes, silica gel) to afford **32** (381 mg, 49%) as a colourless oil.

R_f = 0.21 (10% EtOAc/hexanes); **FTIR** (ν_{max} cm^{-1}, thin film) 3350, 2955, 2928, 2857, 1460, 1377, 1267, 1246, 1167, 1069, 957, 912, 721, 638; **^{1}H NMR (500 MHz, $CDCl_3$)** δ_H = 0.85 – 0.93 (3H, m), 1.24 – 1.40 (8H, m), 1.45 – 1.62 (4H, m), 1.69 – 1.79 (1H, m), 1.94 – 2.08 (4H, m); **^{13}C NMR (126 MHz, $CDCl_3$)** δ_C = 12.3, 14.3, 22.8, 23.5, 29.9, 32.1, 36.1, 39.7, 75.6; **HRMS** (EI+) $C_{10}H_{20}O$ $[M-H_2O]^+$ requires 138.1409, found 138.1410 (+0.7 ppm).

1-(3-Methoxyphenyl)cyclobutan-1-ol (33)

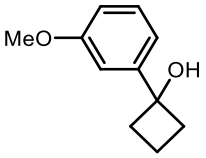

33

Prepared according to General Procedure 3 using 3-bromoanisole (823 µL, 6.50 mmol) in THF (22 mL, 0.3 M), *n*-BuLi (3.10 mL, 2.1 M in hexanes, 6.50 mmol), and cyclobutanone (374 µL, 5.00 mmol) in THF (5 mL, 1.0 M). The resultant crude material was purified by flash column chromatography (15% EtOAc/hexanes, silica gel) to afford **33** (691 mg, 78%) as a white solid.

R_f = 0.10 (10% EtOAc/petrol); **M.p.:** 56-58 °C; **^{1}H NMR (500 MHz, DMSO-d_6)** δ_H = 1.57 – 1.70 (1H, m), 1.86 – 1.95 (1H, m), 2.21 – 2.28 (2H, m), 2.33 – 2.40 (2H, m), 3.75 (3H, s), 5.45 (1H, s), 6.79 (1H, ddd, *J* 8.2, 2.6, 0.9), 7.01 (1H, ddd, *J* 2.6, 1.7, 0.4), 7.05 (1H, ddd, *J* 7.7, 1.7, 0.9), 7.25 (1H, ddd, *J* 8.2, 7.7, 0.4); **^{13}C NMR (126 MHz, DMSO-d_6)** δ_C = 12.8, 37.3, 54.9, 75.1, 110.7, 111.6, 117.1, 128.9, 149.5, 159.1.

These data are consistent with those previously reported in the literature.[1]

1-Bromo-4-(phenylethynyl)benzene (282)

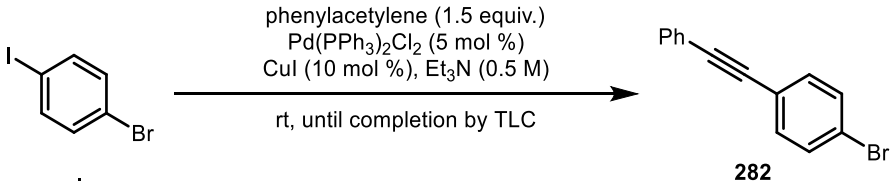

282

Following a modified literature procedure,[4] to a flame-dried RBF were added CuI (95 mg, 0.50 mmol), $Pd(PPh_3)_2Cl_2$ (175 mg, 0.25 mmol), and 1-bromo-4-iodobenzene (1.42 g, 5.00 mmol) in triethylamine (10 mL, 0.50 M). The mixture was stirred for 10 min, before phenylacetylene (824 µL, 7.50 mmol) was added. Upon reaction completion, as monitored by TLC, the mixture was filtered through a silica plug and washed through with hexane, then concentrated under reduced pressure. The resultant crude material was purified by flash column chromatography (hexanes, silica gel) to afford **282** (1.09 g, 84%) as a white solid.

R_f = 0.66 (10% EtOAc/hexanes); **M.p.:** 80-82 °C; **FTIR** (ν_{max} cm^{-1}, thin film) 3049, 2361, 1908, 1599, 1503, 1489, 1477, 1393, 1069, 1007, 829, 820, 750, 685, 509; **^{1}H NMR (500 MHz, $CDCl_3$)** δ_H = 7.31 – 7.42 (5H, m), 7.46 – 7.56 (4H, m); **^{13}C NMR (126 MHz, $CDCl_3$)** δ_C = 88.4, 90.7, 122.4, 122.6, 123.1, 128.5, 128.7, 131.7, 131.8, 133.2; **HRMS** (EI+) $C_{14}H_9Br$ $[M]^+$ requires 255.9888, found 255.9888 (±0.0 ppm).

1-(4-(Phenylethynyl)phenyl)cyclobutan-1-ol (34)

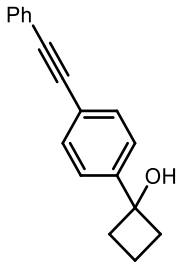

34

Prepared according to General Procedure 3 using **282** (836 mg, 3.25 mmol) in THF (11 mL, 0.3 M), *n*-BuLi (1.41 mL, 2.3 M in hexanes, 3.25 mmol), and cyclobutanone (187 µL, 2.50 mmol) in THF (2.5 mL, 1.0 M). The resultant crude material was purified by flash column chromatography (5-10% EtOAc/hexanes, silica gel) to afford **34** (412 mg, 66%) as a yellow solid.

R_f = 0.14 (10% EtOAc/hexanes); **M.p.:** 95-97 °C; **FTIR** (ν_{max} cm^{-1}, thin film) 3233 (br), 2982, 1503, 1443, 1246, 1132, 1107, 1069, 1107, 839, 756, 689; **^{1}H NMR (500 MHz, $CDCl_3$)** δ_H = 1.69 – 1.78 (1H, m), 1.97 – 2.10 (2H, m), 2.35 – 2.42 (2H, m), 2.53 – 2.60

(2H, m), 7.31 – 7.38 (3H, m), 7.48 – 7.56 (6H, m); **^{13}C NMR (126 MHz, $CDCl_3$)** δ_C = 13.2, 37.1, 77.0, 89.4, 89.6, 122.3, 123.4, 125.1, 128.4, 128.5, 131.7, 131.8, 146.5; **HRMS** (EI+) $C_{18}H_{16}O$ $[M]^+$ requires 248.1201, found 248.1208 (+2.8 ppm).

1-(Benzofuran-2-yl)cyclobutan-1-ol (35)

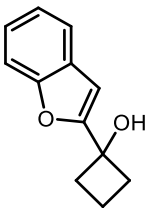

35

Prepared according to General Procedure 3 using benzofuran (358 µL, 3.25 mmol) in THF (11 mL, 0.3 M), *n*-BuLi (1.50 mL, 2.17 M in hexanes, 3.25 mmol), and cyclobutanone (187 µL, 2.50 mmol) in THF (2.5 mL, 1.0 M). The resultant crude material was purified by flash column chromatography (5-10% EtOAc/hexanes, silica gel) to afford **35** (381 mg, 81%) as a pale-yellow solid.

R_f = 0.13 (10% EtOAc/hexanes); **M.p.:** 45-47 °C; **^{1}H NMR (500 MHz, $CDCl_3$)** δ_H = 1.74 – 1.85 (1H, m), 1.92 – 2.02 (1H, m), 2.37 – 2.46 (3H, m), 2.60 – 2.67 (2H, m), 6.68 (1H, s), 7.20 – 7.30 (2H, m), 7.45 – 7.50 (1H, m), 7.53 – 7.57 (1H, m); **^{13}C NMR (126 MHz, $CDCl_3$)** δ_C = 13.0, 35.8, 72.9, 101.7, 111.4, 121.2, 122.9, 124.3, 128.3, 155.2, 160.8.

These data are consistent with those previously reported in the literature.[5]

1-(Phenylethynyl)cyclobutan-1-ol (36)

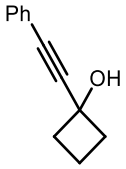

36

Prepared according to General Procedure 3 using phenylacetylene (714 µL, 6.50 mmol) in THF (22 mL, 0.3 M), *n*-BuLi (2.83 mL, 2.3 M in hexanes, 6.50 mmol), and cyclobutanone (374 µL, 5.00 mmol) in THF (5 mL, 1.0 M). The resultant crude material was purified by flash column chromatography (10% EtOAc/petrol, silica gel) to afford **36** (696 mg, 81%) as a yellow oil.

R_f = 0.24 (10% EtOAc/hexanes); **FTIR** (ν_{max} cm^{-1}, thin film) 3318 (br), 2990, 2941, 1597, 1491, 1443, 1244, 1153, 1105, 959, 912, 754, 689, 538; **^{1}H NMR (500 MHz, $CDCl_3$)** δ_H = 1.84 – 1.92 (2H, m), 2.26 (1H, s), 2.31 – 2.39 (2H, m), 2.50 – 2.57 (2H, m), 7.29 –

7.33 (3H, m), 7.42 – 7.47 (2H, m); **^{13}C NMR (126 MHz, $CDCl_3$)** δ_C = 13.1, 38.8, 68.5, 83.6, 92.6, 122.9, 128.4, 128.5, 131.8; **HRMS** (EI+) $C_{12}H_{12}O$ $[M]^+$ requires 172.0888, found 172.0887 (-0.6 ppm).

3-Phenyloxetan-3-ol (37)

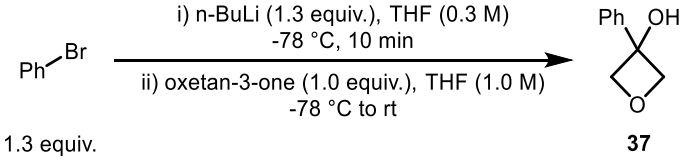

1.3 equiv. **37**

Following a literature procedure,[6] to a flame-dried RBF fitted with a septum seal was added bromobenzene (1.37 mL, 13.0 mmol) and THF (40 mL, 0.3 M). The flask was cooled to -78 °C, and *n*-BuLi (6.20 mL, 2.13 M in hexanes, 13.0 mmol) was slowly added. After stirring for 10 minutes, a solution of oxetan-3-one (641 µL, 10.0 mmol) in THF (10 mL, 1.0 M) was added dropwise. The reaction mixture was stirred for 10 minutes at -78 °C before being allowed to warm to rt. Water (5 mL) was then added, and the layers were separated. The aqueous layer was extracted with Et_2O (20 mL × 3), and the combined organics were washed with brine, dried over $MgSO_4$, filtered, and concentrated under reduced pressure. The resultant crude material was purified by flash column chromatography (40% EtOAc/petrol, silica gel) to afford **37** (1.22 g, 81%) as a colourless oil.

R_f = 0.27 (40% EtOAc/petrol); **FTIR** (ν_{max} cm^{-1}, thin film) 3356 (br), 2951, 2876, 2361, 1495, 1449, 1396, 1337, 1275, 1175, 1138, 1067, 1026, 986, 876, 758, 700, 548; **^{1}H NMR (500 MHz, $CDCl_3$)** δ_H = 2.68 (1H, s), 4.91 (2H, d, *J* 7.0), 4.93 (2H, d, *J* 7.0), 7.32 – 7.37 (1H, m), 7.41 – 7.45 (2H, m), 7.57 – 7.61 (2H, m); **^{13}C NMR (126 MHz, $CDCl_3$)** δ_C = 76.0, 85.8, 124.6, 128.1, 128.9, 142.4; **HRMS** (EI+) $C_9H_{10}O_2$ $[M]^+$ requires 150.0681, found 150.0678 (-2.0 ppm).

Benzyl 3-hydroxy-3-phenylazetidine-1-carboxylate (38)

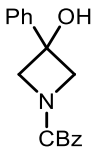

38

Prepared according to General Procedure 3 using bromobenzene (685 µL, 6.50 mmol) in THF (22 mL, 0.3 M), *n*-BuLi (2.77 mL, 2.35 M in hexanes, 6.50 mmol), and benzyl 3-oxoazetidine-1-carboxylate (1.03 g, 5.00 mmol) in THF (5 mL, 1.0 M). The resultant

crude material was purified by flash column chromatography (20-30% EtOAc/hexanes, silica gel) to afford **38** (572 mg, 40%) as a white solid.

R_f = 0.10 (20% EtOAc/hexanes); **M.p.:** 138-140 °C; **FTIR** (ν_{max} cm^{-1}, thin film) 3275 (br), 2962, 2945, 2876, 1670, 1655, 1477, 1456, 1359, 1242, 1209, 1196, 1155, 1076, 948, 750; **^{1}H NMR (500 MHz, $CDCl_3$)** δ_H = 2.45 (1H, s), 4.26 (2H, dd, *J* 9.3, 1.0), 4.37 (2H, app d, *J* 9.3), 5.14 (2H, s), 7.31 – 7.37 (6H, m), 7.39 – 7.42 (2H, m), 7.47 – 7.50 (2H, m); **^{13}C NMR (126 MHz, $CDCl_3$)** δ_C = 64.5, 67.1, 72.1, 124.7, 128.2, 128.3 (2C), 128.7, 128.9, 136.6, 142.9, 156.7; **HRMS** (EI+) $C_{17}H_{17}NO_3$ $[M\text{-}H_2O]^+$ requires 265.1103, found 265.1102 (-0.4 ppm).

1-Phenethylcyclopentan-1-ol (39)

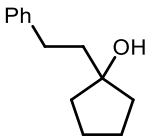

39

Prepared according to General Procedure 1 using magnesium turnings (201 mg, 8.25 mmol), (2-bromoethyl)benzene (1.02 mL, 7.50 mmol), and cyclopentanone (443 µL, 5.00 mmol). The resultant crude material was purified by flash column chromatography (10% EtOAc/hexanes, silica gel) to afford **39** (552 mg, 52%) as a colourless oil.

R_f = 0.24 (10% EtOAc/petrol); **^{1}H NMR (500 MHz, $CDCl_3$)** δ_H = 1.18 (1H, br s), 1.60 – 1.73 (6H, m), 1.79 – 1.87 (2H, m), 1.89 – 1.93 (2H, m), 2.75 – 2.79 (2H, m), 7.16 – 7.23 (3H, m), 7.27 – 7.31 (2H, m); **^{13}C NMR (126 MHz, $CDCl_3$)** δ_C = 24.0, 31.4, 40.0, 43.7, 82.6, 125.9, 128.5, 128.6, 142.9.

These data are consistent with those previously reported in the literature.[7]

1-Ethylcyclobutan-1-ol (40)

40

Prepared according to General Procedure 2 using ethyl magnesium bromide (5.00 mL, 3.0 M in Et_2O, 15.0 mmol), and cyclobutanone (747 µL, 10.0 mmol). The resultant crude material was purified by flash column chromatography (10-20% EtOAc/petrol, silica gel) to afford **40** (323 mg, 32%) as a colourless oil.

R_f = 0.19 (10% EtOAc/petrol); **FTIR** (ν_{max} cm^{-1}, thin film) 3343 (br), 2963, 2932, 2878, 1462, 1296, 1285, 1242, 1173, 1150, 1022, 953, 891, 706, 631; **^{1}H NMR (500 MHz, $CDCl_3$)** δ_H = 0.93 (3H, t, *J* 7.4), 1.44 – 1.57 (2H, m), 1.63 (2H, q, *J* 7.4), 1.70 – 1.78 (1H, m), 1.94 – 2.08 (4H, m); **^{13}C NMR (126 MHz, $CDCl_3$)** δ_C = 7.7, 12.2, 32.2, 35.6, 75.7; **HRMS** (EI+) $C_6H_{12}O$ $[M]^+$ requires 100.0888, found 100.0890 (+2.0 ppm).

1-Cyclohexylcyclobutan-1-ol (41)

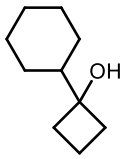

41

Prepared according to General Procedure 2 using cyclohexyl magnesium chloride (11.5 mL, 1.3 M in 1:1 THF/toluene, 15.0 mmol), and cyclobutanone (747 µL, 10.0 mmol). The resultant crude material was purified by flash column chromatography (10% EtOAc/petrol, silica gel) to afford **41** (1.18 g, 77%) as a colourless oil.

R_f = 0.17 (10% EtOAc/petrol); **^{1}H NMR (500 MHz, $CDCl_3$)** δ_H = 0.98 – 1.28 (5H, m), 1.37 (1H, tt, *J* 12.0, 3.1), 1.46 (1H, s), 1.48 – 1.58 (1H, m), 1.65 – 1.94 (8H, m), 2.11 – 2.18 (2H, m); **^{13}C NMR (126 MHz, $CDCl_3$)** δ_C = 12.6, 25.6, 26.6, 26.7, 34.0, 45.7, 78.2.

These data are consistent with those previously reported in the literature.[1]

1-Benzylcyclobutan-1-ol (42)

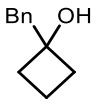

42

Prepared according to General Procedure 2 using benzyl magnesium chloride (10.7 mL, 1.4 M in THF, 15.0 mmol), and cyclobutanone (747 µL, 10.0 mmol). The resultant crude material was purified by flash column chromatography (5% EtOAc/petrol, silica gel) to afford **42** (1.51 g, 93%) as a colourless oil.

R_f = 0.16 (5% EtOAc/petrol); **FTIR** (ν_{max} cm^{-1}, thin film) 3372 (br), 2980, 2932, 2495, 1452, 1265, 1098, 1030, 922, 760, 712, 700, 642, 498; **^{1}H NMR (500 MHz, $CDCl_3$)** δ_H = 1.56 – 1.66 (1H, m), 1.73 (1H, s), 1.77 – 1.85 (1H, m), 1.96 – 2.07 (2H, m), 2.14 – 2.21 (2H, m), 2.91 (2H, s), 7.24 – 7.35 (5H, m); **^{13}C NMR (126 MHz, $CDCl_3$)** δ_C = 12.3, 35.6, 45.6, 75.2, 126.7, 128.5, 130.2, 137.6; **HRMS** (EI+) $C_{11}H_{14}O$ $[M]^+$ requires 162.1045, found 162.1046 (+0.6 ppm).

7-Methylbicyclo[4.2.0]octa-1,3,5-trien-7-ol (43)

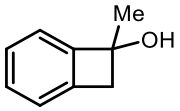

43

Prepared according to General Procedure 2 using methyl magnesium bromide (350 µL, 3.0 M in Et_2O, 1.05 mmol), and bicyclo[4.2.0]octa-1,3,5-trien-7-one (83 mg, 0.70 mmol). The resultant crude material was purified by flash column chromatography (20% Et_2O/petrol, silica gel) to afford **43** (63 mg, 67%) as an off-white solid.

R_f = 0.15 (20% Et_2O/petrol); **M.p.:** 77-79 °C; **FTIR** (ν_{max} cm^{-1}, thin film) 3304 (br), 2918, 1456, 1366, 1231, 1167, 1061, 947, 758, 714; **^{1}H NMR (500 MHz, $CDCl_3$)** δ_H = 1.68 (3H, s), 2.24 (1H, br s), 3.23 (1H, d, *J* 14.1), 3.37 (1H, d, *J* 14.1), 7.15 – 7.20 (2H, m), 7.21 – 7.25 (1H, m), 7.26 – 7.30 (1H, m); **^{13}C NMR (126 MHz, $CDCl_3$)** δ_C = 25.8, 48.5, 78.5, 120.6, 124.2, 127.4, 129.5, 141.3, 151.2; **HRMS** (EI+) $C_9H_{10}O$ $[M]^+$ requires 134.0732, found 134.0738 (+4.5 ppm).

2-Methyl-2,3-dihydro-1*H*-inden-2-ol (44)

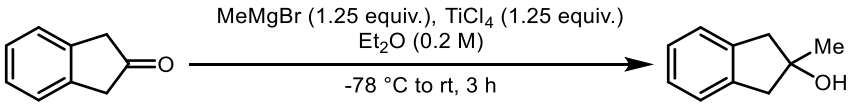

44

Following a modified literature procedure,[8] to a flame-dried RBF was added $TiCl_4$ (1.10 mL, 10.0 mmol) in Et_2O (50 mL, 0.2 M) and the solution was cooled to -78 °C before methyl magnesium bromide (3.30 mL, 3.0 M in Et_2O, 10.0 mmol) was added slowly. The reaction mixture was then allowed to warm to -30 °C before 2-indanone (1.06 g, 8.00 mmol) in Et_2O (5 mL, 1.6 M) was added dropwise. The reaction mixture was then warmed to 0 °C and stirred for 3 h before water (20 mL) was added, the layers were separated, and the aqueous layer was further extracted with EtOAc (30 mL × 3). The combined organics were washed with water, dried over $MgSO_4$, filtered, and concentrated under reduced pressure. The resulting crude residue was purified by flash column chromatography (10-20% EtOAc/petrol, silica gel) to afford **44** (702 mg, 59%) as an orange solid.

R_f = 0.12 (10% EtOAc/petrol); **M.p.:** 54-56 °C; **FTIR** (ν_{max} cm^{-1}, thin film) 3314 (br), 2968, 1481, 1375, 1242, 1128, 1076, 928, 883, 731, 689; **^{1}H NMR (500 MHz, $CDCl_3$)** δ_H = 1.52 (3H, s), 3.00 (2H, d, *J* 15.9), 3.05 (2H, d, *J* 16.1, 7.15 – 7.18 (2H, m), 7.19 – 7.22 (2H,

m); **^{13}C NMR (126 MHz, $CDCl_3$)** δ_C = 27.5, 48.6, 80.4, 125.2, 126.8, 141.7; **HRMS** (EI+) $C_{10}H_{12}O$ $[M]^+$ requires 148.0888, found 148.0894 (+4.1 ppm).

1-Methyl-1,2,3,4-tetrahydronaphthalen-1-ol (45)

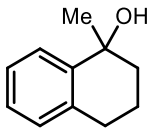

45

Prepared according to General Procedure 2 using methyl magnesium bromide (2.50 mL, 3.0 M in Et_2O, 7.50 mmol), and *α*-tetralone (527 µL, 5.00 mmol). The resultant crude material was purified by flash column chromatography (10-20% EtOAc/hexanes, silica gel) to afford **45** (488 mg, 60%) as a white solid.

R_f = 0.15 (10% EtOAc/petrol); **M.p.:** 95-97 °C; **FTIR** (ν_{max} cm^{-1}, thin film) 3308 (br), 2934, 1487, 1439, 1185, 1103, 989, 930, 760, 727, 557; **^{1}H NMR (500 MHz, $CDCl_3$)** δ_H = 1.57 (3H, s), 1.73 (1H, s), 1.78 – 1.88 (1H, m), 1.89 – 2.00 (3H, m), 2.73 – 2.86 (2H, m), 7.06 – 7.09 (1H, m), 7.15 – 7.19 (1H, m), 7.20 – 7.24 (1H, m), 7.57 – 7.63 (1H, m); **^{13}C NMR (126 MHz, $CDCl_3$)** δ_C = 20.6, 30.0, 30.9, 40.0, 70.8, 126.4, 126.5, 127.3, 129.0, 136.4, 143.0; **HRMS** (EI+) $C_{11}H_{14}O$ $[M\text{-}H_2O]^+$ requires 144.0939, found 144.0938 (-0.7 ppm).

2-Methyl-1,2,3,4-tetrahydronaphthalen-2-ol (46)

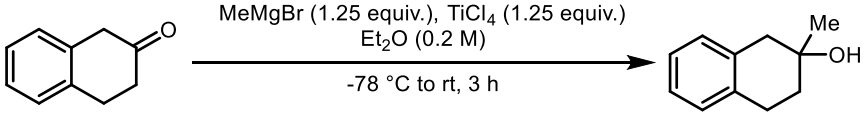

46

Following a modified literature procedure,[8] to a flame-dried RBF was added $TiCl_4$ (1.10 mL, 10.0 mmol) in Et_2O (50 mL, 0.2 M) and the solution was cooled to -78 °C before methyl magnesium bromide (3.30 mL, 3.0 M in Et_2O, 10.0 mmol) was added slowly. The reaction mixture was then allowed to warm to -30 °C before *β*-tetralone (1.06 mL, 8.00 mmol) was added dropwise. The reaction mixture was then warmed to 0 °C and stirred for 3 h before water (20 mL) was added, the layers were separated, and the aqueous layer was further extracted with EtOAc (30 mL × 3). The combined organics were washed with water, dried over $MgSO_4$, filtered, and concentrated under reduced pressure. The resulting crude residue was purified by flash column chromatography (10% EtOAc/petrol, silica gel) to afford **46** (472 mg, 36%) as an orange solid.

R_f = 0.13 (10% EtOAc/petrol); **M.p.:** 43-45 °C; **FTIR** (ν_{max} cm^{-1}, thin film) 3331 (br), 2934, 2920, 1495, 1371, 1273, 1250, 1109, 908, 739, 731; **^{1}H NMR (500 MHz, $CDCl_3$)** δ_H = 1.36

(3H, s), 1.76 – 1.83 (1H, m), 1.87 – 1.92 (1H, m), 2.79 – 2.91 (3H, m), 2.98 – 3.05 (1H, m), 7.05 – 7.09 (1H, m), 7.10 – 7.14 (3H, m); **^{13}C NMR (126 MHz, $CDCl_3$)** δ_C = 26.6, 28.9, 35.9, 43.8, 69.4, 126.0, 126.1, 128.9, 129.8, 134.7, 135.3; **HRMS** (EI+) $C_{11}H_{14}O$ $[M\text{-}H_2O]^+$ requires 144.0939, found 144.0940 (+0.7 ppm).

Ethyl 3-phenylpropanoate (283)

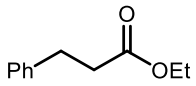

283

Prepared according to General Procedure 4 using 3-phenylpropanoic acid (1.50 g, 10.0 mmol) in EtOH (12.5 mL, 0.8 M), and conc. H_2SO_4 (0.54 mL, 10.0 mmol) to give **283** (1.62 g, 91%) as a colourless oil that was used without further purification.

R_f = 0.40 (10% EtOAc/petrol); **FTIR** (ν_{max} cm^{-1}, thin film) 2980, 1730, 1454, 1371, 1159, 1038, 748, 698; **^{1}H NMR (500 MHz, $CDCl_3$)** δ_H = 1.24 (3H, t, *J* 7.2), 2.60 – 2.64 (2H, m), 2.93 – 2.97 (2H, m), 4.13 (2H, q, *J* 7.2), 7.18 – 7.22 (3H, m), 7.27 – 7.31 (2H, m); **^{13}C NMR (126 MHz, $CDCl_3$)** δ_C = 14.4, 31.1, 36.1, 60.6, 126.4, 128.4, 128.6, 140.7, 173.1; **HRMS** (EI+) $C_{11}H_{14}O_2$ $[M]^+$ requires 178.0994, found 178.0993 (-0.6 ppm).

1-Phenethylcyclopropan-1-ol (47)

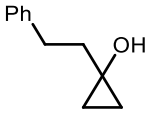

47

Prepared according to General Procedure 5 using **283** (891 mg, 5.00 mmol), Ti(O*i*-Pr)$_4$ (2.07 mL, 7.00 mmol), and ethyl magnesium bromide (4.67 mL, 3.0 M in Et_2O, 14.0 mmol). The resultant crude material was purified by flash column chromatography (25% EtOAc/hexanes, silica gel) to afford **47** (592 mg, 73%) as a white solid.

R_f = 0.38 (10% EtOAc/hexanes); **M.p.:** 49-51 °C; **FTIR** (ν_{max} cm^{-1}, thin film) 3339 (br), 2947, 1493, 1454, 1285, 1248, 1238, 1007, 949, 935, 926, 747, 725, 694, 521; **^{1}H NMR (500 MHz, $CDCl_3$)** δ_H = 0.45 – 0.48 (2H, m), 0.75 – 0.78 (2H, m), 1.77 (1H, s), 1.86 – 1.90 (2H, m), 2.84 – 2.88 (2H, m), 7.17 – 7.24 (3H, m) 7.27 – 7.31 (2H, m); **^{13}C NMR (126 MHz, $CDCl_3$)** δ_C = 13.9, 32.7, 40.6, 56.0, 126.0, 128.5, 128.6, 142.3; **HRMS** (EI+) $C_{11}H_{14}O$ $[M]^+$ 162.1045, found 162.1048 (+1.9 ppm).

Ethyl heptanoate (284)

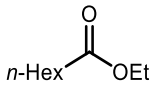

284

Prepared according to General Procedure 4 using heptanoic acid (1.42 mL, 10.0 mmol) in EtOH (12.5 mL, 0.8 M), and conc. H_2SO_4 (0.54 mL, 10.0 mmol) to give **284** (934 mg, 59%) as a colourless oil that was used without further purification.

R_f = 0.92 (10% EtOAc/petrol); **FTIR** (ν_{max} cm^{-1}, thin film) 2930, 2859, 1736, 1456, 1371, 1165, 1099, 1034; **^{1}H NMR (500 MHz, $CDCl_3$)** δ_H = 0.85 – 0.91 (3H, m), 1.23 – 1.35 (9H, m), 1.58 – 1.66 (2H, m), 2.32 – 2.35 (2H, m), 4.12 (2H, t, *J* 7.1); **^{13}C NMR (126 MHz, $CDCl_3$)** δ_C = 14.2, 14.4, 22.6, 25.1, 29.0, 31.6, 34.6, 60.3, 174.1; **HRMS** (EI+) $C_9H_{18}O_2$ $[M]^+$ requires 158.1307, found 158.1306 (-0.6 ppm).

1-Hexylcyclopropan-1-ol (48)

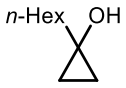

48

Prepared according to General Procedure 5 using **284** (792 mg, 5.00 mmol), Ti(O*i*-Pr)$_4$ (2.07 mL, 7.00 mmol), and ethyl magnesium bromide (4.67 mL, 3.0 M in Et_2O, 14.0 mmol). The resultant crude material was purified by flash column chromatography (10% EtOAc/petrol, silica gel) to afford **48** (287 mg, 40%) as a colourless oil.

R_f = 0.29 (10% EtOAc/petrol); **FTIR** (ν_{max} cm^{-1}, thin film) 3306 (br), 2926, 2855, 1456, 1267, 1236, 1096, 1007, 955, 926, 721; **^{1}H NMR (500 MHz, $CDCl_3$)** δ_H = 0.42 – 0.46 (2H, m), 0.70 – 0.75 (2H, m), 0.86 – 0.93 (3H, m), 1.24 – 1.37 (7H, m), 1.44 – 1.59 (3H, m), 1.73 (1H, s); **^{13}C NMR (126 MHz, $CDCl_3$)** δ_C = 13.7, 14.3, 22.8, 26.0, 29.5, 32.1, 38.5, 56.1; **HRMS** (EI+) $C_9H_{18}O$ $[M]^+$ requires 142.1358, found 142.1365 (+4.9 ppm).

2-Methyl-1-phenethylcyclopropan-1-ol (49)

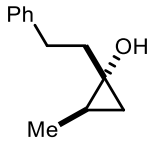

49

Prepared according to General Procedure 5 using **283** (891 mg, 5.00 mmol), Ti(O*i*-Pr)$_4$ (2.07 mL, 7.00 mmol), and isopropyl magnesium chloride (7.00 mL, 2.0 M in THF, 14.0 mmol). The resultant crude material was purified by flash column chromatography

(10-15% EtOAc/petrol, silica gel) to afford **49** (245 mg, 28%) as a colourless oil. The product was obtained as a single diastereoisomer.

R_f = 0.18 (10% EtOAc/petrol); **FTIR** (v_{max} cm^{-1}, thin film) 3294 (br), 2949, 2924, 1495, 1452, 1219, 1061, 907, 750, 698; **^{1}H NMR (500 MHz, $CDCl_3$)** δ_H = 0.03 – 0.10 (1H, m), 0.84 – 0.87 (1H, m), 1.01 – 1.03 (3H, m), 1.05 – 1.12 (1H, m), 1.76 (1H, br s), 1.86 – 1.90 (2H, m), 2.86 – 2.90 (2H, m), 7.17 – 7.25 (3H, m), 7.27 – 7.31 (2H, m); **^{13}C NMR (126 MHz, $CDCl_3$)** δ_C = 14.4, 20.1, 20.9, 32.7, 36.4, 59.0, 126.0, 128.5, 128.6, 142.6; **HRMS** (EI+) $C_{12}H_{16}O$ $[M]^+$ requires 176.1201, found 176.1197 (-2.3 ppm).

5.2.3 Electrochemical Reactions

General Procedure 6 – Electrochemical Deconstructive Chlorination of Cycloalkanols (Standard Procedure)

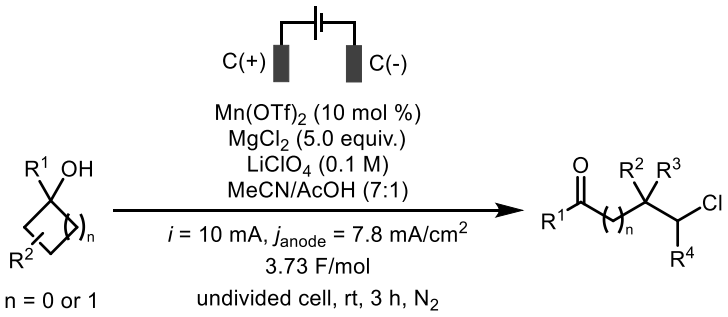

To an oven-dried 10 mL ElectraSyn vial equipped with a magnetic stirrer bar, was added the appropriate cycloalkanol (0.30 mmol), $Mn(OTf)_2$ (11 mg, 0.03 mmol), $MgCl_2$ (143 mg, 1.50 mmol), and $LiClO_4$ (64 mg, 0.60 mmol). The threaded glass was wrapped with PTFE tape and connected to the ElectraSyn cap, which was fitted with a graphite anode and graphite cathode. The vial was subjected to vacuum-nitrogen exchange cycles (× 3), anhydrous MeCN (5.25 mL) was added, followed by AcOH (750 µL), and the mixture was stirred until complete solvation of the $MgCl_2$. The mixture was then purged *via* bubbling with N_2 gas for 10 min. During this time, the vial was connected to an ElectraSyn GoGo module and submerged in a 25 °C water bath mounted on a magnetic stirrer. Electrolysis at 10 mA (j_{anode} = 7.8 mA/cm^2) was conducted for 3 h under N_2 with continuous stirring. After electrolysis was complete, the reaction mixture was left to stir at 25 °C for an additional 30 min before being diluted with Et_2O (10 mL) and washed with a saturated solution of $NaHCO_3$ (aq.) (2 × 15 mL). The layers were separated, and the aqueous layer was further extracted with Et_2O (3 × 10 mL). The combined organics were dried over

$MgSO_4$, filtered, and concentrated under reduced pressure. The resultant crude material was purified by flash column chromatography to afford the desired product.

General Procedure 7 – Electrochemical Deconstructive Chlorination of Cycloalkanols (Syringe Pump Addition of the Substrate)

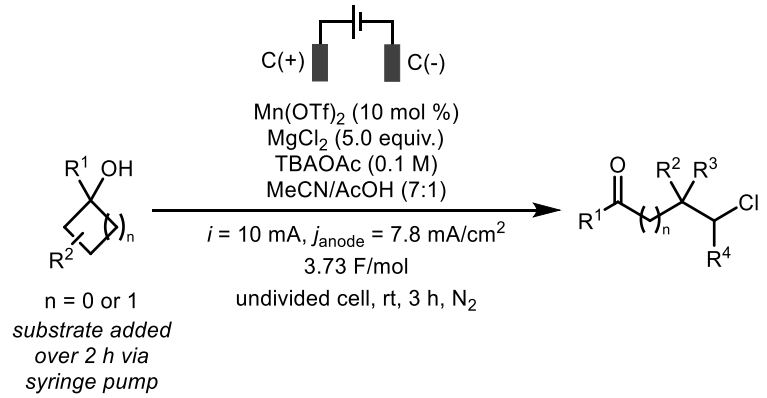

To an oven-dried 10 mL ElectraSyn vial equipped with a magnetic stirrer bar was added $Mn(OTf)_2$ (11 mg, 0.03 mmol), $MgCl_2$ (143 mg, 1.50 mmol), and TBAOAc (181 mg, 0.60 mmol). The threaded glass was wrapped with PTFE tape and connected to the ElectraSyn cap, which was fitted with a graphite anode and graphite cathode. The vial was subjected to vacuum-nitrogen exchange cycles (× 3), anhydrous MeCN (3.25 mL) was added, followed by AcOH (750 µL), and the mixture was stirred until complete solvation of the $MgCl_2$. The mixture was then purged *via* bubbling with N_2 gas for 10 min. During this time, the vial was connected to an ElectraSyn GoGo module and submerged in a 25 °C water bath mounted on a magnetic stirrer. In a separate 5 mL vial was added the appropriate cycloalkanol (0.30 mmol) in MeCN (2 mL) and the solution was purged *via* bubbling with N_2 gas for 2 min before being transferred into a 3 mL disposable syringe and connected to a syringe pump. Electrolysis at 10 mA was conducted for 3 h under N_2 with continuous stirring, while syringe pump addition of the substrate in anhydrous MeCN (1 mL/h) was started after 2 min of electrolysis. After electrolysis was complete, the reaction mixture was left to stir at 25 °C for an additional 30 min before being diluted with Et_2O (10 mL) and washed with a saturated solution of $NaHCO_3$ (aq.) (2 × 15 mL). The layers were separated, and the aqueous layer was further extracted with Et_2O (3 × 10 mL). The combined organics were dried over $MgSO_4$, filtered, and concentrated under reduced pressure. The resultant crude material was purified by flash column chromatography to afford the desired product.

5.2.4 Characterisation of Products

4-Chloro-1-(*o*-tolyl)butan-1-one (51)

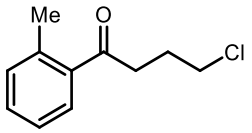

51

Prepared according to General Procedure 7 using 1-(*o*-tolyl)cyclobutan-1-ol (49 mg). The resultant crude material was purified by flash column chromatography (0-6% Et_2O/hexanes, silica gel) to afford **51** (26 mg, 43%) as a light red oil.

R_f = 0.40 (10% EtOAc/hexanes); **FTIR** (ν_{max} cm^{-1}, thin film) 2963, 1682, 1570, 1449, 1300, 1221, 972, 754; **^{1}H NMR (500 MHz, $CDCl_3$)** δ_H = 2.18 – 2.24 (2H, m), 2.50 (3H, s), 3.11 (2H, t, *J* 7.0), 3.67 (2H, t, *J* 6.3), 7.22 – 7.31 (2H, m), 7.35 – 7.42 (1H, m), 7.65 – 7.71 (1H, m); **^{13}C NMR (126 MHz, $CDCl_3$)** δ_C = 21.5, 27.1, 38.3, 44.8, 125.9, 128.6, 131.6, 132.2, 137.8, 138.3, 203.1; **HRMS** (EI+) $C_{11}H_{13}ClO$ $[M]^+$ requires 196.0655, found 196.0647 (-4.1 ppm).

6-Chlorohexan-3-one (69)

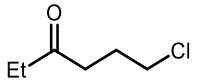

69

Prepared according to General Procedure 6 using **40** (30 mg). The resultant crude material was purified by flash column chromatography (0-6% Et_2O/pentane, silica gel) to afford **69** (8 mg, 19%) as a colourless oil. ^{1}H NMR analysis of the crude reaction mixture indicated a 57% yield.

R_f = 0.27 (10% EtOAc/hexanes); **FTIR** (ν_{max} cm^{-1}, thin film) 2943, 1713, 1445, 1354, 1206, 1034, 861; **^{1}H NMR (500 MHz, $CDCl_3$)** δ_H = 1.07 (3H, t, *J* 7.3), 2.00 – 2.10 (2H, m), 2.41 – 2.49 (2H, m), 2.58 – 2.65 (2H, m), 3.58 (2H, t, *J* 6.3); **^{13}C NMR (126 MHz, $CDCl_3$)** δ_C = 8.0, 26.5, 36.3, 39.0, 44.7, 210.5; **HRMS** (EI+) $C_6H_{11}OCl$ $[M]^+$ requires 134.0498, found 134.0497 (-0.7 ppm).

1-Chlorodecan-4-one (71)

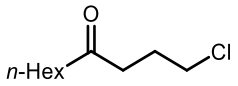

71

Prepared according to General Procedure 6 using **32** (47 mg). The resultant crude material was purified by flash column chromatography (10% Et_2O/pentane, silica gel) to afford **71** (27 mg, 47%) as a colourless oil.

R_f = 0.43 (10% EtOAc/hexanes); **^{1}H NMR (500 MHz, $CDCl_3$)** δ_H = 0.84 – 0.91 (3H, m), 1.23 – 1.32 (6H, m), 1.53 – 1.60 (2H, m), 2.00 – 2.06 (2H, m), 2.41 (2H, t, *J* 7.5), 2.60 (2H, t, *J* 7.0), 3.57 (2H, t, *J* 6.3); **^{13}C NMR (126 MHz, $CDCl_3$)** δ_C = 14.2, 22.6, 24.0, 26.4, 29.0, 31.7, 39.3, 43.2, 44.7, 210.2.

These data are in agreement with those previously reported in the literature.[9]

5-Chloro-1-phenylpentan-2-one (73)

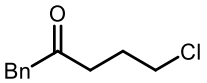

73

Prepared according to General Procedure 6 using **42** (49 mg). The resultant crude material was purified by flash column chromatography (10% Et_2O/pentane, silica gel) to afford **73** (40 mg, 68%) as a colourless oil.

R_f = 0.29 (10% EtOAc/hexanes); **^{1}H NMR (500 MHz, $CDCl_3$)** δ_H = 1.98 – 2.05 (2H, m), 2.65 (2H, t, *J* 7.0), 3.53 (2H, t, *J* 6.3), 3.71 (2H, s), 7.19 – 7.23 (2H, m), 7.25 – 7.30 (1H, m), 7.31 – 7.36 (2H, m); **^{13}C NMR (126 MHz, $CDCl_3$)** δ_C = 26.4, 38.7, 44.5, 50.4, 127.2, 129.0, 129.5, 134.1, 207.3.

These data are in agreement with those previously reported in the literature.[10]

6-Chloro-1-phenylhexan-3-one (74)

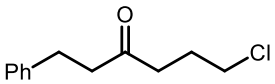

74

Prepared according to General Procedure 6 using **30** (53 mg). The resultant crude material was purified by flash column chromatography (0 – 8% Et_2O/hexanes, silica gel) to afford **74** (41 mg, 65%) as a colourless oil.

R_f = 0.31 (10% EtOAc/hexanes); **FTIR** (ν_{max} cm^{-1}, thin film) 2918, 1711, 1495, 1452, 1408, 1092, 748, 700; **^{1}H NMR (500 MHz, $CDCl_3$)** δ_H = 1.99 – 2.08 (2H, m), 2.59 (2H, t, *J* 7.0), 2.76 (2H, t, *J* 7.7), 2.91 (2H, t, *J* 7.6), 3.55 (2H, t, *J* 6.3), 7.16 – 7.22 (3H, m), 7.26 – 7.30 (2H, m); **^{13}C NMR (126 MHz, $CDCl_3$)** δ_C = 26.4, 29.9, 39.7, 44.5, 44.6, 126.3, 128.4, 128.7, 141.0, 209.0; **HRMS** (EI+) $C_{12}H_{15}ClO$ $[M]^+$ requires 210.0811, found 210.0808 (-1.4 ppm).

1-Chloro-5-phenylpentan-3-one (86)

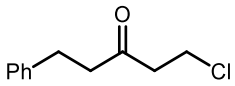

86

Prepared according to General Procedure 7 using **47** (49 mg). The resultant crude material was purified by flash column chromatography (10% Et_2O/pentane, silica gel) to afford **86** (39 mg, 67%) as a colourless oil.

R_f = 0.21 (10% EtOAc/petrol), **^{1}H NMR (500 MHz, $CDCl_3$)** δ_H = 2.78 (2H, t, *J* 7.6), 2.86 (2H, t, *J* 6.6), 2.93 (2H, t, *J* 7.6), 3.73 (2H, t, *J* 6.6), 7.17 – 7.22 (3H, m), 7.27 – 7.32 (2H, m); **^{13}C NMR (126 MHz, $CDCl_3$)** δ_C = 29.6, 38.4, 44.9, 45.3, 126.4, 128.4, 128.7, 140.8, 206.6.

These data are in agreement with those previously reported in the literature.[11]

1-Chlorononan-3-one (87)

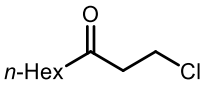

87

Prepared according to General Procedure 7 using **48** (43 mg). The resultant crude material was purified by flash column chromatography (10% Et_2O/pentane, silica gel) to afford **87** (35 mg, 66%) as a colourless oil.

R_f = 0.34 (10% EtOAc/petrol); **FTIR** (ν_{max} cm^{-1}, thin film) 2928, 2855, 1717, 1456, 1368, 1216, 1078, 718, 656; **^{1}H NMR (500 MHz, $CDCl_3$)** δ_H = 0.86 – 0.90 (3H, m), 1.24 – 1.35 (6H, m), 1.56 – 1.62 (2H, m), 2.44 (2H, t, *J* 7.5), 2.88 (2H, t, *J* 6.7), 3.74 (2H, t, *J* 6.7); **^{13}C NMR (126 MHz, $CDCl_3$)** δ_C = 14.2, 22.6, 23.7, 29.0, 31.7, 38.5, 43.5, 45.1, 207.8; **HRMS** (EI+) $C_9H_{17}OCl$ $[M]^+$ requires 176.0968, found 176.0975 (+4.0 ppm).

5-Chloro-1-phenylhexan-3-one (88)

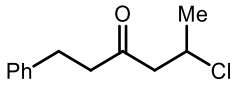

88

Prepared according to General Procedure 7 using **49** (53 mg). The resultant crude material was purified by flash column chromatography (10% Et_2O/pentane, silica gel) to afford **88** (44 mg, 70%) as a colourless oil. This compound was obtained as a 93:7 inseparable mixture of regioisomers.

R_f = 0.29 (10% EtOAc/petrol); **FTIR** (ν_{max} cm^{-1}, thin film) 2934, 1713, 1498, 1452, 1406, 1375, 1128, 1028, 989, 750, 698, 613; **HRMS** (EI+) $C_{12}H_{15}OCl$ $[M]^+$ requires 210.0811, found 210.0815 (+1.9 ppm).

Data for major regioisomer: **^{1}H NMR (500 MHz, $CDCl_3$)** δ_H = 1.52 (3H, d, *J* 6.5), 2.69 (1H, dd, *J* 16.8, 5.7), 2.75 – 2.79 (2H, m), 2.89 – 2.98 (3H, m), 4.46 (1H, dqd, *J* 7.7, 6.6, 5.7), 7.17 – 7.22 (3H, m), 7.26 – 7.30 (2H, m); **^{13}C NMR (126 MHz, $CDCl_3$)** δ_C = 25.3, 29.6, 45.3, 52.5, 52.8, 126.4, 128.5, 128.7, 140.9, 206.5.

Data for minor regioisomer: **^{1}H NMR (500 MHz, $CDCl_3$)** *(selected)* δ_H = 1.15 (3H, d, *J* 7.1), 3.50 (1H, dd, *J* 10.9, 5.8), 3.73 (1H, dd, *J* 10.9, 7.3).

5.2.5 Mechanistic Investigations

5.2.5.1 Cyclic Voltammetry Studies

General Information: Cyclic voltammetry (CV) experiments were conducted with a Metrohm Autolab PGSTAT204 potentiostat and Nova 2.1 software. For all experiments, a glassy carbon working electrode (3 mm dia., BASi), a platinum wire counter electrode, and an $Ag/AgNO_3$ reference electrode were employed. All data was collected at rt. The solution of interest was purged with N_2 for 5 min before data collection. After data collection, ferrocene (5 mM) was added, and an additional scan was run. The parent data was referenced relative to the Fc/Fc^+ couple that was recorded.

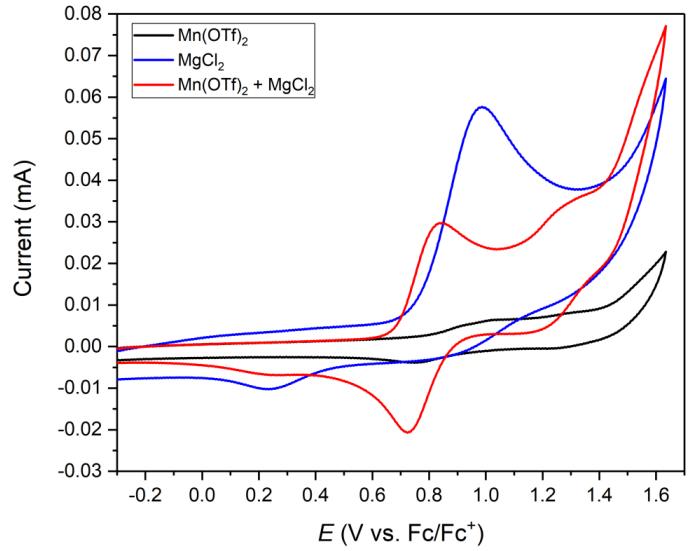

*Figure 5.2: Cyclic voltammogram of $Mn(OTf)_2$, $MgCl_2$, and their mixture in MeCN (5 mL) with AcOH (700 µL) and $LiClO_4$ (0.1 M). **a** (black line) – $Mn(OTf)_2$ (2.0 mM); **b** (blue line) – $MgCl_2$ (8.0 mM); **c** (red line) $Mn(OTf)_2$ (2.0 mM) and $MgCl_2$ (8.0 mM). **Scan rate: 100 mV/s***

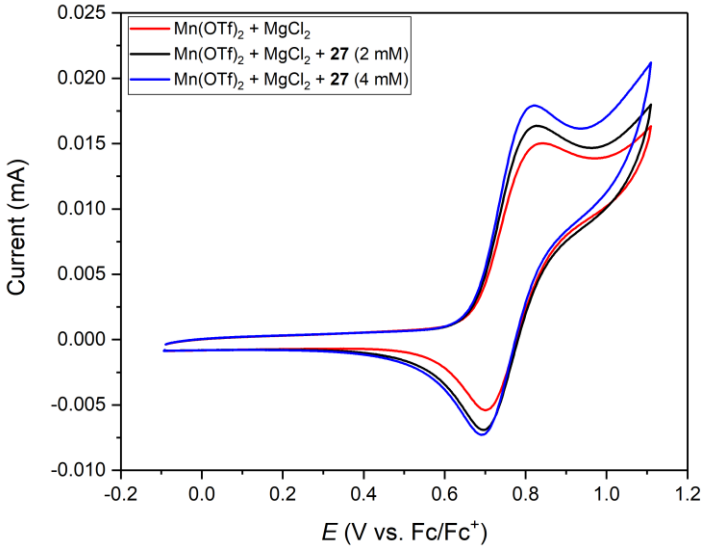

*Figure 5.3: Cyclic voltammogram of $Mn(OTf)_2$, $MgCl_2$, and 1-phenylcyclobutan-1-ol **27** in MeCN (5 mL) with AcOH (700 µL) and $LiClO_4$ (0.1 M). **a** (red line) – $Mn(OTf)_2$ (2.0 mM) and $MgCl_2$ (8.0 mM); **b** (black line) – $Mn(OTf)_2$ (2.0 mM), $MgCl_2$ (8.0 mM), and **27** (2.0 mM); **c** (blue line) – $Mn(OTf)_2$ (2.0 mM), $MgCl_2$ (8.0 mM), and **27** (4.0 mM). **Scan rate: 20 mV/s***

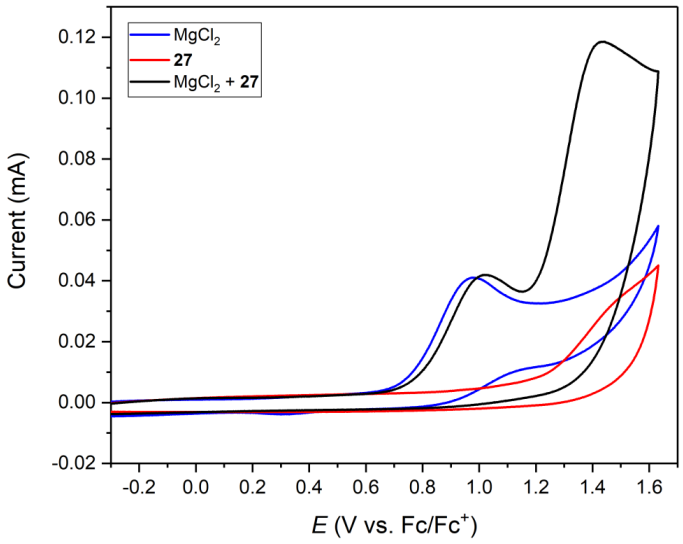

*Figure 5.4: Cyclic voltammogram of $MgCl_2$ and **27** and their mixture in MeCN (5 mL) with AcOH (700 µL) and $LiClO_4$ (0.1 M). **a** (blue line) – $MgCl_2$ (8.0 mM); **b** (red line) – **27** (4.0 mM); **c** (black line) – $MgCl_2$ (8.0 mM) and **27** (4.0 mM). **Scan rate: 50 mV/s***

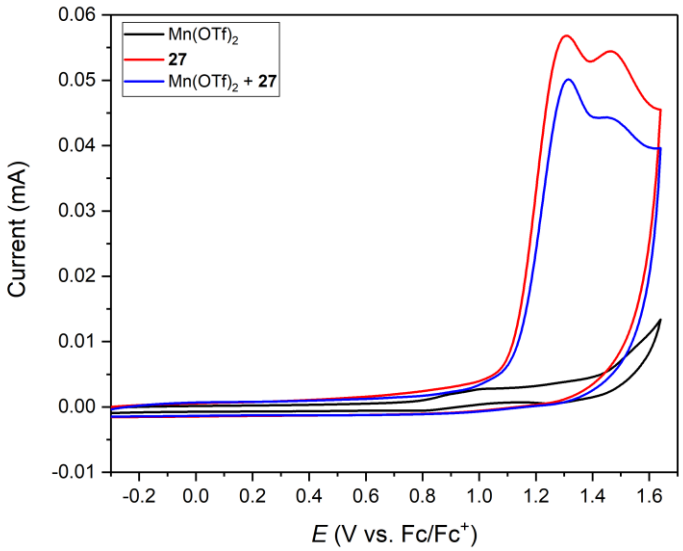

*Figure 5.5: Cyclic voltammogram of $Mn(OTf)_2$ and **27** and their mixture in MeCN (5 mL) with AcOH (700 µL) and $LiClO_4$ (0.1 M). **a** (black line) – $Mn(OTf)_2$ (2.0 mM); **b** (red line) – **27** (4.0 mM); **c** (blue line) – $Mn(OTf)_2$ (2.0 mM) and **27** (4.0 mM). **Scan rate: 20 mV/s***

5.2.5.2 Mechanistic Experiments

(1-Methoxycyclobutyl)benzene (96)

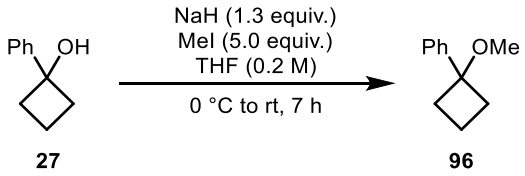

Following a literature procedure,[12] to a solution of **27** (445 mg, 3.00 mmol) in THF (15 mL, 0.2 M) was slowly added NaH (60% dispersed in mineral oil, 156 mg, 3.90 mmol). Once gas evolution had ceased, the solution was cooled to 0 °C and methyl iodide (933 µL, 15.0 mmol) was then added dropwise. The reaction mixture was stirred at rt for 7 h, before being cooled to 0 °C and water (15 mL) was added. The layers were separated, and the aqueous layer was further extracted with Et_2O (2 × 20 mL). The combined organics were then washed with water and brine, dried over $MgSO_4$, filtered, and concentrated under reduced pressure. The resultant crude material was purified by flash column chromatography (5% EtOAc/hexanes, silica gel) to afford **96** (314 mg, 65%) as a colourless oil.

R_f = 0.46 (10% EtOAc/hexanes); **FTIR** (ν_{max} cm^{-1}, thin film) 2978, 2940, 2816, 1443, 1281, 1242, 1126, 1088, 1042, 756, 694; **^{1}H NMR (500 MHz, $CDCl_3$)** δ_H = 1.64 – 1.73 (1H, m), 1.91 – 1.99 (1H, m), 2.34 – 2.46 (4H, m), 2.94 (3H, s), 7.27 – 7.31 (1H, m), 7.36 – 7.40 (2H, m), 7.42 – 7.45 (2H, m); **^{13}C NMR (126 MHz, $CDCl_3$)** δ_C = 13.2, 32.9, 50.6, 81.7, 126.5, 127.3, 128.4, 143.2; **HRMS** (EI^+) $C_{11}H_{14}O$ M^+ requires 162.1045, found 162.1047 (+1.2 ppm).

Subjection of 3-AJ to Parent Reaction Conditions

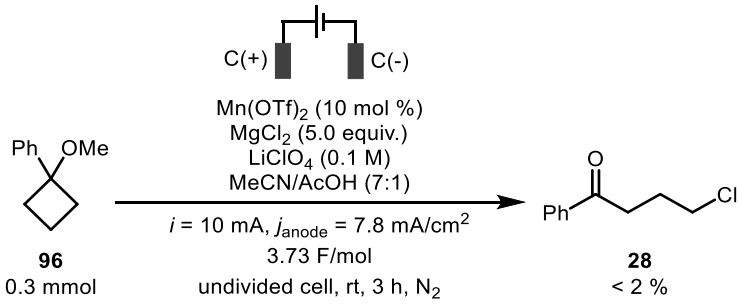

Methyl ether **96** (49 mg) was subjected to the conditions of General Procedure 6. Analysis of the crude reaction mixture by ^{1}H NMR with 1,3,5-trimethylbenzene (14 µL, 0.10 mmol) as an internal standard indicated < 2% formation of **28**, with 82% of **96** recovered.

5.3 Investigations Into the (Photo)Electrochemical Generation of Alkoxy Radicals Using Cerium (III) and (IV) Salts

5.3.1 Substrate Synthesis

General Procedure 8 – Generation and Addition of Grignard Reagents to Cycloalkanones

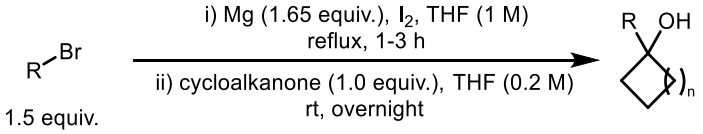

To a three-necked RBF fitted with a condenser, stopper, and septum seal was added magnesium (1.65 equiv.) and the system was flame-dried. After cooling, a crystal of iodine was added before the system was subjected to vacuum-nitrogen exchange cycles (× 3). Anhydrous THF (1 M with respect to the R-Br) was added, followed by dropwise addition of R-Br (1.50 equiv.). After complete addition, the mixture stirred for 5 min at rt or until the exotherm had ceased, before being heated at reflux for 2-3 h. The reaction was allowed to cool to rt, then further cooled to 0 °C. A solution of the cycloalkanone (1.00 equiv.) in anhydrous THF (0.2 M) was added slowly and the reaction was stirred overnight at rt before being quenched with a saturated solution of NH_4Cl (aq.), and a few drops of 1 M HCl (aq.). EtOAc was added, the layers were separated, and the aqueous layer was further extracted with EtOAc (× 3). The combined organics were washed with brine, dried over $MgSO_4$, filtered, and concentrated under reduced pressure. The resultant crude material was purified by flash column chromatography to afford the desired compound.

General Procedure 9 – Generation and Addition of Organolithium Reagents to Cycloalkanone

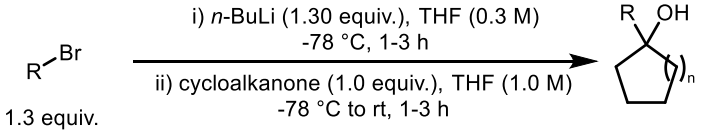

To a flame-dried RBF fitted with a septum seal was added a solution of R-Br (1.30 equiv.) in anhydrous THF (0.3 M). The mixture was cooled to -78 °C, and a solution of *n*-BuLi in hexanes (1.30 equiv.) was added dropwise. The reaction mixture was left to stir for 1-3 h before a solution of the cycloalkanone (1.00 equiv.) in anhydrous THF (1.0 M) was added

dropwise. The solution was left to stir for 1-3 h whilst warming to rt. Water was added dropwise, followed by EtOAc, and the layers were separated. The aqueous layer was further extracted with EtOAc (× 3). The combined organics were washed with brine, dried over $MgSO_4$, filtered, and concentrated under reduced pressure. The resultant crude material was purified by flash column chromatography to afford the desired compound.

5.3.2 Characterisation of Substrates

1-Phenylcyclobutan-1-ol (27)

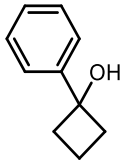

27

Prepared according to General Procedure 8 using magnesium turnings (2.01 g, 82.5 mmol), bromobenzene (7.90 mL, 75.0 mmol), and cyclobutanone (3.74 mL, 50.0 mmol). The crude residue was purified by flash column chromatography (10-20% EtOAc/petrol, silica gel) to afford **27** (6.78 g, 91%) as a colourless solid.

R_f = 0.13 (10% EtOAc/petrol); **M.p.:** 43-46 °C; **^{1}H NMR (500 MHz, DMSO-*d*$_6$)** δ_H = 1.57 – 1.69 (1H, m), 1.85 – 1.97 (1H, m), 2.21 – 2.31 (2H, m), 2.34 – 2.41 (2H, m), 5.44 (1H, s), 7.20 – 7.24 (1H, m), 7.29 – 7.36 (2H, m), 7.45 – 7.50 (2H, m); **^{13}C NMR (126 MHz, DMSO-*d*$_6$)** δ_C = 12.7, 37.2, 75.1, 124.8, 126.3, 127.9, 147.7.

These data are consistent with those previously reported in the literature.[1]

1-Phenethylcyclopentan-1-ol (39)

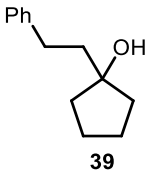

39

Prepared according to General Procedure 8 using magnesium turnings (201 mg, 8.25 mmol), (2-bromoethyl)benzene (1.02 mL, 7.50 mmol), and cyclopentanone (443 µL, 5.00 mmol). The crude residue was purified by flash column chromatography (10% EtOAc/hexanes, silica gel) to afford **5-L** (552 mg, 52%) as a colourless oil.

R_f = 0.24 (10% EtOAc/petrol); **^{1}H NMR (500 MHz, $CDCl_3$)** δ_H = 1.18 (1H, br s), 1.60 – 1.73 (6H, m), 1.79 – 1.87 (2H, m), 1.89 – 1.93 (2H, m), 2.75 – 2.79 (2H, m), 7.16 – 7.23 (3H,

m), 7.27 – 7.31 (2H, m); **^{13}C NMR (126 MHz, $CDCl_3$)** δ_C = 24.0, 31.4, 40.0, 43.7, 82.6, 125.9, 128.5, 128.6, 142.9.

These data are consistent with those previously reported in the literature.[7]

1-Phenylcyclopentan-1-ol (94)

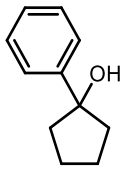

94

Prepared according to General Procedure 9 using bromobenzene (1.37 mL, 13.0 mmol), *n*-BuLi (5.90 mL, 2.2 M in hexanes, 13.0 mmol), and cyclopentanone (887 µL, 10.0 mmol). The crude residue was purified by flash column chromatography (10% EtOAc/petrol, silica gel) to afford **94** (1.06 g, 65%) as a colourless oil.

R_f = 0.29 (10% EtOAc/petrol); **^{1}H NMR (500 MHz, $CDCl_3$)** δ_H = 2.62 (1H, s), 1.81 – 1.88 (2H, m), 1.96 – 2.06 (6H, m), 7.24 – 7.28 (1H, m), 7.33 – 7.37 (2H, m), 7.49 – 7.52 (2H, m); **^{13}C NMR (126 MHz, $CDCl_3$)** δ_C = 24.0, 42.0, 83.6, 125.2, 126.9, 128.3, 147.2.

These data are consistent with those previously reported in the literature.[13]

1-Phenylcyclohexan-1-ol (115)

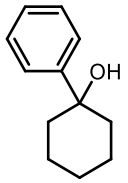

115

Prepared according to General Procedure 9 using bromobenzene (1.37 mL, 13.0 mmol), *n*-BuLi (5.90 mL, 2.2 M in hexanes, 13.0 mmol), and cyclohexanone (1.04 mL, 10.0 mmol). The crude residue was purified by flash column chromatography (10% EtOAc/petrol, silica gel) to afford **115** (1.30 g, 74%) as a colourless solid.

R_f = 0.32 (10% EtOAc/Petrol; **M.p.:** 60-62 °C; **^{1}H NMR (500 MHz, $CDCl_3$)** δ_H = 1.25 – 1.37 (1H, m), 1.58 (1H, s), 1.61 – 1.68 (2H, m), 1.72 – 1.89 (7H, m), 7.23 – 7.27 (1H, m), 7.33 – 7.37 (2H, m), 7.50 – 7.53 (2H, m); **^{13}C NMR (126 MHz, $CDCl_3$)** δ_C = 22.3, 25.7, 39.0, 73.3, 124.7, 126.8, 128.4, 149.6.

These data are consistent with those previously reported in the literature.[13]

1-Phenethylcyclohexan-1-ol (116)

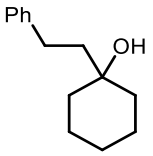

116

Prepared according to General Procedure 8 using magnesium turnings (201 mg, 8.25 mmol), (2-bromoethyl)benzene (1.02 mL, 7.50 mmol), and cyclohexanone (518 µL, 5.00 mmol). The crude residue was purified by flash column chromatography (10% EtOAc/hexanes, silica gel) to afford **116** (601 mg, 59%) as a white solid.

R_f = 0.21 (10% EtOAc/petrol); **M.p.:** 54-56 °C; **FTIR** (ν_{max} cm^{-1}, thin film) 3329 (br), 2924, 2849, 1601, 1449, 1254, 1171, 997, 968, 928, 756, 696, 515; **^{1}H NMR (500 MHz, $CDCl_3$)** δ_H = 1.22 (1H, s), 1.25 – 1.35 (1H, m), 1.46 – 1.66 (9H, m), 1.74 – 1.79 (2H, m), 2.69 – 2.73 (2H, m), 7.16 – 7.22 (3H, m), 7.24 – 7.32 (2H, m); **^{13}C NMR (126 MHz, $CDCl_3$)** δ_C = 22.4, 26.0, 29.6, 37.7, 44.5, 71.6, 125.8, 128.5, 128.6, 143.0; **HRMS** (EI+) $C_{14}H_{20}O$ $[M\text{-}H_2O]^+$ requires 186.1409, found 186.1409 (±0.0 ppm).

***tert*-Butyldimethyl((1-phenylvinyl)oxy)silane (5-AV)**

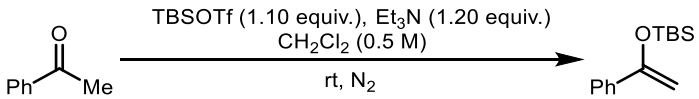

5-AV

Following a literature procedure,[14] to a flame-dried RBF was added acetophenone (1.17 mL, 10.0 mmol) in anhydrous CH_2Cl_2 (20 mL, 0.5 M). Triethylamine (1.67 mL, 12.0 mmol) was added, and the reaction mixture was stirred at rt for 1 h. TBSOTf (2.53 mL, 11.0 mmol) was added dropwise and the reaction mixture was allowed to stir at rt until completion as monitored by TLC analysis. Upon completion, a cold saturated solution of NH_4Cl (aq.) was added, the layers were separated, and the aqueous layer was further extracted with CH_2Cl_2 (2 × 30 mL). The combined organics were washed with brine (20 mL), dried over $MgSO_4$, filtered, and concentrated under reduced pressure. The resultant crude material was purified by flash column chromatography (petrol, triethylamine deactivated silica gel) to afford **5-AV** (2.16 g, 92%) as a colourless oil.

R_f = 0.31 (petrol); **^{1}H NMR (500 MHz, $CDCl_3$)** δ_H = 0.22 (6H, s), 1.01 (9H, s), 4.42 (1H, d, *J* 1.7), 4.89 (1H, d, *J* 1.7), 7.27 – 7.35 (3H, m), 7.60 – 7.62 (2H, m); **^{13}C NMR (126 MHz, $CDCl_3$)** δ_C = -4.5, 26.0, 91.0, 125.4, 128.2, 128.3, 137.9, 156.1.

These data are in accordance with the literature.[15]

5.3.3 Preliminary Investigations

General Procedure 10 – CAN Mediated Deconstructive Functionalisation of Cyclobutanol

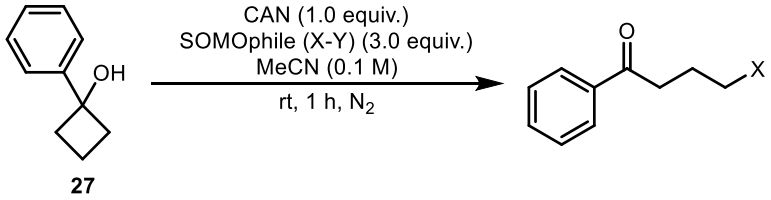

27

To a flame-dried RBF was added **27** (44 mg, 0.30 mmol), CAN (164 mg, 0.30 mmol), and the appropriate SOMOphile (0.90 mmol) in anhydrous MeCN (3 mL, 0.1 M). The reaction mixture was stirred at rt for 1 h before 1,3,5-trimethylbenzene (14 µL, 0.10 mmol) was added to the reaction mixture, stirred for 5 min and then the ^{1}H NMR spectrum was recorded to give a crude reaction yield. Where appropriate, the reaction mixture was concentrated under reduced pressure and the resultant crude material was purified by flash column chromatography.

4-(Benzo[*d*]thiazol-2-yl)-1-phenylbutan-1-one (5-E)

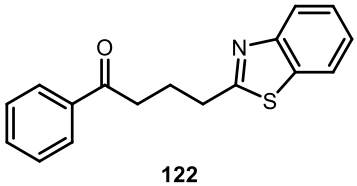

122

Prepared according to General Procedure 10 using benzothiazole **119** (90 µL) as the SOMOphile. The resultant crude material was purified by flash column chromatography (10-20% EtOAc/petrol, silica gel) to afford **122** (36 mg, 43%) as a light-brown solid.

R_f = 0.11 (10% EtOAc/petrol); **M.p.:** 73-75 °C; **^{1}H NMR (400 MHz, $CDCl_3$)** δ_H = 2.36 (2H, app p, *J* 7.2), 3.15 (2H, t, *J* 7.2), 3.25 (2H, t, *J* 7.3), 7.34 – 7.38 (1H, m), 7.43 – 7.48 (3H, m), 7.53 – 7.58 (1H, m), 7.84 – 7.86 (1H, m), 7.94 – 7.99 (3H, m); **^{13}C NMR (101 MHz, $CDCl_3$)** δ_C = 23.9, 33.6, 37.5, 121.7, 122.7, 124.9, 126.1, 128.2, 128.7, 133.3, 135.3, 136.9, 153.4, 171.4, 199.4.

These data are in accordance with the literature.[16]

5.3.4 Electrochemical Reactions

General Procedure 11 – Electrochemical Cerium Mediated Deconstructive Functionalisation of Cycloalkanols

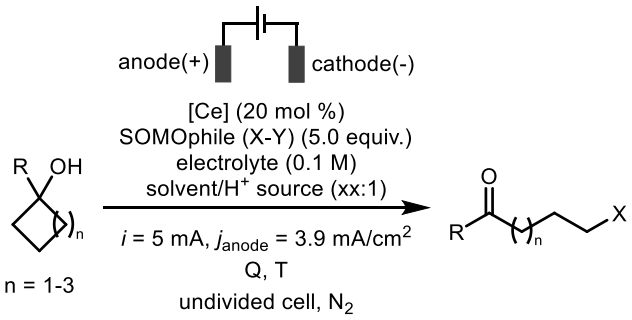

To an oven-dried 10 mL ElectraSyn vial equipped with a magnetic stirrer bar, was added the appropriate cycloalkanol (0.30 mmol), cerium salt (0.06 mmol), SOMOphile (1.50 equiv.), and electrolyte (0.60 mmol). The threaded glass was wrapped with PTFE tape and connected to the ElectraSyn cap, which was fitted with an anode and cathode. The vial was subjected to vacuum-nitrogen exchange cycles (× 3), anhydrous solvent was added, followed by the H^+ source (6 mL total), and the mixture was stirred until complete solvation of the reagents. The mixture was purged *via* bubbling with N_2 gas for 10 minutes. Electrolysis at 5 mA (j_{anode} = 3.9 mA/cm^2) was conducted until the desired amount of charge (F/mol) had passed under N_2 at rt with continuous stirring. After electrolysis was complete, 1,3,5-Trimethylbenzene (14 µL, 0.10 mmol) was added to the reaction mixture, stirred for 5 min and then the ^{1}H NMR spectrum was recorded to give a crude reaction yield.

For full results see sections 3.2.2 to 3.2.5.

5.3.5 Photoelectrochemical Reactions

Photoelectrochemical Cerium Mediated Decarboxylative C-H Heteroarylation

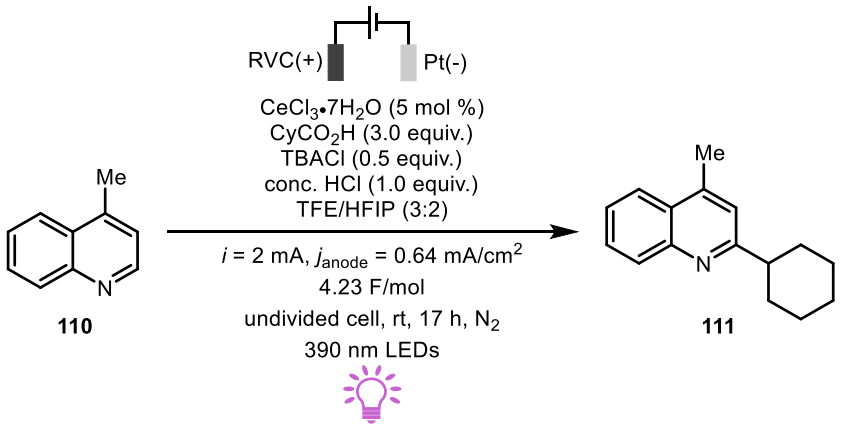

To an oven-dried 10 mL ElectraSyn vial equipped with a magnetic stirrer bar, was added lepidine (40 µL, 0.30 mmol), $CyCO_2H$ (115 mg, 0.90 mmol), $CeCl_3$•$7H_2O$ (6 mg, 0.015 mmol), and TBACl (42 mg, 0.15 mmol). The threaded glass was wrapped with PTFE tape and connected to the ElectraSyn cap, which was fitted with an RVC anode and a platinum foil cathode. The vial was subjected to vacuum-nitrogen exchange cycles (× 3), TFE (3 mL) was added, followed by HFIP (2 mL), and the mixture was stirred until complete solvation of the reagents. The mixture was purged *via* bubbling with N_2 gas for 10 min, after which concentrated HCl (aq.) (25 µL, 0.30 mmol) was added. The vial was placed 2 cm from a 392 nm LED bulb (Kessil: KSPR160L-390), and a fan (Kessil: KSPRRM03) was suspended above the reaction. Electrolysis at 2 mA (j_{anode} = 0.64 mA/cm^2) was conducted for 17 h under N_2 at rt with continuous stirring. After electrolysis was complete, the reaction mixture was diluted with EtOAc (10 mL) and washed with a saturated solution of $NaHCO_3$ (aq.) (2 × 15 mL). The layers were separated, and the aqueous layer was further extracted with EtOAc (3 × 10 mL). The combined organics were washed with brine, dried over $MgSO_4$, filtered, and concentrated under reduced pressure before 1,3,5-trimethylbenzene (14 µL, 0.10 mmol) was added, and then the ^{1}H NMR spectrum was recorded to give a crude reaction yield. Analysis of the crude reaction mixture by ^{1}H NMR indicated a 75% yield of **5-AG**, with the peaks observed in the spectrum matching those in the literature.[17]

General Procedure 12 – Photoelectrochemical Cerium Mediated Deconstructive Heteroarylation of 1-Phenylcyclobutanol (27)

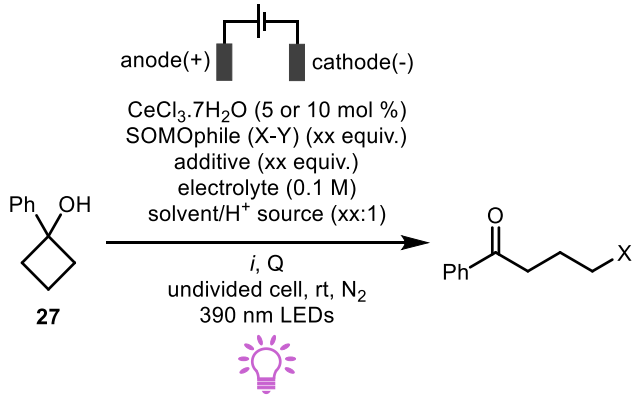

To an oven-dried 10 mL ElectraSyn vial equipped with a magnetic stirrer bar, was added **27** (44 mg, 0.30 mmol), $CeCl_3$•$7H_2O$ (5 or 10 mol %), SOMOphile, additive, and electrolyte (0.60 mmol). The threaded glass was wrapped with PTFE tape and connected to the ElectraSyn cap, which was fitted with an anode and cathode. The vial was subjected to vacuum-nitrogen exchange cycles (× 3), anhydrous solvent was added, followed by the H^+ source (6 mL total), and the mixture was stirred until complete solvation of the reagents. The mixture was purged *via* bubbling with N_2 gas for 10 min. The vial was placed 2 cm from a 392 nm LED bulb (Kessil: KSPR160L-390), and a fan (Kessil: KSPRRM03) was suspended above the reaction. Electrolysis at the appropriate constant current was conducted until the desired amount of charge (F/mol) had passed under N_2 at rt with continuous stirring. After electrolysis was complete, 1,3,5-trimethylbenzene (14 µL, 0.10 mmol) was added to the reaction mixture, and then the ^{1}H NMR spectrum was recorded to give a crude reaction yield.

For full results see section 3.2.6.

5.4 Electrochemical Alkene Azidocyanation *via* 1,4-Nitrile Migration

5.4.1 Substrate Synthesis

General Procedure 13 – Synthesis of Ketones from Acid Chlorides

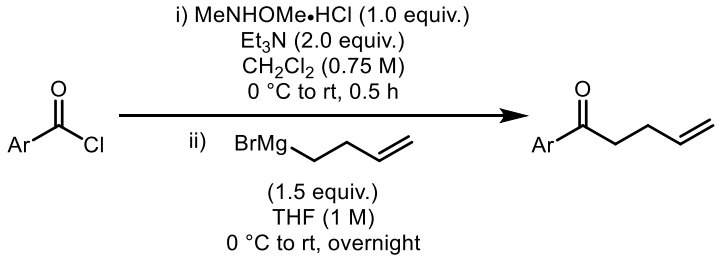

Synthesis of Aryl Weinreb Amide

To a flame-dried RBF fitted with a septum seal was added *N*,*O*-dimethylhydroxylamine hydrochloride (1.0 equiv.) in anhydrous CH_2Cl_2 (0.75 M). The solution was cooled to 0 °C and the appropriate acid chloride (1.0 equiv.) was added dropwise followed by dropwise addition of triethylamine (2.0 equiv.). The reaction suspension was stirred at rt for 30 min before being quenched with a saturated solution of $NaHCO_3$ (aq.). The layers were separated, and the aqueous layer was extracted with CH_2Cl_2 (× 3). The combined organics were washed with water, then brine, dried over $MgSO_4$, filtered, and concentrated under reduced pressure to afford the crude Weinreb amide that was used without further purification.

Formation of Aryl Ketone

To a three-neck RBF fitted with a condenser, stopper, and septum seal was added magnesium (1.65 equiv.) and the system was flame-dried. After cooling, a crystal of iodine was added before the system was subjected to vacuum-nitrogen exchange cycles (× 3). Anhydrous THF (1 M with respect to 4-bromobut-1-ene) was added, followed by the dropwise addition of 4-bromobut-1-ene (1.5 equiv.). After complete addition, the mixture was stirred for 5 min at rt or until the exotherm has ceased, before being heated at reflux for 2-3 h. The reaction was allowed to cool to rt, then further cooled to 0 °C. A solution of Weinreb amide (1.0 equiv.) in anhydrous THF (2 M) was added slowly and the reaction was stirred overnight at rt before being quenched with a saturated solution of NH_4Cl (aq.), and a few drops of 1 M HCl (aq.). EtOAc was added, the layers were separated, and the aqueous layer was further extracted with EtOAc (× 3). The combined organics were washed with brine, dried over $MgSO_4$, filtered, and concentrated under reduced pressure.

The resultant crude material was purified by flash column chromatography to afford the desired compound.

General Procedure 14 – Synthesis of Ketones from Aryl Halides

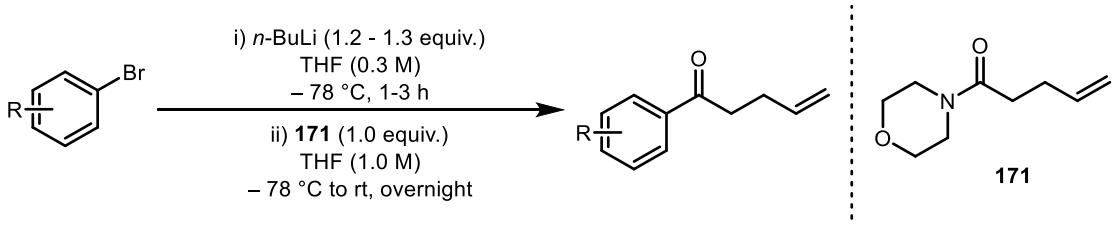

To a flame-dried RBF fitted with a septum seal was added a solution of aryl halide (1.2-1.3 equiv.) in anhydrous THF (0.3 M). The mixture was cooled to -78 °C, and a solution of *n*-BuLi in hexanes (1.2-1.3 equiv.) was added dropwise. The reaction mixture was left to stir for 1-3 h before a solution of **171** (1.0 equiv.) in anhydrous THF (1.0 M) was added dropwise. The solution was left to stir for 1-3 h whilst warming to rt. A saturated solution of NH_4Cl (aq.) was added dropwise, followed by EtOAc, and the layers were separated. The aqueous layer was further extracted with EtOAc (× 3). The combined organics were washed with brine, dried over $MgSO_4$, filtered, and concentrated under reduced pressure. The resultant crude material was purified by flash column chromatography to afford the desired compound.

General Procedure 15 – Synthesis of *α*-Substituted from *β*-Ketoesters

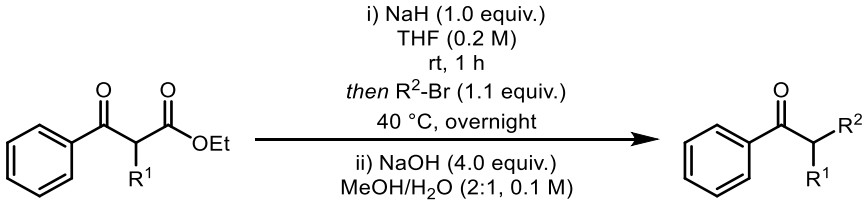

Following a literature procedure,[18] to a flame-dried RBF was added ethylbenzoyl acetate (1.0 equiv.) in THF (0.2 M). NaH (60% dispersion in mineral oil, 1.00 equiv.) was added portion-wise, and the reaction was stirred at rt for 1 h. The appropriate allylic bromide (1.1 equiv.) was added, and the reaction was heated at 40 °C overnight. After cooling to rt, the suspension was diluted with Et_2O, followed by water. The layers were separated, and the aqueous layer was further extracted with Et_2O (× 3). The combined organics were washed with brine, dried over $MgSO_4$, filtered, and concentrated under reduced pressure to give a crude product that was used in the next step without further purification.

To a RBF was added the crude product (1.0 equiv.) in 2:1 MeOH/water (0.1 M), and NaOH (4.0 equiv.) was added. The reaction was heated at reflux for 20 h, before being cooled to rt and concentrated under reduced pressure. EtOAc was added, the layers were separated, and the aqueous layer was further extracted with EtOAc (× 3). The combined organics were washed with brine, dried over $MgSO_4$, filtered, and concentrated under reduced pressure. The resultant crude material was purified by flash column chromatography to afford the desired compound.

General Procedure 16 – Synthesis of Cyanohydrins from Ketones

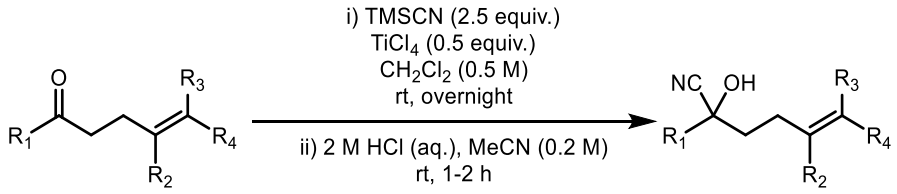

To a flame-dried RBF fitted with a septum seal was added the appropriate ketone (1.0 equiv.) in anhydrous CH_2Cl_2 (0.5 M). TMSCN (2.5 equiv.) was added slowly, followed by $TiCl_4$ (0.5 equiv.) and the reaction mixture was stirred at rt overnight. The reaction mixture was concentrated under reduced pressure and the resulting residue was dissolved in MeCN (0.2 M), before an identical volume of 2 M HCl (aq.) was added. The resulting biphasic mixture was stirred at rt for 1 h, before being diluted with water. The layers were separated, and the aqueous layer was extracted with EtOAc (× 3). The combined organics were washed with brine, dried over $MgSO_4$, filtered, and concentrated under reduced pressure to afford the cyanohydrins that were used without further purification.

5.4.2 Characterisation of Substrates

5.4.2.1 Substrate Precursors

1-Phenylpent-4-en-1-one (162)

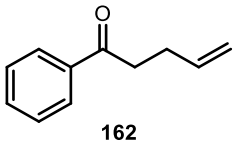

162

Prepared according to General Procedure 13 using *N*,*O*-dimethylhydroxylamine hydrochloride (4.88 g, 50.0 mmol) in CH_2Cl_2 (67 mL), benzoyl chloride (5.80 mL, 50.0 mmol), and triethylamine (14.0 mL, 100 mmol) to form the crude Weinreb amide. The Grignard reagent was prepared using magnesium (2.00 g, 82.5 mmol) in THF (75 mL), and 4-bromobut-1-ene (7.60 mL, 75.0 mmol). The aryl ketone was prepared through the addition of the Weinreb amide in THF (25 mL) to the solution of Grignard reagent. The resultant crude material was purified by flash column chromatography (5% EtOAc/petrol, silica gel) to afford **162** (6.36 g, 79%) as a colourless oil.

R_f = 0.38 (5% EtOAc/petrol); **FTIR** (ν_{max} cm^{-1}, thin film) 3080, 2918, 1684, 1597, 1448, 1205, 912, 743, 689; **^{1}H NMR (500 MHz, $CDCl_3$)** δ_H = 2.48 – 2.52 (2H, m), 3.07 – 3.10 (2H, m), 5.00 – 5.03 (1H, app dq, *J* 17.0, 1.7), 5.07 – 5.12 (1H, ddt, *J* 10.2, 1.7, 1.3), 5.91 (1H, ddt, *J* 17.0, 10.2, 6.5), 7.45 – 7.49 (2H, m), 7.55 – 7.58 (1H, m), 7.96 – 7.98 (2H, m); **^{13}C NMR (126 MHz, $CDCl_3$)** δ_C = 28.3, 37.9, 115.4, 128.2, 128.7, 133.2, 137.0, 137.4, 199.6; **HRMS** (ES+) $C_{11}H_{12}O$ $[M+H]^+$ requires 160.0966, found 161.0970 (+2.5 ppm).

1-(4-Methoxyphenyl)pent-4-en-1-one (166)

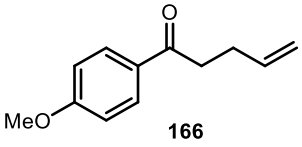

166

Prepared according to General Procedure 13 using *N*,*O*-dimethylhydroxylamine hydrochloride (975 mg, 10.0 mmol) in CH_2Cl_2 (14 mL), *p*-anisoyl chloride (1.35 mL, 10.0 mmol), and triethylamine (2.80 mL, 20.0 mmol) to form the crude Weinreb amide. The Grignard reagent was prepared using magnesium (401 mg, 16.5 mmol) in THF (15 mL), and 4-bromobut-1-ene (1.52 mL, 15.0 mmol). The aryl ketone was prepared through the addition of the Weinreb amide in THF (5 mL) to the solution of Grignard reagent. The resultant crude material was purified by flash column chromatography (10% EtOAc/petrol, silica gel) to afford **166** (1.44 g, 76%) as a low melting colourless solid.

R_f = 0.24 (10% EtOAc/petrol); **FTIR** (ν_{max} cm^{-1}, thin film) 3013, 2905, 1667, 1599, 1250, 1179, 980, 841; **^{1}H NMR (500 MHz, $CDCl_3$)** δ_H = 2.46 – 2.52 (2H, m), 3.00 – 3.04 (2H, m), 3.87 (3H, s), 4.99 – 5.02 (1H, m), 5.06 – 5.11 (1H, m), 5.86 – 5.95 (1H, m), 6.92 – 6.95 (2H, m), 7.93 – 7.97 (2H, m); **^{13}C NMR (126 MHz, $CDCl_3$)** δ_C = 28.5, 37.5, 55.6, 113.8, 115.3, 130.2, 130.4, 137.6, 163.5, 198.2; **HRMS** (ES+) $C_{12}H_{14}O_2$ $[M+H]^+$ requires 191.1072, found 191.1072 (±0.0 ppm).

1-(4-Fluorophenyl)pent-4-en-1-one (167)

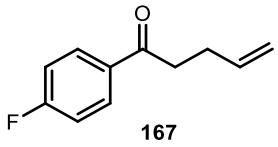

167

Prepared according to General Procedure 13 using *N*,*O*-dimethylhydroxylamine hydrochloride (483 mg, 5.00 mmol) in CH_2Cl_2 (7 mL), 4-fluorobenzoyl chloride (591 µL, 5.00 mmol), and triethylamine (1.39 mL, 10.0 mmol) to form the crude Weinreb amide. The Grignard reagent was prepared using magnesium (201 mg, 8.25 mmol) in THF (7.5 mL), and 4-bromobut-1-ene (761 µL, 7.50 mmol). The aryl ketone was prepared through the addition of the Weinreb amide in THF (5 mL) to the solution of Grignard reagent. The resultant crude material was purified by flash column chromatography (5% EtOAc/petrol, silica gel) to afford **167** (609 mg, 68%) as a colourless oil.

R_f = 0.54 (5% EtOAc/petrol); **FTIR** (ν_{max} cm^{-1}, thin film) 3078, 1684, 1597, 1227, 1206, 1155, 853; **^{1}H NMR (500 MHz, $CDCl_3$)** δ_H = 2.47 – 2.52 (2H, m), 3.01 – 3.08 (2H, m), 4.98 – 5.05 (1H, m), 5.04 – 5.13 (1H, m), 5.83 – 5.95 (1H, m), 7.08 – 7.17 (2H, m), 7.95 – 8.03 (2H, m); **^{13}C NMR (126 MHz, $CDCl_3$)** δ_C = 28.3, 37.8, 115.5, 115.8 (d, *J* 21.8), 130.8 (d, *J* 9.3), 133.5 (d, *J* 3.1), 137.3, 165.8 (d, *J* 254.5), 193.9; **^{19}F{^{1}H} NMR (376 MHz, $CDCl_3$)** δ_F = -105.43; **HRMS** (ES+) $C_{11}H_{11}OF$ $[M+H]^+$ requires 179.0872, found 179.0873 (+0.6 ppm).

1-(4-Chlorophenyl)pent-4-en-1-one (168)

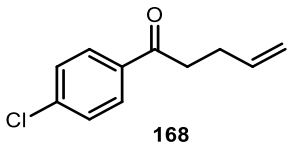

168

Prepared according to General Procedure 13 using *N*,*O*-dimethylhydroxylamine hydrochloride (483 mg, 5.00 mmol) in CH_2Cl_2 (7 mL), 4-chlorobenzoyl chloride (641 µL, 5.00 mmol), and triethylamine (1.39 mL, 10.0 mmol) to form the crude Weinreb amide. The Grignard reagent was prepared using magnesium (201 mg, 8.25 mmol) in THF

(7.5 mL), and 4-bromobut-1-ene (761 µL, 7.50 mmol). The aryl ketone was prepared through the addition of the Weinreb amide in THF (5 mL) to the solution of Grignard reagent. The resultant crude material was purified by flash column chromatography (5% EtOAc/petrol, silica gel) to afford **168** (569 mg, 61%) as a yellow oil.

R_f = 0.57 (5% EtOAc/petrol); **FTIR** (ν_{max} cm^{-1}, thin film) 3076, 1683, 1587, 1400, 1204, 1090; **^{1}H NMR (500 MHz, $CDCl_3$)** δ_H = 2.46 – 2.52 (2H, m), 3.01 – 3.08 (2H, m), 4.98 – 5.04 (1H, m), 5.06 – 5.13 (1H, m), 5.83 – 5.95 (1H, m), 7.42 – 7.45 (2H, m), 7.88 – 7.92 (2H, m); **^{13}C NMR (126 MHz, $CDCl_3$)** δ_C = 28.2, 37.9, 115.6, 129.1, 129.6, 135.4, 137.2, 139.6, 198.3; **HRMS** (ES+) $C_{11}H_{11}OCl$ $[M+H]^+$ requires 195.0577, found 195.0578 (+0.5 ppm).

1-(4-Bromophenyl)pent-4-en-1-one (169)

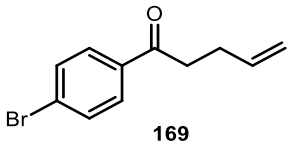

169

Prepared according to General Procedure 13 using *N*,*O*-dimethylhydroxylamine hydrochloride (2.93 g, 30.0 mmol) in CH_2Cl_2 (40 mL), 4-bromobenzoyl chloride (6.58 g, 30.0 mmol), and triethylamine (8.36 mL, 60.0 mmol) to form the crude Weinreb amide. The Grignard reagent was prepared using magnesium (1.20 g, 49.5 mmol) in THF (45 mL), and 4-bromobut-1-ene (4.57 mL, 45.0 mmol). The aryl ketone was prepared through the addition of the Weinreb amide in THF (15 mL) to the solution of Grignard reagent. The resultant crude material was purified by flash column chromatography (5% EtOAc/petrol, silica gel) to afford **169** (5.62 g, 78%) as a white solid.

R_f = 0.52 (10% EtOAc/petrol); **M.p.:** 49-51 °C; **^{1}H NMR (500 MHz, $CDCl_3$)** δ_H = 2.46 – 2.51 (2H, m), 3.02 – 3.05 (2H, m), 5.00 – 5.03 (1H, m), 5.06 – 5.11 (1H, m), 5.89 (1H, ddt, *J* 16.8, 10.2, 6.5), 7.59 – 7.62 (2H, m), 7.81 – 7.84 (2H, m); **^{13}C NMR (126 MHz, $CDCl_3$)** δ_C = 28.2, 37.9, 115.6, 128.3, 129.7, 132.1, 135.8, 137.2, 198.5.

These data are in accordance with the literature.[19]

1-(4-Iodophenyl)pent-4-en-1-one (170)

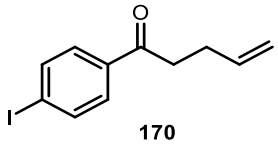

170

Prepared according to General Procedure 13 using *N*,*O*-dimethylhydroxylamine hydrochloride (975 mg, 10.0 mmol) in CH_2Cl_2 (15 mL), 4-iodobenzoyl chloride (2.66 g, 10.0 mmol), and triethylamine (2.79 mL, 20.0 mmol) to form the crude Weinreb amide. The Grignard reagent was prepared using magnesium (401 mg, 16.5 mmol) in THF (15 mL), and 4-bromobut-1-ene (1.52 mL, 15.0 mmol). The aryl ketone was prepared through the addition of the Weinreb amide in THF (5 mL) to the solution of Grignard reagent. The resultant crude material was purified by flash column chromatography (2.5-5% EtOAc/petrol, silica gel) to afford **170** (388 mg, 14%) as a white solid.

R_f = 0.43 (5% EtOAc/petrol); **M.p.:** 64-66 °C; **^{1}H NMR (500 MHz, $CDCl_3$)** δ_H = 2.46 – 2.51 (2H, m), 3.01 – 3.04 (2H, m), 5.00 – 5.03 (1H, m), 5.06 – 5.11 (1H, m), 5.85 – 5.93 (1H, m), 7.66 – 7.68 (2H, m), 7.82 – 7.84 (2H, m); **^{13}C NMR (126 MHz, $CDCl_3$)** δ_C = 28.2, 37.8, 101.1, 115.6, 129.6, 136.3, 137.2, 138.1, 198.8.

These data are in accordance with the literature.[20]

1-Morpholinopent-4-en-1-one (171)

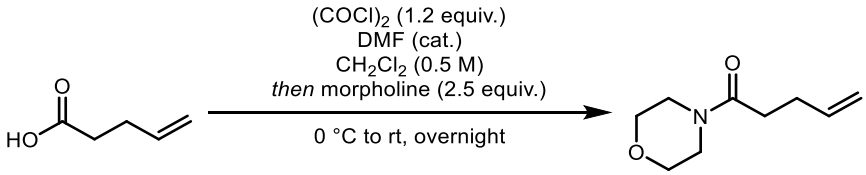

171

To a flame-dried RBF was added 4-pentenoic acid (10.2 mL, 100 mmol) in anhydrous CH_2Cl_2 (200 mL, 0.5 M). The solution was cooled to 0 °C, and oxalyl chloride (8.90 mL, 105 mmol) was added dropwise, followed by the addition of DMF (3 drops). The reaction was warmed to rt and stirred until gas evolution ceased, at which point morpholine (21.9 mL, 250 mmol) was added. The reaction was stirred at rt overnight before being quenched with 2 M HCl (aq.). The layers were separated, and the aqueous layer was extracted with CH_2Cl_2 (× 3). The combined organics were then washed with 2 M HCl (aq.) then brine, dried over $MgSO_4$, filtered, and concentrated under reduced pressure to afford **171** (14.3 g, 85%) as a yellow oil that was used without any further purification.

R_f = 0.18 (25% EtOAc/petrol); **^{1}H NMR (500 MHz, $CDCl_3$)** δ_H = 2.37 – 2.42 (4H, m), 3.44 – 3.47 (2H, m), 3.60 – 3.68 (6H, m), 4.98 – 5.08 (2H, m), 5.80 – 5.90 (1H, m); **^{13}C NMR (126 MHz, $CDCl_3$)** δ_C = 29.3, 32.4, 42.0, 46.1, 66.8, 67.1, 115.5, 137.4, 171.1.

These data are in accordance with the literature.[21]

1-(*p*-Tolyl)pent-4-en-1-one (172)

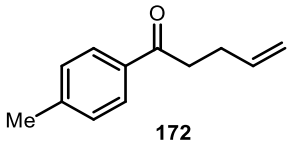

172

Prepared according to General Procedure 14 using **171** (846 mg, 5.00 mmol), 4-bromotoluene (1.11 g, 6.50 mmol), and *n*-BuLi (2.71 mL, 2.4 M in hexanes, 6.50 mmol) in THF (27 mL). The resultant crude material was purified by flash column chromatography (2.5% EtOAc/petrol, silica gel) to afford **172** (394 mg, 45%) as a colourless oil.

R_f = 0.57 (5% EtOAc/petrol); **^{1}H NMR (500 MHz, $CDCl_3$)** δ_H = 2.41 (3H, s), 2.46 – 2.52 (2H, m), 3.03 – 3.07 (2H, m), 4.98 – 5.03 (1H, m), 5.06 – 5.11 (1H, m), 5.85 – 5.95 (1H, m). 7.24 – 7.27 (2H, m), 7.85 – 7.88 (2H, m); **^{13}C NMR (126 MHz, $CDCl_3$)** δ_C = 21.8, 28.4, 37.8, 115.3, 128.3, 129.4, 134.6, 137.5, 143.9, 199.2.

These data are in accordance with the literature.[22]

1-(*m*-Tolyl)pent-4-en-1-one (173)

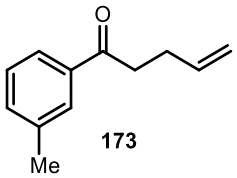

173

Prepared according to General Procedure 14 using **171** (1.52 g, 9.00 mmol), 3-bromotoluene (1.42 mL, 11.7 mmol), and *n*-BuLi (4.68 mL, 2.5 M in hexanes, 11.7 mmol) in THF (50 mL). The resultant crude material was purified by flash column chromatography (0-1% EtOAc/petrol, silica gel) to afford **173** (1.26 g, 80%) as a colourless oil.

R_f = 0.38 (5% EtOAc/petrol); **^{1}H NMR (500 MHz, $CDCl_3$)** δ_H = 2.42 (3H, s), 2.47 – 2.52 (2H, m), 3.05 – 3.08 (2H, m), 5.00 – 5.03 (1H, m), 5.07 – 5.11 (1H, m), 5.87 – 5.95 (1H, m), 7.33 – 7.38 (2H, m), 7.75 – 7.78 (2H, m); **^{13}C NMR (126 MHz, $CDCl_3$)** δ_C = 21.5, 28.4, 37.9, 115.4, 125.4, 128.6, 128.7, 133.9, 137.1, 137.5, 138.5, 199.8.

These data are in accordance with the literature.[23]

1-(*o*-Tolyl)pent-4-en-1-one (174)

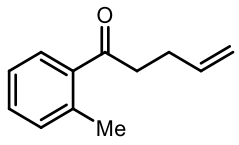

174

Prepared according to General Procedure 14 using **171** (1.52 g, 9.00 mmol), 2-bromotoluene (1.41 mL, 11.7 mmol), and *n*-BuLi (4.68 mL, 2.5 M in hexanes, 11.7 mmol) in THF (50 mL). The resultant crude material was purified by flash column chromatography (1% EtOAc/petrol, silica gel) to afford **174** (622 mg, 40%) as a pale-yellow oil.

R_f = 0.38 (5% EtOAc/petrol); **^{1}H NMR (500 MHz, $CDCl_3$)** δ_H = 2.45 – 2.49 (5H, m), 2.98 – 3.01 (2H, m), 4.99 – 5.02 (1H, m), 5.05 – 5.09 (1H, m), 5.85 – 5.93 (1H, m), 7.24 – 7.27 (2H, m), 7.35 – 7.38 (1H, m), 7.62 – 7.63 (1H, m); **^{13}C NMR (126 MHz, $CDCl_3$)** δ_C = 21.4, 28.5, 40.8, 115.4, 125.8, 128.4, 131.3, 132.1, 137.4, 138.1, 138.2, 203.8.

These data are in accordance with the literature.[24]

1-([1,1'-Biphenyl]-4-yl)pent-3-en-1-one (175)

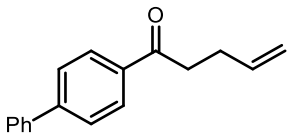

175

Prepared according to General Procedure 14 using **171** (1.692 g, 10.0 mmol), 4-bromo-1,1'-biphenyl (2.80 g, 12.0 mmol), and *n*-BuLi (5.00 mL, 2.4 M in hexanes, 12.0 mmol) in THF (53 mL). The resultant crude material was purified by flash column chromatography (2.5% EtOAc/petrol, silica gel) to afford **175** (1.58 g, 67%) as a white solid.

R_f = 0.51 (5% EtOAc/petrol); **M.p.:** 81-83 °C; **FTIR** (ν_{max} cm^{-1}, thin film) 3038, 1676, 1601, 1199, 982, 903, 754, 687; **^{1}H NMR (500 MHz, $CDCl_3$)** δ_H = 2.50 – 2.56 (2H, m), 3.08 – 3.15 (2H, m), 5.00 – 5.05 (1H, m), 5.08 – 5.15 (1H, m), 5.89 – 5.99 (1H, m), 7.38 – 7.43 (1H, m), 7.45 – 7.50 (2H, m), 7.61 – 7.65 (2H, m), 7.67 – 7.71 (2H, m), 8.02 – 8.06 (2H, m); **^{13}C NMR (126 MHz, $CDCl_3$)** δ_C = 28.4, 38.0, 115.5, 127.39, 127.41, 128.4, 128.8, 129.1, 135.8, 137.5, 140.0, 145.8, 199.2; **HRMS** (CI+) $C_{17}H_{16}O$ $[M+H]^+$ requires 237.1274, found 237.1276 (+1.0 ppm).

1-(4-(Trifluoromethyl)phenyl)pent-4-en-1-one (176)

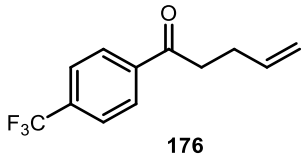

176

Prepared according to General Procedure 14 using **171** (1.69 g, 10.0 mmol), 1-bromo-4-(trifluoromethyl)benzene (1.82 mL, 13.0 mmol), and *n*-BuLi (5.40 mL, 2.4 M in hexanes, 13.0 mmol) in THF (54 mL). The resultant crude material was purified by flash column chromatography (5% EtOAc/petrol, silica gel) to afford **176** (1.65 g, 72%) as a colourless oil.

R_f = 0.63 (5% EtOAc/petrol); **^{1}H NMR (500 MHz, $CDCl_3$)** δ_H = 2.49 – 2.55 (2H, m), 3.07 – 3.14 (2H, m), 5.00 – 5.05 (1H, m), 5.07 – 5.14 (1H, m), 5.84 – 5.96 (1H, m), 7.70 – 7.77 (2H, m), 8.03 – 8.10 (2H, m); **^{13}C NMR (126 MHz, $CDCl_3$)** δ_C = 28.1, 38.2, 115.8, 123.7 (q, *J* 272.7), 125.8 (q, *J* 3.8), 128.5, 134.5 (q, *J* 32.7), 137.0, 139.7, 198.5; **^{19}F{^{1}H} NMR (376 MHz, $CDCl_3$)** δ_F = -63.09.

These data are in accordance with the literature.[25]

1-(4-((*tert*-Butyldimethylsilyl)oxy)phenyl)pent-4-en-1-one (177)

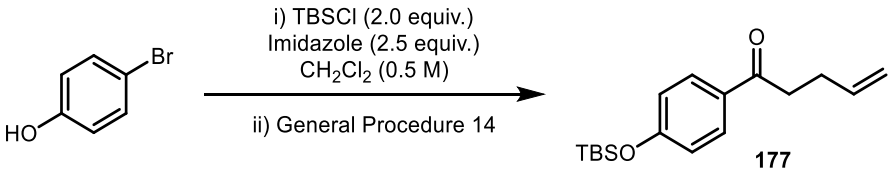

177

To a solution of 4-bromophenol (2.60 g, 15.0 mmol) in CH_2Cl_2 (30 mL, 0.5 M) was added imidazole (2.55 g, 37.5 mmol). The mixture was stirred at rt for 15 min before TBSCl (4.52 g, 30.0 mmol) was added, and the reaction was heated at reflux for 3 h. The reaction mixture was cooled, and a saturated solution of NH_4Cl (aq.) was added. The layers were separated, and the aqueous layer was further extracted with CH_2Cl_2 (× 3). The combined organics were washed with 1 M HCl (aq.), water, then brine, dried over $MgSO_4$, filtered, and concentrated under reduced pressure to afford the crude TBS-protected phenol (4.27 g, 99%) as a colourless oil that was used in the next step without further purification.

The crude TBS-protected phenol (3.92 g, 13.0 mmol) was then subjected to the conditions of General Procedure 14 using **171** (1.69 g, 10.0 mmol) and *n*-BuLi (5.46 mL, 2.38 M in hexanes, 13.0 mmol) in THF (50 mL). The resultant crude material was purified by flash column chromatography (1% EtOAc/petrol, silica gel) to afford **177** (2.03 g, 70%) as a colourless oil.

R_f = 0.59 (1% EtOAc/petrol); **^{1}H NMR (500 MHz, $CDCl_3$)** δ_H = 0.23 (6H, s), 0.99 (9H, s), 2.46 – 2.51 (2H, m), 3.00 – 3.03 (2H, m), 4.99 – 5.02 (1H, m), 5.06 – 5.11 (1H, m), 5.86 – 5.94 (1H, m), 6.86 – 6.88 (2H, m), 7.87 – 7.90 (2H, m); **^{13}C NMR (126 MHz, $CDCl_3$)** δ_C = – 4.2, 18.4, 25.7, 28.5, 37.6, 115.3, 120.1, 130.3, 130.7, 137.7, 160.3, 198.3.

These data are in accordance with the literature.[26]

1-(Naphthalen-1-yl)pent-4-en-1-one (178)

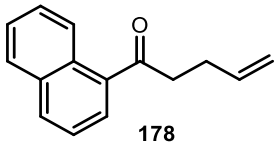

178

Prepared according to General Procedure 14 using **171** (1.52 g, 9.00 mmol), 1-bromonaphthalene (1.63 mL, 11.7 mmol), and *n*-BuLi (4.68 mL, 2.5 M in hexanes, 11.7 mmol) in THF (50 mL). The resultant crude material was purified by flash column chromatography (0-1% EtOAc/petrol, silica gel) to afford **178** (756 mg, 40%) as a pale-yellow oil.

R_f = 0.26 (5% EtOAc/petrol); **FTIR** (ν_{max} cm^{-1}, thin film) 3049, 2976, 2914, 2360, 1678, 1639, 1506, 1435, 1276, 1172, 1089, 997; **^{1}H NMR (500 MHz, $CDCl_3$)** δ_H = 2.54 – 2.59 (2H, m), 3.15 – 3.18 (2H, m), 5.01 – 5.04 (1H, m), 5.08 – 5.13 (1H, m), 5.93 (1H, ddt, *J* 16.8, 10.2, 6.5), 7.49 – 7.55 (2H, m), 7.57 – 7.60 (1H, m), 7.85 – 7.89 (2H, m), 7.98 – 7.99 (1H, m), 8.55 – 8.57 (1H, m); **^{13}C NMR (126 MHz, $CDCl_3$)** δ_C = 28.7, 41.4, 115.6, 124.5, 125.9, 126.9, 127.5, 128.0, 128.5, 130.2, 132.7, 134.1, 136.2, 137.3, 204.1; **HRMS** (CI+) $C_{15}H_{14}O$ $[M]^+$ requires 210.1039, found 210.1039 (-0.2 ppm).

1-(Naphthalen-2-yl)pent-4-en-1-one (179)

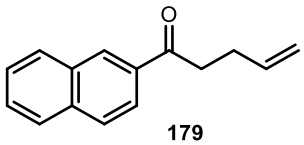

179

Prepared according to General Procedure 14 using **171** (846 mg, 5.00 mmol), 2-bromonaphthalene (1.14 g, 5.50 mmol), and *n*-BuLi (2.20 mL, 2.5 M in hexanes, 5.50 mmol) in THF (27 mL). The resultant crude material was purified by flash column chromatography (0-1% EtOAc/petrol, silica gel) to afford **179** (733 mg, 80%) as an orange oil.

R_f = 0.37 (5% EtOAc/petrol); **FTIR** (ν_{max} cm^{-1}, thin film) 3053, 2976, 2916, 2891, 2360, 1680, 1639, 1624, 1595, 1467, 1435, 1363, 1274, 1172; **^{1}H NMR (500 MHz, $CDCl_3$)**

δ_H = 2.54 – 2.59 (2H, m), 3.20 – 3.24 (2H, m), 5.03 – 5.06 (1H, m), 5.11 – 5.15 (1H, m), 5.91 – 6.00 (1H, m), 7.54 – 7.62 (2H, m), 7.87 – 7.91 (2H, m), 7.97 (1H, d, *J* 8.1), 8.04 (1H, d, *J* 8.6), 8.48 (1H, s); **^{13}C NMR (126 MHz, $CDCl_3$)** δ_C = 28.5, 38.0, 115.5, 124.0, 126.9, 127.9, 128.5, 128.6, 129.7, 129.8, 132.7, 134.4, 135.7, 137.5, 199.5; **HRMS** (ES+) $C_{15}H_{14}O$ $[M+H]^+$ requires 211.1123, found 211.1122 (-0.5 ppm).

1-(4-(((*tert*-Butyldimethylsilyl)oxy)methyl)phenyl)pent-4-en-1-one (180)

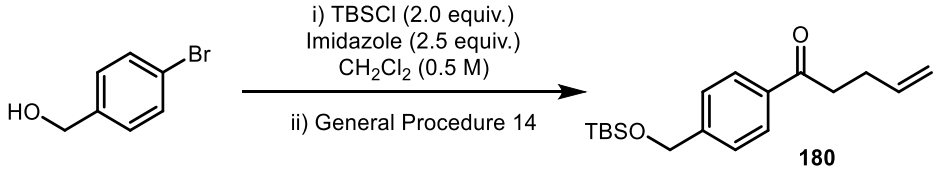

180

To a solution of 4-bromobenzyl alcohol (2.91 g, 15.0 mmol) in CH_2Cl_2 (30 mL, 0.5 M) was added TBSCl (4.52 g, 30.0 mmol) and imidazole (2.55 g, 37.5 mmol). The reaction mixture was stirred at rt overnight before water was added. The layers were separated, and the aqueous layer was further extracted with CH_2Cl_2 (× 3). The combined organics were washed with 1 M HCl (aq.), water, then brine, dried over $MgSO_4$, filtered, and concentrated under reduced pressure to afford the TBS-protected alcohol (4.51 g, 99%) as a colourless oil that was used in the next step without further purification.

The TBS-protected alcohol (3.92 g, 13.0 mmol) was then subjected to the conditions General Procedure 14 using **171** (1.69 g, 10.0 mmol) and *n*-BuLi (5.46 mL, 2.38 M in hexanes, 13.0 mmol) in THF (50 mL). The resultant crude material was purified by flash column chromatography (1% EtOAc/petrol, silica gel) to afford **180** (1.87 g, 61%) as a colourless oil.

R_f = 0.50 (1% EtOAc/petrol); **FTIR** (ν_{max} cm^{-1}, thin film) 2953, 2928, 2857, 1684, 1609, 1252, 1089, 835, 775; **^{1}H NMR (500 MHz, $CDCl_3$)** δ_H = 0.11 (6H, s), 0.95 (9H, s), 2.47 – 2.52 (2H, m), 3.05 – 3.08 (2H, m), 4.79 (2H, s), 5.00 – 5.03 (1H, m), 5.06 – 5.11 (1H, m), 5.87 – 5.95 (1H, m), 7.40 – 7.42 (2H, m), 7.93 – 7.95 (2H, m); **^{13}C NMR (126 MHz, $CDCl_3$)** δ_C = – 5.1, 18.6, 26.1, 28.4, 37.9, 64.6, 115.4, 126.0, 128.3, 135.8, 137.5, 147.1, 199.3; **HRMS** (ES+) $C_{18}H_{28}O_2Si$ $[M+H]^+$ requires 305.1937, found 305.1942 (+1.6 ppm).

4-(Pent-4-enoyl)benzoic acid (181)

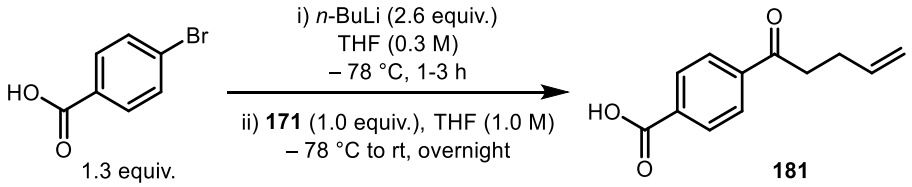

To a flame-dried RBF fitted with a septum seal was added a solution 4-bromobenzoic acid (7.84 g, 39.0 mmol) in anhydrous THF (130 mL, 0.3 M). The mixture was cooled to -78 °C, and a solution of *n*-BuLi (32.5 mL, 2.4 M in hexanes, 78.0 mmol) was added dropwise. The reaction mixture was left to stir for 1 h before a solution of **171** (5.08 g, 30.0 mmol) in anhydrous THF (30 mL, 1.0 M) was added dropwise. The solution was left to stir for 15 min, before a saturated solution of NH_4Cl (aq.) (50 mL) was added. The mixture was warmed to rt and 1 M HCl (aq.) was added. The layers were separated, and the aqueous layer was further extracted with EtOAc (× 3). The combined organics were washed with brine, dried over $MgSO_4$, filtered, and concentrated under reduced pressure. The resultant crude material was suspended in hexane and stirred vigorously, resulting in the formation of a solid. The precipitate was filtered and resuspended in CH_2Cl_2. Slow addition of hexane resulted in the formation of a precipitate that was filtered, and dried under a high vacuum to afford **181** (2.45 g, 40%) as an off-white solid.

R_f = 0.06 (50% EtOAc/petrol); **M.p.:** 154-156 °C; **FTIR** (ν_{max} cm^{-1}, thin film) 2941, 2847, 2544, 1678, 1645, 1504, 1406, 1273, 1204, 930, 901, 752; **^{1}H NMR (500 MHz, DMSO-d_6)** δ_H = 2.35 – 2.40 (2H, m), 3.16 – 3.19 (2H, m), 4.97 – 5.00 (1H, m), 5.05 – 5.10 (1H, m), 5.84 – 5.92 (1H, m), 8.04 – 8.08 (4H, m), 13.24 (1H, br s); **^{13}C NMR (126 MHz, DMSO-d_6)** δ_C = 27.5, 37.3, 115.3, 128.1, 129.6, 134.4, 137.5, 139.7, 166.6, 199.0; **HRMS** (CI+) $C_{12}H_{12}O_3$ $[M+H]^+$ requires 205.0859, found 205.0859 (-0.1 ppm).

1-(4-(1,3-Dioxolan-2-yl)phenyl)pent-4-en-1-one (182)

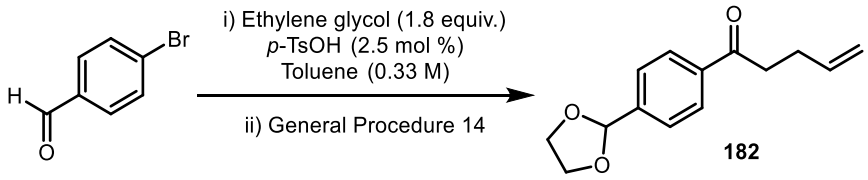

To an RBF fitted with a Dean-Stark condenser was added 4-bromobenzaldehyde (3.70 g, 20.0 mmol), *p*-toluenesulfonic acid (95.0 mg, 0.50 mmol), and ethylene glycol (2.00 mL, 36.0 mmol) in toluene (60 mL, 0.33 M). The mixture was heated at reflux overnight, before being cooled, washed with a saturated solution of $NaHCO_3$ (aq.) (2 × 20 mL), and the aqueous layer was further extracted with EtOAc (3 × 30 mL). The combined organics

were washed with brine, dried with $MgSO_4$, filtered, and concentrated under reduced pressure to afford the crude acetal that was used without further purification.

The crude acetal (2.38 g, 10.4 mmol) was then subjected to the conditions of General Procedure 14 using **171** (1.35 g, 8.00 mmol), and *n*-BuLi (4.33 mL, 2.40 M in hexanes, 10.4 mmol) in THF (43 mL). The resultant crude material was purified by flash column chromatography (5-20% EtOAc/petrol, silica gel) to afford **182** (1.35 g, 73%) as a colourless oil.

R_f = 0.21 (10% EtOAc/petrol); **FTIR** (ν_{max} cm^{-1}, thin film) 2889, 2349, 1682, 1362, 1207, 1080, 970, 941; **^{1}H NMR (500 MHz, $CDCl_3$)** δ_H = 2.47 – 2.52 (2H, m), 3.06 – 3.09 (2H, m), 4.03 – 4.16 (4H, m), 5.00 – 5.03 (1H, m), 5.06 – 5.11 (1H, m), 5.86 – 5.94 (2H, m), 7.56 – 7.59 (2H, m), 7.97 – 7.99 (2H, m); **^{13}C NMR (126 MHz, $CDCl_3$)** δ_C = 28.3, 38.0, 65.5, 103.1, 115.5, 126.8, 128.3, 137.3, 137.6, 142.9, 199.3; **HRMS** (CI+) $C_{14}H_{16}O_3$ $[M+H]^+$ requires 233.1172, found 233.1173 (+0.3 ppm).

1-(4-(2-Methyl-1,3-dioxolan-2-yl)phenyl)pent-4-en-1-one (183)

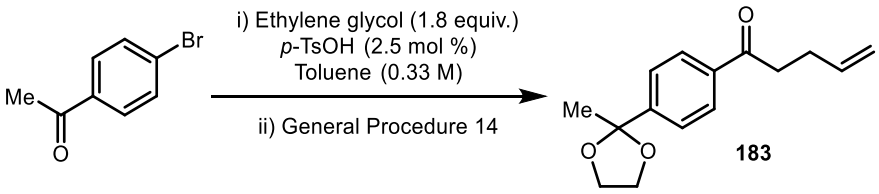

To an RBF fitted with a Dean-Stark condenser was added 4'-bromoacetophenone (3.98 g, 20.0 mmol), *p*-toluenesulfonic acid (95.0 mg, 0.50 mmol), and ethylene glycol (2.00 mL, 36.0 mmol) in toluene (60 mL, 0.33 M). The mixture was heated at reflux overnight, before being cooled, washed with a saturated solution of $NaHCO_3$ (aq.) (2 × 20 mL), and the aqueous layer was further extracted with EtOAc (3 × 30 mL). The combined organics were washed with brine, dried with $MgSO_4$, filtered, and concentrated under reduced pressure to afford the crude ketal that was used without further purification.

The crude ketal (2.53 g, 10.4 mmol) was then subjected to the conditions of General Procedure 14 using **171** (1.35 g, 8.00 mmol), and *n*-BuLi (4.33 mL, 2.40 M in hexanes, 10.4 mmol) in THF (43 mL). The resultant crude material was purified by flash column chromatography (5-10% EtOAc/petrol, silica gel) to afford **183** (1.21 g, 61%) as a colourless oil.

R_f = 0.23 (10% EtOAc/petrol); **FTIR** (ν_{max} cm^{-1}, thin film) 2988, 2889, 2349, 1682, 1607, 1404, 1373, 1244, 1198, 1034, 874; **^{1}H NMR (500 MHz, $CDCl_3$)** δ_H = 1.65 (3H, s), 2.47 –

2.52 (2H, m), 3.06 – 3.09 (2H, m), 3.73 – 3.80 (2H, m), 4.02 – 4.09 (2H, m), 5.00 – 5.03 (1H, m), 5.07 – 5.11 (1H, m), 5.86 – 5.94 (1H, m), 7.56 – 7.59 (2H, m), 7.93 – 7.96 (2H, m); **^{13}C NMR (126 MHz, $CDCl_3$)** δ_C = 27.6, 28.3, 37.9, 64.7, 108.6, 115.5, 125.7, 128.3, 136.6, 137.4, 148.5, 199.3; **HRMS** (CI+) $C_{15}H_{18}O_3$ $[M+H]^+$ requires 247.1329, found 247.1328 (-0.5 ppm).

5-Methyl-1-phenylhex-4-en-1-one (188)

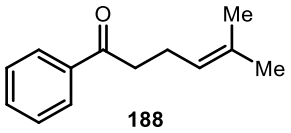

188

Prepared according to General Procedure 15 using ethylbenzoyl acetate (866 µL, 5.00 mmol) in THF (25 mL), NaH (60% dispersion in mineral oil, 200 mg, 5.00 mmol), and 3,3-dimethylallyl bromide (635 µL, 5.50 mmol) to afford the first crude product. The crude product was dissolved in 2:1 MeOH/water (50 mL) and treated with NaOH (800 mg, 20.0 mmol). The resultant crude material was purified by flash column chromatography (1-2% Et_2O/petrol, silica gel) to afford **188** (703 mg, 75%) as a low-melting colourless solid.

R_f = 0.60 (5% EtOAc/petrol); **FTIR** (ν_{max} cm^{-1}, thin film) 3053, 2926, 2904, 1682, 1593, 1579, 1447, 1346, 1273, 1198, 972; **^{1}H NMR (500 MHz, $CDCl_3$)** δ_H = 1.62 – 1.64 (3H, m), 1.68 – 1.70 (3H, m), 2.38 – 2.47 (2H, m), 2.96 – 3.03 (2H, m), 5.13 – 5.22 (1H, m), 7.42 – 7.50 (2H, m), 7.52 – 7.59 (1H, m), 7.93 – 7.99 (2H, m); **^{13}C NMR (126 MHz, $CDCl_3$)** δ_C = 17.8, 23.1, 25.9, 38.9, 123.1, 128.2, 128.7, 132.9, 133.0, 137.2, 200.2; **HRMS** (ES+) $C_{13}H_{17}O$ $[M+H]^+$ requires 189.1279, found 189.1287 (+4.2 ppm).

1-Phenylhex-4-en-1-one (189)

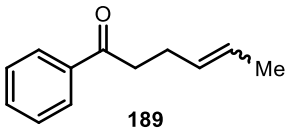

189

Prepared according to General Procedure 15 using ethylbenzoyl acetate (866 µL, 5.00 mmol) in THF (25 mL), NaH (60% dispersion in mineral oil, 200 mg, 5.00 mmol), and 1-bromobut-2-ene (*E*:*Z* ratio = 93:7, 743 mg, 5.50 mmol). The crude product was dissolved in 2:1 MeOH/water (50 mL), and treated with NaOH (800 mg, 20.0 mmol). The resultant crude material was purified by flash column chromatography (2.5% EtOAc/petrol, silica gel) to afford **189** (473 mg, 55%) as a low-melting white solid with an *E*:*Z* ratio of 92:8.

R_f = 0.60 (5% EtOAc/petrol); **FTIR** (ν_{max} cm^{-1}, thin film) 2920, 1680, 1449, 1368, 1202, 970, 737, 685; **HRMS** (ES+) $C_{12}H_{14}O$ $[M+H]^+$ requires 175.1123, found 175.1116 (-4.0 ppm).

Data for (*E*)-**189***:* **^{1}H NMR (500 MHz, $CDCl_3$)** δ_H = 1.63 – 1.66 (3H, m), 2.39 – 2.45 (2H, m), 3.00 – 3.06 (2H, m), 5.46 – 5.56 (2H, m), 7.42 – 7.50 (2H, m), 7.52 – 7.59 (1H, m), 7.94 – 7.98 (2H, m); **^{13}C NMR (126 MHz, $CDCl_3$)** δ_C = 18.1, 27.3, 38.7, 126.1, 128.2, 128.7, 129.9, 133.1, 137.1, 199.9.

Data for (*Z*)-**189** *(selected):* **^{1}H NMR (500 MHz, $CDCl_3$)** δ_H = 2.47 – 2.51 (2H, m); **^{13}C NMR (126 MHz, $CDCl_3$)** δ_C = 12.9, 21.9, 38.6, 125.3, 129.0, 133.1, 137.1.

(*E*)-1,5-Diphenylpent-4-en-1-one (190)

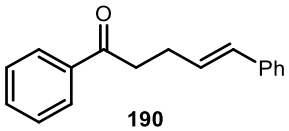

190

Prepared according to General Procedure 15 using ethylbenzoyl acetate (866 µL, 5.00 mmol) in THF (25 mL), NaH (60% dispersion in mineral oil, 200 mg, 5.00 mmol), and (*E*)-cinnamyl bromide (1.08 g, 5.50 mmol) to afford the first crude product. The crude product was dissolved in 2:1 MeOH/water (50 mL), and treated with NaOH (800 mg, 20.0 mmol). The resultant crude material was purified by flash column chromatography (1% EtOAc/petrol, silica gel) to afford **190** (843 mg, 71%) as a white solid.

R_f = 0.43 (5% EtOAc/petrol); **M.p.:** 58-60 °C; **^{1}H NMR (500 MHz, $CDCl_3$)** δ_H = 2.64 – 2.69 (2H, m), 3.15 – 3.18 (2H, m), 6.30 (1H, dt, *J* 15.8, 6.9), 6.47 (1H, dt, *J* 15.8, 1.5), 7.18 – 7.22 (1H, m), 7.27 – 7.31 (2H, m), 7.33 – 7.35 (2H, m), 7.46 – 7.49 (2H, m), 7.55 – 7.59 (1H, m), 7.97 – 8.00 (2H, m); **^{13}C NMR (126 MHz, $CDCl_3$)** δ_C = 27.7, 38.4, 126.2, 127.2, 128.2, 128.6, 128.8, 129.3, 130.9, 133.2, 137.1, 137.6, 199.5.

These data are in accordance with the literature.[27]

2-(Cyclohex-2-en-1-yl)-1-phenylethan-1-one (191)

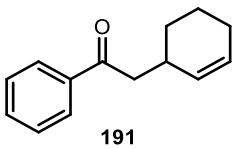

191

Prepared according to General Procedure 15 using ethylbenzoyl acetate (866 µL, 5.00 mmol) in THF (25 mL), NaH (60% dispersion in mineral oil, 200 mg, 5.00 mmol), and 3-bromocyclohexene (633 µL, 5.50 mmol). The crude product was dissolved in 2:1

MeOH/water (50 mL), and treated with NaOH (800 mg, 20.0 mmol). The resultant crude material was purified by flash column chromatography (2.5% EtOAc/petrol, silica gel) to afford **191** (626 mg, 63%) as a white solid.

R_f = 0.66 (5% EtOAc/petrol); **M.p.:** 39-41 °C; **^{1}H NMR (500 MHz, $CDCl_3$)** δ_H = 1.26 – 1.36 (1H, m), 1.52 – 1.65 (1H, m), 1.66 – 1.77 (1H, m), 1.82 – 1.92 (1H, m), 1.96 – 2.04 (2H, m), 2.77 – 2.86 (1H, m), 2.89 – 3.01 (2H, m), 5.56 – 5.63 (1H, m), 5.68 – 5.77 (1H, m), 7.42 – 7.50 (2H, m), 7.52 – 7.59 (1H, m), 7.93 – 8.00 (2H, m); **^{13}C NMR (126 MHz, $CDCl_3$)** δ_C = 21.2, 25.3, 29.2, 31.8, 45.0, 128.1, 128.3, 128.7, 130.9, 133.1, 137.5, 199.8.

These data are in accordance with the literature.[28]

4-Methyl-1-phenylpent-4-en-1-one (192)

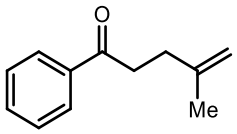

192

Prepared according to General Procedure 15 using ethylbenzoyl acetate (1.73 mL, 10.0 mmol) in THF (50 mL), NaH (60% dispersion in mineral oil, 400 mg, 10.0 mmol), and 3-bromo-2-methylprop-1-ene (1.11 mL, 11.0 mmol). The crude product was dissolved in 2:1 MeOH/water (100 mL), and treated with NaOH (1.60 g, 40.0 mmol). The resultant crude material was purified by flash column chromatography (2% EtOAc/petrol, silica gel) to afford **192** (1.09 g, 63%) as a yellow oil.

R_f = 0.56 (10% EtOAc/petrol); **^{1}H NMR (500 MHz, $CDCl_3$)** δ_H = 1.79 (3H, s), 2.44 – 2.47 (2H, m), 3.11 – 3.14 (2H, m), 4.72 (1H, app s), 4.77 (1H, app s), 7.45 – 7.48 (2H, m), 7.55 – 7.58 (1H, m), 7.97 – 7.99 (2H, m); **^{13}C NMR (126 MHz, $CDCl_3$)** δ_C = 22.9, 32.0, 37.0, 110.3, 128.2, 128.7, 133.1, 137.1, 144.8, 199.9.

These data are in accordance with the literature.[29]

2-Allyl-3,4-dihydronaphthalen-1(2*H*)-one (193)

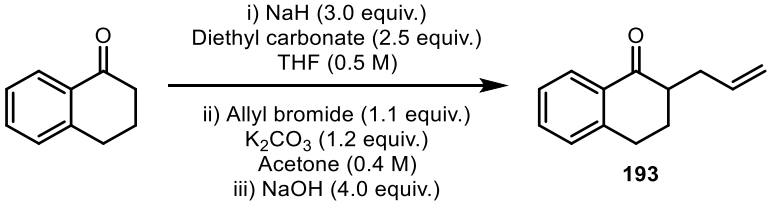

193

To a flame-dried RBF was added NaH (60% suspension in mineral oil, 1.20 g, 30.0 mmol) in THF (20 mL, 1.25 M with respect to diethyl carbonate). The suspension was cooled to

0 °C, diethyl carbonate (5.46 mL, 25.0 mmol) was added, and the mixture was stirred at 0 °C for 30 min. *α*-Tetralone (1.33 mL, 10.0 mmol) was added dropwise, and the mixture was heated at reflux for 4 h. Upon cooling, a saturated solution of $NaHCO_3$ (aq.) was added. The layers were separated, and the aqueous layer was further extracted with Et_2O (× 3). The combined organics were washed with brine, dried over $MgSO_4$, filtered, and concentrated under reduced pressure to give the crude *β*-ketoester that was used without further purification.

The *β*-ketoester was dissolved in acetone (25 mL), then allyl bromide (952 µL, 11.0 mmol) and K_2CO_3 (1.66 g, 12.0 mmol) were added, and the resulting suspension was heated at reflux overnight. Upon cooling, the mixture was filtered, and the filtrate was concentrated under reduced pressure. The crude oil was then dissolved in a 2:1 mixture of EtOH/water (100 mL), NaOH (1.60 g, 40.0 mmol) was added, and the reaction was heated at reflux overnight. Upon cooling to rt the solution was concentrated under reduced pressure. EtOAc was added, the layers were separated, and the aqueous layer was further extracted with EtOAc (× 3). The combined organics were washed with brine, dried over $MgSO_4$, filtered, and concentrated under reduced pressure. The resultant crude material was purified by flash column chromatography (5% EtOAc/petrol, silica gel) to afford **193** (560 mg, 30%) as a colourless oil.

R_f = 0.42 (5% EtOAc/petrol); **^{1}H NMR (500 MHz, $CDCl_3$)** δ_H = 1.82 – 1.91 (1H, m), 2.21 – 2.30 (2H, m), 2.52 – 2.58 (1H, m), 2.74 – 2.79 (1H, m), 2.98 – 3.01 (2H, m), 5.06 – 5.13 (2H, m), 5.81 – 5.89 (1H, m), 7.23 – 7.26 (1H, m), 7.29 – 7.32 (1H, m), 7.45 – 7.48 (1H, app td, *J* 7.5, 1.5), 8.03 – 8.05 (1H, m); **^{13}C NMR (126 MHz, $CDCl_3$)** δ_C = 28.1, 28.8, 34.2, 47.3, 117.0, 126.7, 127.6, 128.9, 132.6, 133.4, 136.4, 144.2, 199.7.

These data are in accordance with the literature.[30]

1-Phenylhex-5-en-1-one (194)

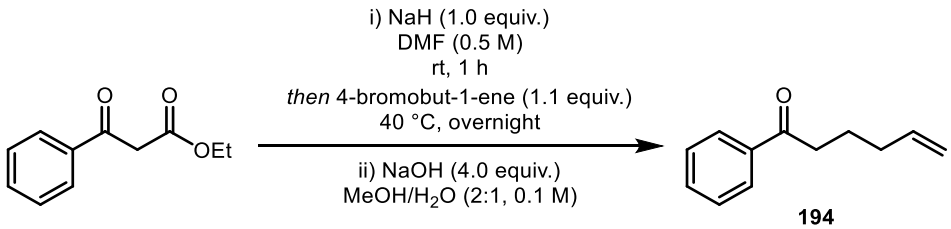

194

Following a literature procedure,[31] to a flame-dried RBF was added ethylbenzoyl acetate (1.73 mL, 10.0 mmol) in DMF (20 mL, 0.5 M). NaH (60% dispersion in mineral oil, 400 mg, 10.0 mmol) was added portion-wise, and the reaction was stirred at rt for 1 h. 4-Bromobut-1-ene (1.12 mL, 11.0 mmol) was added, and the reaction was heated at 40 °C overnight.

After cooling to rt, the suspension was diluted with water, followed by 1 M HCl (aq.) and EtOAc. The layers were separated, and the aqueous layer was further extracted with EtOAc (× 3). The combined organics were washed with water (× 4), then brine, dried over $MgSO_4$, filtered, and concentrated under reduced pressure to give a crude product that was used in the next step without further purification.

To a RBF was added the crude product in 2:1 MeOH/water (100 mL, 0.1 M), and NaOH (1.60 g, 40.0 mmol) was added. The reaction was heated at reflux for 20 h, before being cooled to rt, and concentrated under reduced pressure. EtOAc was added, the layers were separated, and the aqueous layer was further extracted with EtOAc (× 3). The combined organics were washed with brine, dried over $MgSO_4$, filtered, and concentrated under reduced pressure. The resultant crude material was purified by flash column chromatography (0-2% EtOAc/petrol, silica gel) to afford **194** (704 mg, 40%) as a pale-yellow oil.

R_f = 0.40 (5% EtOAc/petrol); **FTIR** (ν_{max} cm^{-1}, thin film) 3067, 2934, 1681, 1639, 1597, 1448, 1408, 1231, 1204, 1178, 1001, 912; **^{1}H NMR (500 MHz, $CDCl_3$)** δ_H = 2.86 (2H, app p, *J* 7.3), 2.14 – 2.19 (2H, m), 2.98 (2H, t, *J* 7.3), 4.99 – 5.07 (2H, m), 5.83 (1H, ddt, *J* 16.9, 10.1, 6.7), 7.44 – 7.47 (2H, m), 7.54 – 7.57 (1H, m), 7.95 – 7.97 (2H, m); **^{13}C NMR (126 MHz, $CDCl_3$)** δ_C = 23.4, 33.4, 37.9, 115.4, 128.2, 128.7, 133.1, 137.2, 138.2, 200.4; **HRMS** (CI+) $C_{12}H_{14}O$ $[M+H]^+$ requires 175.1117, found 175.1115 (-1.7 ppm).

4-(Pent-4-enoyl)benzonitrile (195)

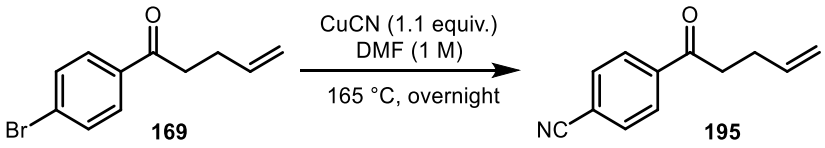

Following a literature procedure,[32] to a flame-dried Schlenk tube was added **169** (2.39 g, 10.0 mmol) in anhydrous DMF (10 mL, 1 M). Copper (I) cyanide (985 mg, 11.0 mmol) was added portion-wise, and the resulting solution was heated to 165 °C overnight. The reaction was cooled to rt, and water was added, followed by CH_2Cl_2. The layers were separated, and the aqueous layer was further extracted with CH_2Cl_2 (× 3). The combined organics were washed with 10% NaCN (aq.) solution, water (× 4), then brine, dried over $MgSO_4$, filtered, and concentrated under reduced pressure. The resultant crude material was purified by flash column chromatography (10% EtOAc/petrol, silica gel) to afford **195** (1.62 g, 87%) as a yellow solid.

R_f = 0.14 (10% EtOAc/petrol); **M.p.:** 48-50 °C; **^{1}H NMR (500 MHz, $CDCl_3$)** δ_H = 2.48 – 2.53 (2H, m), 3.07 – 3.10 (2H, m), 5.02 – 5.05 (1H, m), 5.07 – 5.11 (1H, m), 5.84 – 5.92

(1H, m), 7.76 – 7.79 (2H, m), 8.03 – 8.06 (2H, m); **^{13}C NMR (126 MHz, $CDCl_3$)** δ_C = 28.0, 38.2, 115.9, 116.5, 118.1, 128.6, 132.7, 136.8, 140.0, 198.1.

These data are in accordance with the literature.[19]

1-(4-(4,4,5,5-Tetramethyl-1,3,2-dioxaborolan-2-yl)phenyl)pent-4-en-1-one (196)

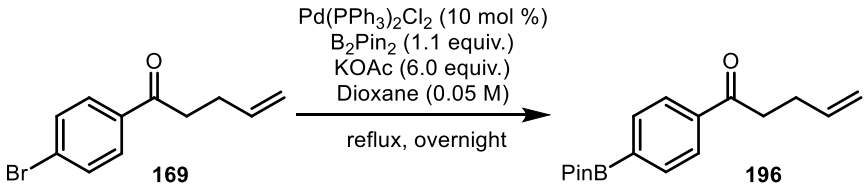

Following a literature procedure,[33] to a flame-dried three-neck RBF fitted with a condenser was added **169** (1.20 g, 5.00 mmol), $Pd(PPh_3)_2Cl_2$ (351 mg, 0.50 mmol), B_2Pin_2 (1.40 g, 5.50 mmol), and KOAc (2.94 g, 30.0 mmol) and the system was subjected to vacuum-nitrogen exchange cycles (× 3). 1,4-Dioxane (100 mL) which has been previously purged with nitrogen gas for 20 min was then added, and the resulting suspension was heated at reflux overnight. Upon cooling, the mixture was filtered through celite, washing with EtOAc, and the filtrate was concentrated under reduced pressure. The resultant crude material was purified by flash column chromatography (2.5-10% EtOAc/petrol, silica gel) to afford **196** (972 mg, 68%) as a colourless oil.

R_f = 0.21 (10% EtOAc/petrol); **FTIR** (ν_{max} cm^{-1}, thin film) 2978, 1686, 1506, 1356, 1142, 1088, 856, 652; **^{1}H NMR (500 MHz, $CDCl_3$)** δ_H = 1.36 (12H, s), 2.47 – 2.52 (2H, m), 3.07 – 3.10 (2H, m), 5.00 – 5.03 (1H, m), 5.06 – 5.11 (1H, m), 5.86 – 5.94 (1H, m), 7.88 – 7.90 (2H, m), 7.92 – 7.94 (2H, m); **^{13}C NMR (126 MHz, $CDCl_3$)** δ_C = 25.0, 28.3, 38.1, 84.4, 115.5, 127.2, 135.1, 137.4, 139.0, 199.9; **HRMS** (ES+) $C_{17}H_{23}{}^{11}BO$ $[M+H]^+$ requires 287.1819, found 287.1826 (+2.4 ppm).

1-(4-Hydroxyphenyl)pent-4-en-1-one (197)

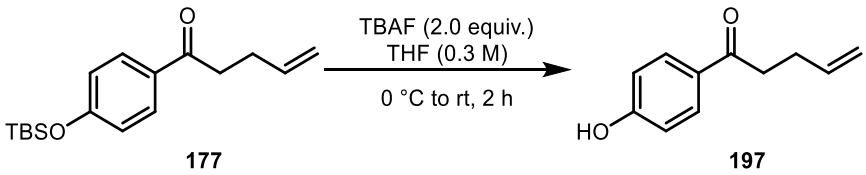

To a flame-dried RBF was added **177** (871 mg, 3.00 mmol) in anhydrous THF (9 mL, 0.3 M). The solution was cooled to 0 °C and TBAF (1 M in THF, 6 mL, 6.00 mmol) was added slowly. The reaction was stirred at rt until completion as monitored by TLC analysis before water was added. The layers were separated, and the aqueous layer was further extracted with EtOAc (× 3). The combined organics were washed with brine, dried over

$MgSO_4$, filtered, and concentrated under reduced pressure. The resultant crude material was purified by flash column chromatography (20% EtOAc/petrol, silica gel) to afford **197** (412 mg, 78%) as a yellow solid.

R_f = 0.17 (20% EtOAc/petrol); **M.p.:** 62-64 °C; **FTIR** (ν_{max} cm^{-1}, thin film) 3157, 3086, 1649, 1582, 1437, 1364, 1283, 1207, 1167, 984, 908, 841; **^{1}H NMR (500 MHz, $CDCl_3$)** δ_H = 2.46 – 2.51 (2H, m), 3.01 – 3.04 (2H, m), 4.99 – 5.02 (1H, m), 5.06 – 5.10 (1H, m), 5.57 (1H, br s), 5.86 – 5.94 (1H, m), 6.87 – 6.90 (2H, m), 7.90 – 7.93 (2H, m); **^{13}C NMR (126 MHz, $CDCl_3$)** δ_C = 28.6, 37.6, 115.4, 115.6, 130.1, 130.9, 137.4, 160.5, 199.0; **HRMS** (EI+) $C_{11}H_{12}O_2$ $[M]^+$ requires 176.0832, found 176.0831 (-0.3 ppm).

1-(4-Hydroxymethyl)phenyl)pent-4-en-1-one (198)

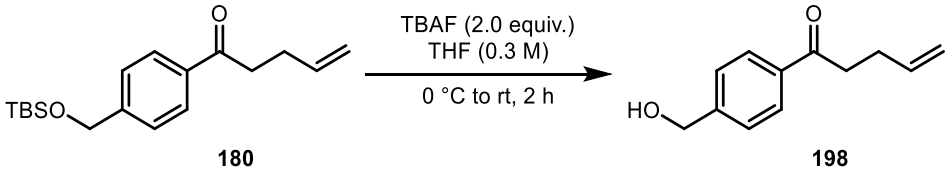

180 **198**

To a flame-dried RBF was added **180** (914 mg, 3.00 mmol) in anhydrous THF (9 mL, 0.3 M). The solution was cooled to 0 °C and TBAF (1 M in THF, 6 mL, 6.00 mmol) was added slowly. The reaction was stirred at rt until completion as monitored by TLC analysis before water was added. The layers were separated, and the aqueous layer was further extracted with EtOAc (× 3). The combined organics were washed with brine, dried over $MgSO_4$, filtered, and concentrated under reduced pressure. The resultant crude material was purified by flash column chromatography (30% EtOAc/petrol, silica gel) to afford **198** (481 mg, 84%) as a yellow solid

R_f = 0.16 (30% EtOAc/petrol); **M.p.:** 47-49 °C; **FTIR** (ν_{max} cm^{-1}, thin film) 3269, 3076, 2909, 1680, 1604, 1406, 1209, 1026, 989, 777; **^{1}H NMR (500 MHz, $CDCl_3$)** δ_H = 1.87 (1H, br s), 2.47 – 2.52 (2H, m), 3.06 – 3.09 (2H, m), 4.78 (2H, s), 5.00 – 5.03 (1H, m), 5.06 – 5.11 (1H, m), 5.86 – 5.94 (1H, m), 7.44 – 7.47 (2H, m), 7.94 – 7.97 (2H, m); **^{13}C NMR (126 MHz, $CDCl_3$)** δ_C = 28.3, 37.9, 64.8, 115.5, 126.8, 128.5, 136.3, 137.4, 146.2, 199.2; **HRMS** (EI+) $C_{12}H_{14}O_2$ $[M]^+$ requires 190.0988, found 190.0987 (-0.6 ppm).

1-Phenylhex-5-en-2-one (199)

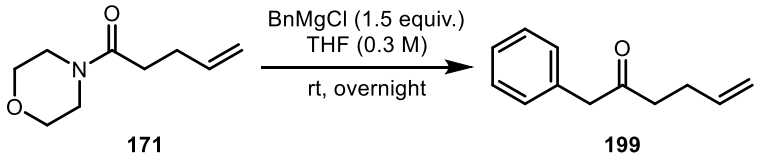

To a flame-dried RBF fitted with a septum seal was added benzyl magnesium chloride (1.4 M in THF, 10.7 mL, 15.0 mmol). After cooling to 0 °C, **171** (1.692 g, 10.0 mmol) in THF (30 mL, 0.3 M) was added dropwise. After complete addition, the resulting mixture was left to warm to rt and stirred overnight. A saturated solution of NH_4Cl (aq.) was added, followed by a few drops of 1 M HCl (aq.), and the mixture was diluted with Et_2O. The layers were separated, and the aqueous layer was further extracted with Et_2O (× 2). The combined organics were dried over $MgSO_4$, filtered, and concentrated under reduced pressure. The resultant crude material was purified by flash column chromatography (5% EtOAc/petrol, silica gel) to afford **199** (503 mg, 28%) as a pale-yellow oil.

R_f = 0.46 (5% EtOAc/petrol); **^{1}H NMR (500 MHz, $CDCl_3$)** δ_H = 2.27 – 2.33 (2H, m), 2.52 – 2.59 (2H, m), 3.69 (2H, s), 4.93 – 5.01 (2H, m), 5.70 – 5.82 (1H, m), 7.19 – 7.22 (2H, m), 7.25 – 7.29 (1H, m), 7.31 – 7.36 (2H, m); **^{13}C NMR (126 MHz, $CDCl_3$)** δ_C = 27.8, 41.2, 50.4, 115.4, 127.2, 128.9, 129.5, 134.3, 137.1, 207.7.

These data are in accordance with the literature.[34]

1-Phenylbut-3-en-1-one (200)

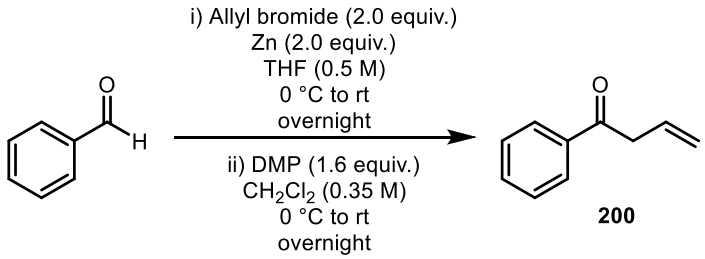

To a RBF fitted with a septum seal was added Zn dust (1.31 g, 20.0 mmol) and the flask was flame-dried. The Zn was suspended in THF (2 mL) and a solution of allyl bromide (1.73 mL, 20.0 mmol) in THF (18 mL, 0.5 M) was added dropwise at 0 °C. The reaction mixture was stirred at rt for 1 h before benzaldehyde (1.02 mL, 10.0 mmol) was added dropwise. The reaction was stirred at rt overnight before being quenched with a saturated solution of NH_4Cl (aq.). The mixture was diluted with EtOAc and 2 M HCl (aq.). The layers were separated, and the aqueous layer was extracted with EtOAc (× 3). The combined organics were washed with brine, dried over $MgSO_4$, filtered, and concentrated under

reduced pressure to give the crude benzyl alcohol that was used in the next step without further purification.

To a flame-dried RBF fitted with a septum seal was suspended DMP (6.79 g, 16.0 mmol) in anhydrous CH_2Cl_2 (16 mL, 1 M). A solution of the crude benzyl alcohol (1.48 g, 10.0 mmol) in CH_2Cl_2 (12.5 mL, 0.8 M) was added at 0 °C, and the reaction mixture was stirred at rt until completion as monitored by TLC analysis. Upon completion, a 1:1 mixture of a saturated solution of $Na_2S_2O_3$ (aq.) and a saturated solution of $NaHCO_3$ (aq.) (20 mL) was added, and the biphasic mixture was stirred for 15 min. The layers were separated, and the aqueous layer was extracted with CH_2Cl_2 (× 3). The combined organics were washed with brine, dried over $MgSO_4$, filtered, and concentrated under reduced pressure. The resultant crude material was purified by flash column chromatography (2-4% EtOAc/petrol, silica gel) to afford **200** (786 mg, 54%) as a colourless oil.

R_f = 0.43 (10% EtOAc/petrol); **^{1}H NMR (500 MHz, $CDCl_3$)** δ_H = 3.74 – 3.77 (2H, m), 5.19 – 5.24 (2H, m), 6.04 – 6.13 (1H, m), 7.44 – 7.47 (2H, m), 7.54 – 7.57 (1H, m), 7.95 – 7.97 (2H, m); **^{13}C NMR (126 MHz, $CDCl_3$)** δ_C = 43.5, 118.8, 128.4, 128.7, 131.1, 133.3, 136.6, 198.1.

These data are in accordance with the literature.[35]

Methyl 4-(pent-4-enoyl)benzoate (201)

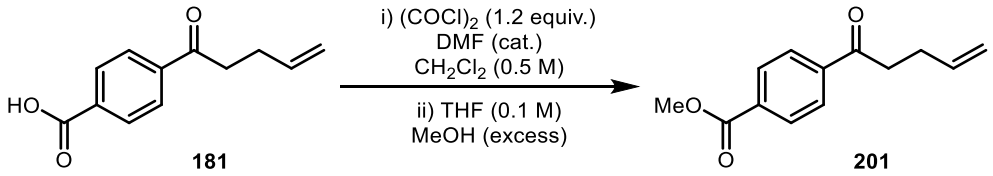

To a flame-dried RBF was added **181** (90 mg, 0.44 mmol) in anhydrous CH_2Cl_2 (2 mL, 0.25 M). The solution was cooled to 0 °C, and oxalyl chloride (45 µL, 0.53 mmol) was added dropwise, followed by the addition of DMF (1 drop). The reaction was warmed to rt and stirred until gas evolution ceased. The mixture was concentrated under reduced pressure, and the resulting crude material was dissolved in anhydrous THF (1 mL, 1.0 M). MeOH (10 mL) was added, and the reaction was stirred at rt overnight before being quenched with a saturated solution of $NaHCO_3$ (aq.). The layers were separated, and the aqueous layer was extracted with EtOAc (× 2). The combined organics were then washed with brine, dried over $MgSO_4$, filtered, and concentrated under reduced pressure. The resultant crude material was purified by flash column chromatography (10-20% EtOAc/petrol, silica gel) to afford **201** (78 mg, 81%) as a white solid.

R_f = 0.36 (15% EtOAc/petrol); **M.p.:** 79-81 °C; **^{1}H NMR (500 MHz, $CDCl_3$)** δ_H = 2.49 – 2.53 (2H, m), 3.09 – 3.12 (2H, m), 3.95 (3H, s), 5.01 – 5.04 (1H, m), 5.07 – 5.12 (1H, m), 5.90 (1H, ddt, *J* 16.9, 10.2, 6.5), 8.00 – 8.02 (2H, m), 8.11 – 8.14 (2H, m); **^{13}C NMR (126 MHz, $CDCl_3$)** δ_C = 28.1, 38.3, 52.6, 115.7, 128.1, 130.0, 134.0, 137.1, 140.3, 166.4, 199.1.

These data are in accordance with the literature.[36]

4-(Pent-4-enoyl)benzamide (202)

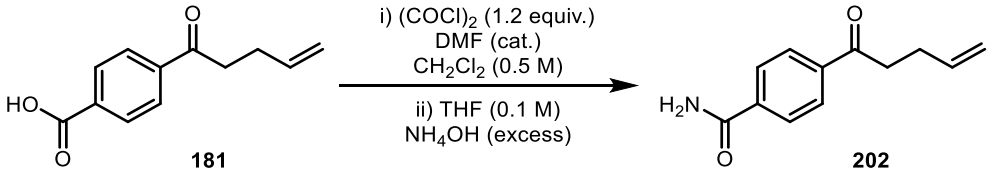

To a flame-dried RBF was added **181** (613 mg, 3.00 mmol) in anhydrous CH_2Cl_2 (6 mL, 0.5 M). The solution was cooled to 0 °C, and oxalyl chloride (305 µL, 3.60 mmol) was added dropwise, followed by the addition of DMF (3 drops). The reaction was warmed to rt and stirred until gas evolution ceased. The mixture was concentrated under reduced pressure, and the resultant crude material was dissolved in THF (3.0 mL, 1.0 M) before being added slowly to 35% NH_3 solution (aq.) (excess) and stirred at rt overnight before being diluted with EtOAc. The layers were separated, and the aqueous layer was further extracted with EtOAc (× 3). The combined organics were then washed with brine, dried over $MgSO_4$, filtered, and concentrated under reduced pressure. The resultant crude material was purified by recrystallisation (CH_2Cl_2) to afford **202** (221 mg, 36%) as a white solid.

R_f = 0.27 (80% EtOAc/petrol); **M.p.:** 168-170 °C; **FTIR** (ν_{max} cm^{-1}, thin film) 3385, 3186, 1678, 1649, 1618, 1568, 1409, 1303, 1273, 1207, 910, 860, 783; **^{1}H NMR (500 MHz, DMSO-*d*$_6$)** δ_H = 2.35 – 2.40 (2H, m), 3.16 – 3.18 (2H, m), 4.97 – 5.00 (1H, m), 5.05 – 5.10 (1H, m), 5.88 (1H, ddt, *J* 16.8, 10.2, 6.4), 7.54 (1H, br s), 7.97 – 7.99 (2H, m), 8.02 – 8.04 (2H, m), 8.13 (1H, br s); **^{13}C NMR (126 MHz, DMSO-*d*$_6$)** δ_C = 27.6, 37.2, 115.3, 127.7, 127.8, 137.5, 138.0, 138.5, 167.1, 199.0; **HRMS** (CI+) $C_{12}H_{13}NO_2$ $[M+H]^+$ requires 204.1019, found 204.1019 (+0.1 ppm).

_N_,_N_-Dimethyl-4-(pent-4-enoyl)benzamide (203)

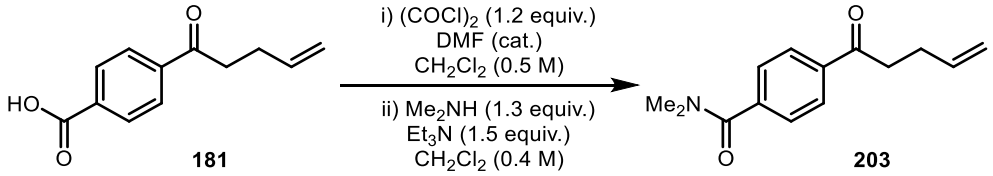

To a flame-dried RBF was added **181** (613 mg, 3.00 mmol) in anhydrous CH_2Cl_2 (6 mL, 0.5 M). The solution was cooled to 0 °C, and oxalyl chloride (305 µL, 3.60 mmol) was added dropwise, followed by the addition of DMF (3 drops). The reaction was warmed to rt and stirred until gas evolution ceased. The mixture was concentrated under reduced pressure, and the resulting crude material was dissolved in anhydrous CH_2Cl_2 (7.5 mL, 0.4 M). Dimethylamine (2.0 M in toluene, 1.95 mL, 3.90 mmol) and triethylamine (627 µL, 4.50 mmol) were added dropwise and the reaction was stirred at rt overnight before being quenched with water. The layers were separated, and the aqueous layer was extracted with CH_2Cl_2 (× 3). The combined organics were then washed with a saturated solution of $NaHCO_3$ (aq.), followed by water, then brine, dried over $MgSO_4$, filtered, and concentrated under reduced pressure. The resultant crude material was purified by flash column chromatography (50% EtOAc/petrol, silica gel) to afford **203** (458 mg, 66%) as a yellow solid.

R_f = 0.16 (50% EtOAc/petrol); **M.p.:** 46-48 °C; **FTIR** (ν_{max} cm^{-1}, thin film) 2938, 1676, 1618, 1508, 1423, 1264, 1206, 1080, 985, 908, 845, 756; **^{1}H NMR (500 MHz, $CDCl_3$)** δ_H = 2.47 – 2.52 (2H, m), 2.95 (3H, s), 3.06 – 3.09 (2H, m), 3.12 (3H, s), 5.00 – 5.03 (1H, m), 5.06 – 5.11 (1H, m), 5.85 – 5.93 (1H, m), 7.49 – 7.51 (2H, m), 7.98 – 8.00 (2H, m); **^{13}C NMR (126 MHz, $CDCl_3$)** δ_C = 28.2, 35.4, 38.0, 39.5, 115.6, 127.4, 128.3, 137.2, 137.6, 140.8, 170.6, 198.9; **HRMS** (ES+) $C_{14}H_{17}NO_2$ $[M+H]^+$ requires 232.1338, found 232.1342 (+1.7 ppm).

5.4.2.2 Substrates

2-Hydroxy-2-phenylhex-5-enenitrile (163)

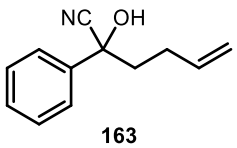

163

Prepared according to General Procedure 16 using **162** (5.77 g, 36.0 mmol) in CH_2Cl_2 (72 mL), trimethylsilyl cyanide (11.3 mL, 90.0 mmol), and $TiCl_4$ (2.00 mL, 18.0 mmol),

followed by MeCN (180 mL) and 2 M HCl (180 mL) to afford **163** (6.68 g, 99%) as a yellow oil that was used without further purification.

R_f = 0.22 (10% EtOAc/petrol); **^{1}H NMR (500 MHz, $CDCl_3$)** δ_H = 2.04 – 2.23 (3H, m), 2.30 – 2.39 (1H, m), 2.97 (1H, br s), 5.00 – 5.03 (1H, m), 5.04 – 5.12 (1H, m), 5.76 – 5.85 (1H, m), 7.38 – 7.46 (3H, m), 7.55 – 7.58 (2H, m); **^{13}C NMR (126 MHz, $CDCl_3$)** δ_C = 28.9, 42.7, 74.7, 116.3, 120.7, 125.0, 129.1, 129.4, 136.6, 139.8.

These data are in accordance with the literature.[37]

2-Hydroxy-2-(*p*-tolyl)hex-5-enenitrile (204)

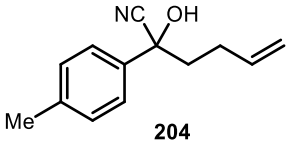

204

Prepared according to General Procedure 16 using **172** (348 g, 2.00 mmol) in CH_2Cl_2 (4 mL), trimethylsilyl cyanide (626 µL, 2.50 mmol), and $TiCl_4$ (110 µL, 0.50 mmol), followed by MeCN (10 mL) and 2 M HCl (10 mL) to afford **204** (345 mg, 86%) as a yellow oil that was used without further purification.

R_f = 0.19 (10% EtOAc/petrol); **^{1}H NMR (500 MHz, $CDCl_3$)** δ_H = 2.03 – 2.11 (1H, m), 2.12 – 2.21 (2H, m), 2.30 – 2.39 (4H, m), 2.86 (1H, br s), 4.98 – 5.04 (1H, m), 5.03 – 5.12 (1H, m), 5.74 – 5.86 (1H, m), 7.20 – 7.25 (2H, m), 7.42 – 7.48 (2H, m); **^{13}C NMR (126 MHz, $CDCl_3$)** δ_C = 21.3, 28.9, 42.6, 74.6, 116.1, 120.8, 124.9, 129.7, 136.7, 136.9, 139.4.

These data are in accordance with the literature.[37]

2-Hydroxy-2-(*m*-tolyl)hex-5-enenitrile (205)

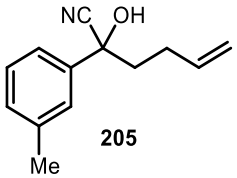

205

Prepared according to General Procedure 16 using **173** (871 mg, 5.00 mmol) in CH_2Cl_2 (10 mL), trimethylsilyl cyanide (1.56 mL, 12.5 mmol), and $TiCl_4$ (274 µL, 2.50 mmol), followed by MeCN (25 mL) and 2 M HCl (25 mL) to afford **205** (951 mg, 94%) as a yellow oil that was used without further purification.

R_f = 0.23 (10% EtOAc/petrol); **^{1}H NMR (500 MHz, $CDCl_3$)** δ_H = 2.03 – 2.11 (1H, m), 2.13 – 2.23 (2H, m), 2.30 – 2.38 (1H, m), 2.40 (3H, s), 2.91 (1H, br s), 5.00 – 5.03 (1H, m), 5.06 – 5.10 (1H, m), 5.77 – 5.85 (1H, m), 7.20 – 7.21 (1H, m), 7.30 – 7.33 (1H, m), 7.35

– 7.37 (2H, m); **^{13}C NMR (126 MHz, $CDCl_3$)** δ_C = 21.7, 28.9, 42.7, 74.7, 116.2, 120.8, 122.0, 125.6, 128.9, 130.2, 136.7, 139.0, 139.8.

These data are in accordance with the literature.[37]

2-Hydroxy-2-(*o*-tolyl)hex-5-enenitrile (206)

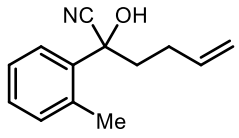

206

Prepared according to General Procedure 16 using **174** (523 mg, 3.00 mmol) in CH_2Cl_2 (6 mL), trimethylsilyl cyanide (938 µL, 7.50 mmol), and $TiCl_4$ (164 µL, 1.50 mmol), followed by MeCN (15 mL) and 2 M HCl (15 mL) to afford **206** (578 mg, 96%) as a yellow oil that was used without further purification.

R_f = 0.20 (10% EtOAc/petrol); **^{1}H NMR (500 MHz, $CDCl_3$)** δ_H = 2.16 – 2.42 (4H, m), 2.58 (3H, s), 2.89 (1H, br s), 5.02 – 5.05 (1H, m), 5.09 – 5.13 (1H, m), 5.79 – 5.88 (1H, m), 7.22 – 7.30 (3H, m), 7.60 – 7.62 (1H, m); **^{13}C NMR (126 MHz, $CDCl_3$)** δ_C = 20.9, 28.9, 39.8, 74.5, 116.3, 120.8, 125.9, 126.4, 129.2, 133.0, 135.3, 136.7, 136.8.

These data are in accordance with the literature.[37]

2-([1,1'-Biphenyl]-4-yl)-2-hydroxyhex-5-enenitrile (207)

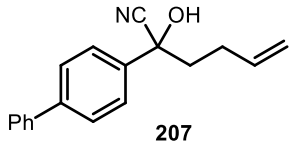

207

Prepared according to General Procedure 16 using **175** (1.18 g, 5.00 mmol) in CH_2Cl_2 (10 mL), trimethylsilyl cyanide (1.55 mL, 12.5 mmol), and $TiCl_4$ (274 µL, 2.50 mmol), followed by MeCN (25 mL) and 2 M HCl (25 mL) to afford **207** (1.25 g, 95%) as an off-white solid that was used without further purification.

R_f = 0.13 (10% EtOAc/petrol); **M.p.:** 81-83 °C; **^{1}H NMR (500 MHz, $CDCl_3$)** δ_H = 2.09 – 2.28 (3H, m), 2.34 – 2.44 (1H, m), 2.97 (1H, br s), 5.02 – 5.05 (1H, m), 5.07 – 5.15 (1H, m), 5.79 – 5.87 (1H, m), 7.35 – 7.42 (1H, m), 7.44 – 7.50 (2H, m), 7.56 – 7.62 (2H, m), 7.60 – 7.69 (4H, m); **^{13}C NMR (126 MHz, $CDCl_3$)** δ_C = 29.0, 42.7, 74.6, 116.3, 120.7, 125.5, 127.2, 127.8, 128.0, 129.1, 136.6, 138.7, 140.1, 142.4.

These data are in accordance with the literature.[37]

2-Hydroxy-2-(4-(trifluoromethyl)phenyl)hex-5-enenitrile (208)

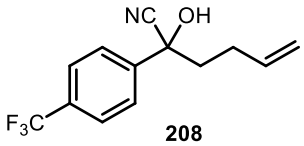

208

Prepared according to General Procedure 16 using **176** (1.14 g, 5.00 mmol) in CH_2Cl_2 (10 mL), trimethylsilyl cyanide (1.55 mL, 12.5 mmol), and $TiCl_4$ (274 µL, 2.50 mmol), followed by MeCN (25 mL) and 2 M HCl (25 mL) to afford **208** (1.26 g, 99%) as a yellow oil that was used without further purification.

R_f = 0.22 (10% EtOAc/petrol); **^{1}H NMR (500 MHz, $CDCl_3$)** δ_H = 2.06 – 2.18 (2H, m), 2.19 – 2.27 (1H, m), 2.32 – 2.41 (1H, m), 3.15 (1H, br s), 5.04 – 5.07 (1H, m), 5.09 – 5.16 (1H, m), 5.75 – 5.87 (1H, m), 7.70 (4H, m); **^{13}C NMR (126 MHz, $CDCl_3$)** δ_C = 28.8, 42.8, 74.2, 116.8, 120.2, 123.8 (q, *J* 272.4), 125.6, 126.1 (q, *J* 3.7), 131.7 (q, *J* 32.8), 136.3, 143.6; **^{19}F{^{1}H} NMR (376 MHz, $CDCl_3$)** δ_F = -62.77.

These data are in accordance with the literature.[37]

4-(1-Cyano-1-hydroxypent-4-en-1-yl)benzonitrile (209)

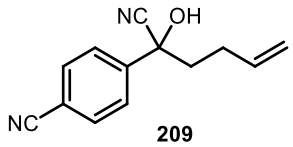

209

Prepared according to General Procedure 16 using **195** (463 mg, 2.50 mmol) in CH_2Cl_2 (5 mL), trimethylsilyl cyanide (782 µL, 6.25 mmol), and $TiCl_4$ (137 µL, 1.25 mmol), followed by MeCN (12.5 mL) and 2 M HCl (12.5 mL) to afford **209** (530 mg, 99%) as a yellow oil that was used without further purification.

R_f = 0.16 (10% EtOAc/petrol); **FTIR** (ν_{max} cm^{-1}, thin film) 3393, 3078, 2926, 2232, 1641, 1609, 1406, 1072, 916, 839; **^{1}H NMR (500 MHz, $CDCl_3$)** δ_H = 2.05 – 2.16 (2H, m), 2.20 – 2.28 (1H, m), 2.32 – 2.40 (1H, m), 3.22 (1H, br s), 5.05 – 5.08 (1H, m), 5.10 – 5.15 (1H, m), 5.77 – 5.85 (1H, m), 7.69 – 7.75 (4H, m); **^{13}C NMR (126 MHz, $CDCl_3$)** δ_C = 28.8, 42.8, 74.1, 113.4, 117.0, 118.1, 119.8, 126.0, 132.9, 136.1, 144.8; **HRMS** (EI+) $C_{13}H_{12}N_2O$ $[M-H]^+$ requires 211.0866, found 211.0866 (-0.1 ppm).

2-(4-Fluorophenyl)-2-hydroxyhex-5-enenitrile (210)

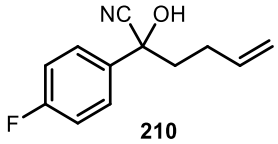

210

Prepared according to General Procedure 16 using **167** (446 mg, 2.50 mmol) in CH_2Cl_2 (5 mL), trimethylsilyl cyanide (782 µL, 6.25 mmol), and $TiCl_4$ (137 µL, 1.25 mmol), followed by MeCN (12.5 mL) and 2 M HCl (12.5 mL) to afford **210** (489 mg, 95%) as a yellow oil that was used without further purification.

R_f = 0.19 (10% EtOAc/petrol); **^{1}H NMR (500 MHz, $CDCl_3$)** δ_H = 2.02 – 2.22 (3H, m), 2.29 – 2.38 (1H, m), 3.05 (1H, br s), 5.02 – 5.04 (1H, m), 5.07 – 5.11 (1H, m), 5.76 – 5.84 (1H, m), 7.09 – 7.14 (2H, m), 7.53 – 7.57 (2H, m); **^{13}C NMR (126 MHz, $CDCl_3$)** δ_C = 28.9, 42.8, 74.2, 116.0 (d, *J* 21.9), 116.5, 120.5, 127.0 (d, *J* 8.5), 135.7, (d, *J* 3.3), 136.5, 163.2 (d, *J* 248.9); **^{19}F{^{1}H} NMR (376 MHz, $CDCl_3$)** δ_F = -112.21.

These data are in accordance with the literature.[37]

2-(4-Chlorophenyl)-2-hydroxyhex-5-ene-nitrile (211)

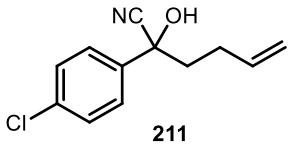

211

Prepared according to General Procedure 16 using **168** (487 mg, 2.50 mmol) in CH_2Cl_2 (5 mL), trimethylsilyl cyanide (782 µL, 6.25 mmol), and $TiCl_4$ (137 µL, 1.25 mmol), followed by MeCN (12.5 mL) and 2 M HCl (12.5 mL) to afford **211** (563 g, 99%) as a yellow oil that was used without further purification.

R_f = 0.22 (10% EtOAc/petrol); **^{1}H NMR (500 MHz, $CDCl_3$)** δ_H = 2.02 – 2.22 (3H, m), 2.30 – 2.36 (1H, m), 3.02 (1H, br s), 5.02 – 5.05 (1H, m), 5.07 – 5.12 (1H, m), 5.76 – 5.84 (1H, m), 7.39 – 7.42 (2H, m), 7.49 – 7.52 (2H, m); **^{13}C NMR (126 MHz, $CDCl_3$)** δ_C = 28.9, 42.7, 74.2, 116.6, 120.4, 126.5, 129.3, 135.4, 136.4, 138.4.

These data are in accordance with the literature.[37]

2-(4-Bromophenyl)-2-hydroxyhex-5-enenitrile (212)

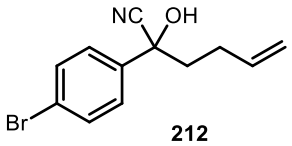

212

Prepared according to General Procedure 16 using **169** (598 mg, 2.50 mmol) in CH_2Cl_2 (5 mL), trimethylsilyl cyanide (782 µL, 6.25 mmol), and $TiCl_4$ (137 µL, 1.25 mmol), followed by MeCN (12.5 mL) and 2 M HCl (12.5 mL) to afford **212** (636 mg, 96%) as a yellow oil that was used without further purification.

R_f = 0.14 (10% EtOAc/petrol); **^{1}H NMR (500 MHz, $CDCl_3$)** δ_H = 2.02 – 2.33 (3H, m), 2.30 – 2.36 (1H, m), 2.99 (1H, br s), 5.02 – 5.05 (1H, m), 5.07 – 5.12 (1H, m), 5.76 – 5.84 (1H, m), 7.43 – 7.45 (2H, m), 7.55 – 7.58 (2H, m); **^{13}C NMR (126 MHz, $CDCl_3$)** δ_C = 28.9, 42.7, 74.2, 116.6, 120.3, 123.6, 126.8, 132.2, 136.4, 138.9.

These data are in accordance with the literature.[37]

2-Hydroxy-2-(4-iodophenyl)hex-5-enenitrile (213)

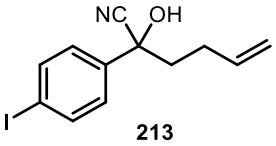

213

Prepared according to General Procedure 16 using **170** (286 mg, 1.00 mmol) in CH_2Cl_2 (2 mL), trimethylsilyl cyanide (313 µL, 2.50 mmol), and $TiCl_4$ (55 µL, 0.50 mmol), followed by MeCN (5 mL) and 2 M HCl (5 mL) to afford **213** (300 mg, 96%) as a yellow oil that was used without further purification.

R_f = 0.14 (10% EtOAc/petrol); **^{1}H NMR (500 MHz, $CDCl_3$)** δ_H = 2.01 – 2.07 (1H, m), 2.09 – 2.22 (2H, m), 2.29 – 2.37 (1H, m), 3.11 (1H, br s), 5.02 – 5.04 (1H, m), 5.07 – 5.11 (1H, m), 5.75 – 5.83 (1H, m), 7.29 – 7.32 (2H, m), 7.75 – 7.78 (2H, m); **^{13}C NMR (126 MHz, $CDCl_3$)** δ_C = 28.8, 42.7, 74.3, 95.3, 116.5, 120.3, 126.9, 136.4, 138.2, 139.6.

These data are in accordance with the literature.[38]

2-Hydroxy-2-(4-methoxyphenyl)hex-5-enenitrile (214)

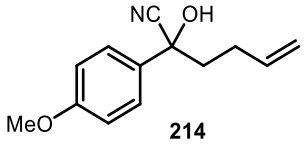

214

Prepared according to General Procedure 16 using **166** (951 mg, 5.00 mmol) in CH_2Cl_2 (10 mL), trimethylsilyl cyanide (1.55 mL, 12.5 mmol), and $TiCl_4$ (110 µL, 2.50 mmol), followed by acetonitrile (25 mL) and 2 M HCl (25 mL) to afford **214** (898 mg, 83%) as a yellow oil that was used without further purification.

R_f = 0.09 (10% EtOAc/petrol); **^{1}H NMR (500 MHz, $CDCl_3$)** δ_H = 2.03 – 2.20 (3H, m), 2.27 – 2.37 (1H, m), 2.80 (1H, br s), 3.83 (3H, s), 5.00 – 5.03 (1H, m), 5.05 – 5.10 (1H, m), 5.76 – 5.84 (1H, m), 6.92 – 6.95 (2H, m), 7.46 – 7.50 (2H, m); **^{13}C NMR (126 MHz, $CDCl_3$)** δ_C = 29.0, 42.6, 55.6, 74.4, 114.4, 116.2, 120.8, 126.4, 131.9, 136.7, 160.4.

These data are in accordance with the literature.[37]

2-Hydroxy-2-(4-(hydroxymethyl)phenyl)hex-5-enenitrile (215)

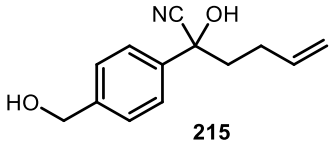

215

Prepared according to General Procedure 16 using **198** (380 mg, 2.00 mmol) in CH_2Cl_2 (4 mL), trimethylsilyl cyanide (626 µL, 5.00 mmol), and $TiCl_4$ (110 µL, 1.00 mmol), followed by acetonitrile (10 mL) and 2 M HCl (10 mL) to afford **215** (426 mg, 98%) as a yellow solid that was used without further purification.

R_f = 0.19 (40% EtOAc/petrol); **M.p.:** 80-82 °C; **FTIR** (ν_{max} cm^{-1}, thin film) 3391 (br), 3148 (br), 2926, 1641, 1436, 1416, 1207, 1080, 1005, 923; **^{1}H NMR (500 MHz, $CDCl_3$)** δ_H = 1.90 (1H, br s), 2.03 – 2.21 (3H, m), 2.29 – 2.37 (1H, m), 3.29 (1H, br s), 4.71 (2H, s), 5.00 – 5.03 (1H, m), 5.05 – 5.09 (1H, m), 5.75 – 5.83 (1H, m), 7.38 – 7.40 (2H, m), 7.52 – 7.55 (2H, m); **^{13}C NMR (126 MHz, $CDCl_3$)** δ_C = 28.9, 42.7, 64.8, 74.4, 116.2, 120.8, 125.3, 127.5, 136.6, 139.3, 142.0; **HRMS** (CI+) $C_{13}H_{15}NO_2$ $[M\text{-}CN]^+$ requires 191.1067, found 191.1066 (-0.5 ppm).

2-Hydroxy-2-(4-hydroxyphenyl)hex-5-enenitrile (216)

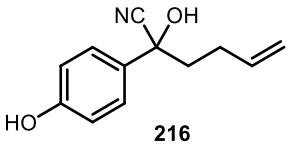

216

Prepared according to General Procedure 16 using **197** (352 mg, 2.00 mmol) in CH_2Cl_2 (4 mL), trimethylsilyl cyanide (626 µL, 5.00 mmol), and $TiCl_4$ (110 µL, 1.00 mmol), followed by acetonitrile (10 mL) and 2 M HCl (10 mL) to afford **216** (405 mg, 99%) as a low melting orange solid that was used without further purification.

R_f = 0.34 (40% EtOAc/petrol); **FTIR** (ν_{max} cm^{-1}, thin film) 3425, 3281 (br), 2929, 1601, 1512, 1442, 1365, 1232, 1213, 1174, 1076, 941, 918, 829; **^{1}H NMR (500 MHz, $CDCl_3$)** δ_H = 2.00 – 2.09 (2H, m), 2.12 – 2.19 (2H, m), 2.27 – 2.37 (1H, m), 2.90 (1H, br s), 5.00 – 5.03 (1H, m), 5.06 – 5.10 (1H, m), 5.76 – 5.84 (1H, m), 6.85 – 6.88 (2H, m), 7.42 – 7.45 (2H, m); **^{13}C NMR (126 MHz, $CDCl_3$)** δ_C = 29.0, 42.6, 74.4, 115.8, 116.2, 120.8, 126.7, 132.1, 136.7, 156.4; **HRMS** (CI+) $C_{12}H_{13}NO_2$ $[M]^+$ requires 203.0941, found 203.0940 (-0.4 ppm).

2-(4-((*tert*-Butyldimethylsilyl)oxy)phenyl)-2-hydroxyhex-5-enenitrile (217)

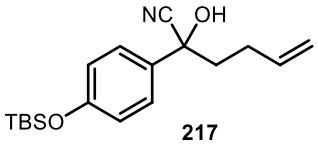

217

Prepared according to General Procedure 16 using **177** (726 mg, 2.50 mmol) in CH_2Cl_2 (5 mL), trimethylsilyl cyanide (782 µL, 6.25 mmol), and $TiCl_4$ (137 µL, 1.25 mmol), followed by acetonitrile (12.5 mL) and 2 M HCl (12.5 mL) to afford **217** (662 mg, 84%) as a yellow oil that was used without further purification.

R_f = 0.16 (10% EtOAc/petrol); **FTIR** (ν_{max} cm^{-1}, thin film) 3406, 2930, 2858, 1607, 1508, 1256, 910, 835, 781; **^{1}H NMR (500 MHz, $CDCl_3$)** δ_H = 0.21 (6H, s), 0.99 (9H, s), 2.02 – 2.10 (1H, m), 2.12 – 2.21 (2H, m), 2.26 – 2.38 (1H, m), 2.79 (1H, br s), 5.00 – 5.03 (1H, m), 5.05 – 5.10 (1H, m), 5.75 – 5.84 (1H, m), 6.86 – 6.88 (2H, m), 7.41 – 7.45 (2H, m); **^{13}C NMR (126 MHz, $CDCl_3$)** δ_C = – 4.3, 18.4, 25.8, 29.0, 42.6, 74.5, 115.8, 116.1, 120.5, 126.4, 132.5, 136.7, 156.7; **HRMS** (EI+) $C_{18}H_{27}NOSi$ $[M]^+$ requires 317.1806, found 317.1804 (-0.6 ppm).

2-Hydroxy-2-(4-(4,4,5,5-tetramethyl-1,3,2-dioxaborolan-2-yl)phenyl)hex-5-enenitrile (218)

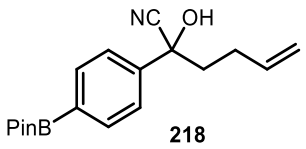

218

Prepared according to General Procedure 16 using **196** (572 mg, 2.00 mmol) in CH_2Cl_2 (4 mL), trimethylsilyl cyanide (626 µL, 5.00 mmol), and $TiCl_4$ (110 µL, 1.00 mmol), followed by MeCN (10 mL) and 2 M HCl (10 mL) to afford **218** (610 mg, 98%) as a yellow solid that was used without further purification.

R_f = 0.27 (20% EtOAc/petrol); **M.p.:** 77-79 °C; **FTIR** (ν_{max} cm^{-1}, thin film) 3402, 2978, 2930, 2238, 1610, 1400, 1360, 1132, 1088, 753; **^{1}H NMR (500 MHz, $CDCl_3$)** δ_H = 1.35 (12H, s), 2.03 – 2.20 (3H, m), 2.30 – 2.36 (1H, m), 3.01 (1H, br s), 4.99 – 5.02 (1H, m), 5.04 – 5.09 (1H, m), 5.75 – 5.83 (1H, m), 7.54 – 7.57 (2H, m), 7.84 – 7.86 (2H, m); **^{13}C NMR (126 MHz, $CDCl_3$)** δ_C = 24.9, 25.0, 28.8, 42.7, 74.7, 84.3, 116.3, 120.6, 124.3, 135.5, 136.6, 142.6; **HRMS** (EI+) $C_{18}H_{24}{}^{11}BNO_3$ $[M-H]^+$ requires 312.1766, found 312.1763 (-0.9 ppm).

4-(1-Cyano-1-hydroxypent-4-en-1-yl)benzoic acid (219)

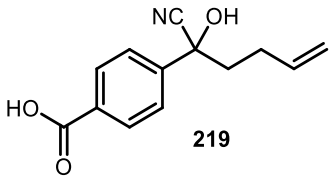

219

Prepared according to General Procedure 16 using **181** (306 mg, 1.50 mmol) in CH_2Cl_2 (7 mL), trimethylsilyl cyanide (469 µL, 3.75 mmol), and $TiCl_4$ (82 µL, 0.75 mmol), followed by MeCN (7.5 mL) and 2 M HCl (7.5 mL) to afford **219** (298 mg, 86%) as an orange solid that was used without further purification.

R_f = 0.09 (50% EtOAc/petrol); **M.p.:** 105-107 °C; **FTIR** (ν_{max} cm^{-1}, thin film) 3397, 2849, 2669, 2550, 2253, 1686, 1610, 1417, 1287, 1078, 914, 864; **^{1}H NMR (500 MHz, DMSO-d_6)** δ_H = 2.03 – 2.11 (4H, m), 4.93 – 5.03 (2H, m), 5.73 – 5.80 (1H, m), 7.44 (1H, s), 7.64 – 7.65 (2H, m), 8.00 – 8.02 (2H, m), 13.07 (1H, br s); **^{13}C NMR (126 MHz, DMSO-d_6)** δ_C = 27.9, 41.8, 72.4, 115.5, 121.4, 125.3, 129.6, 131.0, 136.8, 145.2, 166.8; **HRMS** (ES+) $C_{13}H_{13}NO_3$ $[M+H]^+$ requires 232.0974, found 232.0968 (-2.6 ppm).

Methyl 4-(1-cyano-1-hydroxypent-4-en-1-yl)benzoate (220)

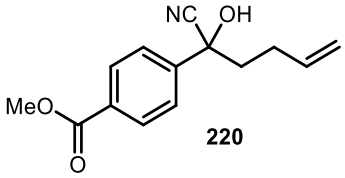

220

Prepared according to General Procedure 16 using **201** (218 mg, 1.00 mmol) in CH_2Cl_2 (2 mL), trimethylsilyl cyanide (313 µL, 2.50 mmol), and $TiCl_4$ (55 µL, 0.50 mmol), followed by MeCN (5 mL) and 2 M HCl (5 mL) to afford **220** (234 mg, 95%) as an orange oil that was used without further purification.

R_f = 0.23 (20% EtOAc/petrol); **FTIR** (ν_{max} cm^{-1}, thin film) 3410 (br), 2955, 1724, 1641, 1610, 1436, 1409, 1278, 1188, 1109, 1018, 916; **^{1}H NMR (500 MHz, $CDCl_3$)** δ_H = 2.05 – 2.24 (3H, m), 2.32 – 2.38 (1H, m), 3.93 (3H, m), 5.01 – 5.04 (1H, m), 5.06 – 5.11 (1H, m), 5.75 – 5.83 (1H, m), 7.62 – 7.65 (2H, m), 8.05 – 8.07 (2H, m); **^{13}C NMR (126 MHz, $CDCl_3$)** δ_C = 28.8, 42.8, 52.6, 74.3, 116.5, 120.3, 125.2, 130.3, 131.0, 136.4, 144.6, 166.6; **HRMS** (AP+) $C_{14}H_{14}NO_3$ $[M+H]^+$ requires 244.0974, found 244.0982 (+3.3 ppm).

4-(1-Cyano-1-hydroxypent-3-en-1-yl)benzamide (221)

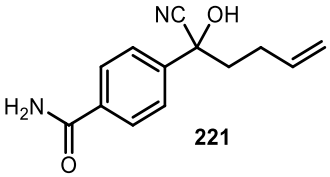

221

Prepared according to General Procedure 16 using **202** (184 mg, 0.90 mmol) in CH_2Cl_2 (4 mL), trimethylsilyl cyanide (563 µL, 4.50 mmol), and $TiCl_4$ (100 µL, 0.90 mmol), followed by MeCN (4.5 mL) and 2 M HCl (4.5 mL) to afford **221** (159 mg, 77%) as an orange solid that was used without further purification.

R_f = 0.24 (80% EtOAc/petrol); **M.p.:** 118-120 °C; **FTIR** (ν_{max} cm^{-1}, thin film) 3414, 3192, 2922, 1653, 1610, 1566, 1413, 1300, 1269, 1207, 1143, 1124, 1072, 991, 910; **^{1}H NMR (500 MHz, DMSO-*d*$_6$)** δ_H = 2.02 – 2.10 (4H, m), 4.93 – 4.96 (1H, m), 4.99 – 5.03 (1H, m), 5.73 – 5.81 (1H, m), 7.37 (1H, s), 7.42 (1H, br s), 7.57 – 7.60 (2H, m), 7.92 – 7.94 (2H, m), 8.02 (1H, br s); **^{13}C NMR (126 MHz, DMSO-*d*$_6$)** δ_C = 27.9, 41.7, 73.3, 115.5, 121.5, 124.9, 127.8, 134.5, 136.8, 143.5, 167.3; **HRMS** (ES+) $C_{13}H_{14}N_2O_2$ $[M+H]^+$ requires 232.1134, found 231.1139 (+2.2 ppm).

4-(1-Cyano-1-hydroxypent-4-en-1-yl)-*N*,*N*-dimethylbenzamide (222)

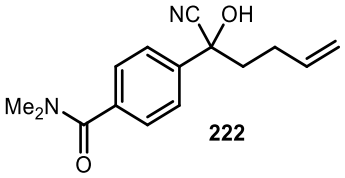

222

Prepared according to General Procedure 16 using **203** (347 mg, 1.50 mmol) in CH_2Cl_2 (3 mL), trimethylsilyl cyanide (469 µL, 3.75 mmol), and $TiCl_4$ (82 µL, 0.75 mmol), followed by MeCN (7.5 mL) and 2 M HCl (7.5 mL) to afford **222** (346 mg, 89%) as an orange oil that was used without further purification.

R_f = 0.19 (60% EtOAc/petrol); **FTIR** (ν_{max} cm^{-1}, thin film) 3242, 2927, 1608, 1517, 1448, 1398, 1265, 1083, 1018, 914, 846; **^{1}H NMR (500 MHz, $CDCl_3$)** δ_H = 1.95 – 1.99 (2H, m), 2.15 – 2.32 (2H, m), 2.92 (3H, s), 3.11 (3H, s), 4.93 – 4.96 (1H, m), 4.99 – 5.03 (1H, m), 5.75 (1H, ddt, *J* 16.8, 10.2, 6.5), 7.21 – 7.23 (2H, m), 7.36 – 7.38 (2H, m); **^{13}C NMR (126 MHz, $CDCl_3$)** δ_C = 28.6, 35.8, 39.7, 43.2, 73.2, 115.6, 121.1 124.9, 127.3, 135.5, 136.9, 142.6, 171.5; **HRMS** (ES+) $C_{15}H_{18}N_2O_2$ $[M+H]^+$ requires 259.1447, found 259.1448 (+0.4 ppm).

2-(4-(1,3-Dioxolan-2-yl)phenyl)-2-hydroxyhex-5-enenitrile (223)

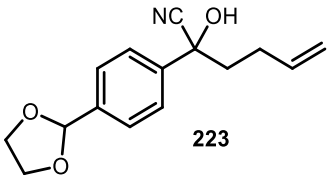

223

Prepared according to General Procedure 16 using **182** (581 mg, 2.50 mmol) in CH_2Cl_2 (5 mL), trimethylsilyl cyanide (782 µL, 6.25 mmol), and $TiCl_4$ (137 µL, 1.25 mmol), followed by acetonitrile (12.5 mL) and 2 M HCl (12.5 mL) to afford **223** (380 mg, 59%) as a yellow oil that was used without further purification.

R_f = 0.10 (30% EtOAc/petrol); **FTIR** (ν_{max} cm^{-1}, thin film) 3408, 2930, 2347, 2324, 1508, 1413, 1271, 1206, 1067, 916, 818; **^{1}H NMR (500 MHz, $CDCl_3$)** δ_H = 1.72 (1H, br s), 2.03 – 2.25 (3H, m), 2.32 – 2.39 (1H, m), 3.73 – 4.00 (4H, m), 5.02 – 5.12 (2H, m), 5.34 – 5.41 (1H, m), 5.76 – 5.85 (1H, m), 7.49 – 7.66 (4H, m); **^{13}C NMR (126 MHz, $CDCl_3$)** δ_C = 28.7, 42.7, 61.6, 70.7, 74.0, 116.4, 116.9, 120.5, 125.9, 128.0, 128.9, 136.7, 137.0, 142.0; **HRMS** (ES+) $C_{15}H_{17}NO_3$ $[M+H]^+$ requires 260.1287, found 260.1282 (-1.9 ppm).

2-Hydroxy-2-(4-(2-methyl-1,3-dioxolan-2-yl)phenyl)hex-5-enenitrile (224)

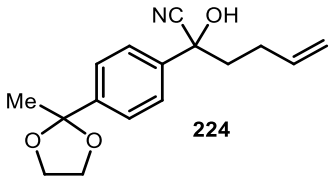

224

Prepared according to General Procedure 16 using **183** (616 mg, 2.50 mmol) in CH_2Cl_2 (5 mL), trimethylsilyl cyanide (782 µL, 6.25 mmol), and $TiCl_4$ (137 µL, 1.25 mmol), followed by MeCN (12.5 mL) and 2 M HCl (12.5 mL) to afford **224** (683 mg, 99%) as a yellow oil that was used without further purification.

R_f = 0.13 (30% EtOAc/petrol); **FTIR** (ν_{max} cm^{-1}, thin film) 3366, 2932, 2326, 1406, 1373, 1229, 1113, 1078, 1044, 1016, 837; **^{1}H NMR (500 MHz, $CDCl_3$)** δ_H = 1.87 (3H, s), 2.06 – 2.14 (2H, m), 2.18 – 2.25 (1H, m), 2.30 – 2.39 (1H, m), 2.61 (s, 1H), 3.31 – 3.39 (1H, m), 3.62 – 3.67 (1H, m), 3.70 – 3.74 (1H, m), 3.77 – 3.81 (1H, m), 5.01 – 5.04 (1H, m), 5.07 – 5.11 (1H, m), 5.76 – 5.84 (1H, m), 7.56 – 7.59 (2H, m), 7.62 – 7.64 (2H, m); **^{13}C NMR (126 MHz, $CDCl_3$)** δ_C = 28.8, 30.6, 42.7, 61.6, 68.1, 74.1, 116.4, 118.8, 120.5, 125.9, 126.1, 136.4, 139.3, 141.4; **HRMS** (ES+) $C_{16}H_{19}NO_3$ $[M+H]^+$ requires 274.1443, found 274.1441 (-0.7 ppm).

2-Hydroxy-2-(naphthalen-2-yl)hex-5-enenitrile (225)

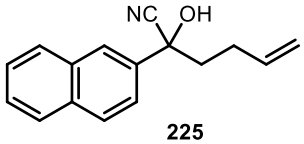

225

Prepared according to General Procedure 16 using **179** (631 mg, 3.00 mmol) in CH_2Cl_2 (6 mL), trimethylsilyl cyanide (938 µL, 7.50 mmol), and $TiCl_4$ (164 µL, 1.50 mmol), followed by acetonitrile (15 mL) and 2 M HCl (15 mL) to afford **225** (704 mg, 99%) as an orange solid that was used without further purification.

R_f = 0.58 (30% EtOAc/petrol); **M.p.:** 85-87 °C; **^{1}H NMR (500 MHz, $CDCl_3$)** δ_H = 2.12 – 2.28 (3H m), 2.32 – 2.40 (1H, m), 3.18 (1H, s), 4.99 – 5.02 (1H, m), 5.05 – 5.09 (1H, m), 5.75 – 5.83 (1H, m), 7.53 – 7.57 (2H, m), 7.58 – 7.60 (1H, m), 7.85 – 7.90 (3H, m), 8.05 – 8.06 (1H, m); **^{13}C NMR (126 MHz, $CDCl_3$)** δ_C = 28.9, 42.4, 74.8, 116.2, 120.7, 122.1, 124.5, 127.0, 127.2, 127.8, 128.5, 129.2, 132.8, 133.5, 136.6, 136.8.

These data are in accordance with the literature.[37]

2-Hydroxy-2-(naphthalen-1-yl)hex-5-enenitrile (226)

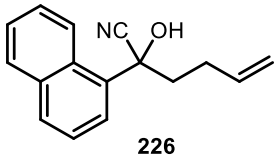

226

Prepared according to General Procedure 16 using **178** (631 mg, 3.00 mmol) in CH_2Cl_2 (6 mL), trimethylsilyl cyanide (938 µL, 7.50 mmol), and $TiCl_4$ (164 µL, 1.50 mmol), followed by MeCN (15 mL) and 2 M HCl (15 mL) to afford **226** (641 mg, 90%) as an orange oil that was used without further purification.

R_f = 0.57 (30% EtOAc/petrol); **^{1}H NMR (500 MHz, $CDCl_3$)** δ_H = 2.20 – 2.27 (1H, m), 2.38 – 2.50 (3H, m), 3.33 (1H, s), 4.98 – 5.09 (2H, m), 5.75 – 5.84 (1H, m), 7.44 – 7.49 (1H, m), 7.51 – 7.59 (2H, m), 7.83 – 7.92 (3H, m), 8.53 – 8.55 (1H, m); **^{13}C NMR (126 MHz, $CDCl_3$)** δ_C = 28.5, 39.6, 75.2, 115.6, 120.4, 124.0, 124.3 (2C), 125.6, 126.2, 128.7, 129.0, 130.2, 133.2, 134.2, 136.1.

These data are in accordance with the literature.[37]

2-Benzyl-2-hydroxyhex-5-enenitrile (227)

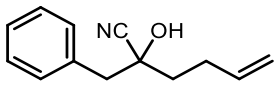

227

Prepared according to General Procedure 16 using **199** (436 mg, 2.50 mmol) in CH_2Cl_2 (5 mL), trimethylsilyl cyanide (782 µL, 6.25 mmol), and $TiCl_4$ (137 µL, 1.25 mmol), followed by MeCN (12.5 mL) and 2 M HCl (12.5 mL) to afford **227** (454 mg, 90%) as a colourless oil that was used without further purification.

R_f = 0.16 (10% EtOAc/petrol); **^{1}H NMR (500 MHz, $CDCl_3$)** δ_H = 1.87 – 2.01 (2H, m), 2.33 – 2.54 (3H, m), 2.95 (1H, d, *J* 13.7), 3.13 (1H, d, *J* 13.7), 5.03 – 5.09 (1H, m), 5.12 – 5.19 (1H, m), 5.81 – 5.94 (1H, m), 7.31 – 7.44 (5H, m); **^{13}C NMR (126 MHz, $CDCl_3$)** δ_C = 28.8, 39.3, 46.7, 72.2, 116.3, 120.6, 128.3, 129.1, 130.6, 133.3, 137.0.

These data are in accordance with the literature.[37]

2-Hydroxy-6-methyl-2-phenylhept-5-enenitrile (232)

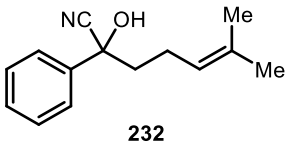

232

Prepared according to General Procedure 16 using **188** (471 mg, 2.50 mmol) in CH_2Cl_2 (5 mL), trimethylsilyl cyanide (782 µL, 6.25 mmol), and $TiCl_4$ (137 µL, 1.25 mmol), followed by acetonitrile (12.5 mL) and 2 M HCl (12.5 mL) to afford **232** (474 mg, 88%) as a yellow oil that was used without further purification.

R_f = 0.19 (10% EtOAc/petrol); **^{1}H NMR (500 MHz, $CDCl_3$)** δ_H = 1.60 – 1.64 (3H, m), 1.66 – 1.71 (3H, m), 1.99 – 2.15 (3H, m), 2.32 – 2.38 (1H, m), 3.03 (1H, br s), 5.10 – 5.13 (1H, m), 7.37 – 7.44 (3H, m), 7.55 – 7.58 (2H, m); **^{13}C NMR (126 MHz, $CDCl_3$)** δ_C = 17.9, 23.7, 25.9, 43.5, 75.0, 120.8, 122.2, 125.0, 129.0, 129.3, 134.4, 140.0.

These data are in accordance with the literature.[37]

2-Hydroxy-2-phenylhept-5-enenitrile (233)

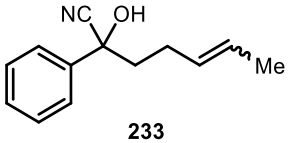

233

Prepared according to General Procedure 16 using **189** (348 mg, 2.00 mmol) in CH_2Cl_2 (4 mL), trimethylsilyl cyanide (626 µL, 5.00 mmol), and $TiCl_4$ (110 µL, 1.00 mmol), followed by MeCN (10 mL) and 2 M HCl (10 mL) to afford **233** (342 mg, 85%) as a yellow solid in an *E*:*Z* ratio of 93:7, that was used without further purification.

R_f = 0.14 (10% EtOAc/petrol); **M.p.:** 56-58 °C; **FTIR** (ν_{max} cm^{-1}, thin film) 3372, 2963, 2933, 2245, 1446, 1377, 1066, 959, 700; **HRMS** (EI+) $C_{13}H_{15}NO$ $[M]^+$ requires 201.1148, found 201.1149 (+0.3 ppm).

Data for (*E*)-**233***:* **^{1}H NMR (500 MHz, $CDCl_3$)** δ_H = 1.60 – 1.65 (3H, m), 2.01 – 2.18 (3H, m), 2.27 – 2.33 (1H, m), 2.95 (1H, br s), 5.38 – 5.44 (1H, m), 5.49 – 5.56 (1H, m), 7.37 – 7.44 (3H, m), 7.55 – 7.59 (2H, m); **^{13}C NMR (126 MHz, $CDCl_3$)** δ_C = 18.1, 27.9, 43.3, 74.9, 120.8, 125.0, 127.3, 129.0, 129.2, 129.3, 140.0;

Data for (*Z*)-**233** *(selected):* **^{1}H NMR (500 MHz, $CDCl_3$)** δ_H = 2.98 (1H, br s); **^{13}C NMR (126 MHz, $CDCl_3$)** δ_C = 13.0, 22.5, 43.2, 126.4, 128.1, 129.1, 129.4.

(*E*)-2-Hydroxy-2,6-diphenylhex-5-enenitrile (234)

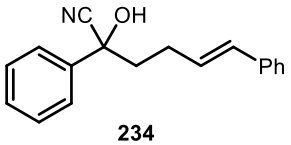

234

Prepared according to General Procedure 16 using **190** (591 mg, 2.50 mmol) in CH_2Cl_2 (5 mL), trimethylsilyl cyanide (782 µL, 6.25 mmol), and $TiCl_4$ (137 µL, 1.25 mmol), followed by acetonitrile (12.5 mL) and 2 M HCl (12.5 mL) to afford **234** (621 mg, 94%) as a yellow solid that was used without further purification.

R_f = 0.10 (10% EtOAc/petrol); **M.p.:** 54-56 °C; **FTIR** (ν_{max} cm^{-1}, thin film) 3387, 3030, 2955, 2247, 1491, 1446, 1064, 966, 748; **^{1}H NMR (500 MHz, $CDCl_3$)** δ_H = 2.14 – 2.20 (1H, m), 2.23 – 2.29 (1H, m), 2.33 – 2.40 (1H, m), 2.48 – 2.56 (1H, m), 2.87 (1H, br s), 6.16 (1H, dt, *J* 15.8, 6.8), 6.43 (dt, *J* 15.8, 1.5), 7.19 – 7.22 (1H, m), 7.27 – 7.32 (4H, m), 7.39 – 7.47 (3H, m), 7.59 – 7.61 (2H, m); **^{13}C NMR (126 MHz, $CDCl_3$)** δ_C = 28.3, 43.2, 74.7, 120.7, 125.0, 126.2, 127.4, 128.1, 128.7, 129.1, 129.5, 131.5, 137.3, 139.8; **HRMS** (EI+) $C_{18}H_{17}NO$ $[M]^+$ requires 263.1305, found 263.1306 (+0.7 ppm).

3-(Cyclohex-2-en-1-yl)-2-hydroxy-2-phenylpropanenitrile (235)

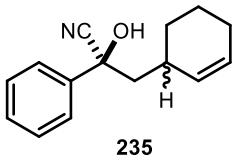

235

Prepared according to General Procedure 16 using **191** (501 mg, 2.50 mmol) in CH_2Cl_2 (5 mL), trimethylsilyl cyanide (782 µL, 6.25 mmol), and $TiCl_4$ (137 µL, 1.25 mmol), followed by MeCN (12.5 mL) and 2 M HCl (12.5 mL) to afford **235** (501 mg, 88%) as an orange oil that was used without further purification. The compound was obtained as a 1:1 inseparable mixture of diastereoisomers.

R_f = 0.14 (10% EtOAc/petrol); **^{1}H NMR (500 MHz, $CDCl_3$)** δ_H = 1.24 – 1.30 (1H, m), 1.37 – 1.44 (1H, m), 1.48 – 1.56 (2H, m), 1.61 – 1.72 (2H, m), 1.74 – 1.80 (1H, m), 1.88 – 2.14 (9H, m), 2.33 – 2.39 (1H, m), 2.43 – 2.50 (1H, m), 2.80 (1H, br s), 2.84 (1H, br s), 5.40 – 5.44 (1H, m), 5.63 – 5.73 (3H, m), 7.37 – 7.45 (6H, m), 7.57 – 7.60 (4H, m); **^{13}C NMR (126 MHz, $CDCl_3$)** δ_C = 21.0, 21.2, 25.0, 25.1, 29.8, 30.0, 32.0, 32.1, 49.7, 49.9, 74.4, 74.5, 121.1, 121.2, 124.9, 125.0, 128.2, 128.4, 129.0, 129.1, 129.3, 129.4, 130.7, 130.8, 140.4, 140.6.

These data are in accordance with the literature.[37]

2-Hydroxy-5-methyl-2-phenylhex-5-enenitrile (236)

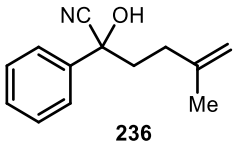

236

Prepared according to General Procedure 16 using **192** (871 mg, 5.00 mmol) in CH_2Cl_2 (10 mL), trimethylsilyl cyanide (1.56 mL, 12.5 mmol), and $TiCl_4$ (274 µL, 2.50 mmol), followed by MeCN (25 mL) and 2 M HCl (25 mL) to afford **236** (993 mg, 99%) as an orange oil that was used without further purification.

R_f = 0.17 (10% EtOAc/petrol); **^{1}H NMR (500 MHz, $CDCl_3$)** δ_H = 1.73 (3H, s), 2.09 – 2.14 (2H, m), 2.18 – 2.26 (1H, m), 2.29 – 2.36 (1H, m), 3.00 (1H, br s), 4.74 (1H, app s), 4.77 (1H, app s), 7.38 – 7.46 (3H, m), 7.57 – 7.59 (2H, m); **^{13}C NMR (126 MHz, $CDCl_3$)** δ_C = 22.7, 32.7, 41.7, 74.9, 111.3, 120.7, 125.0, 129.1, 129.4, 139.9, 144.3.

These data are in accordance with the literature.[37]

2-Allyl-1-hydroxy-1,2,3,4-tetrahydronaphthalene-1-carbonitrile (237)

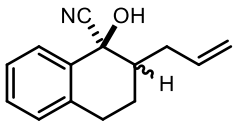

237

Prepared according to General Procedure 16 using **193** (373 mg, 2.00 mmol) in CH_2Cl_2 (4 mL), trimethylsilyl cyanide (626 µL, 5.00 mmol), and $TiCl_4$ (110 µL, 1.00 mmol), followed by MeCN (10 mL) and 2 M HCl (10 mL) to afford **237** (411 mg, 97%) as an orange oil that was used without further purification. Analysis of the reaction mixture indicated a diastereomeric ratio of 3:2.

R_f = 0.33 (20% EtOAc/petrol); **FTIR** (ν_{max} cm^{-1}, thin film) 3408, 2928, 2349, 2326, 1641, 1452, 1363, 1201, 991, 913, 761; **^{1}H NMR (500 MHz, $CDCl_3$)** δ_H = 1.70 – 1.81 (1H, m), 1.95 – 2.10 (2H, m), 2.22 – 2.33 (1H, m), 2.73 – 2.89 (3H, m), 3.12 (1H, s), 5.14 – 5.33 (2H, m), 5.87 – 5.99 (1H, m), 7.12 – 7.18 (1H, m), 7.28 – 7.34 (2H, m), 7.70 – 7.74 (1H, m); **^{13}C NMR (126 MHz, $CDCl_3$)** δ_C = 21.7, 24.6, 27.8, 28.7, 34.9, 35.9, 43.7, 44.5, 72.4, 73.8, 117.9, 118.6, 120.2, 121.9, 127.2, 127.3, 128.5, 129.4, 129.5, 129.7, 130.0 134.9, 135.0, 136.0, 136.2, 136.3, 136.4, 136.5; **HRMS** (ES+) $C_{14}H_{15}NO$ $[M-H]^+$ requires 212.1075, found 212.1079 (+1.9 ppm).

2-Hydroxy-2-phenylhept-6-enenitrile (238)

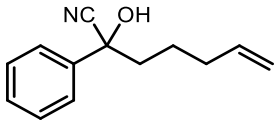

238

Prepared according to General Procedure 16 using **194** (523 mg, 3.00 mmol) in CH_2Cl_2 (6 mL), trimethylsilyl cyanide (938 µL, 7.50 mmol), and $TiCl_4$ (164 µL, 1.50 mmol), followed by acetonitrile (15 mL) and 2 M HCl (15 mL) to afford **238** (588 mg, 97%) as a yellow oil that was used without further purification.

R_f = 0.14 (10% EtOAc/petrol); **^{1}H NMR (500 MHz, $CDCl_3$)** δ_H = 1.44 – 1.53 (1H, m), 1.62 – 1.71 (1H, m), 1.95 – 2.02 (1H, m), 2.05 – 2.12 (3H, m), 2.76 (1H, br s), 4.96 – 5.01 (2H, m), 5.69 – 5.78 (1H, m), 7.38 – 7.45 (3H, m), 7.56 – 7.58 (2H, m); **^{13}C NMR (126 MHz, $CDCl_3$)** δ_C = 23.7, 33.2, 43.0, 74.8, 115.6, 120.8, 125.0, 129.1, 129.4, 137.7, 140.0.

These data are in accordance with the literature.[37]

2-Hydroxy-2-phenylpent-4-enenitrile (239)

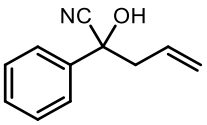

239

Prepared according to General Procedure 16 using **200** (731 mg, 5.00 mmol) in CH_2Cl_2 (10 mL), trimethylsilyl cyanide (1.56 mL, 12.5 mmol), and $TiCl_4$ (274 µL, 2.50 mmol), followed by acetonitrile (25 mL) and 2 M HCl (25 mL) to afford **239** (839 mg, 97%) as an orange oil that was used without further purification.

R_f = 0.11 (10% EtOAc/petrol); **FTIR** (ν_{max} cm^{-1}, thin film) 3402 (br), 3082, 1672, 1641, 1490, 1450, 1257, 1056, 1030, 993, 925; **^{1}H NMR (500 MHz, $CDCl_3$)** δ_H = 2.72 (1H, dd, *J* 13.9, 8.2), 2.82 (1H, dd, *J* 13.9, 6.3), 3.02 (1H, br s), 5.28 – 5. 32 (1H, m), 5.34 – 5.36 (1H, m), 5.83 – 5.91 (1H, m), 7.38 – 7.45 (3H, m), 7.57 – 7.59 (2H, m); **^{13}C NMR (126 MHz, $CDCl_3$)** δ_C = 48.4, 73.4, 120.4, 122.6, 125.1, 129.0, 129.4, 130.5, 139.2; **HRMS** (CI+) $C_{11}H_{11}NO$ $[M+H]^+$ requires 174.0913, found 174.0915 (+ 0.8 ppm).

5.4.3 Electrochemical Reactions

General Procedure 17 – Electrochemical Alkene Azidocyanation

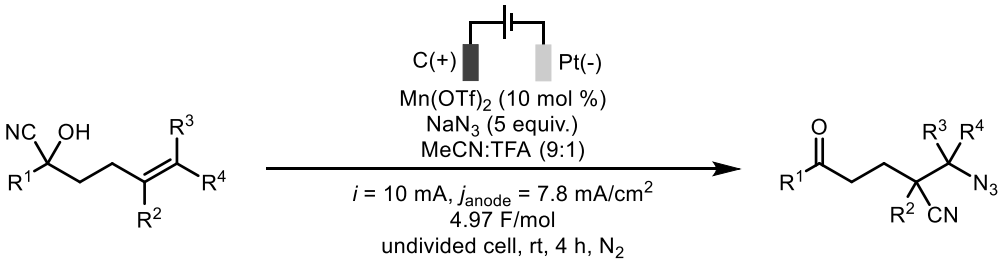

To an oven-dried 10 mL ElectraSyn vial equipped with a magnetic stirrer bar, was added the appropriate cyanohydrin (0.30 mmol), $Mn(OTf)_2$ (11 mg, 0.03 mmol), and NaN_3 (98 mg, 1.50 mmol). The threaded glass was wrapped with PTFE tape and connected to the ElectraSyn cap, which was fitted with a graphite anode and platinum foil cathode. The vial was subjected to vacuum-nitrogen exchange cycles (× 3), anhydrous MeCN (5.4 mL) was added, followed by TFA (600 µL), and the mixture was stirred until complete solvation of the NaN_3. The mixture was purged *via* bubbling with N_2 gas for 10 min. Electrolysis at 10 mA (j_{anode} = 7.8 mA/cm^2) was conducted for 4 h under N_2 at rt with continuous stirring. After electrolysis was complete, the reaction mixture was diluted with EtOAc (10 mL) and washed with a saturated solution of $NaHCO_3$ (aq.) (2 × 15 mL). The layers were separated, and the aqueous layer was further extracted with EtOAc (3 × 10 mL). The combined organics were washed with brine (10 mL), dried over $MgSO_4$, filtered, and concentrated under reduced pressure. The resultant crude material was purified by flash column chromatography to afford the desired product.

5.4.4 Characterisation of Products

2-(Azidomethyl)-5-oxo-5-phenylpentanenitrile (165)

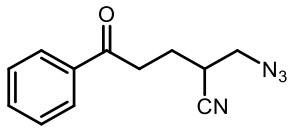

165

Prepared according to General Procedure 17 using **163** (56 mg). The resultant crude material was purified by flash column chromatography (20% EtOAc/petrol, silica gel) to afford **165** (35 mg, 51%) as an orange solid.

1.00 mmol scale

To an oven-dried 20 mL ElectraSyn vial equipped with a magnetic stirrer bar, was added **163** (187 mg, 1.00 mmol), $Mn(OTf)_2$ (35 mg, 0.10 mmol), and NaN_3 (325 mg, 5.00 mmol). The threaded glass was wrapped with PTFE tape and connected to the ElectraSyn cap, which was fitted with a graphite anode and platinum foil cathode. The vial was subjected to vacuum-nitrogen exchange cycles (× 3), anhydrous MeCN (5.4 mL) was added, followed by TFA (600 µL), and the mixture was stirred until complete solvation of the NaN_3. The mixture was purged *via* bubbling with N_2 gas for 10 min. Electrolysis at 10 mA (j_{anode} = 4.0 mA/cm^2) was conducted for 13 h 20 min under N_2 at rt with continuous stirring. After electrolysis was complete, the reaction mixture was diluted with EtOAc (50 mL) and washed with a saturated solution of $NaHCO_3$ (aq.) (2 × 50 mL). The layers were separated, and the aqueous layer was further extracted with EtOAc (3 × 50 mL). The combined organics were washed with brine (50 mL), dried over $MgSO_4$, filtered, and concentrated under reduced pressure. The resultant crude material was purified by flash column chromatography to afford **165** (146 mg, 64%) as an orange solid.

R_f = 0.16 (20% EtOAc/petrol); **M.p.:** 45-47 °C; **^{1}H NMR (500 MHz, $CDCl_3$)** δ_H = 1.98 – 2.09 (1H, m), 2.14 – 2.25 (1H, m), 2.99 – 3.08 (1H, m), 3.18 – 3.33 (2H, m), 3.56 – 3.67 (2H, m), 7.45 – 7.53 (2H, m), 7.57 – 7.64 (1H, m), 7.94 – 8.01 (2H, m); **^{13}C NMR (126 MHz, $CDCl_3$)** δ_C = 24.1 31.8, 35.2, 52.3, 119.6, 128.2, 128.9, 133.8, 136.4, 198.0.

These data are in accordance with the literature.[37]

2-(Azidomethyl)-5-oxo-5-(*p*-tolyl)pentanenitrile (240)

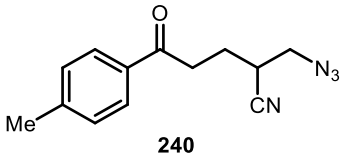

240

Prepared according to General Procedure 17 using **204** (60 mg). The resultant crude material was purified by flash column chromatography (5-15% EtOAc/*n*-hexane, silica gel) to afford **240** (35 mg, 48%) as a yellow oil.

R_f = 0.19 (20% EtOAc/*n*-hexane); **^{1}H NMR (500 MHz, $CDCl_3$)** δ_H = 1.99 – 2.06 (1H, m), 2.15 – 2.22 (1H, m), 2.43 (3H, s), 3.00 – 3.05 (1H, m), 3.16 – 3.28 (2H, m), 3.57 – 3.64 (2H, m), 7.27 – 7.29 (2H, m), 7.86 – 7.88 (2H, m); **^{13}C NMR (126 MHz, $CDCl_3$)** δ_C = 21.9, 24.1, 31.8, 35.0, 52.3, 119.7, 128.3, 129.6, 133.9, 144.7, 197.7.

These data are in accordance with the literature.[37]

2-(Azidomethyl)-5-oxo-5-(*m*-tolyl)pentanenitrile (241)

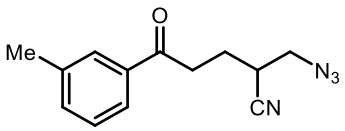

241

Prepared according to General Procedure 17 using **205** (60 mg). The resultant crude material was purified by flash column chromatography (5-15% EtOAc/*n*-hexane, silica gel) to afford **241** (35 mg, 48%) as a yellow oil.

R_f = 0.40 (30% EtOAc/*n*-hexane); **^{1}H NMR (500 MHz, $CDCl_3$)** δ_H = 1.99 – 2.07 (1H, m), 2.15 – 2.22 (1H, m), 2.43 (3H, s), 3.00 – 3.05 (1H, m), 3.18 – 3.29 (2H, m), 3.57 – 3.64 (2H, m), 7.36 – 7.42 (2H, m), 7.75 – 7.78 (2H, m); **^{13}C NMR (126 MHz, $CDCl_3$)** δ_C = 21.5, 24.1, 31.8, 35.2, 52.3, 119.6, 125.4, 128.7, 128.8, 134.5, 136.4, 138.8, 198.2.

These data are in accordance with the literature.[37]

2-(Azidomethyl)-5-oxo-5-(*o*-tolyl)pentanenitrile (242)

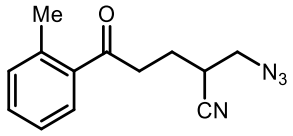

242

Prepared according to General Procedure 17 using **206** (60 mg). The resultant crude material was purified by flash column chromatography (5-15% EtOAc/*n*-hexane, silica gel) to afford **242** (34 mg, 47%) as a yellow oil.

R_f = 0.38 (30% EtOAc/*n*-hexane); **^{1}H NMR (500 MHz, $CDCl_3$)** δ_H = 1.97 – 2.05 (1H, m), 2.14 – 2.20 (1H, m), 2.52 (3H, s), 3.00 – 3.06 (1H, m), 3.13 – 3.22 (2H, m), 2.57 – 3.64 (2H, m), 7.27 – 7.31 (2H, m), 7.39 – 7.43 (1H, m), 7.69 – 7.71 (1H, m); **^{13}C NMR (126 MHz, $CDCl_3$)** δ_C = 21.7, 24.3, 31.8, 37.8, 52.3, 119.6, 126.1, 128.8, 132.1, 132.4, 136.9, 138.8, 201.6.

These data are in accordance with the literature.[37]

5-([1,1'-Biphenyl]-5-yl)-2-(azidomethyl)-5-oxopentanenitrile (243)

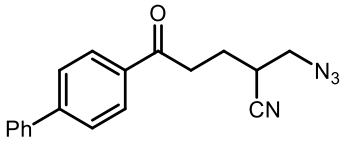

243

Prepared according to General Procedure 17 using **207** (79 mg). The resultant crude material was purified by flash column chromatography (5-20% EtOAc/*n*-hexane, silica gel) to afford **243** (38 mg, 42%) as a white solid.

R_f = 0.13 (20% EtOAc/*n*-hexane); **M.p.:** 123-125 °C; **^{1}H NMR (500 MHz, $CDCl_3$)** δ_H = 2.00 – 2.12 (1H, m), 2.17 – 2.28 (1H, m), 3.02 – 3.09 (1H, m), 3.22 – 3.38 (2H, m), 3.58 – 3.67 (2H, m), 7.39 – 7.44 (1H, m), 7.45 – 7.52 (2H, m), 7.63 – 7.65 (2H, m), 7.70 – 7.74 (2H, m), 8.03 – 8.06 (2H, m); **^{13}C NMR (126 MHz, $CDCl_3$)** δ_C = 24.1, 31.8, 35.2, 52.3, 119.6, 127.4, 127.6, 128.5, 128.8, 129.2, 135.1, 139.8, 146.5, 197.6.

These data are in accordance with the literature.[37]

2-(Azidomethyl)-5-oxo-5-(4-(trifluoromethyl)phenyl)pentanenitrile (244)

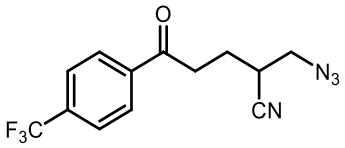

244

Prepared according to General Procedure 17 using **208** (77 mg). The resultant crude material was purified by flash column chromatography (20% EtOAc/*n*-hexane, silica gel) to afford **244** (39 mg, 44%) as a yellow oil.

R_f = 0.19 (20% EtOAc/*n*-hexane); **^{1}H NMR (500 MHz, $CDCl_3$)** δ_H = 2.00 – 2.16 (1H, m), 2.16 – 2.27 (1H, m), 2.99 – 3.08 (1H, m), 3.20 – 3.36 (2H, m), 3.35 – 3.69 (2H, m), 7.73 – 7.80 (2H, m), 8.06 – 8.11 (2H, m); **^{13}C NMR (126 MHz, $CDCl_3$)** δ_C = 23.9, 31.7, 35.6, 52.2, 119.4, 123.6 (q, *J* 272.9), 126.0 (q, *J* 3.7), 128.5, 135.1 (q, *J* 32.8), 138.9, 197.1; **^{19}F{^{1}H} NMR (376 MHz, $CDCl_3$)** δ_F = -63.17.

These data are in accordance with the literature.[37]

4-(5-Azido-4-cyanopentanoyl)benzonitrile (245)

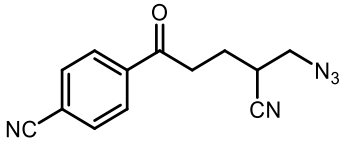

245

Prepared according to General Procedure 17 using **209** (64 mg). The resultant crude material was purified by flash column chromatography (5-30% EtOAc/*n*-hexane, silica gel) to afford **245** (34 mg, 45%) as an orange oil.

R_f = 0.16 (30% EtOAc/*n*-hexane); **FTIR** (ν_{max} cm^{-1}, thin film) 2938, 2230, 2102, 1688, 1404, 1206, 984, 831; **^{1}H NMR (500 MHz, $CDCl_3$)** δ_H = 2.01 – 2.09 (1H, m), 2.16 – 2.23 (1H, m), 3.00 – 3.05 (1H, m), 3.20 – 3.33 (2H, m), 3.59 – 3.66 (2H, m), 7.79 – 7.81 (2H, m), 8.05 – 8.07 (2H, m); **^{13}C NMR (126 MHz, $CDCl_3$)** δ_C = 23.7, 31.6, 35.6, 52.1, 117.0, 117.9, 119.4, 128.5, 132.8, 139.1, 196.7; **HRMS** (CI+) $C_{13}H_{11}N_5O$ $[M\text{-}N_2+H]^+$ requires 226.0975, found 226.0974 (-0.6 ppm).

2-(Azidomethyl)-5-(4-fluorophenyl)-5-oxopentanenitrile (246)

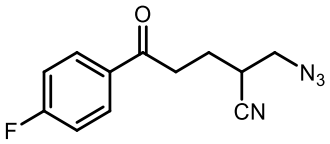

246

Prepared according to General Procedure 17 using **210** (62 mg). The resultant crude material was purified by flash column chromatography (5-15% EtOAc/*n*-hexane, silica gel) to afford **246** (32 mg, 43%) as a yellow oil.

R_f = 0.16 (20% EtOAc/*n*-hexane); **^{1}H NMR (500 MHz, $CDCl_3$)** δ_H = 1.99 – 2.07 (1H, m), 2.16 – 2.22 (1H, m), 3.00 – 3.06 (1H, m), 3.16 – 3.28 (2H, m), 3.58 – 3.64 (2H, m), 7.14 – 7.18 (2H, m), 7.98 – 8.02 (2H, m); **^{13}C NMR (126 MHz, $CDCl_3$)** δ_C = 24.0, 31.8, 35.1, 52.2, 116.1 (d, *J* 21.9), 119.5, 130.8 (d, *J* 9.4), 132.8 (d, *J* 3.0), 166.2 (d, *J* 255.8), 196.4; **^{19}F{^{1}H} NMR (376 MHz, $CDCl_3$)** δ_F = -104.08.

These data are in accordance with the literature.[37]

2-(Azidomethyl)-5-(4-chlorophenyl)-5-oxopentanenitrile (247)

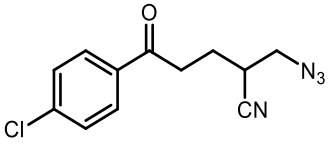

247

Prepared according to General Procedure 17 using **211** (67 mg). The resultant crude material was purified by flash column chromatography (5-15% EtOAc/*n*-hexane, silica gel) to afford **247** (38 mg, 48%) as a white solid.

R_f = 0.16 (20% EtOAc/*n*-hexane); **M.p.:** 51-53 °C; **^{1}H NMR (500 MHz, $CDCl_3$)** δ_H = 1.97 – 2.09 (1H, m), 2.13 – 2.24 (1H, m), 2.97 – 3.07 (1H, m), 3.15 – 3.28 (2H, m), 3.57 – 3.64 (2H, m), 7.45 – 7.48 (2H, m), 7.90 – 7.93 (2H, m); **^{13}C NMR (126 MHz, $CDCl_3$)** δ_C = 24.0, 31.7, 35.2, 52.2, 119.5, 129.3, 129.6, 134.7, 140.3, 196.8.

These data are in accordance with the literature.[37]

2-(Azidomethyl)-5-(4-bromophenyl)-5-oxopentanenitrile (248)

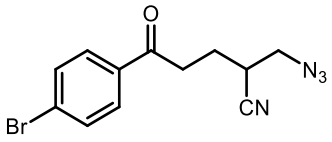

248

Prepared according to General Procedure 17 using **212** (80 mg). The resultant crude material was purified by flash column chromatography (5-20% EtOAc/*n*-hexane, silica gel) to afford **248** (41 mg, 44%) as a yellow solid.

R_f = 0.24 (20% EtOAc/*n*-hexane); **M.p.:** 92-94 °C; **^{1}H NMR (500 MHz, $CDCl_3$)** δ_H = 1.99 – 2.06 (1H, m), 2.15 – 2.22 (1H, m), 2.99 – 3.04 (1H, m), 3.15 – 3.27 (2H, m), 3.57 – 3.64 (2H, m), 7.62 – 7.65 (2H, m), 7.82 – 7.84 (2H, m); **^{13}C NMR (126 MHz, $CDCl_3$)** δ_C = 24.0, 31.7, 35.2, 52.2, 119.5, 129.1, 129.6, 132.3, 135.1, 197.0.

These data are in accordance with the literature.[37]

2-(Azidomethyl)-5-(4-iodophenyl)-5-oxopentanenitrile (249)

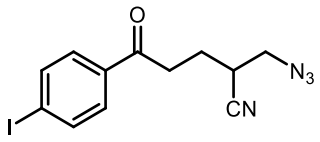

249

Prepared according to General Procedure 17 using **213** (94 mg). The resultant crude material was purified by flash column chromatography (5-12% EtOAc/*n*-hexane, silica gel) to afford **249** (37 mg, 35%) as an orange oil.

R_f = 0.17 (20% EtOAc/*n*-hexane); **FTIR** (ν_{max} cm^{-1}, thin film) 2926, 2243, 2100, 1681, 1579, 1560, 1450, 1392, 1273, 1219, 1205, 1180, 1056, 1004, 977; **^{1}H NMR (500 MHz, $CDCl_3$)** δ_H = 1.99 – 2.06 (1H, m), 2.14 – 2.21 (1H, m), 2.98 – 3.04 (1H, m), 3.13 – 3.26 (2H, m), 3.57 – 3.63 (2H, m), 7.66 – 7.68 (2H, m), 7.84 – 7.87 (2H, m); **^{13}C NMR (126 MHz, $CDCl_3$)** δ_C = 23.4, 31.7, 35.1, 52.2, 101.9, 119.5, 129.5, 135.6, 138.3, 197.3; **HRMS** (AP+) $C_{12}H_{11}N_2OI$ $[M\text{-}N_2+H]^+$ requires 326.9994, found 326.9997 (+0.9 ppm).

2-(Azidomethyl)-5-oxo-5-(4-(4,4,5,5-tetramethyl-1,3,2-dioxaborolan-2-yl)phenyl)pentane nitrile (250)

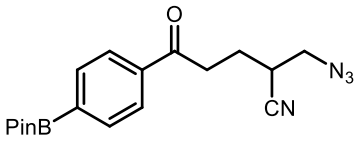

250

Prepared according to General Procedure 17 using **218** (94 mg), but electrolysis was performed for 5 h instead of 4 h. ^{1}H NMR analysis of the crude reaction mixture indicated a 46% yield. **250** was purified by flash column chromatography (5-25% EtOAc/*n*-hexane, silica gel) as a yellow oil.

R_f = 0.38 (30% EtOAc/*n*-hexane); **FTIR** (ν_{max} cm^{-1}, thin film) 2980, 2929, 2360, 2106, 1685, 1508, 1398, 1359, 1327, 1273, 1143, 1089, 1018, 962; **^{1}H NMR (500 MHz, $CDCl_3$)** δ_H = 1.36 (12H, s), 2.00 – 2.07 (1H, m), 2.15 – 2.22 (1H, m), 3.00 – 3.06 (1H, m), 3.20 – 3.32 (2H, m), 3.58 – 3.65 (2H, m), 7.90 – 7.95 (4H, m); **^{13}C NMR (126 MHz, $CDCl_3$)** δ_C = 24.1, 25.0, 31.8, 35.4, 52.3, 84.4, 119.6, 127.1, 135.2, 138.2, 198.3; **HRMS** (ES+) $C_{18}H_{23}{}^{11}BN_4O_3$ $[M\text{-}N_2+H]^+$ requires 327.1880, found 327.1882 (+0.6 ppm).

4-(5-Azido-4-cyanopentanoyl)benzoic acid (251)

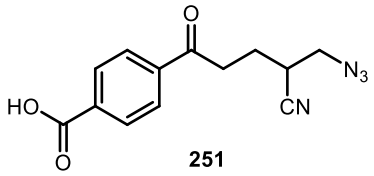

251

Prepared according to General Procedure 17 using **219** (69 mg), but electrolysis was performed for 5 h instead of 4 h. In this example the organic layers were washed with water instead of a saturated solution of $NaHCO_3$ (aq.). ^{1}H NMR analysis of the crude reaction mixture indicated a 45% yield. **251** was purified by flash column chromatography (40-100% EtOAc/*n*-hexane, silica gel) as a yellow solid.

R_f = 0.24 (80% EtOAc/*n*-hexane); **M.p.:** 127-129 °C; **FTIR** (ν_{max} cm^{-1}, thin film) 2922, 2850, 2669, 2546, 2268, 2106, 1678 (br), 1610, 1506, 1425, 1409, 1282, 1205, 1128, 1116, 1014, 981; **^{1}H NMR (500 MHz, DMSO-d_6)** δ_H = 1.94 – 1.99 (2H, m), 3.17 – 3.22 (1H, m), 3.25 – 3.28 (2H, m), 3.68 – 3.78 (2H, m), 8.07 (4H, s), 13.22 (1H, br s); **^{13}C NMR (126 MHz, DMSO-d_6)** δ_C = 23.2, 30.7, 35.5, 50.8, 120.6, 128.1, 129.6, 134.6, 139.4, 166.6, 198.2; **HRMS** (ASAP+) $C_{13}H_{12}N_4O_3$ $[M\text{-}N_2+H]^+$ requires 245.0926, found 245.0930 (+1.6 ppm).

Methyl 4-(5-azido-4-cyanopentanoyl)benzoate (252)

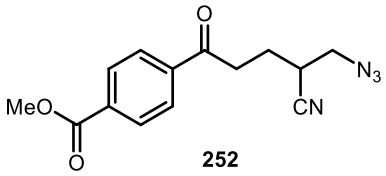

252

Prepared according to General Procedure 17 using **220** (74 mg). The resultant crude material was purified by flash column chromatography (20-30% EtOAc/*n*-hexane, silica gel) to afford **252** (64 mg, 75%) as a white solid.

R_f = 0.21 (30% EtOAc/*n*-hexane); **M.p.:** 66-68 °C; **FTIR** (ν_{max} cm^{-1}, thin film) 2958, 2899, 2202, 2118, 1712, 1681, 1571, 1454, 1433, 1408, 1355, 1282, 1261, 1192, 1111, 1020, 983, 950; **^{1}H NMR (500 MHz, $CDCl_3$)** δ_H = 2.02 – 2.09 (1H, m), 2.17 – 2.24 (1H, m), 3.00 – 3.06 (1H, m), 3.21 – 3.34 (2H, m), 3.59 – 3.65 (2H, m), 3.96 (3H, s), 8.01 – 8.03 (2H, m), 8.14 – 8.16 (2H, m); **^{13}C NMR (126 MHz, $CDCl_3$)** δ_C = 24.0, 31.7, 35.6, 52.2, 52.7, 119.5, 128.1, 130.2, 134.5, 139.5, 166.2, 197.5; **HRMS** (AP+) $C_{14}H_{14}N_4O_3$ $[M\text{-}N_2+H]^+$ requires 259.1083, found 259.1088 (+1.9 ppm).

4-(5-Azido-4-cyanopentanoyl)benzamide (253)

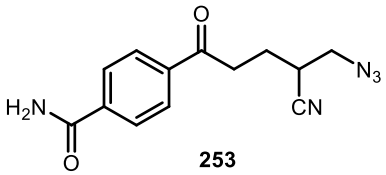

253

Prepared according to General Procedure 17 using **221** (69 mg). The resultant crude material was purified by flash column chromatography (50-90% EtOAc/*n*-hexane, silica gel) to afford **253** (25 mg, 31%) as a white solid.

R_f = 0.16 (80% EtOAc/*n*-hexane); **M.p.:** 136-138 °C; **FTIR** (ν_{max} cm^{-1}, thin film) 3414, 3377, 3165, 2923, 2243, 2092, 1683, 1651, 1620, 1564, 1506, 1409, 1392, 1257, 1203, 1147, 1120, 1016, 981; **^{1}H NMR (500 MHz, DMSO-d_6)** δ_H = 1.91 – 2.01 (2H, m), 3.16 – 3.22 (1H, m), 3.24 – 3.27 (2H, m), 3.68 – 3.78 (2H, m), 7.56 (1H, br s), 7.98 – 8.00 (2H, m), 8.03 – 8.05 (2H, m), 8.14 (1H, br s); **^{13}C NMR (126 MHz, DMSO-d_6)** δ_C = 23.3, 30.7, 35.4, 50.8, 120.6, 127.7, 127.8, 138.1, 132.2, 167.0, 198.2; **HRMS** (ES–) $C_{13}H_{13}N_5O_2$ $[M\text{-}H]^-$ requires 270.0991, found 270.0884 (+1.1 ppm).

4-(5-Azido-4-cyanopentanoyl)-*N*,*N*-dimethylbenzamide (254)

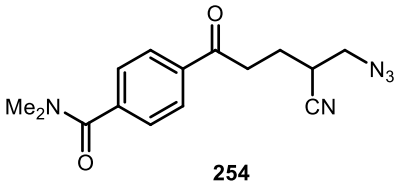

254

Prepared according to General Procedure 17 using **222** (77 mg). The resultant crude material was purified by flash column chromatography (60-90% EtOAc/*n*-hexane, silica gel) to afford **254** (37 mg, 41%) as a yellow oil.

R_f = 0.22 (80% EtOAc/*n*-hexane); **FTIR** (ν_{max} cm^{-1}, thin film) 2933, 2243, 2102, 1683, 1624 (br), 1566, 1512, 1452, 1400, 1265, 1211, 1081, 1016, 981, 918; **^{1}H NMR (500 MHz, $CDCl_3$)** δ_H = 2.00 – 2.08 (1H, m), 2.16 – 2.22 (1H, m), 2.96 (3H, s), 3.00 – 3.06 (1H, m), 3.13 (3H, m), 3.19 – 3.31 (2H, m), 3.57 – 3.64 (2H, m), 7.50 – 7.53 (2H, m), 7.98 – 8.00 (2H, m); **^{13}C NMR (126 MHz, $CDCl_3$)** δ_C = 24.0, 31.7, 35.3, 35.5, 39.5, 52.2, 119.5, 127.6, 128.3, 136.9, 141.2, 170.6, 197.4; **HRMS** (ES+) $C_{15}H_{17}N_5O_2$ $[M+H]^+$ requires 300.1460, found 300.1457 (-1.0 ppm).

2-(Azidomethyl)-5-(4-(2-methyl-1,3-dioxolan-2-yl)phenyl)-5-oxopentanenitrile (255)

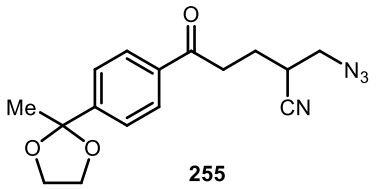

255

Prepared according to General Procedure 17 using **224** (82 mg). The resultant crude material was purified by flash column chromatography (10-50% EtOAc/*n*-hexane, silica gel) to afford **255** (28 mg, 30%) as an orange oil.

R_f = 0.22 (50% EtOAc/*n*-hexane); **FTIR** (ν_{max} cm^{-1}, thin film) 3447, 2934, 2347, 2104, 1684, 1609, 1406, 1225, 1111, 1080, 1044, 831; **^{1}H NMR (500 MHz, $CDCl_3$)** δ_H = 1.89 (3H, s), 2.00 – 2.08 (1H, m), 2.16 – 2.23 (1H, m), 3.00 – 3.06 (1H, m), 3.19 – 3.31 (2H, m), 3.37 – 3.41 (1H, m), 3.58 – 3.65 (2H, m), 3.69 – 3.73 (1H, m), 3.75 – 3.85 (2H, m), 7.66 – 7.68 (2H, m), 8.01 – 8.05 (2H, m); **^{13}C NMR (126 MHz, $CDCl_3$)** δ_C = 23.9, 30.6, 31.7, 35.3, 52.2, 61.6, 68.4, 118.6, 119.5, 126.0, 128.9, 137.1, 143.7, 197.2; **HRMS** (ES+) $C_{16}H_{18}N_4O_3$ $[M+H]^+$ requires 315.1457, found 315.1461 (+1.3 ppm).

2-(Azidomethyl)-5-(naphthalen-1-yl)-5-oxopentanenitrile (256)

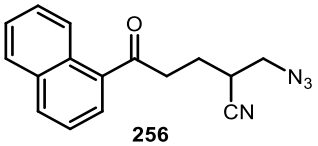

256

Prepared according to General Procedure 17 using **226** (71 mg). The resultant crude material was purified by flash column chromatography (5-25% EtOAc/*n*-hexane, silica gel) to afford **256** (28 mg, 34%) as a yellow oil.

R_f = 0.28 (30% EtOAc/*n*-hexane); **^{1}H NMR (500 MHz, $CDCl_3$)** δ_H = 2.05 – 2.13 (1H, m), 2.23 – 2.30 (1H, m), 3.05 – 3.10 (1H, m), 3.25 – 3.41 (2H, m), 3.60 – 3.66 (2H, m), 7.51 – 7.57 (2H, m), 7.60 – 7.63 (1H, m), 7.89 – 7.91 (1H, m), 7.94 – 7.96 (1H, m), 8.02 – 8.04 (1H, m), 8.63 – 8.65 (1H, m); **^{13}C NMR (126 MHz, $CDCl_3$)** δ_C = 24.5, 31.8, 38.3, 52.3, 119.6, 124.5, 125.7, 126.8, 128.3, 128.4, 128.7, 130.2, 133.6, 134.1, 134.8, 201.9.

These data are in accordance with the literature.[37]

2-(Azidomethyl)-5-oxo-6-phenylhexanenitrile (257)

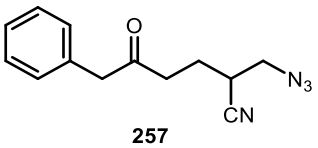

257

Prepared according to General Procedure 17 using **227** (60 mg), but electrolysis was performed for 5 h instead of 4 h. The resultant crude material was purified by flash column chromatography (5-20% EtOAc/*n*-hexane, silica gel) to afford **257** (33 mg, 45%) as a yellow oil.

R_f = 0.21 (30% EtOAc/*n*-hexane); **^{1}H NMR (500 MHz, $CDCl_3$)** δ_H = 1.77 – 1.85 (1H, m), 1.91 – 1.97 (1H, m), 2.65 – 2.77 (2H, m), 2.82 – 2.88 (1H, m), 3.44 – 3.51 (2H, m), 3.72 (2H, s), 7.19 – 7.22 (2H, m), 7.27 – 7.31 (1H, m), 7.33 – 7.37 (2H, m); **^{13}C NMR (126 MHz, $CDCl_3$)** δ_C = 23.6, 31.5, 38.3, 50.4, 52.1, 119.4, 127.5, 129.1, 129.5, 133.7, 206.5.

These data are in accordance with the literature.[37]

2-(1-Azidoethyl)-5-oxo-5-phenylpentanenitrile (262)

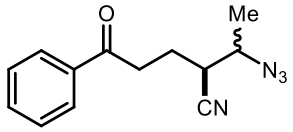

262

Prepared according to General Procedure 17 using **233** (60 mg). The resultant crude material was purified by flash column chromatography (5-15% EtOAc/*n*-hexane, silica gel) to afford the separable diastereoisomers **262-1** (17 mg, 23%) and **262-2** (14 mg, 19%) as yellow oils. Analysis of the crude reaction mixture indicated a diastereomeric ratio of 1:1.

Data for **262-1**

R_f = 0.42 (30% EtOAc/*n*-hexane); **FTIR** (v_{max} cm^{-1}, thin film) 2980, 2245, 2115, 2097, 1672, 1446, 1261, 1209, 974, 738, 685; **^{1}H NMR (500 MHz, $CDCl_3$)** δ_H = 1.52 (3H, d, *J* 6.6), 1.91 – 1.98 (1H, m), 2.22 – 2.29 (1H, m), 2.86 – 2.91 (1H, m), 3.17 – 3.32 (2H, m), 3.73 – 3.78 (1H, m), 7.47 – 7.51 (2H, m), 7.58 – 7.62 (1H, m), 7.96 – 7.99 (2H, m); **^{13}C NMR (126 MHz, $CDCl_3$)** δ_C = 16.9, 23.3, 35.5, 37.7, 57.8, 119.3, 128.2, 128.9, 133.8, 136.4, 198.1; **HRMS** (ES+) $C_{13}H_{14}N_4O$ $[M\text{-}N_2]^+$ requires 215.1184, found 215.1180 (-1.9 ppm).

Data for **262-2**

R_f = 0.33 (30% EtOAc/*n*-hexane); **FTIR** (v_{max} cm^{-1}, thin film) 2976, 2926, 2360, 2243, 2102, 1681, 1635, 1597, 1581, 1448, 1255, 1209, 1180, 1001; **^{1}H NMR (500 MHz, $CDCl_3$)** δ_H = 1.51 (3H, d, *J* 6.6), 2.07 – 2.20 (2H, m), 2.88 – 2.92 (1H, m), 3.19 – 3.31 (2H, m), 3.74 – 3.79 (1H, m), 7.47 – 7.50 (2H, m), 7.56 – 7.62 (1H, m), 7.96 – 7.98 (2H, m); **^{13}C NMR (126 MHz, $CDCl_3$)** δ_C = 17.9, 23.8, 35.2, 37.9, 57.7, 118.9, 128.1, 128.9, 133.8, 136.3, 198.4; **HRMS** (ES+) $C_{13}H_{14}N_4O$ $[M\text{-}N_2\text{+}H]^+$ requires 215.1184, found 215.1177 (-3.3 ppm).

2-Azido-6-(2-oxo-2-phenylethyl)cyclohexane-1-carbonitrile (263)

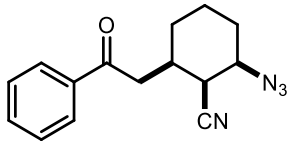

263

Prepared according to General Procedure 17 using **235** (68 mg). The resultant crude material was purified by flash column chromatography (5-10% EtOAc/*n*-hexane, silica

gel) to afford **263** (30 mg, 37%) as a white solid. Analysis of the crude reaction mixture indicated a diastereomeric ratio of > 20:1.

R_f = 0.40 (20% EtOAc/*n*-hexane); **M.p.:** 62-64 °C; **^{1}H NMR (500 MHz, $CDCl_3$)** δ_H = 1.43 – 1.51 (1H, m), 1.66 – 1.75 (3H, m), 1.90 – 1.94 (2H, m), 2.70 – 2.76 (1H, m), 3.04 – 3.15 (2H, m), 3.18 – 3.19 (1H, m), 4.12 – 4.14 (1H, m), 7.46 – 7.50 (2H, m), 7.57 – 7.61 (1H, m), 7.96 – 7.98 (2H, m); **^{13}C NMR (126 MHz, $CDCl_3$)** δ_C = 19.8, 26.3, 28.3, 29.3, 36.9, 42.2, 58.1, 118.5, 128.2, 128.9, 133.7, 136.7, 197.7.

These data are in accordance with the literature.[37]

2-(Azidomethyl)-2-methyl-5-oxo-5-phenylpentanenitrile (264)

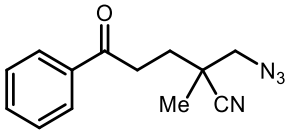

264

Prepared according to General Procedure 17 using **236** (60 mg). The resultant crude material was purified by flash column chromatography (5-15% EtOAc/*n*-hexane, silica gel) to afford **264** (32 mg, 44%) as an orange oil.

R_f = 0.30 (30% EtOAc/*n*-hexane); **^{1}H NMR (500 MHz, $CDCl_3$)** δ_H = 1.43 (3H, s), 1.96 – 2.02 (1H, m), 2.15 – 2.21 (1H, m), 3.15 – 3.29 (2H, m), 3.47 (1H, d, *J* 12.2), 3.53 (1H, d, *J* 12.2), 7.47 – 7.51 (2H, m), 7.58 – 7.61 (1H, m), 7.97 – 7.99 (2H, m); **^{13}C NMR (126 MHz, $CDCl_3$)** δ_C = 22.4, 30.9, 34.1, 37.8, 58.2, 121.9, 128.2, 128.9, 133.7, 136.4, 197.9.

These data are in accordance with the literature.[37]

3-Azido-2-((1-oxo-1,2,3,4-tetrahydronaphthalen-2-yl)methyl)propanenitrile (265)

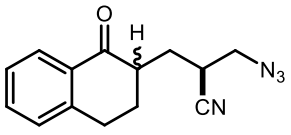

265

Prepared according to General Procedure 17 using **237** (64 mg). The resultant crude material was purified by flash column chromatography (5-15% EtOAc/*n*-hexane, silica gel) to afford the separable diastereoisomers **265-1** (17 mg, 22%) and **265-2** (18 mg, 24%) as yellow oils. Analysis of the crude reaction mixture indicated a diastereomeric ratio of 1:1.

Data for **265-1**

R_f = 0.41 (30% EtOAc/*n*-hexane); **FTIR** (ν_{max} cm^{-1}, thin film) 2918, 2870, 2848, 2243, 2160, 2108, 1672, 1598, 1450, 1436, 1361, 1350, 1273, 1228, 1143, 972, 931; **^{1}H NMR (500 MHz, $CDCl_3$)** δ_H = 1.66 – 1.71 (1H, m), 1.94 – 2.02 (1H, m), 2.11 – 2.17 (1H, m), 2.22 – 2.27 (1H, m), 2.74 – 2.80 (1H, m), 2.98 – 3.03 (1H, m), 3.13 – 3.19 (1H, m), 3.51 – 3.65 (3H, m), 7.25 – 7.26 (1H, m), 7.30 – 7.33 (1H, m), 7.48 – 7.51 (1H, m), 7.97 – 7.99 (1H, m); **^{13}C NMR (126 MHz, $CDCl_3$)** δ_C = 29.3, 30.7, 31.8, 31.9, 45.3, 52.7, 120.2, 126.9, 127.5, 128.9, 132.3, 133.9, 143.9, 199.8; **HRMS** (ASAP+) $C_{14}H_{14}N_4O$ $[M-N_2+H]^+$ requires 227.1184, found 227.1187 (+1.3 ppm).

Data for **265-2**

R_f = 0.38 (30% EtOAc/*n*-hexane); **FTIR** (ν_{max} cm^{-1}, thin film) 2931, 2243, 2100, 1674, 1598, 1454, 1274, 1224, 1155, 1099, 1001, 929; **^{1}H NMR (500 MHz, $CDCl_3$)** δ_H = 1.79 – 1.84 (1H, m), 1.90 – 1.99 (1H, m), 2.27 – 2.33 (1H, m), 2.42 – 2.48 (1H, m), 2.72 – 2.78 (1H, m), 3.01 – 3.06 (2H, m), 3.09 – 3.15 (1H, m), 3.61 – 3.64 (2H, m), 7.25 – 7.27 (1H, m), 7.31 – 7.34 (1H, m), 7.48 – 7.51 (1H, m) 8.01 – 8.03 (1H, m); **^{13}C NMR (126 MHz, $CDCl_3$)** δ_C = 28.7, 29.0, 29.9, 30.0, 45.2, 52.3, 119.7, 127.0, 127.7, 128.9, 132.1, 133.9, 143.8, 198.5; **HRMS** (ASAP+) $C_{14}H_{14}N_4O$ $[M-N_2+H]^+$ requires 227.1184, found 227.1189 (+2.2 ppm).

5.4.5 Alternative Transformations

5-Oxo-5-phenyl-2-(2,2,2-trifluoroethyl)pentanenitrile (164)

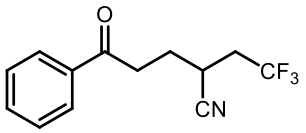

164

Prepared according to General Procedure 17 using **163** (56 mg), but with $NaSO_2CF_3$ (234 mg, 1.50 mmol) in place of NaN_3, $LiClO_4$ (56 mg, 0.53 mmol) as the supporting electrolyte, and the reaction was run for 3 h. The resultant crude material was purified by flash column chromatography (10-20% EtOAc/*n*-hexane, silica gel) to afford **164** (13 mg, 17%) as a colourless oil.

R_f = 0.24 (20% EtOAc/petrol); **^{1}H NMR (500 MHz, $CDCl_3$)** δ_H = 2.00 – 2.08 (1H, m), 2.24 – 2.31 (1H, m), 2.39 – 2.49 (1H, m), 2.55 – 2.65 (1H, m), 3.13 – 3.19 (1H, m), 3.28 – 3.31 (2H, m), 7.48 – 7.52 (2H, m), 7.59 – 7.63 (1H, m), 7.97 – 7.99 (2H, m); **^{13}C NMR**

(126 MHz, $CDCl_3$) δ_C = 25.2 (q, *J* 3.0), 26.5, 35.2, 36.9 (q, *J* 30.0), 119.6, 125.1 (q, *J* 227.3), 128.1, 128.9, 133.9, 136.2, 197.8; **$^{19}F\{^1H\}$ NMR (376 MHz, $CDCl_3$)** δ_F = -64.8.

These data are in accordance with the literature.[39]

5-Oxo-5-phenyl-1-((phenylsulfonyl)methyl)pentanenitrile (266)

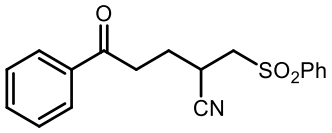

266

Prepared according to General Procedure 17 using **163** (56 mg), but with $NaSO_2Ph$ (246 mg, 1.50 mmol) in place of NaN_3. The resultant crude material was purified by flash column chromatography (5-30% EtOAc/*n*-hexane, silica gel) to afford **266** (40 mg, 41%) as a white solid.

R_f = 0.16 (30% EtOAc/*n*-hexane); **M.p.:** 102-104 °C; **FTIR** (ν_{max} cm^{-1}, thin film) 3059, 2991, 2937, 2239, 1685, 1597, 1583, 1446, 1294, 1278, 1199, 1138, 1083, 997; **^1H NMR (500 MHz, $CDCl_3$)** δ_H = 2.05 – 2.12 (1H, m), 2.30 – 2.37 (1H, m), 3.18 – 3.29 (2H, m), 3.32 (1H, dd, *J* 13.9, 5.0), 3.35 – 3.41 (1H, m), 3.52 (1H, dd, *J* 13.9, 7.8), 7.46 – 7.50 (2H, m), 7.58 – 7.65 (3H, m), 7.71 – 7.75 (1H, m), 7.94 – 7.96 (2H, m), 7.98 – 8.00 (2H, m); **^{13}C NMR (126 MHz, $CDCl_3$)** δ_C = 26.1, 26.6, 35.2, 57.5, 118.9, 128.1, 128.5, 128.9, 129.8, 133.8, 134.8, 136.2, 138.2, 197.5; **HRMS** (ES+) $C_{18}H_{17}NO_3S$ $[M+Na]^+$ requires 350.0827, found 350.0827 (±0.0 ppm).

2-(But-3-en-1-yl)-2-phenylmalononitrile (268)

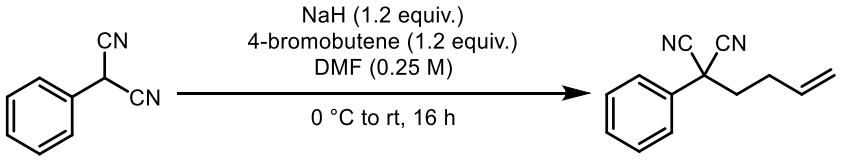

267 **268**

To a flame-dried three-neck RBF fitted with a condenser was added NaH (60% dispersion in mineral oil, 480 mg, 12.0 mmol) in DMF (40 mL, 0.25 M). 2-Phenylmalononitrile **267** (1.42 g, 10.0 mmol) was added at 0 °C and the reaction was stirred at rt for 1 h, 4-bromobut-1-ene (1.22 mL, 12.0 mmol) was added dropwise, and the mixture was heated to 60 °C overnight. Upon completion, the reaction was cooled to rt before a saturated solution of NH_4Cl (aq.) and EtOAc were added. The layers were separated, and the aqueous layer was extracted with EtOAc (× 3). The combined organics were washed with water (× 5) then brine, dried over $MgSO_4$, filtered, and concentrated under reduced pressure. The resultant crude material was purified by flash column

chromatography (10% EtOAc/petrol, silica gel) to afford **268** (1.68 g, 86%) as a pale-yellow oil.

R_f = 0.46 (10% EtOAc/petrol); **^{1}H NMR (500 MHz, $CDCl_3$)** δ_H = 2.29 – 2.34 (2H, m), 2.35 – 2.41 (2H, m), 5.07 – 5.14 (2H, m), 5.72 – 5.80 (1H, m), 7.45 – 7.52 (3H, m), 7.55 – 7.59 (2H, m); **^{13}C NMR (126 MHz, $CDCl_3$)** δ_C = 29.8, 41.9, 42.1, 115.0, 117.5, 125.9, 129.9, 130.1, 132.1, 134.4.

These data are in accordance with the literature.[40]

2-Azido-5-(azidomethyl)-2-phenylhexanedinitrile (269)

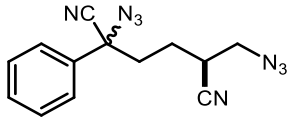

269

Prepared according to General Procedure 17 using **268** (59 mg). The resultant crude material was purified by flash column chromatography (10-20% EtOAc/*n*-hexane, silica gel) to afford **269** (29 mg, 34%) as a yellow oil. Analysis of the crude reaction mixture indicated a diastereomeric ratio of 1:1.

R_f = 0.19 (20% EtOAc/petrol); **^{1}H NMR (500 MHz, $CDCl_3$)** δ_H = 1.71 – 1.84 (2H, m), 1.92 – 1.99 (2H, m), 2.04 – 2.10 (1H, m), 2.12 – 2.19 (1H, m), 2.23 – 2.34 (2H, m), 2.71 – 2.76 (1H, m), 2.80 – 2.85 (1H, m), 3.50 – 3.58 (4H, m), 7.47 – 7.54 (6H, m), 7.55 – 7.58 (4H, m); **^{13}C NMR (126 MHz, $CDCl_3$)** δ_C = 25.1, 25.3, 31.7, 31.9, 39.1, 39.2, 51.8, 51.9, 66.4, 66.5, 117.0, 117.1, 118.7 (2C), 125.7 (2C), 129.8 (2C), 130.5 (2C), 134.8, 135.0.

These data are in accordance with the literature.[40]

5.4.6 Product Derivatisations

5-Oxo-5-phenyl-2-((4-phenyl-1*H*-1,2,3-triazol-1-yl)methyl)pentanenitrile (270)

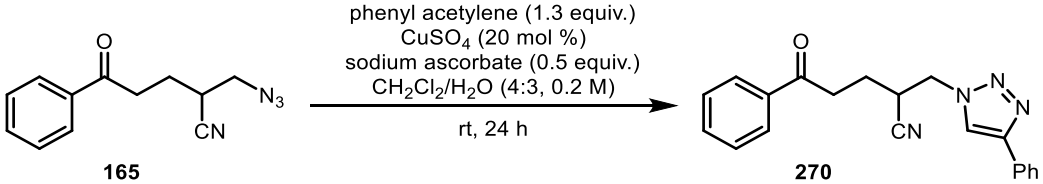

165 **270**

Following a literature procedure,[41] to a flame-dried microwave vial was added **165** (228 mg, 1.00 mmol) and phenylacetylene (143 µL, 1.30 mmol) in CH_2Cl_2 (2.9 mL). Water (2.1 mL) was added, followed by $CuSO_4$ (32 mg, 0.20 mmol). Sodium ascorbate (99 mg, 0.50 mmol) was added portion-wise, and the reaction mixture was stirred at rt for 24 h.

CH_2Cl_2 was added, followed by water and 1 M HCl (aq.). The layers were separated, and the aqueous layer was further extracted with EtOAc (× 3). The combined organics were washed with brine, dried over $MgSO_4$, filtered, and concentrated under reduced pressure. The resultant crude material was purified by recrystallisation (EtOH) to afford **270** (155 mg, 47%) as a white solid.

R_f = 0.12 (30% EtOAc/petrol); **M.p.:** 178-180 °C; **FTIR** (ν_{max} cm^{-1}, thin film) 3086, 2960, 2241, 1739, 1678, 1597, 1462, 1444, 1365, 1226, 1205, 1083, 1041, 974; **^{1}H NMR (500 MHz, DMSO-*d*$_6$)** δ_H = 1.95 – 2.10 (2H, m), 3.30 (2H, t, *J* 7.3), 3.62 – 3.68 (1H, m), 4.79 – 4.86 (2H, m), 7.34 – 7.37 (1H, m), 7.45 – 7.48 (2H, m), 7.53 – 7.56 (2H, m), 7.64 – 7.67 (1H, m), 7.85 – 7.87 (2H, m), 7.99 – 8.01 (2H, m), 8.66 (1H, s); **^{13}C NMR (126 MHz, DMSO-*d*$_6$)** δ_C = 23.4, 31.7, 35.0, 49.6, 119.9, 122.0, 125.2, 127.9, 128.0, 128.7, 129.0, 130.5, 133.4, 136.3, 146.4, 198.3; **HRMS** (CI+) $C_{20}H_{18}N_4O$ $[M+H]^+$ requires 331.1553, found 331.1554 (+0.1 ppm).

***N*'-(5-Azido-4-cyano-1-phenylpentylidene)benzohydrazide (271)**

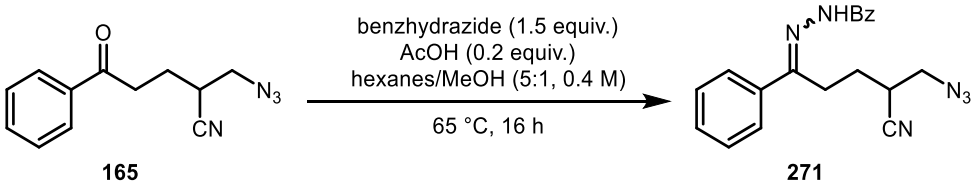

165 **271**

Following a literature procedure,[42] to a RBF was added **165** (114 mg, 0.50 mmol) and AcOH (6 mg, 0.10 mmol) in hexanes (1 mL) and MeOH (0.25 mL). The reaction mixture was heated at reflux overnight. Upon cooling, the mixture was concentrated under reduced pressure. The resultant crude material was purified by flash column chromatography (20-60% EtOAc/petrol, silica gel) to afford **271** (153 mg, 88%) as a pale-yellow solid.

R_f = 0.11 (30% EtOAc/petrol); **M.p.:** 141-143 °C; **FTIR** (ν_{max} cm^{-1}, thin film) 3199, 2931, 2235, 2104, 1639, 1535, 1489, 1463, 1450, 1330, 1278, 1130, 1072; **^{1}H NMR (400 MHz, DMSO-*d*$_6$, 80 °C)** δ_H = 1.82 – 1.93 (2H, m), 3.01 – 3.09 (2H, m), 3.17 – 3.26 (1H, m), 3.65 – 3.75 (2H, m), 7.40 – 7.63 (7H, m), 7.77 – 7.89 (3H, m), 10.71 (1H, br s); **^{13}C NMR (101 MHz, DMSO-*d*$_6$, 80 °C)** δ_C = 23.9, 25.3, 31.0, 50.5, 119.8, 126.1, 127.7, 127.8, 128.0, 129.0, 130.7, 134.0, 136.6; **(126 MHz, DMSO-*d*$_6$, 25 °C)** δ_C = 156.8, 164.4; **HRMS** (ES+) $C_{19}H_{18}N_6O$ $[M+H]^+$ requires 347.1620, found 347.1627 (+2.0 ppm).

5.4.7 Flow Electrochemical Reactions

5.4.7.1 General Information

The flow set-up used PFA tubing with a 0.79±0.1 mm internal diameter and 1.58±0.1 mm outer diameter supplied by Polyflon. All flow fittings and connections were purchased from Kinesis (Gripper fitting nuts, part number: 002103; Adapters, part number: P-618; Omnilok type-p fitting ferrule, part number: 008FT16; Y-Connector, part number: P-512; Threaded union, part number: P-623). Pumps used were the Chemyx Fusion 100 syringe pump and Knauer P4.1S Azura HPLC pump. The residence coils were made from the tubing by taking the appropriate length for the desired volume. The HPLC pumps was calibrated by pumping solvent into a measuring cylinder, recording the time taken for the desired volume to be dispensed and then adjusting the pump's flow rate to the correct value, if required. The power supply used was a Voltcraft LRP-1205 that supplied DC to the electrochemical system. The electrochemical flow cell was purchased from Cambridge Reactor Design, the Ammonite 8 (part number: 74660). The electrochemical flow cell consists of one carbon/PVDF electrode and one platinum foil electrode that are fixed either side of a FFKM gasket with a channel groove length of 1000 mm and an internal volume of 2.5 mL, of which 1 mL is exposed to the electrodes. The inlet and outlet fittings of the ammonite 8 cell were modified from 1/16" ID to accommodate 1/32" ID PFA tubing using Swagelok reducers, nuts, and ferrules.

5.4.7.1 General Procedures

General Procedure 18 – Single Pass Electrochemical Alkene Azidocyanation

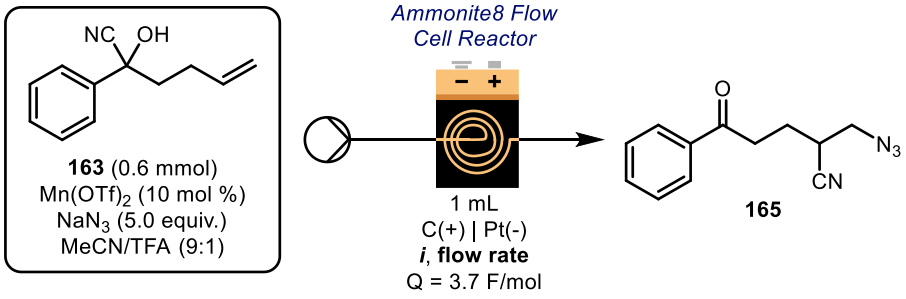

Preparation of reagent solutions

To a flame-dried RBF was added **163** (112 mg, 0.60 mmol), $Mn(OTf)_2$ (21 mg, 0.06 mmol), and NaN_3 (195 mg, 3.00 mmol). The flask was subjected to vacuum-nitrogen exchange cycles (× 3), then anhydrous MeCN (10.8 mL) was added, followed by TFA (1.2 mL), and the mixture was stirred until complete solvation of the NaN_3. The mixture was purged *via* bubbling with N_2 gas for 10 min.

Flow running order

The electrochemical flow system was flushed with nitrogen gas for 5 min by connecting the inlet tubing directly to the dry nitrogen line. The reagent solution was drawn up into a 20 mL syringe and promptly connected to the flow system. The syringe pump was set to the appropriate flow rate. Syringe pumping was initiated, and the outlet of the flow system was set to waste for the first 3 mL (representing 1 whole flow path volume, inclusive of tubing, connectors, and reactor) of reaction mixture to allow the flow system to be filled. After this initial priming, the power supply was switched on and the electrolysis commenced at the appropriate constant current and the outlet stream of the flow system was then collected for 6 mL (representing 0.30 mmol of **163** processed). 1,3,5-Trimethylbenzene (14 µL, 0.10 mmol) was added to the collected mixture, stirred for 5 min and then the ^{1}H NMR spectrum was recorded to give a crude reaction yield.

For full results see section 4.2.4.1.

General Procedure 19 – Recirculating Electrochemical Alkene Azidocyanation

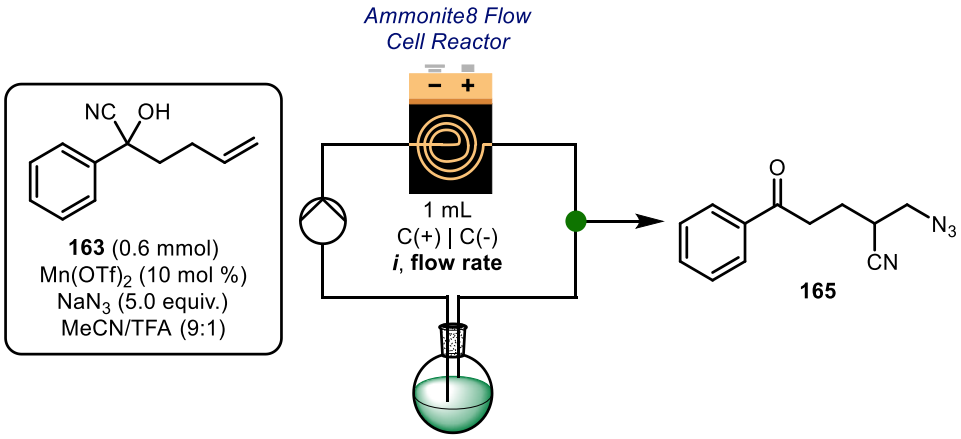

To a flame-dried RBF was added **163** (112 mg, 0.60 mmol), $Mn(OTf)_2$ (21 mg, 0.06 mmol), and NaN_3 (195 mg, 3.00 mmol). The flask was subjected to vacuum-nitrogen exchange cycles (× 3), then anhydrous MeCN (10.8 mL) was added, followed by TFA (1.2 mL), and the mixture was stirred until complete solvation of the NaN_3. The mixture was purged *via* bubbling with N_2 gas for 10 min. The HPLC pump was primed with the reaction mixture and set to recirculate at the appropriate flow rate while the contents of the flask were degassed by bubbling nitrogen for 15 min. The electrolysis was then commenced and conducted at the appropriate constant current. Upon recirculation for the specified time, electrolysis was turned off and the flow system was purged and flushed with clean MeCN (3 × 20 mL). 1,3,5-Trimethylbenzene (28 µL, 0.20 mmol) was added to

the reaction mixture, stirred for 5 min and then the ^{1}H NMR spectrum was recorded to give a crude reaction yield.

For full results see section 4.2.2.1.

5.4.8 Mechanistic Investigations

5.4.8.1 Cyclic Voltammetry Studies

General Information: Cyclic voltammetry (CV) experiments were conducted with a Metrohm Autolab PGSTAT204 potentiostat and Nova 2.1 software. For all experiments, a glassy carbon working electrode (3 mm dia., BASi), a platinum wire counter electrode, and a Ag/$AgNO_3$ reference electrode were employed. All data were collected at rt. The solution of interest was purged with N_2 for 5 min before data collection. After data collection, ferrocene (5 mM) was added, and an additional scan was run. The parent data was referenced relative to the Fc/Fc^+ couple that was recorded. In these studies, $TBAN_3$ was used in place of NaN_3 due to its higher solubility in MeCN, and AcOH was used in place of TFA due to its lower acidity. Both $TBAN_3$ and AcOH proved competent in alkene azidocyanation (see chapter 4).

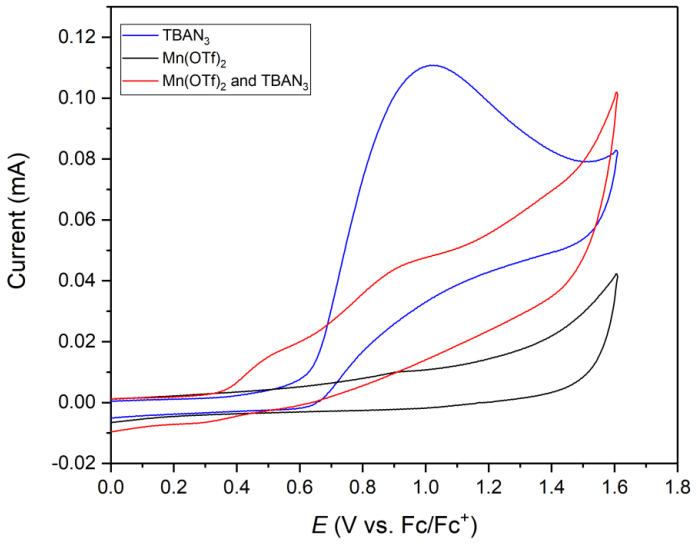

Figure 5.6: Cyclic Voltammogram of $Mn(OTf)_2$, $TBAN_3$, and their mixture in MeCN (6 mL) with AcOH (240 µL) and $LiClO_4$ (0.1 M). a (black line) – $Mn(OTf)_2$ (2.0 mM); b (blue line) – $TBAN_3$ (10 mM); c (red line) – $Mn(OTf)_2$ (2.0 mm) and $TBAN_3$ (10 mM). ***Scan rate: 100 mV/s***

5.5 References

1 H. Zeng, P. Pan, J. Chen, H. Gong and C. J. Li, *Eur. J. Org. Chem.*, 2017, **2017**, 1070–1073.

2 C. W. Cheung and S. L. Buchwald, *J. Org. Chem.*, 2012, **77**, 7526–7537.

3 R. Y. Zhang, L. Y. Xi, L. Shi, X. Z. Zhang, S. Y. Chen and X. Q. Yu, *Org. Lett.*, 2016, **18**, 4024–4027.

4 H. C. Li, C. An, G. Wu, G. X. Li, X. B. Huang, W. X. Gao, J. C. Ding, Y. B. Zhou, M. C. Liu and H. Y. Wu, *Org. Lett.*, 2018, **20**, 5573–5577.

5 Y. Sun, X. Huang, X. Li, F. Luo, L. Zhang, M. Chen, S. Zheng and B. Peng, *Adv. Synth. Catal.*, 2018, **360**, 1082–1087.

6 Z. Wang, Z. Chen and J. Sun, *Angew. Chem., Int. Ed.*, 2013, **52**, 6685–6688.

7 K. Kuroda, Y. Hayashi and T. Mukaiyama, *Tetrahedron*, 2007, **63**, 6358–6364.

8 M. T. Reetz, S. H. Kyung and M. Hüllmann, *Tetrahedron*, 1986, **42**, 2931–2935.

9 L. Huan and C. Zhu, *Org. Chem. Front.*, 2016, **3**, 1467–1471.

10 R. L. Zhai, Y. S. Xue, T. Liang, J. J. Mi and Z. Xu, *J. Org. Chem.*, 2018, **83**, 10051–10059.

11 X. Fan, H. Zhao, J. Yu, X. Bao and C. Zhu, *Org. Chem. Front.*, 2016, **3**, 227–232.

12 S. Sawano, N. Ishida and M. Murakami, *Chem. Lett.*, 2015, **44**, 1521–1523.

13 M. O. Ganiu, A. H. Cleveland, J. L. Paul and R. Kartika, *Org. Lett.*, 2019, **21**, 5611–5615.

14 I. Khan, B. G. Reed-Berendt, R. L. Melen and L. C. Morrill, *Angew. Chem., Int. Ed.*, 2018, **57**, 12356–12359.

15 J. F. Zhao, B. H. Tan and T. P. Loh, *Chem. Sci.*, 2011, **2**, 349–352.

16 S. C. Lu, H. S. Li, S. Xu and G. Y. Duan, *Org. Biomol. Chem.*, 2017, **15**, 324–327.

17 X. L. Lai, X. M. Shu, J. Song and H. C. Xu, *Angew. Chem., Int. Ed.*, 2020, **59**, 10626–10632.

18 J. Davies, N. S. Sheikh and D. Leonori, *Angew. Chem., Int. Ed.*, 2017, **56**, 13361–13365.

19 D. M. Hodgson, P. G. Humphreys, S. M. Miles, C. A. J. Brierley and J. G. Ward, *J. Org. Chem.*, 2007, **72**, 10009–10021.

20 S. Arava, J. N. Kumar, S. Maksymenko, M. A. Iron, K. N. Parida, P. Fristrup and A. M. Szpilman, *Angew. Chem., Int. Ed.*, 2017, **56**, 2599–2603.

21 S. Samadi and A. Orellana, *ChemCatChem*, 2016, **8**, 2472–2475.

22 S. Giboulot, F. Liron, G. Prestat, B. Wahl, M. Sauthier, Y. Castanet, A. Mortreux and G. Poli, *Chem. Commun.*, 2012, **48**, 5889–5891.

23 F. Huang and S. Zhang, *Org. Lett.*, 2019, **21**, 7430–7434.

24 C. S. Penkett, J. A. Woolford, T. W. Read and R. J. Kahan, *J. Org. Chem.*, 2011, **76**, 1295–1304.

25 J. Wu, X. Yang, Z. He, X. Mao, T. A. Hatton and T. F. Jamison, *Angew. Chem., Int. Ed.*, 2014, **53**, 8416–8420.

26 S. Scaringi and C. Mazet, *ACS Catal.*, 2021, **11**, 7970–7977.

27 D. J. Fox, D. S. Pedersen and S. Warren, *Chem. Commun.*, 2004, 2598–2599.

28 E. C. Burger and J. A. Tunge, *Org. Lett.*, 2004, **6**, 4113–4115.

29 R. Suresh, A. K. Simlandy and S. Mukherjee, *Org. Lett.*, 2018, **20**, 1300–1303.

30 J. A. Murphy, M. Mahesh, G. McPheators, R. Vijaya Anand, T. M. McGuire, R. Carlinga and A. R. Kennedy, *Org. Lett.*, 2007, **9**, 3233–3236.

31 S. Hok and N. E. Schore, *J. Org. Chem.*, 2006, **71**, 1736–1738.

32 K. Usami, E. Yamaguchi, N. Tada and A. Itoh, *Org. Lett.*, 2018, **20**, 5714–5717.

33 S. Wang, L. Ma, Q. Wang, P. Shao, D. Ma, S. Yuan, P. Lei, P. Li, X. Feng and B. Wang, *J. Mater. Chem. C*, 2018, **6**, 5369–5374.

34 J. F. Hayes, M. Shipman and H. Twin, *J. Org. Chem.*, 2002, **67**, 935–942.

35 K. Moriyama, M. Takemura and H. Togo, *J. Org. Chem.*, 2014, **79**, 6094–6104.

36 W. S. Bechara, G. Pelletier and A. B. Charette, *Nat. Chem.*, 2012, **4**, 228–234.

37 Z. Wu, R. Ren and C. Zhu, *Angew. Chem., Int. Ed.*, 2016, **55**, 10821–10824.

38 Y. Kwon and Q. Wang, *Org. Lett.*, 2020, **22**, 4141–4145.

39 N. Wang, L. Li, Z. L. Li, N. Y. Yang, Z. Guo, H. X. Zhang and X. Y. Liu, *Org. Lett.*, 2016, **18**, 6026–6029.

40 C. Chang, H. Zhang, X. Wu and C. Zhu, *Chem. Commun.*, 2022, **58**, 1005–1008.

41 X. Creary, A. Anderson, C. Brophy, F. Crowell and Z. Funk, *J. Org. Chem.*, 2012, **77**, 8756–8761.

42 X. L. Yang, X. X. Peng, F. Chen and B. Han, *Org. Lett.*, 2016, **18**, 2070–2073.